ABSORBANCE SPECTROSCOPY BASED EVALUATION OF HUMIC ACID UNDER NON-OXIDATIVE AND OXIDATIVE CONDITIONS

by

Müge Paçal

BS. in Environmental Engineering, Yıldız Technical University, 2006

Submitted to the Institute of Environmental Sciences in partial fulfillment of

The requirements for the degree of

Master of Science

in

Environmental Sciences

Boğaziçi University

2011

ACKNOWLEDGEMENT

Master was an important step for my education. I would like to express my grateful for support, guidance I have received from my thesis supervisor ‘Miray Bekbölet’. She provided me with many valuable scientific, opportunities, and personal experiences. I would also like to express my appreciation to the members of my thesis Prof.Dr. Ferhan Çeçen, Yrd.Doç.Dr. Aslıhan Kerç for their valuable comments and time.

I owe special thanks to my family for their support and patient during my thesis. I also would like to express my kindness to support and provide me comfortable condition during my master thesis.

ABSTRACT

The aim of this study was to examine the mathematical relationships between humic acid concentration and UV-vis spectroscopic parameters under oxidative and non-oxidative conditions. Humic acid concentration was represented by dissolved organic carbon contents (DOC). UV-vis spectroscopic parameters were presented by absorbance measurements at wavelength λ = 436 nm as $Color_{436}$, λ= 365 nm as UV_{365}, λ=280 nm as UV_{280}, and λ= 254 nm as UV_{254}. Humic acids were selected as representing terrestrial humic acids (FHA, AHA and RHA) and aquatic humic acid (NHA).

As a lot of different humic molecules in very diverse physical associations are mixed together in natural environments, it is difficult to determine their exact concentrations (units of ppm, mg L^{-1} or mol L^{-1}) and allocate them to a certain class of organic molecules. Since direct determination of humic acid concentraton is not possible to the unspecified chemical structure,various methods have been developed to express the humic acid contents of the aqueous humic solutions. Due to the fact that humic acid does not have a well identified structure, the researchers applied some methods to represent the humic acid concentration as a function of DOC concentration and/or UV-vis parameters (UV_{254}, UV_{280}, UV_{365} and $Color_{436}$).This study includes evaluation of the experimental work performed on the UV-vis parameters in relation to the humic acid “prepared” concentration and DOC contents. The mathematical relationships between i. DOC concentration and HA “prepared” concentration, ii. DOC concentration and UV-vis parameters (UV_{254}, UV_{280}, UV_{365} and $Color_{436}$) and iii. HA “prepared” concentration and UV-vis parameters (UV_{254}, UV_{280}, UV_{365} and $Color_{436}$) were investigated for NHA, FHA, AHA and RHA under the non-oxidative conditions.

DOC concentrations, corresponding to HA concentration (NHA, FHA, AHA, and RHA), were correlated with UV-vis parameters (UV_{254}, UV_{280}, UV_{365} and $Color_{436}$) under the non-treatment condition and HA concentrations (NHA, FHA, AHA, and RHA) were correlated with UV-vis parameters (UV_{254}, UV_{280}, UV_{365} and $Color_{436}$) with high regression coefficient under the non-treatment condition. Furthermore, the overall humic

acids (NHA, FHA, AHA, and RHA) and also DOC concentrations of the overall humic acids were correlated with UV-vis parameters.

The same steps were done under the oxidative treatment conditions where photocatalytic treatment was applied. In general, photocatalytic oxidation can be considered as an example of innovative technologies collectively known as ‘‘Advanced Oxidation Processes’’ that rely on the generation of very reactive oxygen radicals. Those reactive species are subsequently used to degrade non selectively organic compounds. The known concentrations of NHA and AHA was treated by photocatalytic treatment. The removal of DOC concentration of NHA and AHA were determined by using TOC analyzer and the removal of UV-vis parameter (UV_{254}, UV_{280}, UV_{365} and $Color_{436}$) was determined by using UV-vis spectrophotometer after the photocatalytic treatment.The mathematical relationships between DOC concentration of NHA and AHA, and UV-vis parameters (UV_{254}, UV_{280}, UV_{365} and $Color_{436}$) were investigated after the photocatalytic treatment.

DOC concentrations of NHA (in the presence of 0.25 mg mL^{-1} TiO_2) and AHA (in the presence of 0.10, 0.25 and 1.00 mg mL^{-1} TiO_2) were correlated with UV-vis parameters under the treatment condition (the photocatalytic treatment). Some researchers represented the removal of HA as a function of UV-vis parameter under the photocatalytic treatment. Moreover, DOC ‘DOC_{calc}’ was calculated as a function of UV_{254}, UV_{280}, UV_{365} and $Color_{436}$ parameter of the removed HA concentration, by using the non-treatment Equations of NHA and AHA. The mathematical relationship between DOC_{obs} and DOC_{calc} was evaluated.

ÖZET

Bu çalışmanın amacı, humik asit konsantrasyonuyla ultraviyole görülebilir parametreler arasındaki ilişkiyi arıtım olan ve arıtım olmayan şartlar arasında incelemekti. Hümik asit konsantrasyonu, çözünmüş oksijen içeriği olarak ifade edilir. 254, 280, 365 ve 436 dalga boyunda, absorbans ölçümleri tarafından ultraviyole görülebilir parametreler ifade edildi. Toprak humik asitlerini ifade etmek üzere FHA, AHA ve RHA, su humik asitini ifade etmek üzere NHA seçildi.

Çeşitli fiziksel yapıda farklı hümik molekülleri doğada bulunduğundan dolayı, gerçek konsantrasyonları tahmin etmek ve (ppm, mg L^{-1} veya mol L^{-1}) onları belirli organik molekül sınıflarına koymak zordur. Belirli kimyasal yapısını tahmin etmek zor olduğu için, humik asit konsantrasyonlarının içeriğini ifade edebilmek için farklı methodlar uygulandı. Humik asitin iyi tanımlanabilir yapısı olmadığından dolayı, araştırmacılar humik asit konsantrasyonlarını çözünmüş organik konsantrasyonu ve ultraviyole görülebilir parameterler ve renk parametresi (UV_{254}, UV_{280}, UV_{365} and $Color_{436}$) cinsinden ifade etmek için bazı methodlara başvurmuştur. Bu çalışma, çözünmüş organik konsantrasyon içeriğinin, humik asitin hazırlanmış konsantrasyonuna bağlı olarak ultraviyole parametrelerine dayalı bilimsel bir çalışma oluşturmuştur. i. Çözünmüş organik karbon konsantrasyon ile humik asit hazırlanmış konsantrasyon arasında, ii. Çözünmüş organik karbon konsantrasyon ile ultraviyole görülebilir parametreler arasında, iii. Humik asit çözünmüş konsantrasyon ile ultraviyole görülebilir parametreler arasında arıtım olmayan şartlar arasında matematiksel ilişki, NHA, FHA, AHA ve RHA için, incelendi.

HA konstansantrasyonuna (NHA, FHA, AHA ve RHA) karşılık gelen çözünmüş organik karbon ile ultraviyole parametreleri oksidatif olmayan şartlarda korole edildi ve HA konstantrasyonu (NHA, FHA, AHA ve RHA) ile ultraviyole parametreler yüksek regrasyon eşitliğiyle, oksidatif olmayan şartlarda, korole edildi. Öte yandan, bütün hümik asitler ve hümik asitlere karşılık gelen çözünmüş organik karbon ultraviyole parametrelerle korole edildi.

Aynı adımlar oksidatif şartlar için uygulandı ve oksidatif şart için fotokatalitik arıtım seçildi. Genellikle, ileri oksidasyon teknolojileri gibi ileri teknoloji örneği olarak gözönünde bulundurulur ve aktif oksijen radikallerinin üretimine cevap verir. Bu reaktif türler organik bileşenlerinin giderimi için kullanılır. Bilinen konsantrasyondaki NHA ve AHA fotokatalitik yöntemle arıtıldı. Çözünmüş organik karbon konsantrasyonu, toplam organik karbon konsantrasyonu cinsinden ve ultraviyole görülebilir parametreler ve renk (UV_{254}, UV_{280}, UV_{365} and $Color_{436}$) cinsinden tayin edildi. Fotokatalitik arıtımdan sonra, NHA ve AHA nın çözünmüş organik karbon konsantrasyonuyla ultraviyole görülebilir parametreler (UV_{254}, UV_{280}, UV_{365} and $Color_{436}$) arasındaki ilişki incelendi.

Fotokatalitik arıtma esnasında, NHA çözünmüş oksijen konsantrasyonu ile ultraviyole görülebilir parametreler (UV_{254}, UV_{280}, UV_{365} and $Color_{436}$) ile korole edildi (0.25 mg mL^{-1} TiO_2 olduğu durumda). AHA çözünmüş organik karbon konsantrasyonu ile ultraviyole görülebilir parametreler (UV_{254}, UV_{280}, UV_{365} and $Color_{436}$) ile korole edildi (0.10, 0.25 and 1.00 mg mL^{-1} TiO_2 olduğu durumda). Bazı araştırmacılar, fotokatalitik şartlar altında, HA giderimini ultraviyole görülebilir parametreler (UV_{254}, UV_{280}, UV_{365} and $Color_{436}$) cinsinden ifade etti. Öte yandan, fotokatalitik esnasında giderilmiş hümik asitin, UV_{254}, UV_{280}, UV_{365} ve $Color_{436}$ parametreleri cinsinden NHA ve AHA nın oksidatif olmayan denklemleri kullanarak çözünmüş organik karbon konsantrasyonu hesaplandı. Hesaplanan çözünmüş organik karbon ile gözlemlenen çözünmüş organik karbon arasındaki matematiksel ilişki incelendi.

TABLE OF CONTENTS

LIST OF FIGURES

LIST OF TABLES

LIST OF SYMBOLS/ABBREVIATIONS

Symbol	Explanation
λ	Wavelength
AHA	Aldrich Humic Acid
AOP	Advanced Oxidation Processes
$Color_{436}$	Absorbance at 436 nm
DOC	Dissolved Organic Carbon
FA	Fulvic Acid
FHA	Fluka Humic Acid
HA	Humic Acid
HOMO	Highest Occupied Molecular Orbital
HS	Humic Substances
Ir	Irradiation Time (min)
k	Pseudo First Order Reaction Rate Constant (min^{-1})
K_{LH}	Adsorption Coefficient (m^{-1})
k_{LH}	Reaction Rate Constant (m^{-1} min^{-1})
L-H	Langmuir Hinshelwood
LUMO	Lowest Unoccupied Molecular Orbital
NHA	Nordic Humic Acid
NOM	Natural Organic Matter
RHA	Roth Humic Acid
SCOA	Specific Color Absorbance
$SCOA_{436}$	Specific Color Absorbance at 436 nm
SUVA	Specific UV absorbance
$SUVA_{254}$	Specific UV absorbance at 254 nm
$SUVA_{365}$	Specific UV absorbance at 365 nm
UV_{254}	Absorbance at 254 nm
UV_{280}	Absorbance at 280 nm
UV_{365}	Absorbance at 365 nm

1. INTRODUCTION

Natural organic matter occuring in aquatic systems and terrestrial environments are defined as withering material from plants and animals as well as their degradation products. Natural organic matter consists of humic substances. Humic substances are structurally polyelectrolytic, complex, dark colored organic acids that are found in sediments, soils, and natural waters. Humic acids and related pigments, collectively referred to as humic substances, are widely distributed in soils, natural waters, marine and lake sediments, peat, carbonaceous shales, lignites, brown coals, and miscellaneous other deposits.

Organic compounds that are aromatic or that have conjugated double bounds absorb light in the ultraviolet wavelength region. UV absorbance is a good technique for measuring the presence of humic acids because they include aromatic moieties and are the dominant form of organic matter in natural waters (Alberts et al., 1982; Schnitzer et al., 1972).

Advanced oxidation process are used to oxidize complex organic constituents found in wastewater that are difficult to degrade biologically into a simpler end products (Rice, 1996). In general, photocatalysis can be considered as a set of new technologies collectively known as 'Advanced Oxidation Processes' that rely on the generation of very reactive free radicals ($^{\bullet}OH$).

UV-vis parameters (UV_{254}, UV_{280}, UV_{365} and $Color_{436}$) of NHA, FHA, AHA and RHA was correlated with NHA, FHA, AHA and RHA concentrations under the non-treatment condition. Moreover, DOC concentration of NHA, FHA, AHA and RHA was presented as a function of UV-vis parameters (UV_{254}, UV_{280}, UV_{365} and $Color_{436}$) under the non-treatment condition. In addition to the non-treatment condition, the same steps were done under the treatment condition. The photocatalytic treatment was chosen as the treatment method. Equations, obtained from the correlation between UV-vis parameters (UV_{254}, UV_{280}, UV_{365} and $Color_{436}$) and HA concentrations (NHA, FHA, AHA and RHA)

as well as UV-vis parameters and DOC concentration under the non-treatment and the treatment condition (the photocatalytic treatment), were evaluated .

2. THEORETICAL BACKGROUND

2.1.Natural Organic Matter

The compositions of naturally occurring organic molecules are dominated by a relatively small number of structural moieties (such as benzene rings, aliphatic segments, hexose and pentose units, amino acids), functional groups (such as carboxyl, hydroxyl, amine), and linkages (such as ester, amide, ether) (MacCarthy, 2001a). Natural organic matter (NOM) in the environment can be broadly divided into two classes of compounds: non-humic substances (for example, polysaccharides and amino acids) and humic substances (Jones and Bryan, 1998; Davies and Ghabbour, 1998).

The content of natural organic material occurring in terrestrial environments and aquatic systems are defined as withering material from plants and animals as well as their degradation products. Total organic carbon is the most comprehensive measurement to quantify the presence of organic matter in aquatic systems and often used as synonymous to natural organic matter. The simplest characterization of natural organic matter can be based on the subdivision of total organic carbon into operationally defined fractions such as dissolved organic carbon and particule organic carbon. Dissolved organic carbon represents the organic carbon smaller than 0.45 μm in diameter whereas particulate organic carbon signifies the fraction of total organic carbon that is retained on a 0.45 μm porosity membrane. Dissolved organic carbon concentrations in water range from 0.1 mg L^{-1} in groundwater to 50 mg L^{-1} in bogs. On the other hand, particule organic carbon accounts for a minor fraction below 10 % (Thurman, 1985).

Natural organic matter includes humic substances (mainly humic and fulvic acids) and non humic materials including proteins, polysaccharides and other labile components. NOM is derived from both allochtonous (watershed or terrestrial) and autochtonous (algal or in situ) sources. Allochtonous NOM generally exhibits more of a humic signature while autochtonous NOM largely consists of algal organic matter (AOM) (Table 2.1). It is well known that AOM also exhibits some humic like material along with some lower and higher molecular size components of low UV absorptivity. Although much has been learned about

the chemical characteristics of terrestrially derived NOM, knowledge about autochtonous NOM remains limited. Algae give out anabolic products into the surrounding environment, which are known as extracellular organic matter (EOM). Cell biopolymers within the algae are known as intercellular organic matter (IOM). The EOM and IOM are together referred to as algogenic organic matter. AOM includes biopolymers such as nucleic acids, proteins, and polysaccharides (Tulonen, 2004).

Table 2.1. Acronyms of commonly used terms of organic matter in water (Thurman, 1985; Frimmel, 2000).

Acronym	**Meaning**
DOC	Dissolved organic carbon
SOC	Suspended organic carbon
POC	Particulate organic carbon
TOC	Total organic carbon
DOM	Dissolved organic matter
POM	Particulate organic matter
ROM	Recalcitrant organic matter
ROS	Refractory organic substances
SOM	Soil organic matter
CDOM	Chromophoric dissolved organic matter
EOM	Extracellular organic matter
EfOM	Effluent organic matter
IOM	Intercellular organic matter
AOM	Algal organic matter

The understanding of natural organic matter properties as a function of size, as well as the molecular weight of NOM, is a crucial factor to determine treatability of dissolved organic matter. The polydispersity of molar masses and the chemical structures comprising NOM give it a multifunctional role in natural environment and in water treatment processes. Natural organic matter in water originates basically in soil and the amount, properties and characteristics mainly depend on climate, geology and topography of the area and are also influenced by POC inputs such as runoff or algal blooms. Hence, site specific response of NOM would be expected during different stages of water treatment. It is reviewed the importance of natural organic material in water and soil while emphasizing the interactions between natural organic matter and environmental pollutants (Kördel et al., 1997).

Table 2.2. Proposed composition of NOM fractions separated using fractionation techniques (Świetlik et al., 2004).

Fraction	Organic compound class	Reference
Humic acid	Portion of humic substances precipitated at pH 1.	Peuravuori and Pihlaja,1997
Hydrophobic Acid	Soil fulvic acids, C_5–C_9 aliphatic carboxylic acids, 1- and 2-ring aromatic carboxylic acids, 1- and 2-ring phenols.	Leenheer, 1981; Aiken et al., 1992; Marhaba et al., 2000; Barber et al., 2001
Hydrophobic Base	1- and 2-ring aromatics (except pyridine), proteinaceous substances.	Leenheer, 1981; Marhabaet al., 2000; Barber et al., 2001
Hydrophobic neutral	Mixture of hydrocarbons, >C_5 aliphatic alcohols, amides, aldehydes, ketones, esters, >C_9 aliphatic carboxylic acids and amines, >3 ring aromatic carboxylic acids and amines.	Leenheer, 1981; Marhabaet al., 2000; Barber et al., 2001
Hydrophilic Acid	Mixtures of hydroxy acids, <C_5 aliphatic carboxylic acids, polyfunctional carboxylic acids.	Leenheer, 1981; Aiken et al., 1992; Marhaba et al., 2000; Barber et al., 2001
Hydrophilic Base	Pyridine, amphoteric proteinaceous material (i.e. aliphatic amino acids, amino sugars, <C_9 aliphatic amines, peptides and proteins).	Leenheer, 1981; Marhabaet al., 2000; Barber et al., 2001
Hydrophilic neutral	<C_5 aliphatic alcohols, polyfunctional alcohols, short-chain aliphatic amines, amides, aldehydes, ketones, esters, cyclic amides, polysaccharides and carbonhydrates.	Leenheer, 1981; Marhabaet al., 2000; Barber et al., 2001

The chemical properties of NOM and its role in most soil processes, such as metal complexation, cation exchange capacity and chemical weathering have been well identified (Stevenson, 1982). There are many other studies on the role, properties and characterization of natural organic matter (Frimmel, 1998; Gjessing et al., 1999a; Barrett et

al., 2000; Knabner, 2000; Nikolaou and Lekkas, 2001; Frimmel et al., 2002; Leenheer and Croue, 2003; Ritchie and Perdue, 2003; Zsolnay, 2003). The character of the organics can be explained in terms of MW, solubility, hydrophobicity, charge density and functional group composition (Edzwald, 1993; Korshin et al., 1997; Schlautman and Morgan, 1994; Vuorio et al., 1998).

NOM found in natural waters consists of both hydrophobic and hydrophilic fractions. NOM consists of three kinds of hydrophobic and hydrophilic fractions (Table 2.2). These hydrophobic fractions are hydrophobic acid, hydrophobic base and hydrophobic neutral. The hydrophilic fractions are hydrophilic acid, hydrophilic base and hydrophilic neutral. The largest fraction is generally hydrophobic acids, which make up approximately 50% of the TOC in water (Thurman, 1985).

Natural organic matter is a complex entity that comprises organic materials formed ubiquitously in surface and groundwaters (Aiken et al.,1985a; Suffet and MacCharty, 1989; Stevenson, 1994; Croue et al., 2000; Frimmel and Abbt-Braun, 2009). Dissolved organic carbon represents the dissolved portion of natural organic matter (Marhaba et al., 2000).

2.2. Dissolved Organic Carbon Content in Aquatic Environment

Dissolved organic carbon (DOC) in aquatic environments represents one of the largest active organic carbon reservoirs in the biosphere (Amon and Benner, 1996). DOC is operationally defined as the fraction of organic matter that passes through a 0.45 μm filter. While this definition of DOC has been adopted and widely used (Kalbitz et al., 2000). The use of the 0.45 μm pore size is one of convenience, and it has recently come under criticism, as being inadequate for the removal of colloidal species, and a compromise between flow rate and rejection of clay minerals (Peuravuori and Pihlaja, 1999). Nevertheless, the operational definition of DOC has remained. Other forms of organic matter present in riverine environments may also be operationally defined by particle size, including coarse particulate organic matter (CPOM, >1mm in diameter) and fine particulate organic matter (FPOM, <1mm in diameter). From a compositional perspective, DOC can be viewed as having two parts: a non-humic fraction, that consists of

known biomolecular classes of compounds, including lipids, carbohydrates, polysaccharides, amino acids, proteins, waxes and resins (Piccolo et al.,2001) and a humic fraction, which can be defined as being a category of naturally occurring, biogenic, heterogeneous organic substances that can generally be characterized as being yellow to black in colour, of high molecular weight, and refractory (MacCarthy et al.,1990). Further to this, they have been described as consisting of polyelectrolytic organic acids (Thurman, 1985; Zavarzina et al., 2002), having a wide range of molecular sizes (Thurman, 1985), and being macromolecular (Zavarzina et al., 2002).The major fraction of NOM is composed of humic substances (humic and fulvic acids) which comprise over 50% of the dissolved organic carbon (DOC), and are mainly responsible for the colour in natural waters (Fan et al., 2001).

DOM is very heterogeneous in that it contains many classes of high molecular weight organic compounds. Humic substances (HS) constitute a major portion of the dissolved organic carbon (DOC) from surface waters 50-65% (Thurman, 1985; Collins et al.,1986). They are complex mixtures of organic compounds with relatively unknown structures and chemical composition. Aquatic humic substances are polar, strawcolored, organic acids that are derived from soil humus and terrestrial and aquatic plants as defined. (Thurman and Malcolm, 1981).

2.3. Humic Substances

Humic substances are structurally polyelectrolytic, complex, dark colored organic acids that are found in sediments, soils, and natural waters. Moreover, the term humic substances is defined as the product of a heteropolycondensation of carbohydrates, proteins, fatty acids, lignins, tannins and many other materials depending on their origin (Gjessing, 1976). Humic substances are structurally complex large macromolecules, presenting a dark yellow to black appearance. They contain a core structure of phenols and phenolic acids, such as hydrobenzoic acids, vanillic acid, etc. These aromatic groups are linked together by short saturated aliphatic chains, possibly on three or four positions on the aromatic ring (Stone and Morgan, 1984; Jones and Bryan, 1998). The conformational and structural characterization of humics is extremely challenging because of their highly

heterogeneous nature. Hence, continued development of new analytical methods and approaches is required for the characterization and analysis of humic substances .

Humic substances account for 40-80% of the dissolved organic matter in water. Typical freshwater concentrations may be in the range of 1-25 mg L^{-1} expressed as dissolved organic carbon (DOC). The role of humic substances in natural aquatic systems has deserved specific attention. A variety of review papers and books exist on the principles of soil and aquatic humic substances providing detailed information on genesis, extraction, fractionation, purification, chemical properties as well as interactions with organic and inorganic species (Schnitzer and Khan, 1972; Aiken et al., 1985; Hayes et al., 1989; Senesi et al., 1991; Piccolo, 1996; Gaffney et al., 1996; Davies and Ghabbour, 1998; Frimmel, 2001; Hofrichter and Steinbüchel, 2001; MacCarthy, 2001; Senesi and Loffredo, 2001; Struyk and Sposito, 2001; Tipping, 2002; Janos, 2003). Aquatic humic substances have been shown to be precursors of THMs on chlorination and affect the transport and fate of other organic and inorganic species through complexation/partition/adsorption, catalytic and photolytic reactions (Schnitzer and Khan, 1972; Tipping, 2002).

Two general conceptual models have been discussed in literature for the formation of humic substances. The first one assumes that they are formed from the breakdown of plant materials and oxidation due to extracellular enzymes and abiotic processes. The second concept states a polymerization of simple compounds like quinones that are derived from degraded plant material. Based on their solubility properties humic substances have been classified into three fractions such as humic acid, fulvic acid and humin (Leenheer, 1981; Thurman and Malcolm, 1981; Suffet and MacCarthy, 1989). Humic acid is that fraction of humic substances that is not soluble in water under acid conditions (below pH 2), but becomes soluble at greater pH. Fulvic acid is that fraction of humic substances that is soluble under all pH conditions. Humin is that fraction of humic substances that is not soluble in water at any pH value (Aiken et al.,1985).

Humic acids and related pigments, collectively referred to as humic substances, are widely distributed in soils, natural waters, marine and lake sediments, peat, carbonaceous shales, lignites, brown coals, and miscellaneous other deposits. These constituents are best described as a series of acidic, yellow-to-black-colored polyelectrolytes that have

properties dissimilar to the biocolloids of living organisms. The current view is that they represent an extremely heterogeneous mixture of molecules, which, in any given soil or sediment, may range in molecular weight from as low as several hundred to perhaps over 300,000 (Dubach and Mehta, 1963; Flaig et al., 1975; Hayes and Swift, 1978; Schnitzer, 1978; Stevenson, 1982).

The fulvic acid fraction has a straw-yellow color at low pH values and turns to wine-red at high pH values, passing through an orange color at a pH near 3.0. There is little doubt that compounds of a nonhumic nature are present. The term fulvic acid should be reserved as a class name for the pigmented components of the acid-soluble fraction (Stevenson et al., 1985). Humin is commonly defined as the class of sedimentary humic matter that remains insoluble when sediments are treated with dilute alkali to extract the soluble humic and fulvic acids. Because of its insolubility and macromolecular nature, humin has been the least studied of all humic fractions (Hatcher et al., 1985). Molecular weight is an important criterion for defining humic substances. Soil humic substances appear to have higher molecular weights than their aquatic counterparts. Molecular weight measurements on humic substances are highly dependent on the method used, as well as pH, concentration, and ionic strength (Ghosh and Schnitzer, 1980). Humic acids have reported number average molecular weight ranges of 3000-1,000,000; fulvic acids range from 500 to 5000 in molecular weight (Stevenson, 1982). Differences between humic acids and fulvic acids can be explained by variations in molecular weight, the number of functional groups (carboxyl and phenolic OH) and the extent of polymerization. In general, fulvic acids have lower molecular weights than humic acids. It is also known that soil derived humic materials are larger than aquatic humic substances (Gaffney et al., 1996).

Humic acids are thought to be complex aromatic macromolecules with amino acids, amino sugars, peptides, aliphatic compounds involved in linkages between the aromatic groups. They can not be regarded as single chemical entities described by unique, chemically defined molecular structures. However, generic structural models of humic and fulvic acids have been proposed in literature on the basis of available compositional, structural and functional data (Schnitzer and Khan, 1972; Stevenson, 1982; Buffle, 1988; Hofrichter and Steinbüchel, 2001).

The hypothetical structure for humic acid as shown in Figure 2.1 consists of side aliphatic chains and a hydrophobic aromatic core that is highly substituted with functional groups such as free and bound phenolic OH groups, quinone structures, nitrogen and oxygen as bridge units and COOH groups. The model features both hydrophilic and hydrophobic sites, a highly polyelectrolytic character and several sites potentially available to bind with metal ions, mineral surfaces and organic compounds.

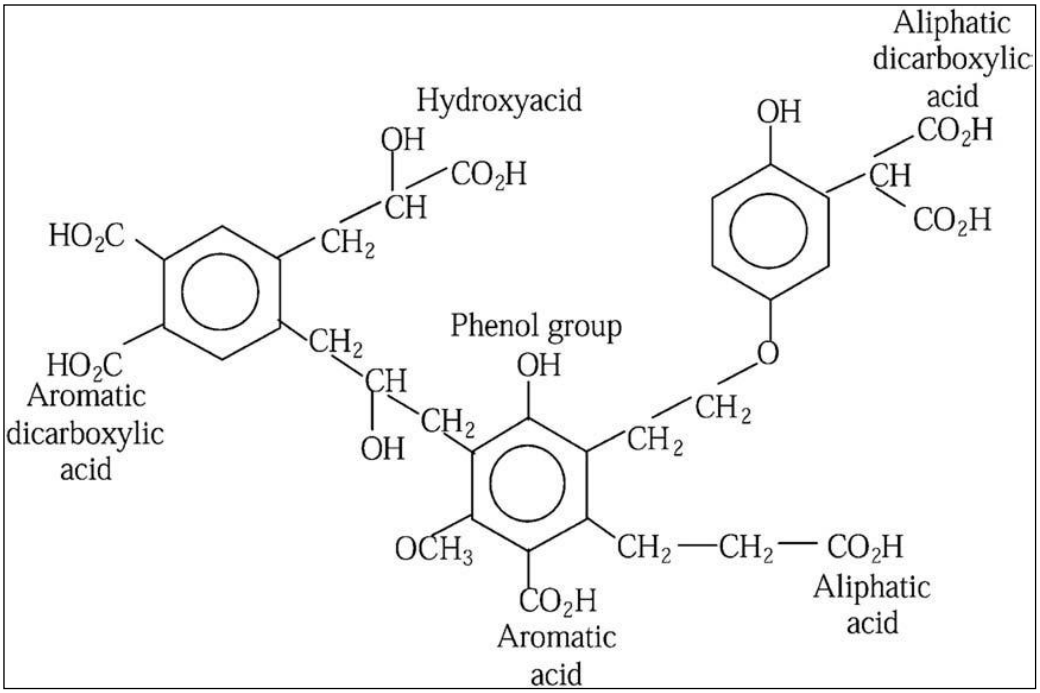

Figure 2.1. Hypothetical molecular structure of humic acid (Duan and Gregory, 2003).

The structure and composition of humic acids are apparently more complex than those of fulvic acids (Duan and Gregory, 2003). The greater water solubility of fulvic acids compared to humic acids can be attributed to the higher content of polar groups, particularly carboxyl groups. Among the other functional groups present in smaller quantities are ether, aldehyde and amine (Figure 2.1).

The model structure of fulvic acid contains both aliphatic and aromatic structures, both extensively substituted with oxygen-containing functional groups (Figure 2.2). However, the structures of fulvic acid are more aliphatic and less aromatic than humic acids. The reason for their high solubility in water at all pH values is mainly due to the

presence of carboxylic acid, phenolic and ketonic groups in appreciable amounts (MacCarthy, 2001b).

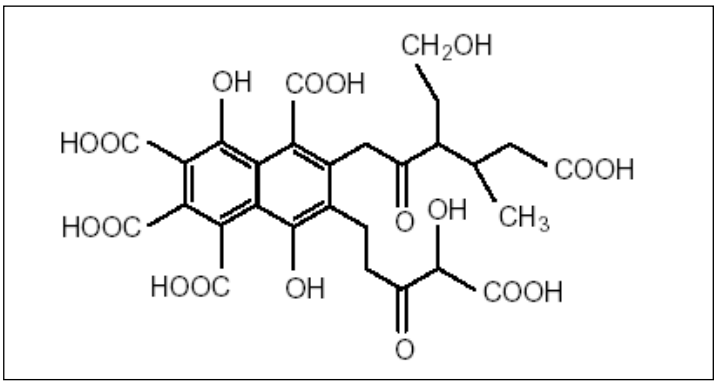

Figure 2.2. Structure of fulvic acid (Buffle, 1988).

Fulvic acids are more soluble, smaller in average molecular weight, and more highly charged than humic acids. Fulvic acids also typically have higher oxygen content, with higher carboxylic acid (COOH) and lower aromatic hydroxyl (ArOH) content than humic acids (Hayes et al., 1989). It was concluded that fulvic acids consist in part of phenolic and benzenecarboxylic acids, held together through hydrogen bonds to form a polymeric structure of considerable stability (Schnitzer and Khan, 1972). A model structure of fulvic acid contains aromatic and aliphatic components extensively substituted with oxygen-containing functional groups. Both structures show an abundance of COOH groups (Buffle et al., 1977).

Despite the heterogeneity of HS, many similarities can also be found in samples from different sources. The elemental composition of humic and fulvic acids from various sources seems to be similar, although the function may vary greatly (MacCarthy, 2001b). The complex polymeric nature and interaction between component chains of humic material make structural analysis difficult; however, compositional information can be obtained from elemental and functional group analysis in Table 2.3.

Table 2.3. Elemental analysis ranges for soil humic and fulvic acids (Schnitzer and Khan, 1972).

	Humic acid	Fulvic acid
Element, wt%		
C	53.6-58.7	40.7-50.6
H	3.2-6.2	3.8-7.0
N	0.8-5.5	0.9-3.3
O	32.8-38.3	39.7-49.8
S	0.1-1.5	0.1-3.6
Functional group*		
Total acidic groups	5.6-8.9	6.4-14.2
Carboxyl, COOH	1.5-5.7	5.2-11.2
Phenolic OH	2.1-5.7	0.3-5.7
Alcoholic OH	0.2-4.9	2.6-9.5
Quinoid/keto, C=O	0.1-5.6	0.3-3.1
Methoxy, OCH_3	0.3-0.8	0.3-1.2

*mequiv g^{-1}equivalentto mmol of each group per g of humic substances.

The elemental analysis of humic and fulvic acids from a range of soils show that the atomic H/C ratio is quite low, and is lower for humic acid than fulvic acid, which is consistent with a higher aromatic content for humic acid (Schnitzer and Khan, 1972). The atomic O/C ratio is also lower for humic acid than fulvic acid, reflecting the higher content of polar groups in fulvic acid. Oxygen is the major heteroatom in humic substances and occurs predominantly in the following functional groups: COOH, phenolic and alcoholic OH, ketonic and quinoid C=O, and OCH_3 (ether and ester).The estimated abundances of these groups in soil humic and fulvic acids are given in Table 2.3 (Schnitzer and Khan, 1972). Depending on the pH of the solution functional groups in humic molecule they are dissociated or protonated. Dissociated functional groups carry negative charges. Electrostatic repulsions between neighboring negatively charged sites causes stretching of themolecule. Furthermore, the electrostatic forces are influenced by ionic strength, by the presence of cationic species etc. (Ghosh and Schnitzer, 1980). It was reported that humic molecules can change from a large, flexible and linear shape at high pH, low ionic strength ana low humic concentration, to a small, rigid and spherocolloidal conformation at low pH, high ionic strength and high humic concentration (Ghosh and Schnitzer, 1980).

2.4. Spectroscopic Characterization of Humic Substances

2.4.1. UV-vis Spectroscopy

Generally, ultraviolet-visible spectroscopy corresponds to electronic excitations between the energy levels that equivalent to the molecular orbitals of the systems (UV=200-400 nm, visible= 400-800 nm). For a molecule, this is a process where electrons are promoted from their electronic ground state to an excited electronic state. As a result, energetically favored electron promotion will be from the highest occupied molecular orbital (HOMO) to the lowest unoccupied molecular orbital (LUMO). The electronic structure of a molecule determines its UV light absorbance. Therefore, the UV spectrum indicates the existence of specific bonding arrangements in the molecule. Different electronic excitation that can occur in organic molecules by UV light absorption was demonstrated in (Skoog and Lineary, 1992).

Organic compounds that are aromatic or that have conjugated double bounds absorb light in the ultraviolet (UV) wavelength region. UV absorbance is a good technique for measuring the presence of naturally occuring organic matter, such as humic substances, because they contain aromatic moieties and are the dominant form of organic matter in natural waters (Schnitzer et al., 1972; Alberts et al., 1982). Statictically significant regressions was found between UV absorbance and TOC concentration for several river waters, both raw and treated (Dobbs et al., 1972; Smart et al., 1976). Spectroscopic measurements in various regions of the electromagnetic spectrum provide information about functionality of humic substances. Many of the spectroscopic methods are often limited when applied to HS. This is because the spectra of HS represent the summation of a whole mixture of compounds and in otherwords are the response of many different functional groups.

UV-vis spectra of humic substances are featureless with absorption increasing at lower wavelengths and contain no discrete absorption bands due to the overlapping of the broad absorption bands of the chromophores. The absorption in the UV region is mainly caused by the excitation of electron lone pair, usually oxygen ($n \rightarrow \pi^*$) and by conjugated C = C double bonds ($\pi \rightarrow \pi^*$). The absorption in the visible region is caused by lone pair

electrons and charge-transfer systems. The absorbance decreases as the wavelength increases which is typical for humic substances (Schnitzer and Khan, 1972; Stevenson, 1982). A slight maximum could be indicated at approximately 275 nm, which is probably due to quinone structure (Schnitzer and Khan, 1972). The spectral absorption exhibits a dependence on pH values (Chen et al., 1977; Langhals et al., 2000) with decreasing absorbance as solution pH decreases. This dependence reflects the acid-base forms of the chromophores within the molecules or, as suggested, an increase in particle size due to macromolecular associations is expected (Chen et al.,1977). UV-vis light absorption of humic substances appears to increase with increase in degree of condensation of aromatic rings, total C content, molecular weight and ratio of C in aromatic rings to C in aliphatic side chains (Senesi and Loffredo, 2001).

In general, light absorbance of humic substances in the water will increase with the degree of aromatic rings in the humic substances, the ratio of carbon in aromatic nuclei to carbon in aliphatic or alicyclic side chains, the total carbon contents in the water, and the molecular weights of the humic acids (Choudhry, 1984). Although the UV-vis spectra of HS have little structure, there is a useful application for determining the absorption at distinct wavelengths. A number of UV–vis absorption ratios have been measured to provide information about the state of humification and content of humic material in the DOC.

Absorbances at 254 nm (UV_{254}) and 436 nm ($Color_{436}$) are generally used for the quantification of humic substances. UV_{254} is interchangeably measured with TOC as a surrogate parameter to represent the natural organic matter content in natural waters (Najm et al., 1994).The UV absorptivity at 280 nm was also introduced to represent total aromaticity, because, $\pi \rightarrow \pi^*$ electron transition occurs in this UV region (ca. 270-280 nm) for phenolic arenes, benzoic acids, aniline derivatives, polyenes and polycyclic aromatic hydrocarbons with two or more rings (Traina et al., 1990; Chin et al., 1994). UV_{365} represents the molecular weight and aromaticity in humic acids (Peuravuori and Pihlaja, 1997). $Colour_{436}$ expresses the colour forming moieties that are the chromophoric groups containing conjugated double bond systems (delocalised electrons) and heteroatoms with lone pair of electrons like O, N and S (Bekbolet et al.,2002). It was suggested using the absorption at 203 nm which is the absorption band for benzonoid compounds (generally

referred to as the benzoid band) and 253 nm which is the absorption band attributed to charge-transfer transition (CT) (Korshin et al.,1997). Those wavelengths were used for an estimation of the degree of functionality of the aromatic ring. While the strength of the benzoid band stays relatively constant upon changes in the functionality of the aromatic ring, charge transfer band is strongly altered. Therefore, change in the ratio of these wavelenghts was considered to be indicative of alterations in the functionality of the aromatic system. The ratio of the UV/vis absorption at 254 nm to that at 203 nm was used in a recent study (Kumke et al.,2001).Various absorption wavelengths at 250, 254, 270, 280, 300, 365, 400, 436 and 465 nm as well as ratios like E_2/E_3 (Abs_{250}/Abs_{365}), E_3/E_4 (Abs_{300}/Abs_{400}) and E_4/E_6 (Abs_{465}/Abs_{665}) have also been cited in literature for the spectral differentiation of humic substances (Chen et al., 1977; De Haan et al., 1982; Stevenson, 1982; Buffle et al., 1982; Bloom and Leenheer, 1989; Hayes et al., 1989; Traina et al., 1990; Wang et al., 1990; Chin et al., 1994; Peuravuori and Pihlaja, 1997b; Chen et al., 2002; Abbt-Braun and Frimmel, 2002). However, they usually served as additional indexes characterizing humic materials (Choudhry, 1981). A summary of related data compiled from literature is presented in Table 2.4.

Irrespective of what proportion of the humic molecules contribute to the absorbance at a particular wavelength, the UV-visible spectroscopy does have many useful applications (Table 2.4) for purposes other than determining functionality in humic substance research. Chromophores responsible for the absorbance consist of conjugated double bonds and unbonded electrons like those associated with oxygen, sulphur, and halogen atoms (MacCarthy and Rice, 1985). Absorbance is probably mainly due to the aromatic ring structure (Bloom and Leenheer, 1989). Also internal vibration and rotation of the molecules and intermolecular interactions affect the spectra (Korshin et al., 1997). Absorbance increases with pH, aromaticity, total C-content and molecular weight (Chen et al., 1977). In general, it is showed that UV absorption is a good indicator of the unsaturated C content of samples and that it can be used as a fast, simple and sensitive method for molecular characterization (Table 2.4). Therefore, the absorption spectra with reference to the selective wavelengths exhibit structural information as well as DOC content.

Table 2.4. UV-vis spectroscopic characterization of aquatic humic substances (Hautala et al., 2000).

Wavelength, nm	Correlative characteristics	References
250, 330, 350	DOC, TOC	De Haan et al.,1982; Moore, 1985
285	DOC	Buffle et al., 1982
254	DOC, TOC, COD, BOD	Mrkva, 1983; Reynolds and Ahmad, 1997
272, 280	Aromaticity, molecular weight	Trainaet al., 1990; Chin et al., 1994; Li et al., 1998
250/365 (E_2/E_3)	Aromaticity, molecular weight	Peuravuori and Pihlaja, 1997
465/665 (E_4/E_6)	Humification, molecular weight, condensation of aromatic carbon	Bloom and Leenheer, 1989; Stevenson, 1982; Chen et al., 1977

Humic waters are yellow-brown and a raw regression exists between the darkness of water and its humus content. Thus, measuring the colour of water is largely accepted as an easy way to estimate the humus content in natural waters. Molecular weight and aggregation of humic matter are positively correlated with colour (Wang et al., 1990), and it has been also noted that colour increases with increasing pH (Packham, 1964). Various wavelengths have been proposed for measuring the colour of humic water with spectrophotometer: 410 or 450-465 nm (Hongve and Akesson, 1996), 456 nm (Bennett and Drikas, 1993) and 465 nm (Stevenson, 1982). SUVA values offer a simple characterization of the nature of the NOM based on measurements of UV absorbance and DOC. The ratio of the UV absorbance at 254 nm (UV_{254}) with the DOC content, provides an estimate of the abundance of UV absorbing species, and may also be used for comparison of the aromaticity of various humic materials (Kronberg et al., 1999).

$$SUVA_{254} = UV_{254}\ (cm^{-1}) * 100 / DOC\ (mg\ L^{-1}) \quad (2.1)$$

SUVA value is achieved as UV_{254} absorbance divided by the TOC concentration (Equation 2.1). High SUVA value indicates that the organic matter is composed largely of hydrophobic, high molar mass (HMM) organic material, in comparison of low SUVA

value which means that water includes mainly organic compounds which are hydrophilic, low molar mass (LMM) and low in charge density (Edzwald and Tobiason, 1999; Sharp et al., 2006 a,b).

The assumption that humic substances are polymers has promulgated the use of simple physical-chemical measurements to characterize humic substances, such as the E_4/E_6 ratio (Etelka et al., 1999). Frequently, the E_4/E_6 (absorbance at 465 nm and 665 nm) ratio and E_2/E_3 (ratio of absorbances at 250 nm and 365 nm) are used to indicate an inverse relationship with progressive humification and increased condensation, or molecular weight (De Lourdes et al., 2002). The spectroscopic ratios calculated for the different types of humic substances show differences depending on their source. The quotient E_{250}/E_{365}, which is a property of aquatic humic substances, increases as the aromaticity and molecular size decreases (Peuravuori et al., 1997b). The ratio of E_{254}/E_{436} gives a good impression about the intensity of the UV absorbing functional groups compared to the colored ones (Battin, 1998). Normalization of absorbance to TOC defined as specific absorbance value (SUVA) is very useful for comparing different samples. It was also reported that a plot of the specific absorption in the visible range ($Color_{436}$/DOC) against the specific absorption in the UV range (UV_{254}/DOC) exhibit higher values for HA fractions for both the UV and visible range than that of FA fractions. This result indicates that the double bond density is related to the hydrophobic character (Abbt-Braun et al., 2004).

2.5. Advanced Oxidation Process

Advanced oxidation process are used to oxidize complex organic constituents found in wastewater that are difficult to degrade biologically into a simpler end products. When chemical oxidation is used, it may not be necessary to oxidize completely a given compound or group of compounds. In many cases, partial oxidation is sufficient to render specific compounds more amenable to subsequent biological treatment or to reduce their toxicity. The oxidation of specific compounds may be characterized by the extent of degradation of the final oxidation products as follows (Tchobanoglous et al., 2003):

1. Primary degradation. A structural change in the parent compound.

2. Acceptable degradation (defusing). A structural change in the parent compound to the extent taht toxicity is reduced.
3. Ultimate degradation (mineralization). Conversion of organic carbon to inorganic CO_2.
4. Unacceptable degradation (fusing). A structural change in the parent compound resulting in increased toxicity.

Advanced oxidation processes typically involve the generation and use of the hydroxyl free radical ($HO^{\bullet}$) as a strong oxidant to destroy compounds that cannot be oxidized by conventional oxidants such as oxygen, ozone, and chlorine. The hyroxyl radicals reacts with the dissolved constituents, initiating a series of oxidation reactions until the constituents are completely mineralized. Nonselective in their mode of attack and able to operate at normal temperature and pressures, hyroxyl radicals are capable of oxidizing almost all reduced materials present without restriction to specific classes or groups of compounds, as compared to other oxidants.

Advanced oxidation processes differ from the other treatment processes discussed (such as ion exhange or stripping) because wastewater compounds are degraded rather than concentrated or transferred into a different phase. Because secondary waste materials are not generated, there is no need to dispose of or regenerate materials.

2.5.1. Oxidation of Refractory Organic Compounds

For the reasons cited above hyroxyl radicals are not used for conventional disinfection: instead they are used more commonly for the oxidation of trace amounts of refractory organic compounds found in highly treated effluents. The hyroxyl radicals, once generated, can attack organic molecules by radical addition, hyrogen abstraction, electron transfer, radical combination (Tchobanoglous et al., 2003).

i. By radical addition. The addition of the hyroxyl radical to an unsaturated aliphatic or aromatic organic compound (C_6H_6) results in the production of a radical organic compound that can be oxidized further by compounds such as oxygen or ferrous

iron to produce stable oxidized end products. In the following reactions the abbreviation R is used to denote the reacting organic compound.

$$R + HO^{\bullet} \rightarrow \quad ROH \qquad (2.2)$$

ii. By hydrogen abstraction. The hydroxyl radical can be used to remove a hydrogen atom from organic compounds. The removal of a hydrogen atom results in the formation of a radical organic compound, initiating a chain reaction where the radical organic compound reacts with oxygen, producing a peroxyl radical, which can react with another organic compound, and so on.

$$R + HO^{\bullet} \rightarrow \quad R^{\bullet} + H_2O \qquad (2.3)$$

iii. By electron transfer. Electron transfer results in the formation of ions of a higher valence. Oxidation of a monovalent negative ion will result in the formation of an atom or a free radical.

$$R^n + HO^{\bullet} \rightarrow \quad R^{n-1} + OH^- \qquad (2.4)$$

iv. By radical combination. Two radicals can be combine to form a stable product.

$$HO^{\bullet} + HO^{\bullet} \rightarrow \quad H_2O_2 \qquad (2.5)$$

In general, the reaction of hyroxyl radicals with organic compounds, at completion, will produce water, carbon dioxide, and salts; this process is also known as minera. Photocatalytic oxidation process is the one of the advanced oxidation processes, that is applied for the treatment of organic matters. Photocatalysis has been continuously developed as a promising alternative technology for environment purification (Hoffmann et al., 1995; Hermann, 1999; Zhang and Wang, 2005).

2.5.2. Photocatalytic Oxidation Process

In general, photocatalysis can be considered as a set of new technologies collectively known as “Advanced Oxidation Processes” that rely on the generation of very reactive free radicals (e.g. $^{\bullet}OH$). Those reactive species are subsequently used to degrade the organic

pollutants or microorganisms. The principles underpinning photocatalysis and its environmental applications have been reviewed extensively since 1985 (Ollis, 1985; Serpone and Pelizzetti, 1989; Ollis et al., 1991; Fox and Dulay, 1993; Legrini et al., 1993; Hoffmann et al., 1995; Rajeshwar, 1995; Mills and Le Hunte, 1997; Herrmann**,** 1999; Blake, 2001; Bhatkhande et al., 2002; Bahnemann, 2004; Emeline et al., 2005).

Heterogeneous photocatalytic process relies on utilizing the near UV radiation to photoexcite a semiconductor catalyst in the presence of oxygen. Under these circumstances oxidizing species, either bound hydroxyl radical or free holes are generated. The process is heterogeneous in nature since two active phases; solid and liquid are involved during the reaction sequence. Many semiconducting oxides as catalysts have been tested, although TiO_2 in the anatase form performed the most interesting and efficient features, such as high stability, good performance, ready availability, low toxicity and low cost (Rajeshwar, 1995). The optical absorption of TiO_2 in the near UV region is the major advantage of the photocatalytic method over UV-C driven AOPs (O_3/UV, H_2O_2/UV) that require light of shorter wavelengths (λ<300 nm) and hence can not make use of a part of solar irradiation. A simplified TiO_2, photocatalytic mechanism is summarized in Figure 2.3.

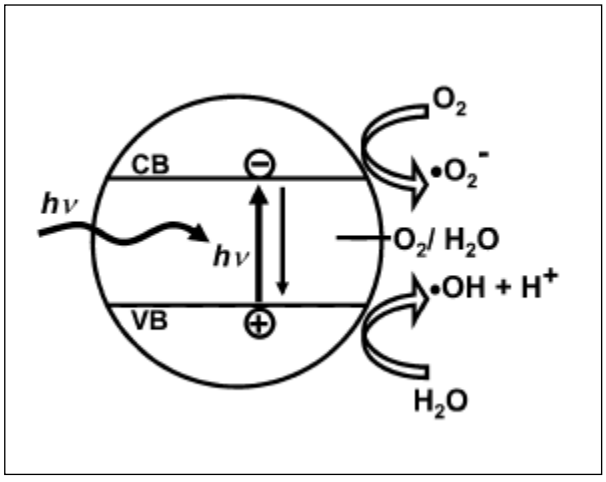

Figure 2.3. The simplified TiO_2, photocatalytic mechanism

Continuous band-gap irradiation (Ebg is 3.2eV (390 nm) in anatase and 3.05 eV (420 nm) in rutile) of an aqueous semiconductor dispers ion excites an electron from the valenceband (VB) to the conduction band (CB), creating an electron-hole pair. TiO_2 is only

active in the ultraviolet region which is < 10% of the overall solar intensity. The formation of redox pair could either be followed by respective reactions or a recombination reaction resulting in the dissipation of the reactive species (Equations 2.6-2.7).

i. Formation of redox pair through light absorption ($E_{hv}>E_{bg}$):

$$TiO_2 + hv\ (UV) \rightarrow TiO_2\ (e^-_{CB} + h^+_{VB}) \quad (2.6)$$

ii. Direct recombination reaction leading to the inactivation of the electron hole pair:

$$TiO_2\ (e^-_{CB} + h^+_{VB}) \rightarrow TiO_2 + \text{heat} \quad (2.7)$$

iii. Photogenerated holes (h^+_{VB}) may directly oxidize the organic substrate, S (organic substrate) anchored to the oxide surface. The principal hole traps are adsorbed H_2O molecules and OH^- forming $HO^\bullet$ radicals. The $HO^\bullet_{(s)}$ radicals adsorbed on the semiconductor surface are the prominent reactive species due to their high oxidant power (E= +2.80 V) and possible competing reaction leads to the formation of hydrogen peroxide. (S: organicsubstrate).

$$h^+_{VB} + S \rightarrow S^{\bullet+} \quad (2.8)$$

$$h^+_{VB} + H_2O \rightarrow HO^\bullet + H^+ \quad (2.9)$$

$$h^+_{VB} + OH^- \rightarrow HO^\bullet \quad (2.10)$$

$$HO^\bullet + HO^\bullet \rightarrow H_2O_2 \quad (2.11)$$

iv. On the other hand, in the presence of electron scavengers (i.e. O_2) reduction reactions may take place leading to the following sequence of the reactions:

$$e^-_{CB} + O_2 \rightarrow O_2^{\bullet-} \quad (2.12)$$

$$e^-_{CB} + H_2O_2 \rightarrow OH^- + HO^\bullet \quad (2.13)$$

$$O_2^{\bullet-} + H^+ \rightarrow HO_2^\bullet \quad (2.14)$$

$$O_2^{\bullet-} + HO_2^\bullet \rightarrow HO_2^- + O_2 \quad (2.15)$$

$$HO_2^\bullet + HO_2^\bullet \rightarrow O_2 + H_2O_2 \quad (2.16)$$

$$H_2O_2 \leftrightarrow HO_2^- + H^+ \qquad pK_a=11.6 \quad (2.17)$$

$$HO^\bullet + HO_2^\bullet \rightarrow H_2O + O_2 \quad (2.18)$$

Heterogeneous photocatalytic process takes place through a complex sequence of reactions. The relevant reactions at the TiO_2 surface causing the degradation of the organic compounds could be outlined by Equations (2.6)-(2.18).

Hydroxyl radicals are created from water when UV light is absorbed by the titanium dioxide layer. The energy causes electrons to move to the conduction band of the TiO_2. The positive holes remaining in the valance band can accept electrons from molecules. A •OOH radical is formed from the reduction of the dissolved oxygen in the aqueous solution combining with a hydroxyl radical.

2.5.3. Photocatalyst Type

A semiconductor comprises a manifold of electron energy levels filled with electrons called the valence band, and at a higher energy, a manifold of largely vacant electron energy levels called the conduction band. Although there are many semiconducting materials in this world (e.g., ZnO, SnO_2, WO_3, CdS, and ZnS), TiO_2 has been by far the most popular photocatalyst due to its superior features (Rajeshwar, 1995).

2.5.4. Light Intensity

The key to semiconductor-induced reactions is the light source that will emit photons at the optimum wavelength for excitation of valence band electrons, an optimum that varies between semiconductors (Serpone and Pelizzetti, 1989). To excite titanium dioxide's valence band electrons, a light source must have a wavelength shorter than 387.5 nm to overcome the band-gap energy. Medium-pressure ultraviolet lamps provide the most effective source of photons for titanium dioxide systems emitting wavelengths concentrated in the 200 to 400 nm range. Wavelengths shorter than 387.5 nm are emitted by the sun but in a much less concentrated and consistent manner, making the utilization of solar energy possible but much less advantageous than artificial sources (Legrini et al., 1993).

Most bench-scale ultraviolet/titanium dioxide systems utilize suspensions of titanium dioxide particles and are operated in batch mode. These systems are an effective means to screen contaminant species for UV/TiO_2 applicability, to determine specific reaction rate

constants, and to optimize operating conditions such as contaminant concentration, TiO_2 loading, and use of oxidant. However, the suspended titanium dioxide must be recovered from the effluent via centrifuge, filtration, or coagulation and flocculation, none of which are applicable at a larger scale (Hoffmann et al., 1995). An industrially applicable UV/TiO_2 system will have to immobilize titanium dioxide particles to avoid expensive recovery and resuspension mechanisms.

In most of the laboratory scale studies, only the light source output energy was indicated although some of the papers reported the light intensities determined by actino metric measurements in terms of absorbed photons $time^{-1}$ (minuteorsecond) or Einstein $time^{-1}$ (minuteorsecond). Solar photocatalysis wasdemonstrated by expressing solar photon flow, as $1.51x10^{-6}$ mol s^{-1}, based on the value of 0.38 mol/(m^2 h) photons from the Sun on Earth's surface for $\lambda<400$ nm. The kinetic evaluation of the degradation of the dissolved natural organic matter was achieved by photonic efficiency assuming an average molar mass of 1200 g mol^{-1} (Ljubas, 2005).

A remarkable research study was reported on the sensitized degradation of humic acids on TiO_2 under visible light ($\lambda> 420$ nm) irradiation (Cho and Choi, 2002). The photolysis rates were found to be strongly influenced by pH due to the pH-dependent adsorption of humic acids on TiO_2 with the maximum rate observed under acidic conditions (pH ~ 3). Reduction in the UV–visible absorbance and fluorescence emission (λ_{ex}= 350 nm) of humic acids was observed during the irradiation. A plausible explanation was set forward that humic acids acting as a sensitizer for injecting electrons from their excited state to the conduction band of TiO_2 were subsequently transformed and decolorized through a series ofelectron transfer reactions. However, the dissolved organic carbon (DOC) of humic acid solutions remained almost unchanged under visible light while the UV-irradiation was able to remove part of the total DOC.

Chromophoric groups in humic molecules may absorb radiation in the UV-vis region leading to degradation via direct photochemical route. Since the lower wavelength limit for solar radiation reaching the surface of the earth is approximately 300 nm, only chromophores that absorb radiation of 300 nm or greater would undergo transitions to excited states. Aromatic and heteroaromatic functional groups, and conjugated polyenes

and carbonyl groups undergo π - π* and n- π * transitions at these wavelengths; most other functional groups commonly present in NOM absorb at wavelengths shorter than 300 nm and are, therefore, inactive (Brown, 1999). On the other hand, in the case of UV light source (λ= 253.7 nm), direct photolytic degradation of humic is also expected as a result of competitive and consecutive radical pathways. NOM may also undergo photochemical reactions by indirect processes in which photo-activated organic or inorganic species react with unactivated molecules (Goldstone et al., 2002; Faust, 1999; Larson and Marley, 1999; Zafiriou et al., 1984). Tay and co-workers performed photocatalytic degradation experiments using 15 W low pressure Hg UV lamps with a major emission at 253.7 nm (Tay et al., 2001). The light intensity in the system was subjected to variation in the range of $1.31x10^{-4}$ to $6.70x10^{-5}$ Einstein min^{-1} and an enhancement in the degradation rate as expressed by both $Color_{400}$ and TOC was assessed in relation to the increased light intensity.

Considering the well defined kinetic model of (Serpone et al., 1992), it would be more appropriate to express the role of light intensity in terms of quantified light energy terms in the reaction medium. On the other hand, several research results cover the modeling of light intensity in relation to the reactor geometry thereby revealing the significance of the effect (Cassano et al., 1995; Cassano and Alfano, 2000).

The use of exact terminology for the assessment of the light intensity effects on photocatalysis was explained in detail by two major reports of IUPAC Commission. Considering the importance of removal efficiencies, it would be more appropriate to refer to these reports for the evaluation of the light effects (Serpone and Salinaro, 1999 and Salinaro et al., 1999). On the other hand, the incorporation of light intensity into the kinetic modeling would provide a comparative basis for simplicity purposes (Turchi and Ollis, 1990; Mills and Moris, 1993, Meng et al., 2002).

2.5.5. pH and Adsorption Effects

Due to the surface oriented nature of photocatalysis, adsorption of humic acids onto TiO_2 should also be considered as an effective parameter for the efficiency of degradation. It was considered initial adsorption effects on the degradation rate of humic acids in relation to pH temperature and light intensity conditions (Palmer et al., 2002). It was

reported the adsorption effects by DRIFT spectroscopy indicating that at acidic pH, humic acids were adsorbed on TiO_2 mainly as carboxylate surface groups (Wiszniowski et al., 2002).

2.6. Characterization and Quantification Parameters of Natural Organic Matter and Humic Acids

AHA was presented as a function of $Color_{436}$ parameter and TOC concentration, corresponding to AHA, was determined by TOC analyzer during the photocatalytic treatment (Zhang et al., 2009). AHA, studied in range of 10-100 mg L^{-1}, was presented as a function of UV_{254} parameter during the photocatalytic treatment. Moreover, UV_{350} parameter and $Color_{436}$ parameter, was determined by using the photocatalytic treatment (Tsimas et al., 2009). 10 mg L^{-1} of AHA, was presented as a function of UV_{254} parameter and UV_{280} parameter and $Color_{455}$ parameter were determined by UV-vis spectrophotometer during the photocatalytic treatment (Portjanskaja et al., 2009). TOC concentration, corresponding to AHA, was determined by TOC analyzerand UV-vis parameter was determined by UV-vis spectrophotometer, during the photocatalytic treatment (Gomes et al., 2009). The removal of TOC concentration (8.4 mg L^{-1}) and the removal of UV_{254} parameter (0.69 cm^{-1}) were determined by using TOC analyzer and UV-vis spectrophotometer (Selcuk and Bekbolet, 2008). 10 mg L^{-1} of AHA was presented as a function of UV_{254} parameter during the photocatalytic treatment. Moreover, $Color_{455}$ parameter was determined by using UV-vis spectrophotometer (Portjanskaja et al., 2006).UV_{254}, UV_{280} and $Color_{436}$ parameter, corresponding to AHA concentration, were determined by Kerc et al., 2003a and Kerc et al., 2003b during the photocatalytic treatment. UV_{254} parameter, corresponding to AHA, was determined UV-vis spectrophotometer (Palmer et al., 2002). TOC concentration of AHA, studied in range of 5 and 50 mg L^{-1}, was determined by TOC analyzer (Minero et al., 1999). AHA, studied in range of 7 and 10 mg L^{-1}, was presented as a function of Abs_{465} during the photocatalytic treatment (Tsarenko et al., 2006). TOC concentration of AHA was determined during the photocatalytic treatment. Moreover, $Color_{436}$, $Color_{400}$, UV_{365}, UV_{300}, UV_{280}, and UV_{254} parameter was determined during the photocatalytic treatment (Uyguner andBekbolet, 2005b).

Table 2.5.Substrate specification in relation to the reaction conditions during photocatalytic treatment of natural organic matter (Table 3.,Uyguner-Demirel and Bekbolet, 2011).

Table 3
Substrate specification in relation to the reaction conditions during photocatalytic treatment of natural organic matter.

NOM model compounds	Reactor type/irradiation source	Filter type, pore size, material	Parameter	References
Humic acid, Aldrich, 50 mg L^{-1}	TiO_2 nanowire, TiO_2 Degussa P-25, batch reactor, low pressure Hg lamp, 254 nm, 2000 W cm^{-2}	0.20 μm microfiltration membrane, Advantec MFS, Inc.	Absorbance at 436 nm, TOC $HA_{conc} = Color_{436}$ First order kinetics	Zhang et al. (2009)
Humic acid, Aldrich, 10–100 mg L^{-1} 1 M NaOH pH = 3	TiO_2 Degussa P-25, batch type, laboratory scale photoreactor, UV-A irradiation, 9 W (Radium Ralutec), 350–400 nm, $I_o = 4.69 \times 10^{-6}$ E s^{-1}	0.45 μm disposable filter	Absorbance at 254 nm, 350 nm and 436 nm No kinetics $HA_{conc} = UV_{254}$	Tsimas et al. (2009)
Humic acid, Aldrich, 10 mg L^{-1}	Immobilized TiO_2 Degussa P-25 attached to buoyant hollow glass microspheres, anode oxidized titanium and titanium dioxide doped with sulfur and boron atoms attached to various supports, low-pressure luminescent mercury UV-lamp (Phillips TLD), 360 nm, $I_o = 0.7$ mW cm^{-2}	Filtration is indicated as a means of separation of the buoyant micro spheres	Absorbance at 455 nm, 280 nm, and 254 nm $HA_{conc} = UV_{254}$	Portjanskaja et al. (2009)
Humic acid, Aldrich, 6.9 mg L^{-1}	TiO_2 Degussa P-25, TiO_2 coated on a paper matrix type NW10 Ahlstrom paper, compound parabolic collectors, UV-A lamp (Radium Suprablack, HBT), 125 W	No information was provided	TOC, UV–vis and other parameters *i.e.*, pH, temperature, dissolved oxygen and conductivity	Gomes et al. (2009)
Humic acid, Aldrich, TOC = 8.4 mg L^{-1} $UV_{254} = 0.69$ cm^{-1}	Thin film electrodes coated with titanium, Oriel model 6262, 450 W Xe-Hg arc lamp, $I_o = 18.6$ and 100 mW cm^{-2}		TOC, UV_{254} no kinetics	Selcuk and Bekbolet (2008)
Humic acid, Aldrich, 10 mg L^{-1}	TiO_2 Degussa P-25 and immobilized TiO_2 attached to buoyant hollow glass microspheres, batch reactors, low-pressure luminescent mercury UV lamp (Phillips TLD), 360 nm, $I_o = 0.7$ mW cm^{-2}	Filtration with a membrane filter, no information was provided	Absorbance at 455 nm and 254 nm $HA_{conc} = UV_{254}$	Portjanskaja et al. (2006)
Humic acid, Aldrich	TiO_2 Degussa P-25, batch reactor, BLF, 365 nm, 125 W	0.45 μm cellulose acetate membrane, Millipore	UV_{254}, UV_{280}, $Color_{436}$ First order kinetics	Kerc et al. (2003a)
Humic acid, Aldrich	TiO_2 Degussa P-25, batch reactor, BLF, 365 nm, 125 W, $I_o = 2.84 \times 10^{-6}$ E min^{-1}	0.45 μm cellulose acetate membrane, Millipore	UV_{254}, UV_{280}, $Color_{436}$ First order kinetics	Kerc et al. (2003b)
Humic acid, Aldrich, DOC = 5–40 mg L^{-1}	TiO_2 Degussa P-25, batch reactor, medium pressure mercury lamp, 365 nm, 250 W	0.22 μm pore size filter	UV_{254}, DOC, CO_2 HPSEC First order kinetics	Palmer et al. (2002)
Humic acid, Aldrich, 100 mg L^{-1} pH = 1.9–11	TiO_2 Degussa P-25, Solar box Atlas Suntest CPS+, Vapor Xenon lamp, 300 nm < λ < 800 nm	0.45 μm cellulose nitrate membrane, Whatman	TOC, BOD_5	Wiszniowski et al. (2002)
Humic acid, Aldrich, 5–50 mg L^{-1}	TiO_2 Degussa P-25, cylindrical Pyrex glass cells, Solar box,1500 watt Xenon lamp simulating AMI solar light with a 340 nm cut off filter, $I_o = 1.35 \times 10^{-5}$ E min^{-1}	0.45 μm cellulose acetate membrane, Millipore	TOC	Minero et al. (1999)
Humic acid, Aldrich, 7–10 mg L^{-1}	TiO_2: OSCh 7–3 (Russia), R-O3 (DAK Titan, Armyansk, Ukraine), and Degussa P-25, photocatalytic membrane reactor, UV irradiation a high pressure mercury lamp, $I_o = 18.9$ W m^{-2}	Membranes UPM-67, UPM-20, and OPMN-P (Vladipor, Vladimir, Russia)	Absorbance at 465 nm $HA_{conc} = Abs_{465}$ Kinetics	Tsarenko et al. (2006)
Humic acid, Aldrich	TiO_2 Degussa P-25, batch reactor, BLF lamp, $I_o = 2.84 \times 10^{-6}$ E min^{-1}	0.45 μm cellulose acetate membrane, Millipore	TOC, $Color_{436}$, $Color_{400}$, UV_{365}, UV_{300}, UV_{280}, UV_{254}, $SUVA_{254}$, $SUVA_{365}$, $SCOA_{436}$, absorbance ratios, fluorescence	Uyguner and Bekbolet (2005b)
Humic acid, Aldrich, 100 mg L^{-1}	TiO_2 Degussa P-25, compound parabolic collectors (CPC) reactor pilot plant scale, solar irradiation	0.2 μm and 0.45 μm filters, Millipore	DOC, BOD_5, UV_{254}, $Color_{400}$	Wiszniowski et al. (2004)
Humic acid, Aldrich, DOC = 1.2 mg mL^{-1}	TiO_2 Degussa P-25, immersion batch type reactor, medium pressure mercury lamp, 365 nm, $I_o = 5.25 \times 10^{-4}$ E min^{-1}	0.45 μm syringe filter	UV_{254}, DOC $Color_{400}$ L-H kinetics	Al-Rasheed and Cardin (2003a)
Humic acid, Aldrich	TiO_2 Degussa P-25, TiO_2 (anatase) Sigma, TiO_2 (Rutile) Aldrich, TiO_2 (Mesoporous) Aldrich and ZnO Aldrich, platinized metal oxides, immersion batch-type reactor, medium pressure mercury lamp, $I_o = 5.25 \times 10^{-4}$ E min^{-1}	0.45 μm syringe filter	UV_{254} first order kinetics	Al-Rasheed and Cardin (2003b)
Humic acid, Aldrich, pH = 3.4, 7.8 and 11.5 HA = 100 mg L^{-1}	TiO_2 Degussa P-25, Solar box Atlas Suntest CPS+, Vapor Xenon lamp	No filtration, direct injection for analysis	TOC no kinetics	Wiszniowski et al. (2003)
Humic acid, Aldrich, HA = 1–25 mg L^{-1}	TiO_2 Degussa P-25, Batch reactor, 300 W Xe arc lamp	0.45 μm nylon membrane filter, Gelman Sciences	DOC, absorbance at 250 nm, fluorescence emission spectra No kinetics	Cho and Choi (2002)
Humic acid, Aldrich, HA = 100 mg L^{-1} $UV_{254} = 2.4$ m^{-1}	TiO_2 Degussa P-25, batch reactor, medium pressure mercury lamp, 365 nm, 250 W	0.22 μm nylon syringe filters	Hazen color, absorbance at 254 nm and 400 nm, fluorescence (emission at 400 nm after excitation at 237 nm), DOC, COD No kinetics	Eggins et al. (1997)
Humic acid, Aldrich, TOC = 9 mg L^{-1}	TiO_2 Degussa P-25, membrane reactor, UV lamp, 254 nm (Philips, TUV 8 W/G8 T5)	0.45 μm cellulose acetate membrane, Whatman	UV_{254}, DOC, SUVA No kinetics	Syafei et al. (2008)

(*continued on next page*)

Table 2.5. Continued

Table 3 (*continued*)

NOM model compounds	Reactor type/irradiation source	Filter type, pore size, material	Parameter	References
Humic acid, Fluka, 15 mg L^{-1}	TiO_2 nanowire, batch reactor, low pressure Hg lamp, 254 nm, 2000 W cm^{-2}	0.45 μm glass filter, Advantec, GC-50	Absorbance at 436 nm, TOC HA_{conc} = $Color_{436}$ L-H kinetics	Zhang et al. (2008)
Humic acid, Fluka, DOC = 10 mg L^{-1}	TiO_2 Degussa P-25, annular photoreactor, UV lamp (20 W NEC black light blue), 365 nm, I_o = 20.3 μE L^{-1} s^{-1}	0.45 μm cellulose acetate membrane, Millipore	UV_{254}, DOC, HPSEC-UV_{260} No kinetics	Liu et al. (2008a)
Humic acid, Fluka, 20 mg L^{-1} pH = 3, 5, 7, 9	TiO_2 Degussa P-25, batch reactor (borosilicate glass) 125 W high pressure mercury lamp, I_o = 4.38 mW cm^{-2}	0.45 μm syringe filters, Millipore	Color in Hazen, UV_{254}, TOC First order kinetics HA_{conc} = UV_{254}	Li et al. (2002)
Humic acid, Fluka, 20 mg L^{-1} pH = 3, 5, 7, 9	TiO_2 coated hematite, UV bubble photocatalytic reactor, medium pressure mercury lamp, 12 W	0.45 μm membrane filter	TOC, $Color_{400}$ major emission wavelength set at 253.7 nm	Qiao et al. (2002)
Humic acid, Fluka, TOC = 32.13 mg L^{-1} pH = 7	TiO_2 Degussa P-25, UV multipurpose cabinet, low pressure UV mercury lamp, 253.7 nm, 9 × 15 W	0.45 μm membrane filter	TOC, $Color_{400}$,UV_{254} First order and L-H kinetics	Tay et al. (2001)
Humic acid, Roth, TOC = 4.46 mg L^{-1}	TiO_2 Degussa P-25, batch reactor, 125 W BLF lamp, 350 nm, I_o = 2.84 μE min^{-1}	0.45 μm cellulose acetate membrane, Millipore	TOC, $Color_{436}$, UV_{254}, $SUVA_{254}$, $SCOA_{436}$,fluorescence (FI_{emis}, FI_{syn}, SFI_{syn} L-H and first order kinetics	Uyguner and Bekbolet (2010)
Humic acid, Roth, DOC = 4.45–10.48 mg L^{-1}	TiO_2 Degussa P-25, batch reactor, 125 W BLF lamp, I_o = 2.85 × 10^{16} quanta s^{-1}	0.45 μm cellulose acetate membrane, Millipore	DOC, UV_{254} First order kinetics	Uyguner and Bekbolet (2009)
Humic acid, Roth, HA = 10 mg L^{-1}	TiO_2 Degussa P-25, batch reactor, 125 W BLF lamp, 350 nm, I_o = 2.84 μE min^{-1}	0.45 μm cellulose acetate membrane, Millipore	$Color_{436}$, UV_{254}	Uyguner and Bekbolet (2007a)
Humic acid, Roth, HA = 5–20 mg L^{-1}	TiO_2 Degussa P-25, Hombikat UV-100, Millennium PC-100 and PC-500, Merck, batch reactor, 125 W BLF lamp, 350 nm, I_o = 0.89 μE min^{-1}–3.44 μE min^{-1}	0.45 μm cellulose acetate membrane, Millipore	UV_{254}	Uyguner and Bekbolet (2004a)
Humic acid, Roth, HA = 10–50 mg L^{-1}	TiO_2 Degussa P-25, Hombikat UV-100, batch reactor, 125 W BLF lamp, I_o = 2.84 × 10^{-6} E min^{-1}	0.45 μm cellulose acetate membrane, Millipore	$Color_{436}$	Bekbolet et al. (2002)
Humic acid, Roth	TiO_2 Degussa P-25, batch reactor, BLF	0.45 μm cellulose acetate membrane, Millipore	TOC	Gonenc and Bekbolet (2001)
Humic acid, Roth, 20 mg L^{-1} pH = 7.2	TiO_2 Degussa P-25, Kronos-1002 (Kronos Titan-GmbH, Germany), and DT-51 (Rhone-Poulenc, France), batch system, 150 W Xe-high pressure lamp	0.22 μm membrane filter, Roth	UV–vis spectra	Bems et al. (1999)
Humic acid, Roth	TiO_2 Degussa P-25, batch reactor, 125 W BLF lamp, 350 nm	0.45 μm cellulose acetate membrane, Millipore	$Color_{436}$, $Color_{400}$	Bekbolet et al. (1998)
Humic acid, Roth	TiO_2 Degussa P-25, batch reactor, 125 W BLF lamp	0.45 μm syringe filter, Millipore	TOC, COD, BOD_5	Bekbolet (1996)
Humic acid, Roth	TiO_2 Degussa P-25, batch reactor, 125 W BLF lamp	0.45 μm syringe filter, Millipore	TOC, COD, BOD_5, $Color_{400}$, UV_{280}, UV_{254}	Bekbolet et al. (1996)
Humic acid, Roth	TiO_2 Degussa P-25, batch reactor, 125 W BLF lamp	0.45 μm syringe filter, Millipore	TOC,COD, $Color_{400}$, UV_{254}	Bekbolet and Balcioglu (1996)
Humic acid, Roth	TiO_2 Degussa P-25, batch reactor, 125 W BLF lamp	0.45 μm syringe filter, Millipore	TOC, $Color_{400}$	Bekbolet and Ozkosemen (1996)
Humic acid, Waco, 0–20 mg L^{-1} HA pH = 4, 7, 10	TiO_2 Degussa P-25, reaction tube, UV lamp, 365 nm, 15 W	0.2 μm membrane filter	Absorbance at 254 nm No kinetics, Removal %	Yang and Lee (2006)
A sodium salt of humic acid, Acros organics, HA = 100 mg L^{-1}	Palladium-modified nitrogen doped titanium oxide prepared by sol gel, metal halogen desk lamp, I_o = 1.6 mW cm^{-2}	No filtration	Absorption spectra HA_{conc} = UV_{280} First order kinetics	Li et al. (2007)
Humic acids mixture, Acros Organics	TiO_2 Degussa P-25, cylindrical batch reactor, 125 W immersed medium pressure Hg lamp	Nanofiltration membranes; NF-PES010(Celgard, Germany) polyethersulphone, NTR-7410 (Nitto-Denko, Japan) sulphonated polyethersulphone	Absorbance at 254 nm, TOC TC-IC = TOC No kinetics	Molinari et al. (2002)
Humic acid, IHSS peat; fulvic acid, IHSS; Humic acid, Aldrich; HA = 5–25 mg L^{-1}	TiO_2 Degussa P-25, 1049 Ahlstrom paper containing TiO_2 Degussa P-25, cylindrical stainless steel photoreactor and Solar Cocentric Parabolic Concentrator reactor, high-pressure mercury lamp, 254 nm, I_o = 300 W m^{-2}	No information was provided	TOC, Gel permeation chromatography (GPC) using a high-erformance liquid chromatography system by Metrohm First order kinetics	Remoundaki et al. (2009)
NOM, IHSS humic acid TOC = 2.3 ± 0.2 mg L^{-1}	TiO_2 Degussa P-25, UV annular reactor, low pressure UV lamp, 254 nm, 75 W	Flat sheet 0.22 μm polyvinylene fluoride membrane, GVHP Millipore	TOC L-H kinetics	Le-Clech et al. (2006)
Humic substance, Biohumic from the Bioiberica Company (Spain) DOC = 10 mg L^{-1}	TiO_2 Degussa P-25, batch reactor and a continuous reactor system of three stainless steel reactors, UV lamps, 3 × 8 W	No information was provided	DOC/TOC	Areerachakul et al. (2008)
IHSS Suwannee River NOM TOC = 10 mg L^{-1}	TiO_2 Aeroxide P25 (Degussa), photoreactor, low pressure mercury lamp, 254 nm, 8 W	0.2 μm PVDF filter	Absorbance at 254 nm, TOC L-H kinetics	Huang et al. (2008)
Humic acid, Aldrich and	Polymethylmethacrylate rings coated by TiO_2	No filtration	UV–vis spectra, UV_{254}	Rizzo et al.

Table 2.5. Continued

NOM model compounds	Reactor type/irradiation source	Filter type, pore size, material	Parameter	References
surface water	nanofilm, UV lamp, 335 nm, I_o = 3.0 mW cm^{-2} at the inner ring diameter and 1.1 mW cm^{-2} at the outer ring diameter			(2007)
IHSS soil humic acids, IHSS humic acid, IHSS fulvic acid, Aldrich humic acid, Roth humic acid HA = 50 mg L^{-1}	TiO_2 Degussa P-25, batch reactor, 125 W BLF lamp, 350 nm, I_o = 2.84 μE min^{-1}	0.45 μm cellulose acetate membrane, Millipore	TOC, $Color_{436}$, $Color_{400}$, UV_{365}, UV_{300}, UV_{280}, UV_{254}, $SUVA_{254}$	Uyguner and Bekbolet (2005a)
Fulvic acid (Beijing BioChem Corp.), TOC = 12 mg L^{-1} UV_{254} = 0.18	TiO_2 Degussa P-25, continuous flow photocatalytic membrane reactor, low pressure UV lamp, 253.7 nm, 11 W, I_o = 0.75 mW cm^{-2}	0.2 μm Polypropylene ultrafiltration membrane	UV_{254}, TOC First order kinetics	Fu et al. (2006a)
Fulvic acid (Beijing BioChem Corp.), TOC = 11.95 mg L^{-1}	Nano-structured TiO_2/silica gel photocatalyst, TiO_2 Degussa P-25, submerged membrane photocatalysis reactor, low pressure UV lamp (Philips), 253.7 nm, 11 W	0.2 μm microfiltration membrane polyvinylidene (PVDF) hollow fiber, and filtration area 0.2 m^2	TOC First order kinetics	Fu et al. (2006b)
Humic acids, Aldrich, IHSS and humic acid extracted from a river	TiO_2 from Nanasolution Co. (photocatalyst hollow bead), rotating photoreactor, UV-A (352 nm), UV-C lamp (254 nm) (Sankyo, Japan), 15 W		UV_{254}, TOC	Han et al. (2006)
Humic acid, Wako, Nordic aquatic humic acid, Nordic aquatic fulvic acid and IHSS fulvic acid HA = 7.6 mg L^{-1}	SiO_2-Ti, batch reactor, black light irradiation, 365 nm, I_o = 370 mW cm^{-2}	0.45-μm PTFE membrane filter, DISMIC-13HP, Advantec Japan	Absorbance at 250 nm, 350 nm, and 450 nm No kinetic modeling	Moriguchi et al. (2006)
Natural NOM				
Source water DOC = 10.6–3.5 mg L^{-1} UV_{254} = 0.365–0.067 cm^{-1}	TiO_2 Degussa P-25, annular photoreactor,blacklight blue fluorescent lamp (NEC 20 W T10), 365 nm, I_o = 20.3 μE (Ls)$^{-1}$	0.45 μm cellulose acetate membrane	Absorbance spectra 200–800 nm DOC No kinetics	Liu et al. (2010)
Raw water, DOC = 10 mg L^{-1}	TiO_2 Degussa P-25, laboratory-scale annular photoreactor UV lamp (20 W NEC black light blue), 365 nm, I_o = 20.3 μE L^{-1} s^{-1}	0.45 μm cellulose acetate membrane	UV_{254}, DOC, HPSEC-UV_{260} No kinetics	Liu et al. (2008b)
Lake water, DOC = 21 mg L^{-1}	TiO_2 Degussa P-25, batch type solar UV simulator, I_o = 1 × 10^{-7} E s^{-1}	0.45 μm cellulose acetate membrane	Size exclusion chromatograms were recorded using the SEC DOC/UV system No kinetics	Espinoza et al. (2009)
Groundwater TOC = 0.3 mg L^{-1} UV_{254} = 0.8 m^{-1}	TiO_2 Degussa P-25, batch reactor, 125 W black light fluorescent lamp, 350 nm, I_o = 1309 μW cm^{-2}	0.45 μm borosilicate filters, Millipore	DOC, UV_{254} First order kinetics	Rizzo et al. (2008)
Humic acid extracted from water reservoir HA = 8 mg L^{-1}	TiO_2 Degussa P-25, Silver deposited TiO_2 photocatalyst, batch reactor, fluorescent black light blue lamp, 355 nm, 20 W	0.45 μm PTFE membrane filter	Absorbance at 254 nm and TOC = TC-IC No kinetics	Bansal et al. (2008)
Humic acid, Aldrich and lake water sample TOC = 4.80 mg L^{-1}	TiO_2 Degussa P-25, photocatalytic membrane reactor, a dual cylindrical chamber (1 L), UV black light blue lamp (Sankyo, Japan), 8 W	0.1 μm submerged microfiltration membrane fibers, Mitsubishi	Absorbance at 254 nm and TOC No kinetics	Choo et al. (2008)
Source water, TOC = 5.4–24.9 mg L^{-1}	TiO_2 pellets from Sachtleben Chemie Gmbh, TiO_2 Hombikat UV-100, bench and pilot scale TiO_2 columns, mercury arc UV lamp, 365 nm, 100 W, I_o = 21700–8900 μW cm^{-2}	Glass microfiber filter paper	Absorbance at 254 nm, DOC, HPSEC-UV_{254} No kinetics	Murray et al. (2007)
Humic acid, Aldrich DOC = 10 mg L^{-1} and raw water DOC = 9.64 mg L^{-1}, UV_{254} = 42.83 m^{-1}	Six sol–gel solutions and commercial TiO_2 suspensions (Hombikat UV-100, Degussa P-25 and Millennium PC 100) were used to coat glass microscope slides, batch reactor UV lamp, 365 nm	No information was provided	UV_{254} absorbance, DOC and specific UV absorbance (SUVA) No kinetics	Murray and Parsons (2006)
Lake water, DOC = 7 mg L^{-1}	TiO_2 Degussa P-25, Hombikat UV-100, Solar UV Simulator (Oriel Corp.)	0.1 μm PVDF membrane filter, Millipore or centrifugation	UV–vis spectra, DOC	Doll and Frimmel (2005)
Surface water DOC = 3.78–5.29 mg L^{-1}	TiO_2 Degussa P-25, batch reactor, 125 W BLF lamp, I_o = 2.84 μE min^{-1}	0.45 μm cellulose acetate membrane, Millipore	DOC, UV_{280}, UV_{254}, fluorescence	Uyguner et al. (2007a)
Lake water, TOC = 2.47–3.61 mg L^{-1}	TiO_2 Degussa P-25, batch reactor, 125 W BLF lamp, I_o = 2.85 × 10^{16} quanta s^{-1}	0.45 μm cellulose acetate membrane, Millipore	TOC, UV_{280}, UV_{254}	Bekbolet et al. (2005)
Lake water, DOC = 4.55–5.10 mg L^{-1} UV_{254} = 0.11–0.135 cm^{-1}	TiO_2 Aldrich, TiO_2 Degussa P-25 Solar System	0.45 μm cellulose nitrate membrane, Sartorius	DOC, absorbance at 254 nm, turbidity No kinetics	Ljubas (2005)
Humic acid, Aldrich, ground water HA = 10 mgL^{-1}	TiO_2 Degussa P-25 attached to buoyant hollow glass microspheres, batch reactor, low pressure mercury lamp, 15 W, 0.7 mW cm^{-2}	0.45 μm membrane filter for humic acid, Advantec MFS	Absorbance at 455 nm, 254 nm HA_{conc} = UV_{254}	Portjanskaja et al. (2004)
Humic acid, Wako, surface water, TOC = 1.1 and 3.5 mg L^{-1} TOC_{HA} = 4.9 mg L^{-1}	TiO_2 granules (ST-B11, Ishihara Techno Corp.), fluidized photocatalysis reactor, UV lamp, 254 nm, 20 W	Glass fiber filter	Absorbance at 260 nm, TOC First order kinetics	Lee and Ohgaki (1999)
River water TOC = 48 mg L^{-1}	TiO_2 electrode coated by sol gel method, two compartment isolated by a membrane, 450 W Xe-Hg arc UV lamp, I_o = 6 mW cm^{-2}		UV_{254}, Color, TOC	Selcuk et al. (2004)

DOC concentration, UV_{254}, and $Color_{400}$ parameter, correspondingto AHA, was determined by TOC analyzer and UV-vis spectrophotometer (Wisziowski et al., 2004). UV_{254} parameter and $Color_{400}$ parameter (Al-Rasheed and Cardin, 2003b), corresponding to AHA, was determined by TOC analyzer (Al-Rasheed ana Cardin, 2003a). TOC concentration, corresponding to 100 mg L^{-1} AHA, was determined during the photocatalytic treatment (Wiszniowski et al., 2003). DOC concentration, corresponding to AHA (1-25 mg L^{-1}), was determined by TOC analyzer (Cho and Choi, 2002). UV_{254} parameter, $Color_{400}$ parameter and Hazen color, corresponding to AHA, were determined by UV-vis spectrophotometer (Eggins et al., 1997). UV_{254} parameter, DOC concentration, corresponding to AHA, were determined by using UV-vis spectrophotometer and TOC analyzer during the photocatalytic treatment (Syafei et al., 2008) and furthermore, SUVA was calculated as a function of DOC concentration and UV_{254} parameter. The removal of 15 mg L^{-1} of FHA was presented as a function of $Color_{436}$ parameter during the photocatalytic treatment (Zhang et al., 2008). The removal of UV_{254} parameter and DOC concentration (10 mg L^{-1}) were determined by UV-vis spectrophotometer and TOC analyzer (Liu et al., 2008a). The removal of FHA (20 mg L^{-1}) was presented as a function of UV_{254} parameter and TOC concentration was determined by TOC analyzer (Li et al., 2002) at pH=3, 5, 7 and 9. TOC concentration was determined by TOC analyzer and $Color_{400}$ parameter was determined by UV-vis spectrophotometer (Qiao et al., 2002). The removal of TOC concentration, $Color_{400}$ and UV_{254} parameter (32.13 mg L^{-1}) were determined by TOC analyzer and UV-vis spectrophotometer for FHA (Tay et al., 2001). The removal of TOC concentration, $Color_{436}$ parameter and UV_{254} parameter by using TOC analyzer and UV-vis spectrophotometer for RHA (Uyguner and Bekbolet, 2010). Moreover, $SUVA_{254}$ and $SCOA_{436}$ parameter were calculated. The removal of DOC concentration (4.45-10.48 mg L^{-1}) and UV-vis spectrophotometer (Uyguner and Bekbolet, 2009). The removal of $Color_{436}$ parameter and UV_{254} parameter were determined by UV-vis spectrophotometer (Uyguner and Bekbolet, 2007a) for 10 mg L^{-1} of RHA. The removal of UV_{254} parameter was determined by UV-vis spectrophotometer (Uyguner and Bekbolet, 2004a). The removal of $Color_{436}$ parameter, (10-50 mg L^{-1} RHA), was determined during the photocatalytic treatment (Bekbolet et al., 2002).

The removal of TOC concentration was determined during the photocatalytic treatment (Gonenc and Bekbolet, 2001). UV-vis spectra was determined during the

photocatalytic treatment for 20 mg L^{-1} of RHA (Bems et al., 1999).The removal of $Color_{436}$ and $Color_{400}$ parameter were determined by UV-vis spectrophotometer for RHA during the photocatalytic treatment (Bekbolet et al., 1998). TOC concentration of RHA (Bekbolet, 1996), $Color_{400}$, UV_{280}, and UV_{254} (Bekbolet and Balcioglu, 1996; Bekbolet and Ozkösemen, 1996) parameter were determined by UV-vis spectrophotometer (Bekbolet et al., 1996) during the photocatalytic treatment.The removal of UV_{254} parameter was determined for 0-20 mg L^{-1} Waco, HA at pH=4, 7 and 10 during the photocatalytic treatment (Yang and Lee, 2006). The removal of a sodium salt of humic acid (Acros organics) was presented as a function of UV_{280} parameter during the photocatalytic treatment (Li et al., 2007). The removal of UV_{254} parameter and TOC concentration were determined for humic acid mixture, Acros organics (Molinari et al., 2002). The removal of TOC concentration was determined for humic acid, Aldrich (5 to 25 mg L^{-1}) (Remoundaki et al., 2009) and the removal of TOC concentration was determined for IHSS humic acid during the photocatalytic treatment (Le-Chech et al., 2006). DOC/TOC was determined for humic substances (Areerachakul et al., 2008) during the photocatalytic treatment. The removal of UV_{254} parameter and TOC concentration were determined during the photocatalytic treatment. The removal of UV_{254} parameter and TOC concentration were determined during the photocatalytic treatment (Huang et al., 2008). The removal of UV_{254} parameter was determined by UV-vis spectrophotometer during the photocatalytic treatment for AHA and surface water (Rizzo et al., 2007). TOC concentration was determined by TOC analyzer, $Color_{436}$, $Color_{400}$, UV_{365}, UV_{300}, UV_{280} and UV_{254} were determined by UV-vis spectrophotometer during the photocatalytic treatment for IHSS soil humic acids, IHSS humic acid, IHSS fulvic acid, AHA and RHA (Uyguner and Bekbolet, 2005a). The removal of UV_{254} parameter and TOC concentration were determined during the photocatalytic treatment for AHA, IHSS, and humic acid extracted from a river (Han et al., 2006). The removal of UV_{250} parameter, UV_{350} parameter and $Color_{450}$ parameter were determined during the photocatalytic treatment for Waco humic acid, Nordic humic acid, Nordic Fulvic Acid and IHSS fulvic acid (Moriguchi et al., 2006). The removal of DOC concentration and UV-vis spectra (200-800 nm) were determined during the photocatalytic treatment (Liu et al., 2010). The removal of UV_{254} parameter and DOC concentration, corresponding to raw water, were determined by UV-vis spectrophotometer and TOC analyzer during the photocatalytic treatment (Liu et al., 2008b). The removal of DOC concentration and UV_{254} parameter were determined by TOC analyzer and UV-vis

spectrophotometer (Rizzo et al., 2008). The removal of UV_{254} parameter and TOC concentration, corresponding to humic acid extracted from water reservoir, were determined by UV-vis spectrophotometer and TOC analyzer (Bansal et al., 2008). The removal of UV_{254} parameter and TOC concentration were determined for humic acid, AHA and lake water sample during the photocatalytic treatment (Choo et al., 2008). The removal of UV_{254} parameter and DOC concentration were determined for source water (Murray et al., 2007) and for AHA and raw water (Murray and Parsons, 2006) during the photocatalytic treatment.The removal of UV-vis spectra and DOC concentration were determined during the photocatalytic treatment (Doll and Frimmel, 2005). The removal of DOC concentration (Uyguner et al., 2007a), TOC concentration (Bekbolet et al., 2005), UV_{280} and UV_{254} parameter (Uyguner et al., 2007a; Bekbolet et al., 2005) during the photocatalytic treatment. The removal of DOC concentration and UV_{254} parameter were determined by using TOC analyzer and UV-vis spectroscopy during the photocatalytic treatment (Ljubas, 2005).The removal of AHA concentration was determined as a function of UV_{254} parameter for AHA, groundwater during the photocatalytic treatment and the removal of $Color_{455}$ parameter was determined during the photocatalytic treatment (Portjanskaja et al., 2004). The removal of UV_{260} parameter and TOC concentration were determined during the photocatalytic treatment for humic acid, Wako, surface water (Lee and Ohgaki, 1999). The removal of UV_{254} parameter, color, and TOC were determined during the photocatalytic treatment (Selcuk et al., 2004).

3. MATERIALS AND METHODOLOGY

3.1. Materials

3.1.1. Humic Acid Solution

Humic substances of different origin (terrestrial and aquatic) were used in bench scale experiments. Nordic humic acid (aquatic), Fluka humic acid (terrestrial), Aldrich humic acid (terrestrial) and Roth humic acid (terrestrial) were used as humic acid sources.

A stock solution of 1000 mg L^{-1} was prepared by dissolving humic acid in distilled deionized water and filtered through filter paper except for RHA which was prepared according to Urano et al., (1983). Stock solution was stored in amber glass bottles and were protected from light to prevent decomposition. A series of standards were prepared by diluting with distilled deionized water 1 mL, 2 mL, 3 mL, 4 mL and 5mL of standard solution to 100 mLwith distilled water. These standards are equivalent to 10, 20, 30, 40 and 50 mg L^{-1} humic acid solution.

A stock solution of 1000 mg L^{-1} (Roth) was prepared by dissolving in 1000 ml of 0.1 N NaOH solution. After 1 day, the solution was diluted with distilled dionized water and filtered through filter paper. A series of standards were prepared by diluting with distilled deionizedwater 0.25 mL, 0.5mL, 1 mL, 2 mL, 3 mL, 4 mL and 5mL of Standard Roth Humic Acid solution to 100 mL with distilled water. These standards are equivalent to 2.5, 5, 10, 20, 30, 40 and 50 mg L^{-1} Roth Humic Acid solution.

3.2. Methods and Methodology

3.2.1. Experimental Procedure

UV-vis measurements, and DOC analysis were done in accordance with the below given methods (Dissolved Organic Carbon (DOC) Analysis and UV-vis measurements).

3.2.1.1.Dissolved Organic Carbon (DOC) Analysis. Dissolved organic carbon content (DOC, mg L^{-1}) measurements of humic substances were performed on a Shimadzu TOC-V WP Total Organic Carbon Analyzer. Calibration of the instrument was done using potassium hydrogenphthalate concentration in range of 5-25 mg L^{-1}.

3.2.1.2. UV-vis Absorbance Measurements. UV-vis absorption spectra were recorded on a Perkin Elmer Lambda 35 UV/VIS Spectrophotometer employing Hellma quartz cuvettes of 1.0 cm optical pathlength.The absorbance values expressed as UV_{254}, UV_{280}, UV_{365} and $Color_{436}$ parameter were used as parameters that indicate organicmatter and color, in studied humic acids (NHA, FHA, AHA and RHA), respectively. Specific UV absorbance ($SUVA_{254}$, cm^{-1} $mg^{-1}L$) was used to represent DOC normalized the organic carbon content (UV_{254}). $SUVA_{280}$ was calculated as the ratio of the UV_{280} absorbing species to DOC, $SUVA_{365}$ was also calculated in a similar fashion as the ratio of the UV_{365} absorbing species to DOC, and specific color absorbance ($SCOA_{436}$, cm^{-1} mg^{-1} L) was defined as $Color_{436}$/DOC to signify organic carbon normalized color forming moieties.

3.2.1.3.Regression Analysis. Regression analysis, concerns the study of relationships between variables with the object of identifying, estimating, and validating the relationship. The estimated relationship can then be used to predict one variable from the value of the other variable(s). A regression problem involving a single predictor (also called simple regression) arises when the aim is to study the relation between two variables x and y and use it to predict y from x. The variable x acts as an independent variable whose values are controlled by the experimenter. The variable y depends on x and is also subjected to unaccountable variationsor errors. Recall that if the relation between y and x is exactly a straightline, then the variables are connected by the formula (Equation 3.1) where

β_o indicates the intercept of the line with the y-axisand β_1 represents the slope of the line, or the change in y per unit change

$$y = \beta_o + \beta_1 x \quad (3.1)$$

Regression analysis deals with studying the manner in which the response variable y depends on a predictor variable x. Thefirstimportant step in studying the relation between the variables y and x is to plot the scatter diagram of the data (x_i, y_i), i=1,…….,n. If this plot indicates an approximate linear relation, a straight-line regression model (Equation 3.2 andEquation 3.3) is formulated (Johnson ana Bhattacharyya, 1996):

Response = (A straightline in x) + (Random error) (3.2)

$$y_i = \beta_1 x_i + e_i \quad (3.3)$$

The random errors are assumed to be independent, normally distributed , and have mean 0. The error may be regarded as the sum of two components:

i. Measurement error. In our study, UV-vis parameter of the types of humic acids were measured by UV-vis spectroscopy and DOC concentrations were measured by TOC analyzer. For example, in measuring DOC concentrations of humic acids and UV-vis parameter of humicacids, there may be an error resulting from in accurate solubility of the types of humic acid.
ii. Even if there were no measurement error, repetititon of an experiment using exactly the same amount of fertilizer would result in somewhat different yields. Forexample, to measure UV-vis parameters and DOC concentrations more than once could cause an error in measurement result (Wonnacott andWonnacott, 1990).

The correlation coefficient, denoted by R, is a measure of strength of the linear relation between the x and y variables. Some important features of the correlation coefficient was outlined and discussed the manner in which it serves to measure the strength of a linear relation.

i. The value of R is always between -1 and +1.

ii. The magnitude of R indicates the strength of a linear relation, whereas its sign indicates the direction. More specifically,

R> 0 if the pattern of (x,y) values is a band that runs from lower left to upper right.

R = +1 if all (x,y) values lie exactly on a straight linewith a positive slope (perfect positive linear relation).

R= -1 if all (x,y) values lie exactly on a straight line with a negatives lope (perfect negative linear relation).

iii. A value of R close to zero means that the linear association is very weak (Johnson and Bhattacharyya, 1996).

4. RESULTS AND DISCUSSION

Since humic acids are known to express chemical properties with respect to their source and origin, humic acids, originating from aquatic and terrestrials sources, were selected as representatives of humic compounds. In this study, model compounds of originally aquatic humic acid (Nordic), and terrestrial humic acids (Fluka, Roth and Aldrich) were characterized with respect to their UV-vis parameters (UV_{254}, UV_{280}, UV_{365} and $Color_{436}$) and DOC concentrations of the humic acids. The data (HA concentrations and UV-vis parameter, corresponding to these humic acids and DOC concentrations of HAs) was reported by Ilgun et al., 2010. According to the determination of DOC concentration and UV-vis parameter results (UV_{254}, UV_{280}, UV_{365} and $Color_{436}$) from HA source, UV-vis parameter were correlated with DOC concentrations and DOC concentrations were correlated with HA concentrations. After complete the correlation for each humic acid source, these results were done for the overall humic acids (NHA, FHA, AHA and RHA). In other words, the overall humic acids were correlated with UV-vis parameters, corresponding to these humic acids, furthermore, UV-vis parameters, corresponding to these humic acids, were correlated with DOC concentrations of these HAs (NHA, FHA, AHA and RHA).

In addition to non-treatment condition, where humic acids were investigated in relation to their UV-vis parameters (UV_{254}, UV_{280}, UV_{365} and $Color_{436}$), the same steps were applied for the treatment conditions. The photocatalytic oxidation was used as treatment method for the humic acids. The photocatalytic oxidation of model humic acids was accomplished using TiO_2 Degussa P-25 as the photocatalyst. The data for the photocatalytic oxidation (HA concentrations and UV-vis parameter, corresponding to these humic acids and DOC concentrations of HAs) were reported previously (Ilgun, 2010). According to the data attained by photocatalytic treatment of AHA and NHA, UV-vis parameter results were correlated with the DOC concentration results. Furthermore, these equations, attained by the correlations, were evaluated with each other. The least square regression method was applied for the determination of correlation equation and correlation coefficients.

4.1. Specific Analysis of Humic Acids

4.1.1 Humic Acid, Nordic

For the basic characterization of humic acid (NHA, Nordic), studied in the range of 10 to 50 mg L^{-1}, DOC concentrations of NHA as well as UV-vis (UV_{254}, UV_{280}, UV_{365} and $Color_{436}$) parameters were presented in Table 4.1.

Table 4.1. UV-vis Parameters and DOC Concentrations of Nordic Humic Acid (NHA).

Nordic Humic Acid					
HA, mg L^{-1}	DOC, mg L^{-1}	UV-vis parameters			
		UV_{254}, cm^{-1}	UV_{280}, cm^{-1}	UV_{365}, cm^{-1}	$Color_{436}$, cm^{-1}
10	5.450	0.2792	0.2285	0.0820	0.0317
20	9.640	0.4690	0.3834	0.1285	0.0420
30	13.22	0.7436	0.6071	0.2071	0.0690
40	19.48	1.0385	0.8996	0.2549	0.0845
50	23.01	1.2294	1.0041	0.3398	0.1140

Depending on the concentration of the working humic acid solutions, UV-vis parameters (UV_{254}, UV_{280}, UV_{365} and $Color_{436}$) and DOC concentrations of humic acid displayed certain values. The aquatic humic acid exhibited UV_{254} parameter in the range of 0.2792 cm^{-1} to 1.2294 cm^{-1}, UV_{280} parameter in the range of 0.2285 cm^{-1} to 1.0041 cm^{-1}, UV_{365} parameter in the range of 0.0820 cm^{-1} to 0.3398 cm^{-1} and $Color_{436}$ parameter in the range of 0.0317 cm^{-1} to 0.1140 cm^{-1}. Moreover, humic acid displayed DOC concentration in the range of 5.450 mg L^{-1} to 23.01 mg L^{-1}. The humic acid (Nordic) exhibited DOC concentration in the range of 5.450 mg L^{-1} to 23.01 mg L^{-1}, representing approximately 50 % organic carbon. When NHA was increased 5 times of its initial concentration, the increase in DOC concentration exhibited 24 % of its initial value, the increase in UV_{254} parameter displayed 23 % of its initial value, the increase in UV_{280} parameter exhibited 23 % of its initial value, the increase in UV_{365} parameter exhibited 24 % of its initial value and $Color_{436}$ parameter displayed 28 % of its initial value.

4.1.1.1.The Relationship between HA and DOC Concentrations of NHA. HA concentrations of NHA were correlated with DOC concentrations as presented in Figure 4.1.

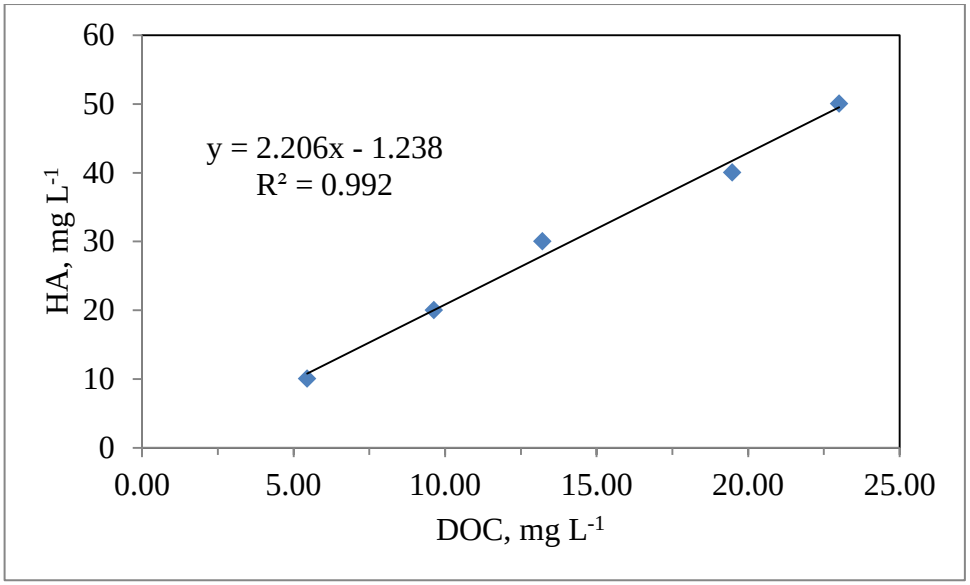

Figure 4.1. The correlation between HA and DOC concentrations of NHA.

Reckhow et al. (1990) showed that the elemental composition for the humic acids is carbon (52-56%), hydrogen (4.5-5 %), oxygen (33-39 %), and minor percentages of nitrogen, sulfur, and phosphorus. As mentioned before, DOC represents organic carbon in a sample. As a result, DOC is expected a linear increase with increasing HA concentration due to include organic carbon, as shown above. On the other hand, DOC could not represent well, due to the experimental conditions. As mentioned before, DOC concentration is determined by TOC analyzer in a humic acid sample. The solubility of humic acid is very important for the productivity of experiments, in other words, to determine DOC content in a humic acid sample. More specifically, as shown in Table 4.1, DOC concentration represented 50 % of NHA for each HA concentration. Humic substances account for 40-80% of the dissolved organic matter in water, as a consequence, this result was consistent with this explanation.

$$HA\ (mg\ L^{-1}) = 2.206 * DOC\ (mg\ L^{-1}) - 1.238 \qquad R^2 = 0.992 \qquad (4.1)$$

Figure 4.1 illustrated the linear correlation between NHA and DOC concentrations of NHA. HA and DOC Equation was produced from the least-squares regression analyses (Equation 4.1). The regression coefficient was found to be as R^2= 0.992.

4.1.1.2.The Relationships between HA and DOC Concentrations of NHA and UV-vis Parameters. According to Table 4.1, the calibration curves between HA and DOC concentrations of NHA and respective UV-vis parameters (UV_{254}, UV_{280}, UV_{365}, and $Color_{436}$) were presented in Figure 4.2. The linear equation of the correlation between UV-vis parameters (UV_{254}, UV_{280}, UV_{365} and $Color_{436}$) and DOC concentration and the correlation between UV-vis parameters and HA concentrations were listed below.

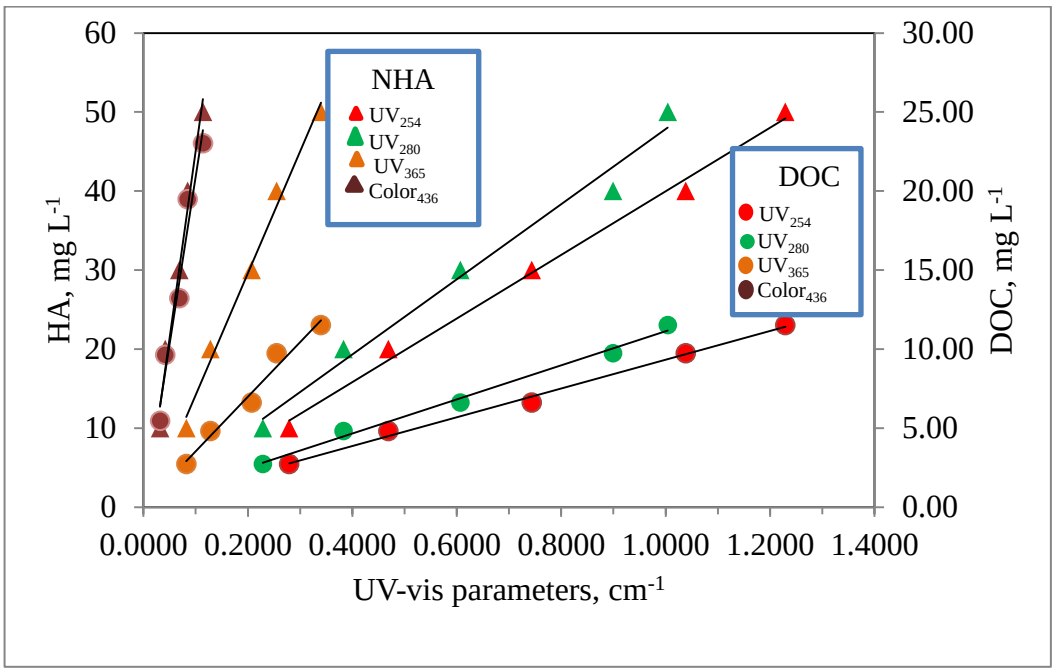

Figure 4.2. The correlation between HA and DOC concentrations of NHA and UV-vis parameters.

DOC concentration represented as a function of UV_{254} parameter, representing the natural organic matter content in a humic acid (Najm et al., 1994) (Equation 4.2) and NHA concentration was represented as a function of UV_{254} parameter (Equation 4.3). The regression coefficient, was found to be as R^2=0.995 (Equation 4.2) and R^2=0.994 (Equation 4.3). Depending on these high regression coefficients, it could be inferred that

UV_{254} parameter was good indicator of DOC concentration of NHA and good indicator of NHA concentration. DOC concentration was represented as a function of UV_{280} parameter, representing total aromaticity such as phenolic arenes, benzoic acids, aniline derivatives, polyenes and polycyclic aromatic hydrocarbons with two or more rings in a humic acid sample (Chin et al., 1994; Traina et al.,1990) (Equation 4.4) and NHA concentration was represented as a function of UV_{280} parameter (Equation 4.5). The regression coefficient, was found to be as R^2=0.992 (Equation 4.4) and R^2=0.983 (Equation 4.5). According to these high regression coefficients, it could be inferred that UV_{280} parameter was good indicator of DOC concentration of NHA and good indicator of NHA concentration.

$$DOC\ (mg\ L^{-1}) = 18.18*UV_{254}\ (cm^{-1}) + 0.493 \qquad R^2=0.995 \qquad (4.2)$$

$$HA\ (mg\ L^{-1}) = 40.25*\ UV_{254}\ (cm^{-1}) - 0.263 \qquad R^2=0.994 \qquad (4.3)$$

$$DOC\ (mg\ L^{-1}) = 21.56*UV_{280}\ (cm^{-1}) + 0.696 \qquad R^2=0.992 \qquad (4.4)$$

$$HA\ (mg\ L^{-1}) = 47.52*UV_{280}\ (cm^{-1}) + 0.319 \qquad R^2=0.983 \qquad (4.5)$$

$$DOC\ (mg\ L^{-1}) = 69.05*UV_{365}\ (cm^{-1}) + 0.180 \qquad R^2=0.974 \qquad (4.6)$$

$$HA\ (mg\ L^{-1}) = 154.25*UV_{365}\ (cm^{-1}) - 1.234 \qquad R^2=0.990 \qquad (4.7)$$

$$DOC\ (mg\ L^{-1}) = 211.66*Color_{436}\ (cm^{-1}) - 0.284 \qquad R^2=0.963 \qquad (4.8)$$

$$HA\ (mg\ L^{-1}) = 472.55*Color_{436}\ (cm^{-1}) - 2.246 \qquad R^2=0.979 \qquad (4.9)$$

Previously, it was reported that UV_{365} parameter represented aromatic moieties such as quinones, aromatic ketons, and polyphenols in humic chemical composition (Polewski et al., 2005). The correlation between DOC concentration and UV_{365} parameter was presented by Equation 4.6 and NHA concentration was represented as a function of UV_{365} parameter (Equation 4.7). The regression coefficient, was found to be as R^2=0.974 (Equation 4.6) and R^2=0.990 (Equation 4.7). Depending on these high regression coefficients, it could be inferred that UV_{365} parameter was good indicator of DOC concentration of NHA and good indicator of NHA concentration. DOC concentration was represented as a function of $Color_{436}$ parameter, representing color forming moieties (Equation 4.8) and NHA concentration was represented as a function of $Color_{436}$ parameter (Equation 4.9). The regression coefficient, was found to be as R^2=0.963 (Equation 4.8) and R^2=0.979 (Equation 4.9). According to these high regression coefficients, it could be inferred that $Color_{436}$ parameter was good indicator of DOC concentration of NHA and good indicator of NHA concentration. In other words, these specified UV-vis parameter

(UV_{254}, UV_{280}, UV_{365} and $Color_{436}$) could significantly indicate a good correlation with DOC contents due to the presence of sufficient-carbon-contents that the attained correlations represented by the regression coefficients close to $R^2 \leq 1$.

4.1.2. Humic Acid, Fluka

For the basic characterization of humic acid (FHA, Fluka), DOC concentrations as well as UV-vis (UV_{254}, UV_{280}, UV_{365} and $Color_{436}$) parameters were presented in Table 4.2. Like the aquatic humic acid (Nordic), the terrestrial humic acid (Fluka) displayed DOC concentration in the range of 3.780 mg L^{-1} to 20.30 mg L^{-1}. UV_{254}, UV_{280}, UV_{365} and $Color_{436}$ parameter exhibited absolute values depending on the concentration of working humic acid solutions (Table 4.2).

Table 4.2. UV-vis Parameters and DOC Concentrations of Fluka Humic Acid (FHA).

Fluka Humic Acid					
HA, mg L^{-1}	DOC, mg L^{-1}	UV-vis parameters			
		UV_{254}, cm^{-1}	UV_{280}, cm^{-1}	UV_{365}, cm^{-1}	$Color_{436}$, cm^{-1}
10	3.780	0.2598	0.2241	0.0970	0.0475
20	7.910	0.5292	0.4607	0.2137	0.1074
30	11.22	0.7777	0.6740	0.3087	0.1527
40	15.48	1.0385	0.8996	0.4149	0.2054
50	20.30	1.2924	1.1174	0.5160	0.2540

The humic acid exhibited the following UV-vis properties as UV_{254} parameter in the range of 0.2598 cm^{-1} to 1.2924 cm^{-1}, UV_{280} parameter in the range of 0.2241 cm^{-1} to 1.1174 cm^{-1}, UV_{365} parameter in the range of 0.0970 cm^{-1} to 0.5160 cm^{-1} and $Color_{436}$ parameter in the range of 0.0475 cm^{-1} to 0.2540 cm^{-1}. The humic acid (Fluka) displayed DOC concentration in the range of 3.780 mg L^{-1} to 20.30 mg L^{-1}, representing approximately 40 % organic carbon.

4.1.2.1.The Relationship between HA and DOC Concentrations (Fluka). According to Table 4.2, HA concentrations of FHA were correlated with DOC concentrations (Figure 4.3). More specifically, as shown in Table 4.2, it was observed that FHA concentration,

studied in range of 10 and 50 mg L^{-1}, expressed 25-30 % DOC concentration. Generally, humic substances account for 40-80% of the dissolved organic matter in water. Moreover a significant part of humic substances are presented as humic acids insoluble fraction.

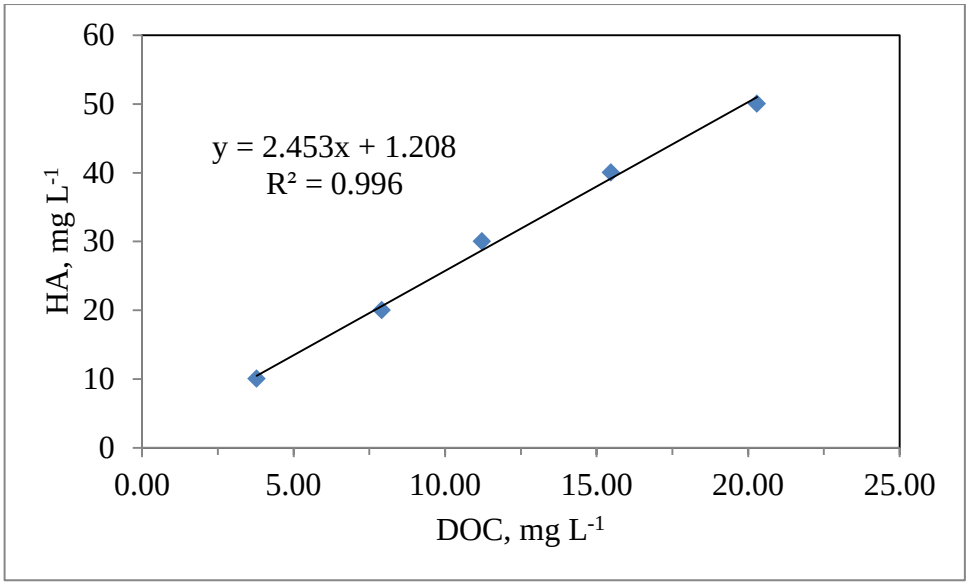

Figure 4.3. The correlation between HA and DOC concentrations of FHA.

It could be inferred that FHA exhibited lower DOC concentration than NHA. Figure 4.3 illustrated the linear correlations between HA and DOC concentrations of FHA.

$$HA\ (mg\ L^{-1}) = 2.453*DOC\ (mg\ L^{-1}) + 1.208 \qquad R^2=0.996 \qquad (4.10)$$

HA-DOC Equation was produced from the least-squares regression analyses (Equation 4.10). The regression coefficient was found to be as R^2= 0.996.

4.1.2.2. The Relationship between HA and DOC Concentrations of FHA and UV-vis Parameters. According to data presented in Table 4.2, the correlation curves constructed between FHA concentration and DOC concentrations of FHA and UV-vis parameters (UV_{254}, UV_{280}, UV_{365} and $Color_{436}$) were presented in Figure 4.4. The linear equations, obtained from the correlation between UV-vis parameters (UV_{254}, UV_{280}, UV_{365} and $Color_{436}$) and DOC concentrations and also the correlation between UV-vis parameters and HA concentrations were listed below. DOC concentration was represented as a function of

UV_{254} parameter, that represents the natural organic matter content in humic acids (Najm et al., 1994) (Equation 4.11) and FHA concentration was represented as a function of UV_{254} parameter (Equation 4.12). The regression coefficient, was found to be as R^2=0.995 (Equation 4.11) and R^2=1.000 (Equation 4.12). According to these high regression coefficients, it could be inferred that UV_{254} parameter was good indicator of DOC concentration of FHA and good indicator of FHA concentration.

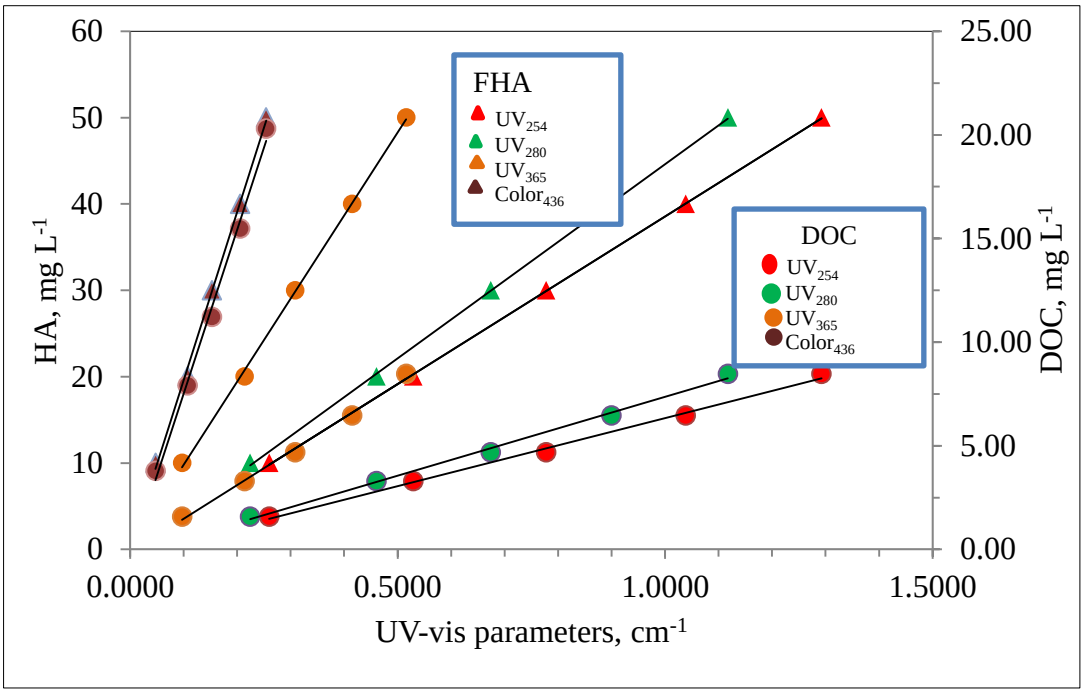

Figure 4.4. The correlation between HA, DOC concentrations of FHA and UV-vis parameters.

DOC concentration was represented as a function of UV_{280} parameter, representing total aromaticity such as phenolic arenes, benzoic acids, aniline derivatives, polyenes and polycyclic aromatic hydrocarbons with two or more rings in a sample, (Chin et al., 1994; Traina et al.,1990) (Equation 4.13) and FHA concentration was represented as a function of UV_{280} parameter (Equation 4.14). The regression coefficient, was found to be as R^2=0.996 (Equation 4.13) and R^2=1.000 (Equation 4.14). According to these high regression coefficients, it could be inferred that UV_{280} parameter was good indicator of DOC concentration of FHA and good indicator of FHA concentration.

$DOC\ (mg\ L^{-1}) = 15.77*UV_{254}\ (cm^{-1}) - 0.557$ $R^2=0.995$ (4.11)

$HA\ (mg\ L^{-1}) = 38.84*\ UV_{254}\ (cm^{-1}) - 0.275$ $R^2=1.000$ (4.12)

$DOC\ (mg\ L^{-1}) = 18.24*UV_{280}\ (cm^{-1}) - 0.579$ $R^2= 0.996$ (4.13)

$HA\ (mg\ L^{-1}) = 44.92*UV_{280}\ (cm^{-1}) - 0.330$ $R^2=1.000$ (4.14)

$DOC\ (mg\ L^{-1}) = 39.05*\ UV_{365}\ (cm^{-1}) - 0.367$ $R^2=0.995$ (4.15)

$HA\ (mg\ L^{-1}) = 96.15*\ UV_{365}\ (cm^{-1}) + 0.189$ $R^2=0.999$ (4.16)

$DOC\ (mg\ L^{-1}) = 79.34*\ Color_{436}\ (cm^{-1}) - 0.432$ $R^2=1.000$ (4.17)

$HA\ (mg\ L^{-1}) = 195.37*\ Color_{436}\ (cm^{-1}) + 0.030$ $R^2=0.994$ (4.18)

As mentioned before, it was reported that UV_{365} parameter represented aromatic moieties such as quinones, aromatic ketons, and polyphenols in humic chemical composition (Polewski et al., 2005) . The correlation between DOC concentration and UV_{365} parameter was presented by Equation 4.15 and FHA concentration represented as a function of UV_{365} parameter (Equation 4.16). The regression coefficient, was found to be as $R^2=0.995$ for Equation 4.15 and $R^2=0.999$ for Equation 4.16. Depending on these high regression coefficients, it could be inferred that UV_{365} parameter could be a good indicator of DOC concentration of FHA and good indicator of FHA concentration. DOC concentration was represented as a function of $Color_{436}$ parameter, which indicates the presence of color forming moieties in a humic acid structure, by Equation 4.17 and FHA concentration was represented as a function of $Color_{436}$ parameter by Equation 4.18. The regression coefficient, was found to be as $R^2=1.000$ (Equation 4.17) and $R^2=0.994$ (Equation 4.18). Depending on these high regression coefficients, it could be inferred that $Color_{436}$ parameter could be a good indicator of DOC concentration of FHA and good indicator of FHA concentration. These different UV absorbing centers and color forming chromophoric groups as expressed by various UV-vis spectroscopic parameters (UV_{254}, UV_{280}, UV_{365} and $Color_{436}$), exhibited dissolved organic carbon (DOC) in FHA with high regression coefficient results. In other words, these specified UV-vis parameters (UV_{254}, UV_{280}, UV_{365} and $Color_{436}$) could significantly indicate a good correlation with DOC contents due to the presence of sufficient-carbon contents that the achieved correlations represented by the regression coefficients close to $R^2 \leq 1$.

4.1.3. Humic Acid, Aldrich

For the basic characterization of humic acid (AHA, Aldrich), DOC concentrations as well as UV-vis (UV_{254}, UV_{280}, UV_{365} and $Color_{436}$) parameters were presented in Table 4.3. UV_{254} displayed a variation in range of 0.2398 cm^{-1} to 1.2620 cm^{-1}; UV_{280} exhibited a variation in range of 0.1961 cm^{-1} to 0.9850 cm^{-1}; UV_{365} displayed a variation in range of 0.1155 cm^{-1} to 0.7012 cm^{-1}.

Table 4.3. UV-vis Parameters and DOC Concentrations of Aldrich Humic Acid (AHA).

Aldrich Humic Acid					
HA, mg L^{-1}	DOC, mg L^{-1}	UV-vis parameters			
		UV_{254}, cm^{-1}	UV_{280}, cm^{-1}	UV_{365}, cm^{-1}	$Color_{436}$, cm^{-1}
10	3.330	0.2398	0.1961	0.1155	0.0405
20	6.940	0.4646	0.3811	0.2948	0.0820
30	10.97	0.7043	0.5452	0.3652	0.1411
40	15.48	0.9588	0.6874	0.4942	0.2580
50	19.49	1.2620	0.9850	0.7012	0.4310

Color forming moieties as expressed by $Color_{436}$ exhibited a range of 0.0405 cm^{-1} to 0.4310 cm^{-1}. DOC concentration displayed in the range of 3.330 mg L^{-1} to 19.49 mg L^{-1} for AHA concentration. Likewise to NHA, and FHA, the specified UV-vis parameters as UV_{254}, UV_{280}, UV_{365} and $Color_{436}$ and DOC concentrations showed absolute increasing trend with increasing concentration of the working Aldrich humic acid solutions as expected (Table 4.3). When AHA concentration was increased 5 times higher than its initial concentration, the increase in DOC concentration exhibited 17 % of its inital concentration, the increase in UV_{254} parameter displayed 19 % of its initial value, the increase in UV_{280} parameter exhibited 20 % of its initial value, the increase in UV_{365} parameter displayed 16 % of its initial value and the increase in $Color_{436}$ parameter displayed 26 % of its initial value. The humic acid (Aldrich) displayed DOC concentration in the range of 3.330 mg L^{-1} to 19.49 mg L^{-1}, representing approximately 30 % organic carbon.

4.1.3.1.The Relationship between HA and DOC Concentrations (Aldrich). According to the data presented in Table 4.3, HA concentrations of AHA (10 mg L^{-1}-50 mg L^{-1}) were correlated with the determined DOC concentrations (3.330 mg L^{-1}- 19.49 mg L^{-1}), corresponding to AHA (Figure 4.5).

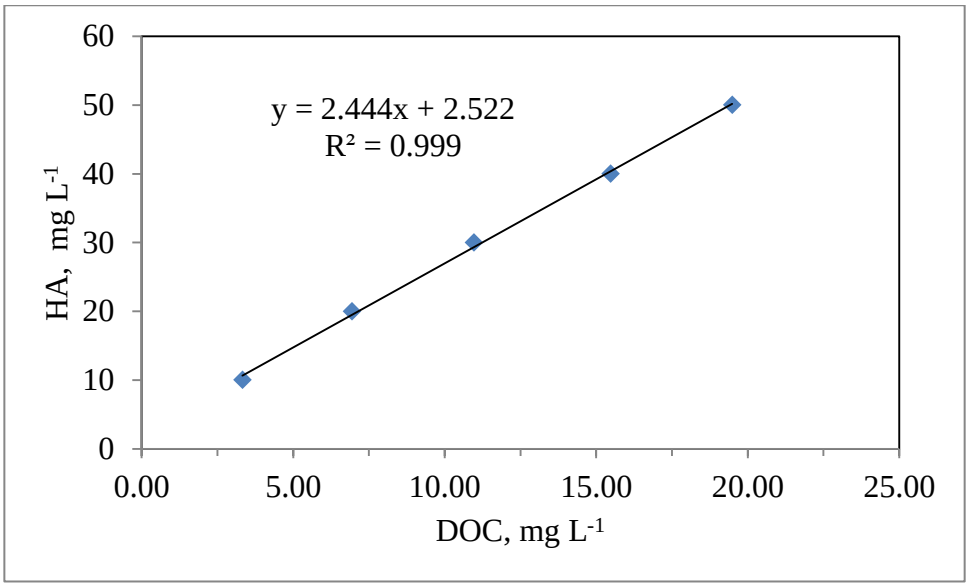

Figure 4.5. The correlation between HA and DOC concentrations of AHA.

More specifically, as shown in Table 4.3, it was observed that AHA concentration, studied in range of 10 and 50 mg L^{-1}, included 25-30 % DOC concentration. Humic substances account for 40-80 % of the dissolved organic matter in water. As a consequence, it could be inferred that DOC concentration, representing dissolved organic carbon in AHA, was lower than in NHA whereas, DOC concentration of AHA was closed to FHA.

$$HA\ (mg\ L^{-1}) = 2.444*DOC\ (mg\ L^{-1}) + 2.522 \quad R^2=0.999 \qquad (4.19)$$

Figure 4.5 illustrated the linear correlation between AHA and DOC concentrations of AHA. HA-DOC Equation produced from the least-squares regression analyses (Equation 19). The regression coefficient was found to be as R^2= 0.999 .

4.1.3.2. The Relationship between HA and DOC Concentrations of AHA and UV-vis Parameters. According to Table 4.3, the correlation curves between AHA concentrations and DOC concentrations of AHA and UV-vis parameters (UV_{254}, UV_{280}, UV_{365} and $Color_{436}$) were drawn in Figure 4.6. The linear equations, obtained the correlation between UV-vis parameters (UV_{254}, UV_{280}, UV_{365} and $Color_{436}$) and DOC concentration and also the correlation between UV-vis parameters and AHA concentration were listed below. DOC concentration was represented as a function of UV_{254} parameter, representing the natural organic matter content in humic acid (Najm et al., 1994) (Equation 4.20) and AHA concentration was represented as a function of UV_{254} parameter (Equation 4.21). The regression coefficient, was found to be as R^2=0.998 (Equation 4.20) and R^2=0.997 (Equation 4.21).

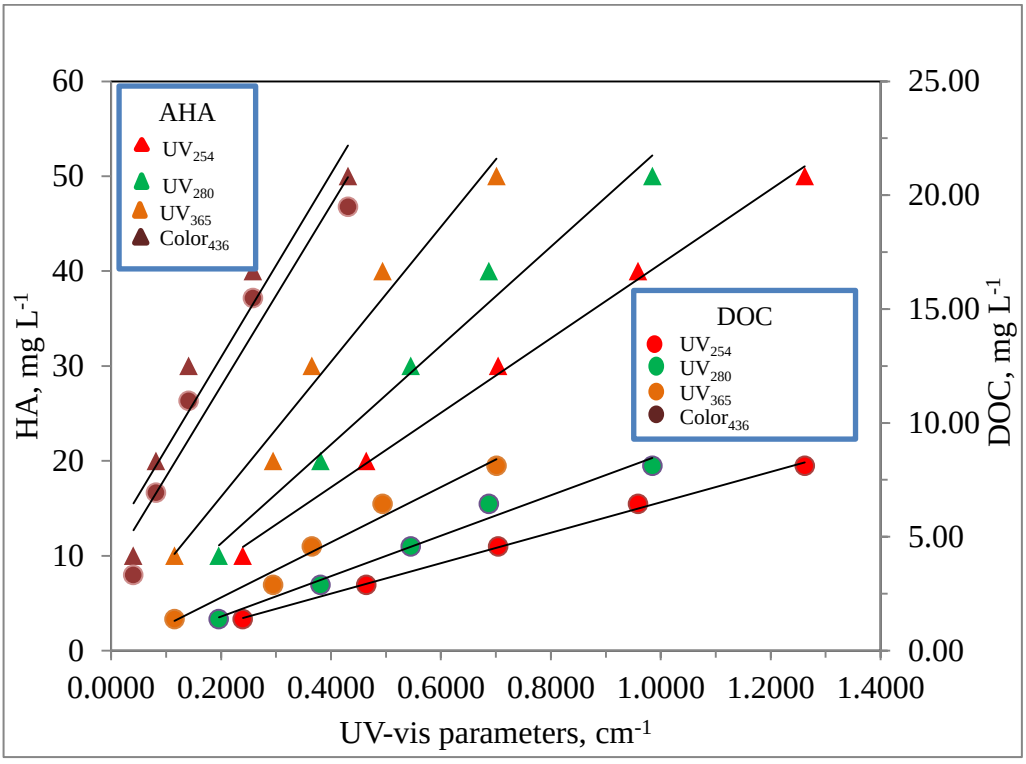

Figure 4.6. The correlation between HA, DOC concentrations of AHA and UV-vis parameters.

Depending on these high regression coefficients, it could be inferred that UV_{254} parameter was good indicator of DOC concentration of AHA and good indicator of AHA concentration. DOC concentration was represented as a function of UV_{280} parameter,

representing total aromaticity such as phenolic arenes, benzoic acids, aniline derivatives, polyenes and polycyclic aromatic hydrocarbons with two or more rings in a sample (Chin et al., 1994; Traina et al.,1990) (Equation 4.22) and AHA concentration was represented as a function of UV_{280} parameter (Equation 4.23). The regression coefficient, was found to be as R^2=0.981 (Equation 4.22) and R^2=0.982 (Equation 4.23). According to these high regression coefficients, it could be inferred that UV_{280} parameter was good indicator of DOC concentration of AHA and good indicator of AHA concentration. DOC concentration was represented as a function of UV_{365} parameter, representing aromatic moieties such as quinones, aromatic ketons and polyphenols in a sample (Polewski et al., 2005) (Equation 4.24) and AHA concentration was represented as a function of UV_{365} parameter (Equation 4.25). The regression coefficient, was found to be as R^2=0.973 (Equation 4.24) and R^2=0.975 (Equation 4.25). According to these high regression coefficients, it could be inferred that UV_{365} parameter was good indicator of DOC concentration of AHA and good indicator of AHA concentration.

$$DOC\ (mg\ L^{-1}) = 16.06*UV_{254}\ (cm^{-1}) - 0.415 \qquad R^2=0.998 \qquad (4.20)$$

$$HA\ (mg\ L^{-1}) = 39.26*UV_{254}\ (cm^{-1}) + 1.504 \qquad R^2=0.997 \qquad (4.21)$$

$$DOC\ (mg\ L^{-1}) = 21.30*UV_{280}\ (cm^{-1}) - 0.661 \qquad R^2=0.981 \qquad (4.22)$$

$$HA\ (mg\ L^{-1}) = 52.12*UV_{280}\ (cm^{-1}) + 0.867 \qquad R^2=0.982 \qquad (4.23)$$

$$DOC\ (mg\ L^{-1}) = 29.05*UV_{365}\ (cm^{-1}) - 0.209 \qquad R^2=0.973 \qquad (4.24)$$

$$HA\ (mg\ L^{-1}) = 71.16*UV_{365}\ (cm^{-1}) + 1.951 \qquad R^2=0.975 \qquad (4.25)$$

$$DOC\ (mg\ L^{-1}) = 39.72*Color_{436}\ (cm^{-1}) + 3.674 \qquad R^2=0.935 \qquad (4.26)$$

$$HA\ (mg\ L^{-1}) = 96.56*Color_{436}\ (cm^{-1}) + 11.60 \qquad R^2=0.924 \qquad (4.27)$$

DOC concentration was represented as a function of $Color_{436}$ parameter, representing color forming moieties (Equation 4.26) and AHA concentration was represented as a function of $Color_{436}$ parameter (Equation 4.27). The regression coefficient, was found to be as R^2=0.935 (Equation 4.26) and R^2=0.924 (Equation 4.27). Depending on these high regression coefficients, it could be inferred that $Color_{436}$ parameter was good indicator of DOC concentration of AHA and good indicator of AHA concentration. These various aromatic moieties absorbing various UV-vis parameter (UV_{254}, UV_{280}, UV_{365} and $Color_{436}$), exhibited dissolved organic carbon in AHA with high regression coefficient results. In other words, these specified UV-vis parameters (UV_{254}, UV_{280}, UV_{365} and

$Color_{436}$) could significantly indicate a good correlation with DOC contents due to the presence of sufficient-carbon-contents that the achieved correlations represented by the regression coefficients close $R^2 \leq 1$.

4.1.3.3. Humic Acid (pH:4.5-8.15) (Aldrich) (Al-Rasheed- et al., 2003a). As showed below, the correlation studies were done in similar pH conditions (neutral media). A pH dependent data was applied for the correlation between UV-vis parameter (UV_{254} and $Color_{400}$) and DOC concentration. This correlation result was evaluated for the different pH condition. The researcher reported the study on the photocatalytic oxidation of AHA in artificial seawater (Al-Rasheed et al., 2003a). The aim was to establish whether photocatalytic treatment of saline waters could minimize dissolved organic matter, and lead to less toxic by-products. AHA, used for these experiments, was not completely soluble in water.

Table 4.4. DOC, UV_{254} and $Color_{400}$ parameters of Aldrich humic acid taken from Al-Rasheed et al., 2003a.

Humic Acid, Aldrich*				
DOC mg L^{-1}	UV-vis parameters			
	UV_{254}, cm^{-1}	$Color_{400}$, cm^{-1}	UV_{254}, cm^{-1}	$Color_{400}$, cm^{-1}
	pH=4.5		pH=8.15	
2.86	0.21	-	0.21	--
10.48	0.87	0.11	0.68	0.11
22.86	1.50	0.21	1.42	0.16
33.33	2.15	0.37	2.21	0.26
40.95	2.84	0.53	2.84	0.37
51.43	3.31	0.68	3.37	0.53
64.76	3.47	0.84	3.52	0.63

* Al-Rasheed et al., 2003a.

AHA solution was prepared by dissolving AHA in artifial seawater. Prior to applying the photocatalytic treatment of humic acid (AHA), DOC concentration of AHA were correlated with UV_{254} parameter, corresponding to DOC concentrations of AHA in both acidic (pH=4.5), and alkaline media (pH=8.15). DOC concentrations were determined by

the high temperature combustion method, using a Shimadzu Model TOC-5000 and also, UV/VIS spectra were recorded on a Kontron Uvikon-860 instrument in quartz cells for the determination of UV_{254} and $Color_{400}$ parameter. Moreover, DOC concentrations of AHA were correlated with $Color_{400}$ parameter in both acidic and alkaline media. DOC concentrations of AHA was between 2.86 mg L^{-1} and 64.76 mg L^{-1}, UV_{254} parameter, corresponding to DOC concentrations, was between 0.21 cm^{-1} and 3.47 cm^{-1} at pH 4.5; was between 0.21 cm^{-1} and 3.52 cm^{-1} at pH 8.15. $Color_{400}$ parameter, corresponding to DOC concentration (2.86 mg L^{-1}- 64.76 mg L^{-1}), was between 0.00 cm^{-1} and 0.84 cm^{-1} at pH 4.5; was between 0.00 cm^{-1} and 0.63 cm^{-1} at pH 8.15 (Table 4.4). According to the data given in Table 4.4, UV_{254} parameter exhibited the same absorbance parameter at both acidic and alkaline condition for DOC concentration of 2.86 mg L^{-1}, UV_{254} parameter at alkaline condition, displayed 78 % UV_{254} parameter at acidic condition for DOC concentration of 10.48 mg L^{-1}, UV_{254} parameter at alkaline condition, displayed 95 % UV_{254} parameter at acidic condition for DOC concentration of 22.86 mg L^{-1}, UV_{254} parameter at acidic condition, exhibited 97 % UV_{254} parameter at alkaline condition for DOC concentration of 33.33 mg L^{-1}, UV_{254} parameter at acidic condition, exhibited 100 % UV_{254} parameter at alkaline condition for DOC concentration of 40.95 mg L^{-1}, UV_{254} parameter at acidic condition, exhibited 98 % UV_{254} parameter at alkaline condition for DOC concentration of 51.43 mg L^{-1}, and UV_{254} parameter at acidic condition, exhibited 99 % UV_{254} parameter at alkaline condition for DOC concentration of 64.76 mg L^{-1}. $Color_{400}$ parameter at alkaline condition, displayed 100 % $Color_{400}$ parameter at acidic condition for DOC concentration of 10.48 mg L^{-1}, $Color_{400}$ parameter at alkaline condition, displayed 76 % $Color_{400}$ parameter at acidic condition for DOC concentration of 22.86 mg L^{-1}, $Color_{400}$ parameter at alkaline condition, displayed 70 % $Color_{400}$ parameter at acidic condition for DOC concentration of 33.33 mg L^{-1}, $Color_{400}$ parameter at alkaline condition, displayed 70 % $Color_{400}$ parameter at acidic condition for DOC concentration of 40.95 mg L^{-1}, $Color_{400}$ parameter at alkaline condition, displayed 78 % $Color_{400}$ parameter at acidic condition for DOC concentration of 51.43 mg L^{-1}, and $Color_{400}$ parameter at alkaline condition, displayed 75 % $Color_{400}$ parameter at acidic condition for DOC concentration of 64.76 mg L^{-1}.

4.1.3.4.The Relationship between DOC Concentrations of AHA and UV-vis Parameters.

According to the data, given in Table 4.4, DOC concentrations of AHA were correlated

with UV-vis parameters (UV_{254} and $Color_{400}$) with respect to pH conditions (pH= 4.5-8.15) (Table 4.7). UV_{254} parameter data, exhibited in range of 0.21 cm^{-1} to 3.47 cm^{-1}, was plotted against DOC concentration, studied in range of 2.86 mg L^{-1} to 64.76 mg L^{-1}, at pH=4.5, UV_{254} parameter data, displayed in range of 0.21 cm^{-1} to 3.52 cm^{-1}, was plotted against DOC concentration of AHA, studied in range of 2.86 mg L^{-1} to 64.76 mg L^{-1} at pH=8.15, $Color_{400}$ parameter data, exhibited in range of 0.00 cm^{-1} to 0.84 cm^{-1}, was plotted against DOC concentration of AHA at pH=4.5 and $Color_{400}$ parameter data, displayed in range of 0.00 cm^{-1} to 0.63 cm^{-1}, was plotted against DOC concentration of AHA at pH=8.15 in Figure 4.7.

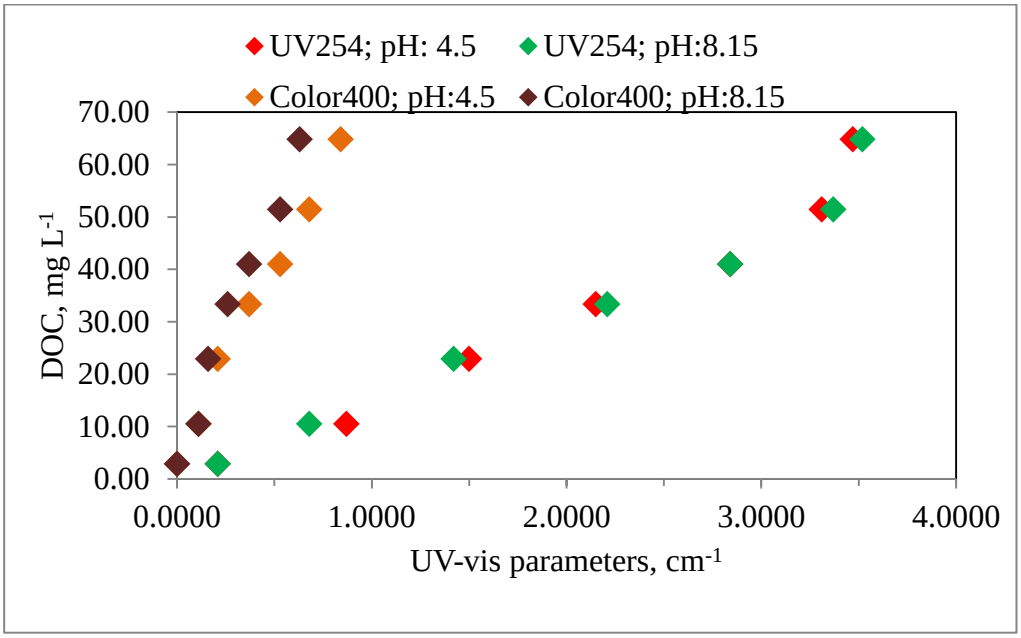

Figure 4.7. The relationship between DOC concentrations of AHA and UV-vis parameters (pH:4.5; pH:8.15).

Equation 4.28 was attained from the correlation between UV_{254} parameter and DOC concentration at acidic condition (pH=4.5), Equation 4.29 was obtained from the correlation between UV_{254} parameter and DOC concentration at alkaline condition (pH=8.15), Equation 30 was attained from the correlation between $Color_{400}$ parameter and DOC concentration at acidic condition (pH=4.5) and Equation 4.31 was obtained from the correlation between $Color_{400}$ parameter and DOC concentration at alkaline condition (pH=8.15). As seen below, the linear correlation equations displayed very high correlation

coefficients (Equation 4.28, R^2=0.965; Equation 4.29, R^2=0.967; Equation 4.30, R^2=0.990; Equation 4.31, R^2=0.978) irrespective of the pH of the reaction medium.

DOC (mg L^{-1}) = 17.41*UV_{254} (cm^{-1}) – 3.310	(pH:4.5)	R^2=0.965	(4.28)
DOC (mg L^{-1}) = 16.65*UV_{254} (cm^{-1}) – 1.508	(pH:8.15)	R^2=0.967	(4.29)
DOC (mg L^{-1}) = 71.35*$Color_{400}$ (cm^{-1}) + 4.452	(pH:4.5)	R^2=0.990	(4.30)
DOC (mg L^{-1}) = 95.54*$Color_{400}$ (cm^{-1}) + 4.264	(pH:8.15)	R^2=0.978	(4.31)

Considering a representative AHA solution expressing UV_{254}=0.5000 cm^{-1} and $Color_{400}$=0.1000 cm^{-1} the DOC contents could be calculated as 5.395 mg L^{-1} (UV_{254}, Equation 4.28), 11.59 mg L^{-1} ($Color_{400}$, Equation 4.30) at pH=4.5 and 6.817 mg L^{-1} (UV_{254}, Equation 4.29), 13.82 mg L^{-1} ($Color_{400}$, Equation 4.31) at pH 8.15, difference in DOC, whereas AHA at neutral pH conditions exhibited 7.615 mg L^{-1} DOC. According to these results, the highest DOC result exhibited in neutral media, whereas the lowest DOC result displayed in acidic media for UV_{254} parameter. Moreover, DOC result in alkaline media exhibited more than DOC result in acidic media for $Color_{400}$ parameter. According to these results, DOC concentration as a function of UV_{254} parameter and $Color_{400}$ parameter, exhibited different values in the different pH media. One of the reason could be the behavior of functional groups depending on pH media. As mentioned before, humic acids can include the different types of functional groups mainly expressed by carboxylic and phenolic groups. These functional groups consist of organic carbon and as the pH alters, the structure of these functional group could change, as well through deprotonation and protonation equilibrium. As a consequence, the alteration in the functional groups could cause the structural and conformational changes in a humic acid sample. Moreover,the change in pH could also affect the absorption profile of humic acid expressed by UV_{254} parameter and $Color_{400}$ parameter. The aromatic moieties, absorbing UV_{254} parameter, and the color forming moieities, absorbing $Color_{400}$ parameter, could display the different value of UV-vis parameter in acidic, neutral and alkaline media. DOC concentration, as a function of UV_{254} and $Color_{400}$ parameter, exhibited the different value, depending on the pH media. It could be inferred that pH could affect DOC concentration in humic acid and the absorbance of humic acid in UV-vis parameter.

4.1.4. Humic Acid, Roth

For the basic characterization of humic acid (RHA, Roth), DOC concentrations as well as UV-vis (UV_{254}, UV_{280}, UV_{365} and $Color_{436}$) parameters were showed with respect to RHA concentration in the range of 2.5 mg L^{-1} – 50 mg L^{-1} in Table 4.5. Likewise NHA, FHA, and AHA, UV_{254}, UV_{280}, UV_{365} and $Color_{436}$ parameters and DOC concentrations indicated an absolute increasing trend with increasing of studied humic acid concentrations of RHA (Table 4.5).

Table 4.5. UV-vis Parameters and DOC Concentrations of Roth Humic Acid (RHA).

Roth Humic Acid					
HA, mg L^{-1}	DOC, mg L^{-1}	UV-vis parameters			
		UV_{254}, cm^{-1}	UV_{280}, cm^{-1}	UV_{365}, cm^{-1}	$Color_{436}$, cm^{-1}
2.5	1.650	0.0850	0.0520	0.0420	0.0310
5	3.240	0.1870	0.1600	0.1010	0.0580
10	6.670	0.3730	0.3200	0.2000	0.1170
20	10.50	0.7340	0.6280	0.3960	0.2320
30	15.30	1.1090	0.9850	0.5990	0.3480
40	20.10	1.4660	1.2300	0.7710	0.4500
50	24.70	1.9120	1.6430	1.0250	0.6030

The humic acid (Roth) displayed DOC concentration in the range of 3.240 mg L^{-1} to 24.70 mg L^{-1}, representing approximately 50 % organic carbon. When RHA was increased 20 times of its value, the increase in UV_{254} parameter exhibited 4 % of its initial value, the increase in UV_{280} parameter displayed 3 % of its initial value, the increase in UV_{365} parameter exhibited 4 % of its initial value and the increase in $Color_{436}$ parameter exhibited 5 % of its value (Table 4.5).

4.1.4.1.The Relationship between HA and DOC Concentrations (Roth). According to Table 4.5, HA concentrations of RHA were correlated with DOC concentrations, corresponding to RHA concentration (Figure 4.8).

As shown in Table 4.5, it was observed that DOC concentration represented 50 % of RHA concentration, studied in range of 2.5 mg L^{-1} to 50 mg L^{-1}. Humic substances account for 40-80% of the dissolved organic matter in water, as a consequence, this result was consistent with this explanation.

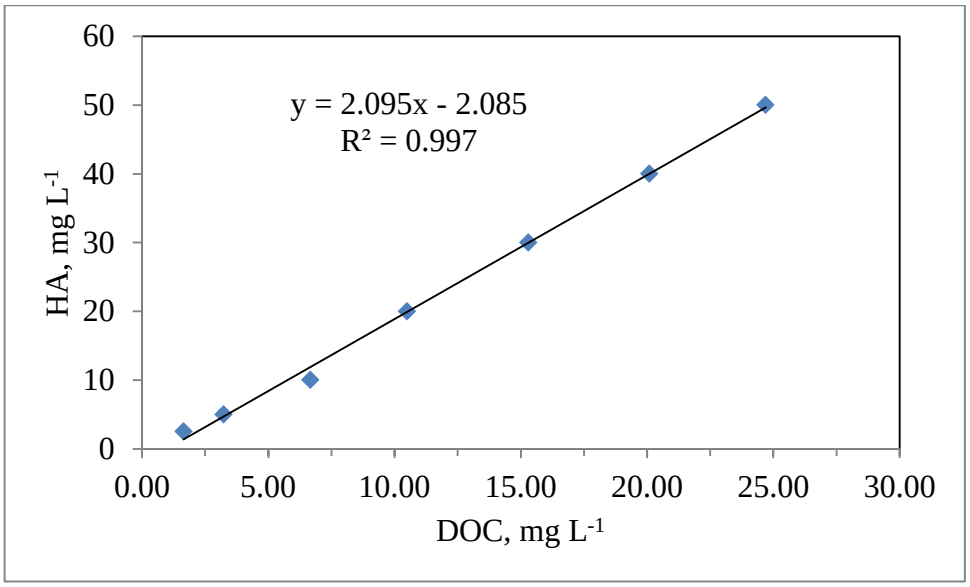

Figure 4.8. The correlation between HA and DOC concentrations of RHA.

It could be inferred that DOC concentration, representing dissolved organic carbon in RHA, was similar to NHA and higher than FHA and AHA. Likewise to NHA, FHA and AHA, RHA concentration was correlated with DOC concentration of RHA. Figure 4.8 illustrated the linear correlation between RHA concentration and DOC concentration of RHA.

$$HA\ (mg\ L^{-1}) = 2.095*DOC\ (mg\ L^{-1}) - 2.085 \qquad R^2=0.997 \qquad (4.32)$$

HA-DOC Equation was produced from the least-squares regression analyses (Equation 4.32). The regression coefficient was found to be as R^2= 0.997.

4.1.4.2. The Relationship between HA and DOC Concentrations of RHA and UV-vis Parameters. According to the information presented in Table 4.5, the correlation curves

constructed between HA concentration and DOC concentration of RHA and the respective UV-vis parameters (UV_{254}, UV_{280}, UV_{365} and $Color_{436}$) were presented in Figure 4.9.

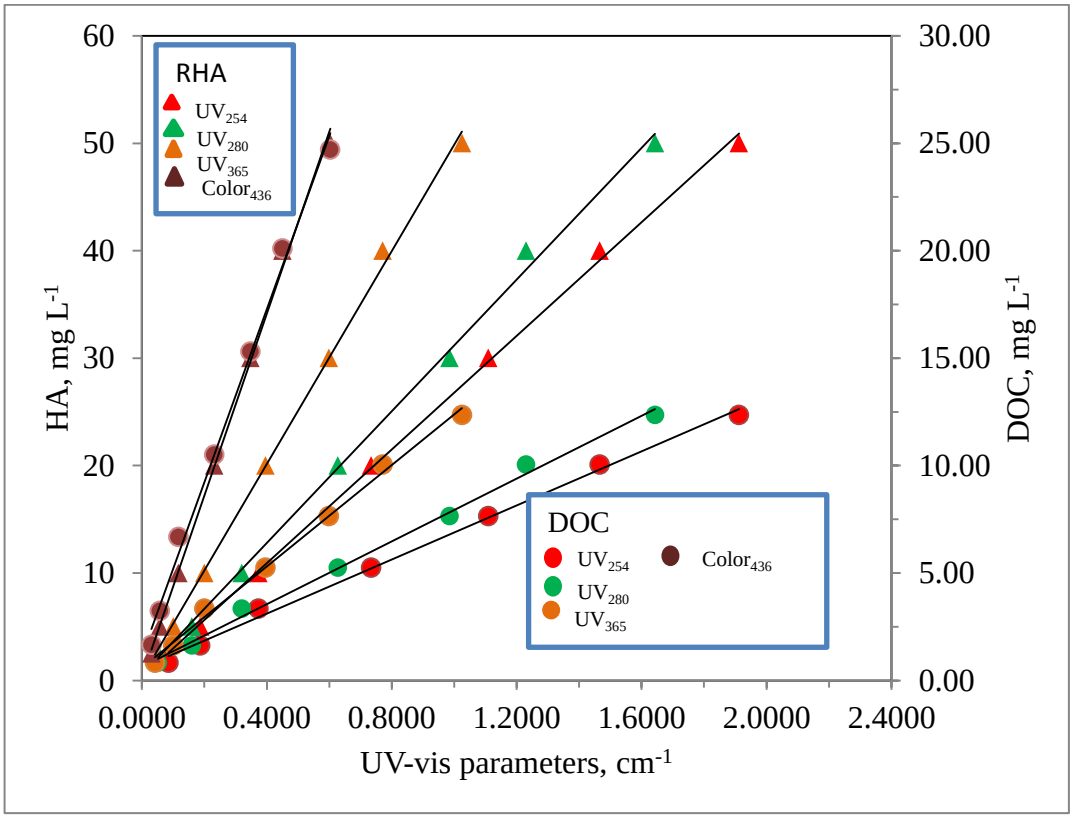

Figure 4.9. The correlation between HA, DOC concentrations of RHA and UV-vis parameters.

The linear equations, obtained the correlation between UV-vis parameters (UV_{254}, UV_{280}, UV_{365} and $Color_{436}$) and DOC concentration of RHA and the correlation between UV-vis parameters and RHA concentration were listed below. DOC concentration was represented as a function of UV_{254} parameter, representing the natural organic matter content in humic acid (Najm et al., 1994) (Equation 4.33) and RHA concentration was represented as a function of UV_{254} parameter (Equation 4.34). The regression coefficient, was found to be as R^2=0.996 (Equation 4.33) and R^2=0.999 (Equation 4.34). Depending on these regression coefficients, it could be inferred that UV_{254} parameter was good indicator of DOC concentration of RHA and good indicator of RHA concentration. DOC concentration was represented as a function of UV_{280} parameter, representing total aromaticity such as phenolic arenes, benzoic acids, aniline derivatives, polyenes and

polycyclic aromatic hydrocarbons with two or more rings in a sample (Chin et al., 1994; Traina et al.,1990) (Equation 4.35) and RHA concentration was represented as a function of UV_{280} parameter (Equation 4.36). The regression coefficient, was found to be as R^2=0.996 (Equation 4.35) and R^2=0.998 (Equation 4.36). According to these regression coefficients, it could be inferred that UV_{280} parameter was good indicator of DOC concentration of RHA and good indicator of RHA concentration.

$$DOC\ (mg\ L^{-1}) = 12.59*UV_{254}\ (cm^{-1}) + 1.185 \qquad R^2=0.996 \qquad (4.33)$$

$$HA\ (mg\ L^{-1}) = 26.45*UV_{254}\ (cm^{-1}) + 0.339 \qquad R^2=0.999 \qquad (4.34)$$

$$DOC\ (mg\ L^{-1}) = 14.60*UV_{280}\ (cm^{-1}) + 1.272 \qquad R^2=0.996 \qquad (4.35)$$

$$HA\ (mg\ L^{-1}) = 30.65*UV_{280}\ (cm^{-1}) + 0.529 \qquad R^2=0.998 \qquad (4.36)$$

$$DOC\ (mg\ L^{-1}) = 23.57*UV_{365}\ (cm^{-1}) + 1.183 \qquad R^2=0.996 \qquad (4.37)$$

$$HA\ (mg\ L^{-1}) = 49.51*UV_{365}\ (cm^{-1}) + 0.336 \qquad R^2=0.998 \qquad (4.38)$$

$$DOC\ (mg\ L^{-1}) = 40.35*Color_{436}\ (cm^{-1}) + 1.136 \qquad R^2=0.994 \qquad (4.39)$$

$$HA\ (mg\ L^{-1}) = 84.77*Color_{436}\ (cm^{-1}) + 0.229 \qquad R^2=0.998 \qquad (4.40)$$

DOC concentration was represented as a function of UV_{365} parameter, representing aromatic moieties such as quinones, aromatic ketons and polyphenols in a sample (Polewski et al., 2005) (Equation 37) and RHA concentration was represented as a function of UV_{365} parameter (Equation 38). The regression coefficient, was found to be as R^2=0.996 (Equation 4.37) and R^2=0.998 (Equation 4.38). According to these regression coefficients, it could be inferred that UV_{365} parameter was good indicator of DOC concentration of AHA and good indicator of RHA concentration. DOC concentration was represented as a function of $Color_{436}$ parameter, representing color forming moieties (Equation 4.39) and RHA concentration was represented as a function of $Color_{436}$ parameter (Equation 4.40). The regression coefficient, was found to be as R^2=0.994 (Equation 4.39) and R^2=0.998 (Equation 4.40). Depending to these regression coefficients, it could be inferred that $Color_{436}$ parameter was good indicator of DOC concentration of RHA and good indicator of RHA concentration. These various aromatic moieties absorbing various UV-vis parameters (UV_{254}, UV_{280}, UV_{365} and $Color_{436}$), exhibited dissolved organic carbon in RHA with high regression coefficient results. In other words, these specified UV-vis parameters (UV_{254}, UV_{280}, UV_{365} and $Color_{436}$) could significantly indicate a good correlation with DOC contents due to the presence of sufficient-carbon contents that the

achieved correlations represented by the regression coefficients close to $R^2 \leq 1$. As mentioned above, the curves, representative of the correlation between Nordic humic acid and UV-vis parameters, were characterized by highly aromatic components with high relative UV_{254} parameter, UV_{280} parameter, UV_{365} parameter and by highly color forming components with high $Color_{436}$ parameter (Figure 4.2). Similar to Nordic humic acid, the curves, obtained from the correlation between each humic acid (Fluka, Aldrich and Roth) and UV-vis parameters, were emphasized strong aromatic character with high relative UV_{254} parameter, UV_{280} parameter, UV_{365} parameter and were characterized by highly color forming components with high $Color_{436}$ parameter (Figure 4.4, Figure 4.6 and Figure 4.9).

4.2. Comparative Evaluation of the Correlations Attained between Humic Acid Concentration and DOC Concentration of NHA, FHA, AHA and RHA in relation to their respective UV-vis Parameters

The origin of humic acids were divided into two parts, namenly terrestrial and aquatic humic acids. It was compared functional group contents of humic materials of both terrestrial and aquatic origins (Visser et al., 1982). It was observed that aquatic humic acids contained more COOH and fewer phenolic OH groups than their terrestrial counterparts. Fluka humic acid and Roth humic acid and Aldrich humic acid were terrestrial origin, whereas Nordic humic acid was aquatic origin. DOC concentrations, corresponding to the studied overall humic acid solutions, were correlated with these humic acid solutions (NHA, FHA, AHA and RHA). UV-vis parameters (UV_{254}, UV_{280}, UV_{365} and $Color_{436}$), corresponding to the studied overall humic acid solutions, were correlated with these humic acid solutions, and DOC concentrations of the humic acid solutions.

4.2.1.The Relationship between HA Concentrations and DOC Concentrations of NHA, FHA, AHA and RHA

The studied humic acid concentrations, including the overall types, were correlated with dissolved organic carbon concentrations corresponding to these humic acids (Figure 4.11). DOC concentrations were between 1.650 mg L^{-1} and 24.70 mg L^{-1} for RHA (Table 4.5), between 3.780 mg L^{-1} and 20.30 mg L^{-1} for FHA (Table 4.2), between 5.450 mg L^{-1}

and 23.01 mg L^{-1} for NHA (Table 4.1), between 3.33 mg L^{-1} and 19.49 mg L^{-1} for AHA (Table 4.3).

As mentioned before, NHA, FHA and AHA concentration was studied in range of 10 to 50 mg L^{-1} and RHA concentration was also studied in 2.5 mg L^{-1} and .5 mg L^{-1}. The relationship between the overall humic acids (NHA, FHA, AHA and RHA) and DOC concentration were presented in Figure 4.10. DOC concentration of AHA exhibited 61 %, 88 %, and 50 % DOC concentration of NHA, FHA and RHA for 10 mg L^{-1} of HA concentration. Moreover, DOC concentration of AHA displayed 85 %, 96 % and 79 % DOC concentration of NHA, FHA and RHA for 50 mg L^{-1} of HA concentration.

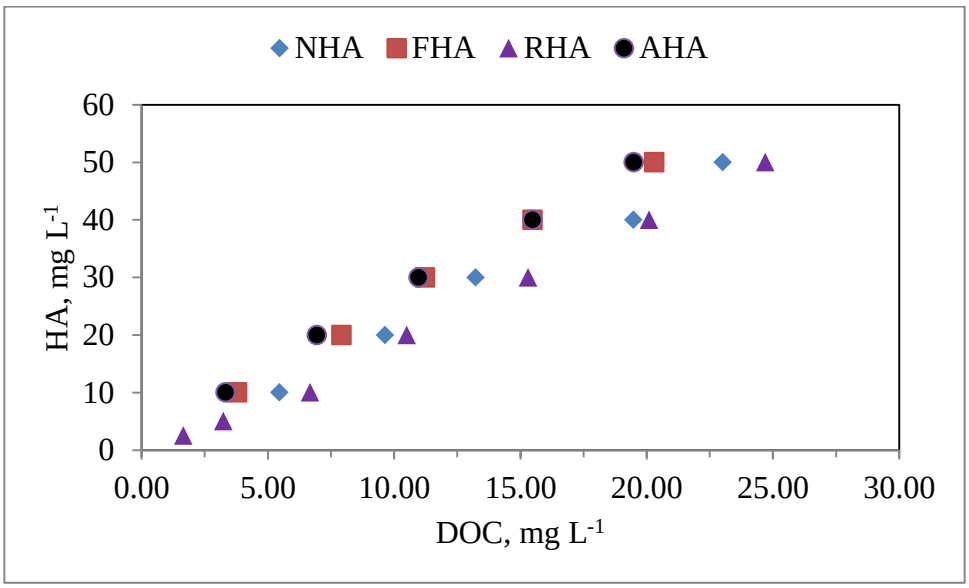

Figure 4.10. The relationship between HA and DOC concentrations of NHA, FHA, AHA, and RHA.

As mentioned below, the slope of the curves, representing the relationship between DOC concentration and the overall humic acids followed decreasing trend, AHA>FHA>NHA>RHA under the same DOC concentrations (Figure 4.10). For the same DOC concentrations, AHA exhibited the highest HA concentration, whereas RHA displayed the lowest HA concentration.

$$HA\ (mg\ L^{-1}) = 2.201*DOC\ (mg\ L^{-1}) + 0.811 \qquad R^2=0.936 \qquad (4.41)$$

The correlations between humic acid concentration and DOC contents were presented for Nordic HA by Equation 4.1 (R^2=0.992), for Fluka HA by Equation 4.10 (R^2=0.996), for Aldrich HA by Equation 4.19 (R^2=0.999) and for Roth HA by Equation 4.32 (R^2=0.997). The overall correlation composed of all of the studied humic acid samples (NHA, FHA, AHA and RHA) were presented by the linear Equation 4.41. A linear relationship between DOC concentration, corresponding to HA concentration, and HA concentration for the overall humic acids (NHA, FHA, AHA and RHA) with a high correlation (R^2=0.936) was attained.

4.2.2. The Relationship between HA Concentrations and UV_{254} Parameter of NHA, FHA, AHA and RHA.

In Figure 4.11, the working solutions of the overall humic acid (2.5 to 50 mg L^{-1}) were plotted against the specific absorption UV range (UV_{254}). The data expressed UV_{254} parameter, corresponding HA concentrations, in Table 4.1 for NHA, in Table 4.2 for FHA, in Table 4.3 for AHA and in Table 4.5 for RHA were used in graph.

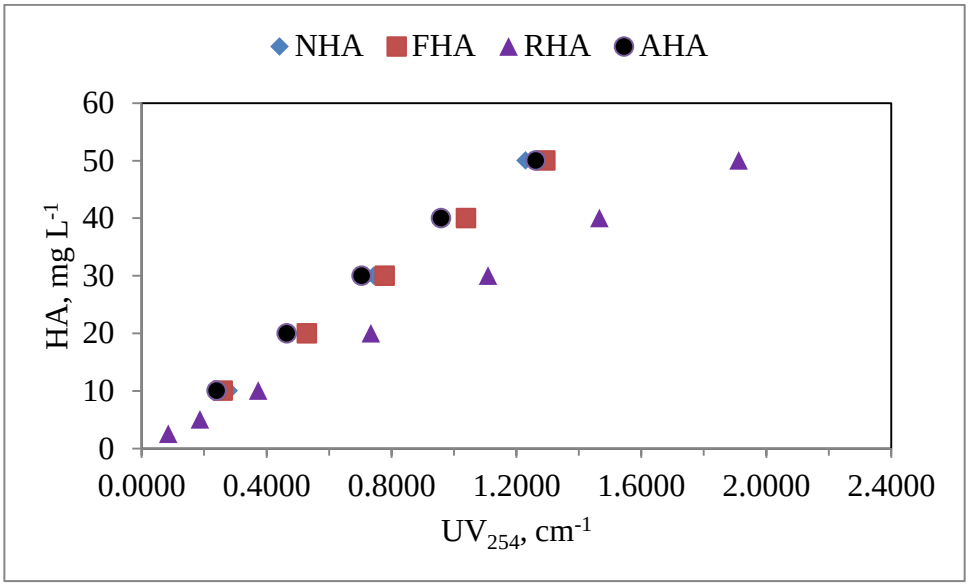

Figure 4.11. The relationship between HA concentrations and UV_{254} of NHA, FHA, AHA and RHA.

According to the data given in Table 4.1 (NHA), Table 4.2 (FHA), Table 4.3 (AHA) and Table 4.5 (RHA), UV_{254} parameter of AHA exhibited 86 %, 92 % and 64 % UV_{254} parameter of NHA, FHA, and RHA for 10 mg L^{-1} of HA concentration. UV_{254} parameter of AHA displayed 99 %, 88 %, and 63 % UV_{254} parameter of NHA, FHA and RHA for 20 mg L^{-1} of HA concentration. UV_{254} parameter of AHA exhibited 95 %, 91 % and 64 % UV_{254} parameter of NHA, FHA and RHA for 30 mg L^{-1} of HA concentration. UV_{254} parameter of AHA displayed 92 %, 92 % and 65 % UV_{254} parameter of NHA, FHA and RHA for 40 mg L^{-1} of HA and UV_{254} parameter of NHA exhibited 95 %, 97 % and 64 % UV_{254} parameter of FHA, AHA and RHA for 50 mg L^{-1} of HA concentration. The curves, representing the relationship between UV_{254} parameter and the overall humic acids, were examined. According to 4.11, the curve, representing the relationship between UV_{254} parameter and AHA, was the highest, whereas the curve, representing the relationship between UV_{254} parameter and RHA, was the lowest for the same UV_{254} parameter.

The correlations between humic acid concentration and UV_{254} parameter were presented for Nordic HA by Equation 4.3 (R^2= 0.994), for Fluka HA by Equation 4.12 (R^2= 1.000), for Aldrich HA by Equation 4.21 (R^2= 0.997) and for Roth HA (R^2= 0.999) by Equation 4.34.

$$HA\ (mg\ L^{-1}) = 30.77 * UV_{254}\ (cm^{-1}) + 3.621 \qquad R^2=0.866 \qquad (4.42)$$

The overall correlation composed of all of the studied humic acid samples were presented by the linear Equation 4.42. The relationship between UV_{254} parameter and HA concentration for the overall humic acids (NHA, FHA, AHA and RHA) was obtained with a good correlation (R^2=0.866). This result showed that UV_{254} parameter, representing the natural organic matter in HA, was good indicator of HA concentration for the overall humic acids (NHA, FHA, AHA and RHA).

4.2.3. The Relationship between DOC Concentrations and UV_{254} Parameter of NHA, FHA, AHA and RHA.

Figure 5.3 showed DOC concentrations as a function of the change in UV_{254} parameters for the specified types of humic acids. DOC concentration of NHA (Table 4.1),

FHA (Table 4.2), AHA (Table 4.3) and RHA (Table 4.5) and UV_{254} parameter, corresponding to these DOC concentrations were used in graph (Figure 4.12).

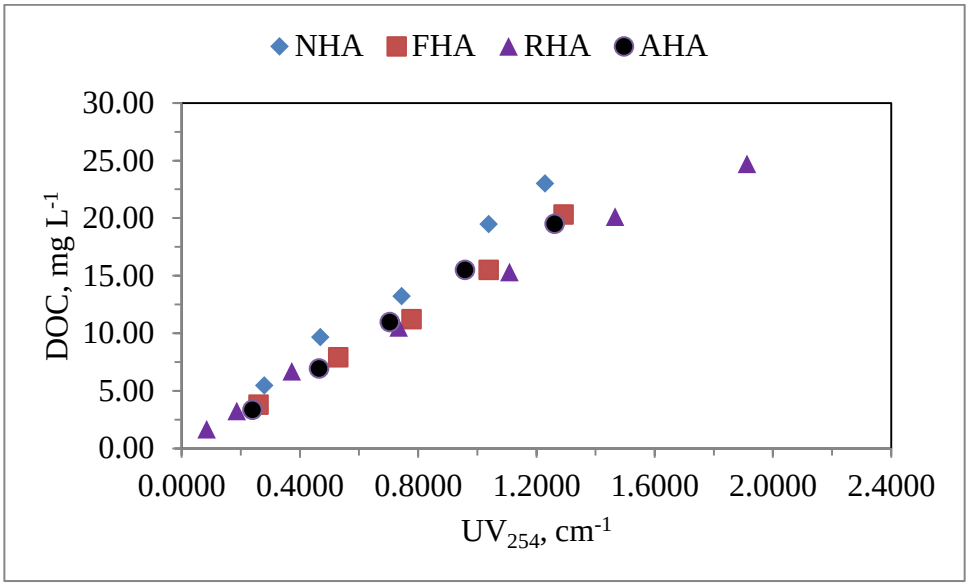

Figure 4.12. The relationship between UV_{254} parameter and DOC concentrations of NHA, FHA, AHA and RHA.

As seen in Figure 4.12, the curves, obtained from the correlation between UV_{254} parameter and the overall humic acids (NHA, FHA, AHA and RHA), were examined. Depending on Figure 4.12, NHA exhibited the highest DOC concentration whereas, RHA displayed the lowest DOC concentration for the same UV_{254} parameter. On the other hand, AHA and FHA exhibited very close slope to each other for the same UV_{254} parameter. The correlations between DOC contents and UV_{254} parameter were presented for Nordic HA by Equation 4.2 (R^2= 0.995), for Fluka HA by Equation 4.11 (R^2=0.995), for Aldrich HA by Equation 4.20 (R^2= 0.998), and for Roth HA (R^2= 0.996) by Equation 4.33. The overall correlation composed of all of the studied humic acid samples were presented by the linear Equation 4.43. The relationship between UV_{254} parameter and DOC concentration of the overall humic acids was attained with a high correlation (R^2=0.936).

$$DOC\ (mg\ L^{-1}) = 14.06 * UV_{254}\ (cm^{-1}) + 1.215 \qquad R^2=0.936 \qquad (4.43)$$

This result demostrated that UV_{254} parameter was a good indicator of DOC concentration for the overall humic acids. Moreover, as mentioned above, the correlation coefficient, obtained from the correlation between UV_{254} parameter and DOC concentration of NHA, FHA, AHA and RHA were found to be as R^2=0.995, R^2=0.995, R^2=0.998 and R^2=0.996, respectively. It could be concluded that even though, humic acids belong to the different types of origin, the result point out that UV_{254} parameter could predict DOC content well, in these humic acids (NHA, FHA, AHA and RHA).

4.2.4. The Relationship between HA Concentrations and UV_{280} Parameter of NHA, FHA, AHA and RHA.

In Figure 4.13, the working solutions of the overall humic acid (2.5 to 50 mg L^{-1}) were plotted against the specific absorption UV range (UV_{280}). The data expressed UV_{280} parameter, corresponding HA concentrations, in Table 4.1 for NHA, in Table 4.2 for FHA, in Table 4.3 for AHA and in Table 4.5 for RHA were used in graph.

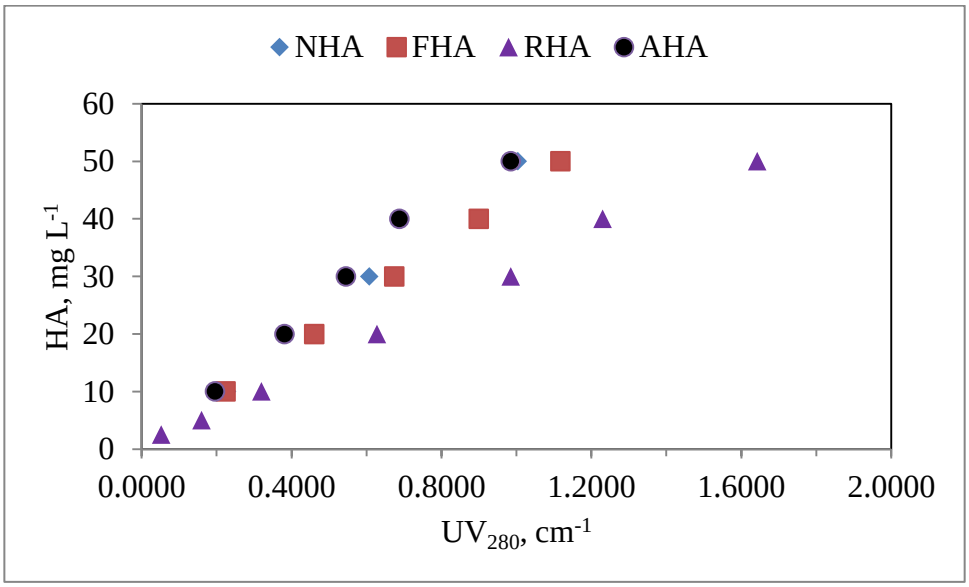

Figure 4.13. The relationship between HA concentrations and UV_{280} parameter of NHA, FHA, AHA, RHA.

According to the data given in Table 4.1 (NHA), Table 4.2 (FHA), Table 4.3 (AHA) and Table 4.5 (RHA), UV_{280} parameter of AHA exhibited 86 %, 88 % and 61 % of NHA,

FHA and RHA, respectively, for 10 mg L^{-1} of HA concentration. UV_{280} parameter of AHA displayed 99 %, 83 % and 61 % UV_{280} parameter of NHA, FHA and RHA, respectively, for 20 mg L^{-1} of HA concentration. UV_{280} parameter of AHA exhibited 90 %, 81 % and 55 % UV_{280} parameter of NHA, FHA and RHA, respectively, for 30 mg L^{-1} of HA concentration, UV_{280} parameter of AHA displayed 76 %, 76 % and 56 % UV_{280} parameter of NHA, FHA and RHA, respectively, for 40 mg L^{-1} of HA concentration and UV_{280} parameter of AHA exhibited 98 %, 88 % and 60 % UV_{280} parameter of NHA, FHA and RHA, respectively, for 50 mg L^{-1} of HA concentration.

As mentioned above (Figure 4.13), the slope of the curve, representing the relationship between UV_{280} parameter and AHA, was the highest among the slope of the other curves, representing the relationship between UV_{280} parameter and RHA, NHA and FHA, respectively for the same UV_{280} parameter. On the other hand, RHA displayed the lowest HA concentration whereas, NHA and AHA exhibited close HA concentrations for the same UV_{280} parameter. FHA displayed lower HA concentration than RHA for the same UV_{280} parameter. The correlations between humic acid concentration and UV_{280} parameter were presented for Nordic HA by Equation 4.5 (R^2= 0.983), for Fluka HA by Equation 4.14 (R^2= 1.000), for Aldrich HA by Equation 4.23 (R^2= 0.982) and for Roth HA by Equation 4.36 (R^2=0.998). The overall correlation composed of all of the studied humic acid samples were presented by the linear Equation 4.44.

$$HA\ (mg\ L^{-1}) = 35.32 * UV_{280}\ (cm^{-1}) + 4.637 \qquad R^2=0.826 \qquad (4.44)$$

A linear relationship between UV_{280} parameter and HA concentration for the overall humic acids with a good correlation (R^2=0.826) was obtained.This result showed that UV_{280} parameter was good indicator of HA concentration for the overall humic acids.

4.2.5. The Relationship between DOC Concentrations and UV_{280} Parameter of NHA, FHA, AHA and RHA.

Figure 4.14 presented DOC concentration as a function of the alteration in UV_{280} parameter for the types of humic acids. DOC concentration of NHA (Table 4.1), FHA

(Table 4.2), AHA (Table 4.3) and RHA (Table 4.5) and UV_{280} parameter, corresponding to these DOC concentrations, were used in graph.

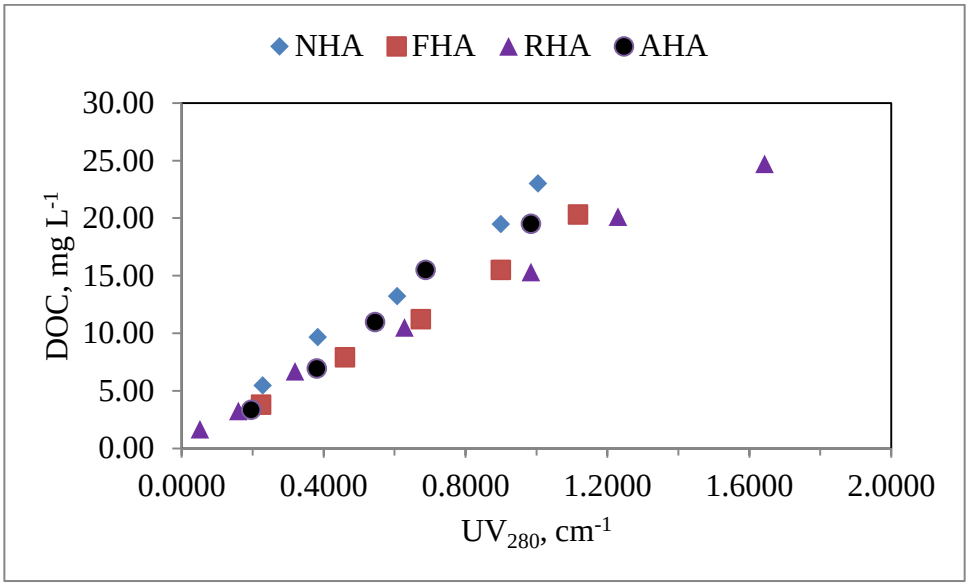

Figure 4.14. The relationship between UV_{280} parameter and DOC concentrations for NHA, FHA, AHA and RHA.

As seen in Figure 4.14, NHA exhibited the highest DOC concentration whereas, RHA displayed the lowest DOC concentration for the same UV_{280} parameter. Moreover, NHA and AHA exhibited close DOC concentration to each other while, FHA and RHA displayed close DOC concentration to each other for the same UV_{280} parameter. The correlations between DOC contents and UV_{280} parameter were presented for Nordic HA by Equation 4.4 (R^2= 0.992), for Fluka HA by Equation 4.13 (R^2= 0.996), for Aldrich HA by Equation 4.22 (R^2= 0.981), and for Roth HA by Equation 4.35 (R^2= 0.996). The overall correlation composed of all of the studied humic acid samples were presented by the linear Equation 4.45. The relationship between UV_{280} parameter and DOC concentration of the overall humic acids was obtained with a high correlation (R^2=0.939). This result demostrated that UV_{280} parameter was good indicator of DOC concentration for the overall humic acids.

$$DOC\ (mg\ L^{-1}) = 16.07*UV_{280}\ (cm^{-1}) + 1.559 \qquad R^2=0.939 \qquad (4.45)$$

Moreover, as mentined above, the correlation coefficient, obtained from the correlation between UV_{280} and DOC concentration of NHA, FHA, AHA and RHA were found to be as R^2=0.992, R^2=0.996, R^2=0.981 and R^2=0.996. It could be concluded that even though, humic acids belong to the different types of origin, the result point out that UV_{280} parameter could predict well, DOC content in these humic acids.

4.2.6. The Relationship between HA Concentrations and UV_{365} Parameter of NHA, FHA, AHA and RHA.

In Figure 4.15, the working solutions of the overall humic acid (2.5 to 50 mg L^{-1}) were plotted against the specific absorption UV range (UV_{365}). The data expressed UV_{365} parameter, corresponding HA concentrations, in Table 4.1 for NHA, in Table 4.3 for FHA, in Table 4.5 for AHA and in Table 4.9 for RHA were used in graph. According to the data given in Table 4.1 (NHA), 4.2 (FHA), 4.3 (AHA) and 4.5 (RHA), UV_{365} parameter of NHA exhibited 86 %, 71 % and 41 % UV_{365} parameter of FHA, AHA and RHA, respectively, for 10 mg L^{-1} of HA concentration. UV_{365} parameter displayed 60 %, 44 % and 32 % UV_{365} parameter of FHA, AHA and RHA, respectively, for 20 mg L^{-1} of HA concentration, UV_{365} parameter of AHA displayed 61 %, 61 % and 33 % UV_{365} parameter of FHA, AHA and RHA, respectively, for 40 mg L^{-1} of HA concentration and UV_{365} parameter of NHA exhibited 66 %, 49 % and 33 % UV_{365} parameter of FHA, AHA and RHA, respectively, for 50 mg L^{-1} of HA concentration. As seen in Figure 4.15, HA concentrations displayed increasing trend NHA>FHA>AHA>RHA for the same UV_{365} parameter. Moreover, FHA and AHA displayed close HA concentrations, when UV_{365} parameter was less than 0.1000 cm^{-1}.

$$HA\ (mg\ L^{-1}) = 48.61 * UV_{365}\ (cm^{-1}) + 10.67 \qquad R^2=0.605 \qquad (4.46)$$

The correlations between humic acid concentration and UV_{365} pameter were presented for Nordic HA by Equation 4.7 (R^2=0.990), for Fluka HA by Equation 4.16 (R^2= 0.999), for Aldrich HA by Equation 4.25 (R^2= 0.975) and for Roth HA by Equation 4.38 (R^2= 0.998). The overall correlation composed of all of the studied humic acid samples were presented by the linear Equation 4.46.

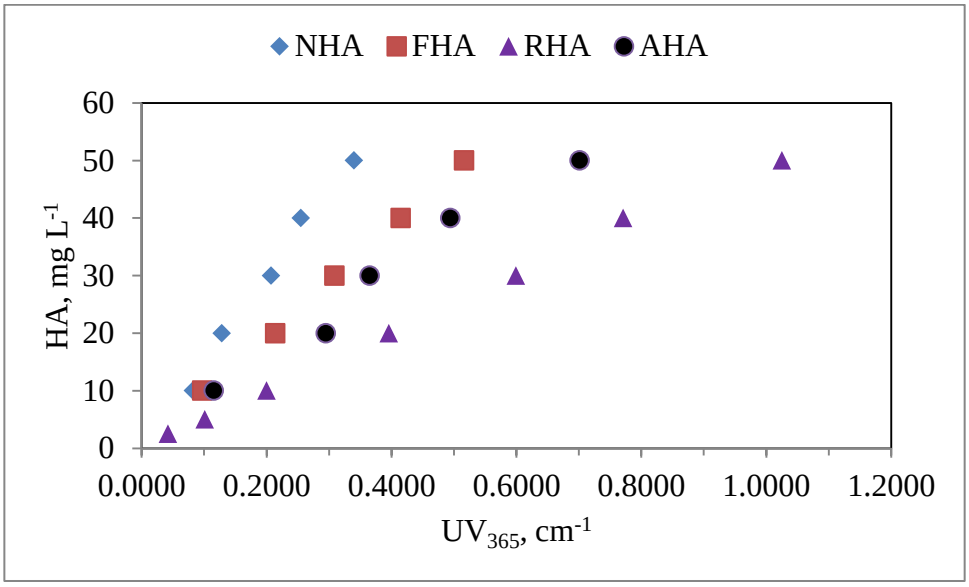

Figure 4.15. The relationship between HA concentrations and UV_{365} parameters of NHA, FHA, AHA, and RHA.

A linear relationship between UV_{365} parameter, represented aromatic moieties such as quinones, aromatic ketons, and polyphenols in humic chemical composition (Polewski et al., 2005), and HA concentration for the overall humic acids with low correlation (R^2=0.605) was obtained. This result showed that UV_{365} parameter, was not good indicator of HA concentration for the overall humic acids (NHA, FHA, AHA and RHA).

4.2.7. The Relationship between DOC Concentrations and UV_{365} Parameter of NHA, FHA, AHA and RHA.

Figure 4.16 showed DOC concentration as a function of the change in UV_{365} parameter for the types of humic acids. DOC concentration of NHA (Table 4.1), FHA (Table 4.2), AHA (Table 4.3) and RHA (Table 4.5) and UV_{365} parameter, corresponding to these DOC concentrations were used in graph.

As seen in Figure 4.16, NHA exhibited the highest DOC concentration whereas, RHA displayed the lowest DOC concentration for the same UV_{365} parameter. Moreover, AHA exhibited higher DOC concentration than RHA did, and lower DOC concentration than RHA. The correlations between DOC contents and UV_{365} parameter were presented

for Nordic HA by Equation 4.6 (R^2= 0.974), for Fluka HA by Equation 4.15 (R^2= 0.995), for Aldrich HA by Equation 4.24 (R^2= 0.973), and for Roth HA by Equation 4.37 (R^2= 0.996). The overall correlation composed of all of the studied humic acid samples (NHA, FHA, AHA and RHA) were presented by the linear Equation 4.47.

$$DOC\ (mg\ L^{-1}) = 22.22*UV_{365}\ (cm^{-1}) + 4.431 \qquad R^2=0.655 \qquad (4.47)$$

The relationship between UV_{365} parameter and DOC concentration of the overall humic acids was obtained with low correlation (R^2=0.655). This result demostrated that UV_{365} parameter was not good indicator of DOC concentration for the overall humic acids.

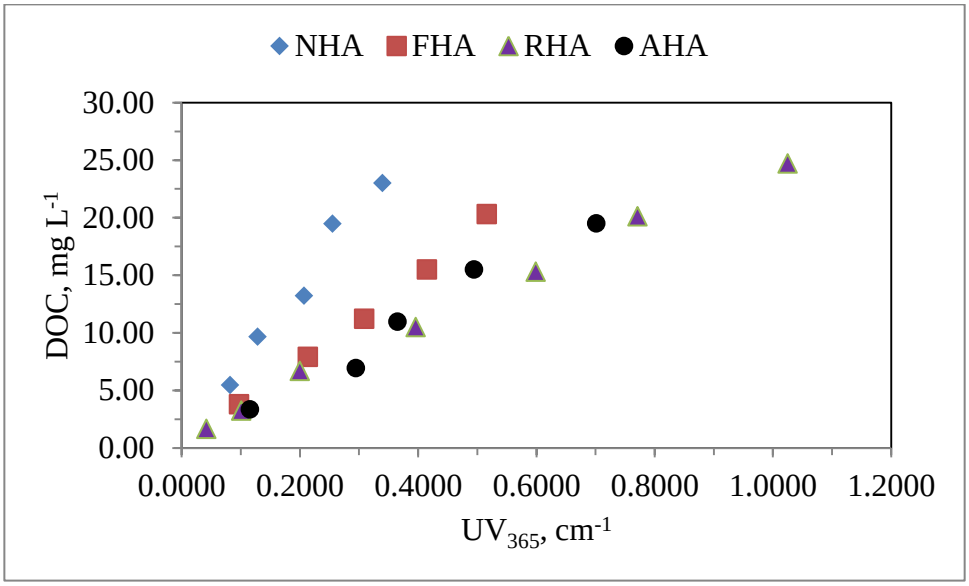

Figure 4.16. The relationship between UV_{365} parameter and DOC concentrations for NHA, FHA, AHA and RHA.

As mentioned above, the correlation coefficient, obtained from the correlation between UV_{365} and DOC concentration of NHA, FHA, AHA and RHA were found to be as R^2=0.974, R^2=0.995, R^2=0.973 and R^2=0.996. It could be concluded that UV_{365} parameter indicated DOC content in humic acid, representing a type of humic acid well, while, UV_{365} parameter could not predict DOC content in the overall humic acids (NHA, FHA, AHA and RHA).

4.2.8. The Relationship between HA Concentrations and $Color_{436}$ Parameter of NHA, FHA, AHA and RHA.

In Figure 4.18, the working solutions of the overall humic acid (2.5 to 50 mg L^{-1}) were plotted against the specific absorption UV range ($Color_{436}$). The data expressed UV_{365} parameter, corresponding HA concentrations, in Table 4.1 for NHA, in Table 4.2 for FHA, in Table 4.3 for AHA and in Table 4.5 for RHA were used in graph. According to the data given in Table 4.1 (NHA), Table 4.2 (FHA), Table 4.3 (AHA) and Table 4.5 (RHA), $Color_{436}$ parameter of NHA exhibited 67 %, 78 % and 27 % $Color_{436}$ parameter of FHA, AHA and RHA, respectively, for 10 mg L^{-1} of HA concentration. $Color_{436}$ parameter of NHA displayed 39 %, 51 % and 18 % $Color_{436}$ parameter of FHA, AHA and RHA, respectively, for 20 mg L^{-1} of HA concentration. $Color_{436}$ parameter of NHA exhibited 45 %, 49 % and 20 % $Color_{436}$ parameter of FHA, AHA and RHA, respectively, for 30 mg L^{-1} of HA concentration, $Color_{436}$ parameter of NHA displayed 41 %, 33 % and 19 % $Color_{436}$ parameter of FHA, AHA and RHA, respectively, for 40 mg L^{-1} of HA concentration, $Color_{436}$ parameter of NHA exhibited 45 %, 27 % and 19 % $Color_{436}$ parameter of FHA, AHA and RHA, respectively, for 50 mg L^{-1} of HA concentration.

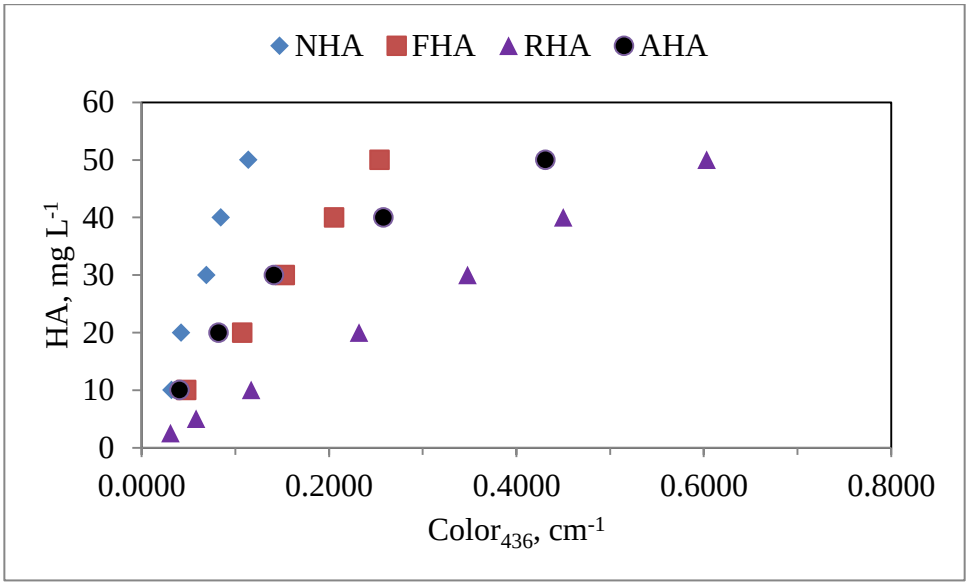

Figure 4.17. The relationship between HA concentrations and $Color_{436}$ parameters of NHA, FHA, AHA, and RHA.

According to Figure 4.17, NHA exhibited the highest HA concentration, whereas RHA displayed the lowest HA concentration for the same $Color_{436}$ parameter. When $Color_{436}$ parameter was lower than 0.1500 cm^{-1}, FHA and AHA exhibited close HA concentrations to each other. When $Color_{436}$ parameter was higher than 0.2000 cm^{-1}, HA concentration displayed decreasing trend, NHA>FHA>AHA>RHA.

$$HA\ (mg\ L^{-1}) = 68.59 * Color_{436}\ (cm^{-1}) + 15.46 \qquad R^2=0.465 \qquad (4.48)$$

The correlations between humic acid concentration $Color_{436}$ were presented for Nordic HA by Equation 4.9 (R^2= 0.979), for Fluka HA by Equation 4.18 (R^2= 0.994), for Aldrich HA by Equation 4.27 (R^2= 0.924) and for Roth HA by Equation 4.43 (R^2= 0.998). The overall correlation composed of all of the studied humic acid samples were presented by the linear Equation 4.48. A linear relationship between $Color_{436}$ parameter and HA concentration for the overall humic acids (R^2=0.465). This result showed that $Color_{436}$ parameter was not good indicator of HA concentration for the overall humic acids.

4.2.9. The Relationship between DOC Concentrations and $Color_{436}$ Parameter of NHA, FHA, AHA, RHA.

Figure 4.18 presented DOC concentration as a function of the alteration in $Color_{436}$ parameter for the types of humic acids. DOC concentration of NHA (Table 4.1), FHA (Table 4.2), AHA (Table 4.3) and RHA (Table 4.5) and $Color_{436}$ parameter, corresponding to these DOC concentrations were used in graph.

Depending on Figure 4.18, NHA exhibited the highest DOC concentration, whereas RHA displayed the lowest DOC concentrations for the same $Color_{436}$ parameter. When $Color_{436}$ parameter was lower than 0.1800 cm^{-1}, FHA and AHA displayed DOC concentrations to each other. The correlations between DOC contents and $Color_{436}$ were presented for Nordic HA by Equation 4.8 (R^2= 0.963), for Fluka HA by Equation 4.17 (R^2= 1.000), for Aldrich HA by Equation 4.26 (R^2= 0.935), and for Roth HA by Equation 4.39 (R^2= 0.994). The overall correlation composed of all of the studied humic acid samples (NHA, FHA, AHA and RHA) were presented by the linear Equation 4.49.

$$DOC\ (mg\ L^{-1}) = 32.16*Color_{436}\ (cm^{-1}) + 6.474 \qquad R^2=0.530 \qquad (4.49)$$

The relationship between $Color_{436}$ parameter and DOC concentration of the overall humic acids was attained with low correlation (R^2=0.530). This result demostrated that $Color_{436}$ parameter was not good indicator of DOC concentration for the overall humic acids. On the other hand, as mentioned above, the correlation coefficient, obtained from the correlation between UV_{365} and DOC concentration of NHA, FHA, AHA and RHA were found to be as R^2=0.963, R^2=1.000, R^2=0.935 and R^2=0.994.

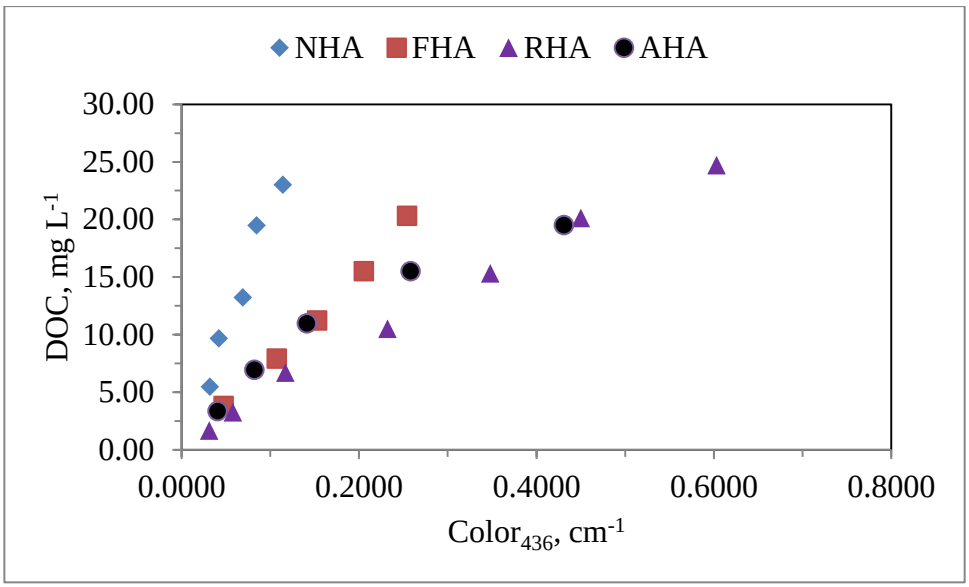

Figure 4.18. The relationship between $Color_{436}$ parameter and DOC concentrations for NHA, FHA, AHA and RHA.

It could be inferred that $Color_{436}$ parameter indicated DOC content in a humic acid, representing a type of humic acid, well, while $Color_{436}$ parameter could not predict DOC content in the overall humic acids (NHA, FHA, AHA and RHA).

4.2.10.The Evaluation of the overall Humic Acids

The combination of the experimental results and reference (Al-Rasheed et al., 2003) was applied for the evaluation. The source of humic acids were NHA, the data given in Table 4.1, FHA, the data given in Table 4.2, AHA, the data given in Table 4.3, and RHA, the data given in Table 4.5; furthermore, AHA (Table 4.4) was used from the reference.

4.2.11. The overall Relationship between DOC and UV_{254}

From the data given in Table 4.1 (NHA), Table 4.2 (FHA), Table 4.3 (AHA), Table 4.4 (AHA, Al-Rasheed et al., 2003a) and Table 4.5 (RHA), UV_{254} parameter were between 0.085 cm^{-1} and 3.520 cm^{-1} whereas, DOC concentration, correspondend to UV_{254} parameters, was between 1.65 mg L^{-1} and 64.76 mg L^{-1}. The correlation between DOC concentration and UV_{254} parameter were presented in Figure 4.19. As mentioned before, UV_{254} parameter, corresponded to NHA (10-50 mg L^{-1}), FHA (10-50 mg L^{-1}), AHA (10-50 mg L^{-1}), and RHA (2.5-50 mg L^{-1}) obtained from the experimental results, and AHA (both in acidic and alkaline media), attained from the reference (Al-Rasheed et al., 2003). Likewise to UV_{254} parameter, DOC concentration, corresponded to NHA (10-50 mg L^{-1}), FHA (10-50 mg L^{-1}), AHA (10-50 mg L^{-1}), and RHA (2.5-50 mg L^{-1}) obtained from the experimental results, and AHA, attained from the reference (both in acidic and alkaline media) (Al-Rasheed et al., 2003). UV_{254} parameter was correlated with DOC concentration (Figure 4.19). As mentioned below, Equation 4.50 was attained from the correlation between UV_{254} parameter and DOC concentration. As seen in Figure 4.19 showed more scatter in the data at the lower values of the variables than at the higher values of these variables (UV_{254} and DOC). Figure 4.19 illustrated the linear correlation between UV_{254} parameter and DOC concentration.

$$DOC\ (mg\ L^{-1}) = 16.24 * UV_{254}\ (cm^{-1}) - 0.517 \qquad R^2=0.970 \qquad (4.50)$$

$$DOC\ (mg\ L^{-1}) = 14.06 * UV_{254}\ (cm^{-1}) + 0.217 \qquad R^2=0.936 \qquad (4.43)$$

DOC concentration-UV_{254} parameter Equation was produced from the least-squares regression analyses (Equation 4.50). The regression coefficient was found to be as R^2=0.970. According to this result, UV_{254} parameter could predict DOC concentration with high regression coefficient. If the UV_{254} parameter was the same, the result of DOC concentration, obtained from Equation 4.43 would be higher than the result of DOC concentration, obtained from Equation 4.50.

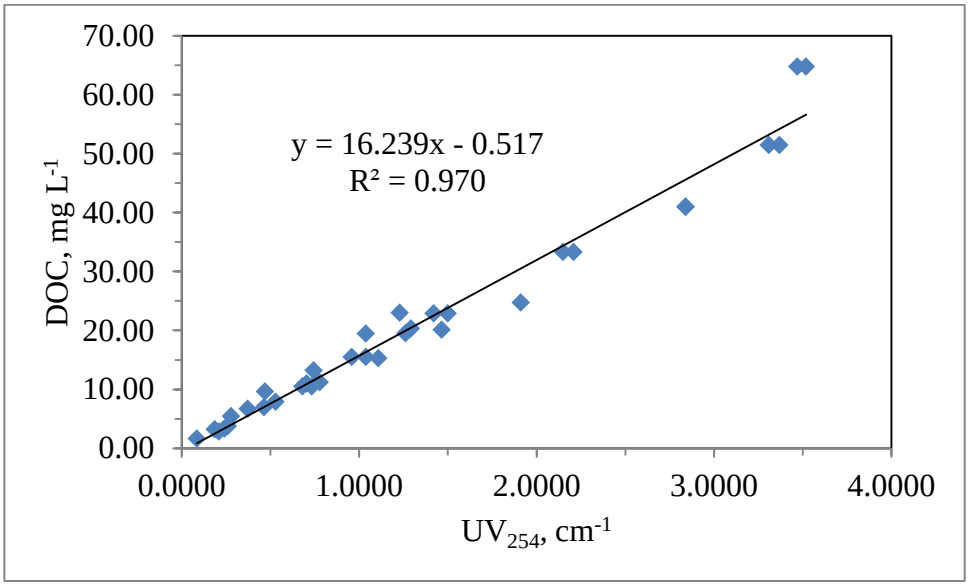

Figure 4.19. UV-vis parameter and DOC concentration for the overall types of humic acids.

As mentioned before, Equation 4.43 represents the correlation between DOC concentration and UV_{254} parameter data, including NHA, FHA, AHA and RHA (the experimental results). On the other hand, Equation 4.50 represents the correlation between DOC concentration and UV_{254} parameter data, consisting both the experimental results and reference. As mentioned above, the data used in Equation could exhibit different DOC concentration results (DOC (Equation 4.43)> DOC (Equation 4.50).

4.2.12. The Relationship between the Calculated DOC Contents and the Observed DOC Contents of the Humic Acids.

DOC concentrations were correlated with the calculated DOC contents (DOC_{calc}) using the UV_{254}-DOC overall Equation (Equation 4.50) (Figure 4.22). From Table Table 4.1 (NHA), Table 4.2 (FHA), Table 4.3 (AHA), Table 4.4 (AHA, Al-Rasheed et al., 2003a) and Table 4.5 (RHA), DOC concentrations of humic acid ranged from 1.65 mg L^{-1} to 64.76 mg L^{-1} whereas, DOC_{calc} concentrations ranged from 0.86 mg L^{-1} to 56.64 mg L^{-1} respectively. Figure 4.20 illustrated the least correlation between DOC_{calc} concentrations and DOC concentrations of humic acid. DOC-DOC_{calc} equation was produced from the least-squares regression analyses (Equation 4.51).

The regression coefficient was found to be as R^2=0.970. As seen Equation 4.51, the regression coefficient was found to be closed to R^2=1. DOC_{calc}, obtained by Equation 4.50 as a function of UV_{254} parameter, could predict DOC_{obs}, the data given in Table 4.1 (NHA), Table 4.2 (FHA), Table 4.3 (AHA), Table 4.4 (AHA, Al-Rasheed et al., 2003a) and Table 4.5 (RHA).

$$DOC_{calc}(mg\ L^{-1}) = 0.970*DOC\ (mg\ L^{-1}) +0.615 \qquad R^2=0.970 \qquad (4.51)$$

As mentioned before, the data in Table 4.1 (NHA), Table 4.2 (FHA), Table 4.3 (AHA), Table 4.4 (AHA, Al-Rasheed et al., 2003a) and Table 4.5 (RHA) includes the studied HA concentrations at neutral conditions and the data studied AHA concentration both at acidic and alkaline conditions by the researcher (Al-Rasheed et al., 2003a).

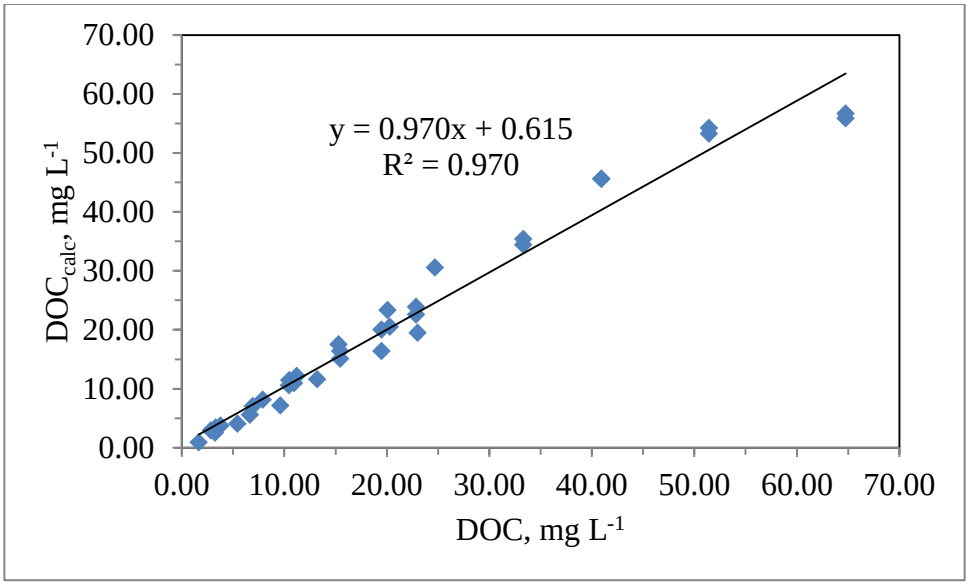

Figure 4.20. The correlation between DOC_{calc} and DOC, including the overall humic acids and reference (Al-Rasheed et al., 2003a).

Under the different pH conditions (acidic, neutral and alkaline) and the various humic acid sources (aquatic and terrestrial), a good correlation displayed. As a result, the some conditions, such as pH and the humic acid sources could not change the result.

4.2.13. The Relationship between DOC and DOC_{calc} (A model verification check)

Before the treatment of NOM in a sample, the relationship between water quality parameter and the character and reactivity of NOM was identified. Data from 88 water sources from 10 references was (Goslan et al., 2003) collated. UV_{254} parameter of the water resources was determined by UV-vis spectrophotometer and DOC concentration of the water resources was determined by TOC analyzer. UV_{254} parameter was correlated with dissolved organic carbon concentration (Equation 52). The Equation 4.52 , formed from the correlation between UV_{254} and DOC, was applied for the calculation of DOC concentration. DOC_{calc} was obtained as a function of UV_{254} parameter, including the overall humic acids and reference results (Al-Rasheed et al., 2003a), by using Equation 4.52.

$$DOC\ (mg\ L^{-1}) = 21.37 * UV_{254}\ (cm^{-1}) + 112.05 \quad (4.52)$$

DOC concentrations of humic acid ranged from 1.65 mg L^{-1} to 64.76 mg L^{-1} whereas, DOC_{calc} concentrations ranged from 2.94 mg L^{-1} to 76.34 mg L^{-1} as a function of UV_{254} parameter. DOC_{calc} was correlated with DOC (Equation 4.53) (Figure 4.22)

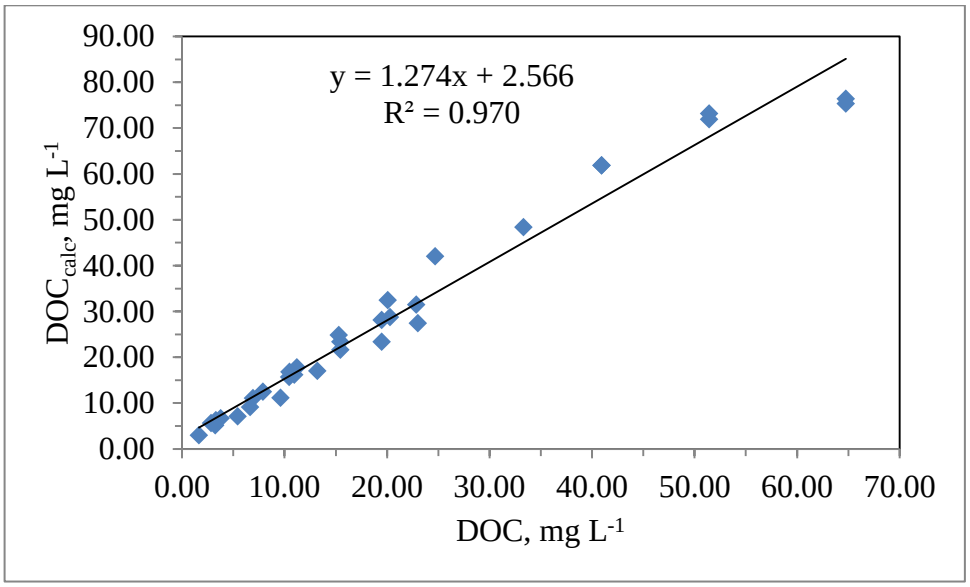

Figure 4.21. The correlation between DOC and $DOC_{calc,}$ including the overall humic acids and reference (Al-Rasheed et al., 2003a).

DOC_{calc} was obtained as a function of UV_{254} parameter, including the overall humic acids and reference results (Al-Rasheed et al., 2003a), by using Equation 4.52. DOC concentrations of humic acid ranged from 1.65 mg L^{-1} to 64.76 mg L^{-1} whereas, DOC_{calc} concentrations ranged from 2.94 mg L^{-1} to 76.34 mg L^{-1} as a function of UV_{254} parameter. DOC_{calc} was correlated with DOC (Equation 4.53) (Figure 4.22). DOC_{calc} was correlated with DOC (Equation 4.53) (Figure 4.23). From Table 4.12, DOC concentrations of humic acid ranged from 1.65 mg L^{-1} to 64.76 mg L^{-1} whereas, DOC_{calc} concentrations ranged from 2.94 mg L^{-1} to 76.34 mg L^{-1}.

Figure 4.21 showed more scatter in the data at the lower values of the variables than at the higher values of these variables (DOC and DOC_{calc}). Figure 4.21 illustrated the least correlation between DOC_{calc} parameter and DOC parameter.

$$DOC_{calc}\ (mg\ L^{-1}) = 1.274*DOC\ (mg\ L^{-1}) + 2.566 \qquad R^2=0.970 \qquad (4.53)$$

DOC-DOC_{calc} equation was produced from the least-squares regression analyses (Equation 4.53). The regression coefficient was found to be as R^2=0.970. With high regression coefficient, it could be inferred that DOC was a good indicator of DOC_{calc}.

4.2.14. Sample Calculation

4.2.14.1. Purpose, Hypothetical Composition and Calculated DOC and HA Concentrations of NHA, FHA, AHA and RHA and the overall Humic Acids. A humic sample, whose UV-vis parameters were known, was used to determine the DOC concentration and HA concentration of the types of humic acid. By using equations, that was achieved by the correlation between UV-vis parameter and DOC concentrations for each types of humic acid and the correlation between DOC concentrations and HA concentrations for each types of humic acid, DOC and HA concentrations were calculated.

Considering a humic acid sample expressing UV_{254}: 0.5000 cm^{-1}, UV_{280}: 0.4000cm^{-1}, UV_{365}: 0.1150 cm^{-1} and $Color_{436}$: 0.0550 cm^{-1}. HA and DOC contents were calculated according to the respective equations (4.1- 4.9) for NHA, equations (4.10- 4.18) for FHA, equations (4.19- 4.27) for AHA and equations (4.32- 4.40) for RHA. Moreover, Equation

4.43, 4.44, 4.45, 4.46, 4.47 and 4.49 were used for All HAs. As shown below, If the sample, expressing UV_{254} parameter was NHA, the result of DOC concentration would be 9.58 mg L^{-1} , If the sample, expressing UV_{254} parameter was FHA, the result of DOC concentration would be 7.33 mg L^{-1}; If the sample, expressing UV_{254} parameter was AHA, the result of DOC concentration would be 7.61 mg L^{-1}; If the sample, expressing UV_{254} parameter was RHA, the result of DOC concentration would be 7.48 m L^{-1}.

The DOC concentration results of NHA was higher than the other humic acids for each UV-vis parameter. The DOC concentration of RHA, expressing UV_{254} parameter was 22 % less than the DOC concentration of NHA expressing UV_{254} parameter. The DOC concentration of RHA, expressing UV_{365} parameter was 48 % less than the DOC concentration of NHA expressing UV_{365} parameter. The DOC concentration of FHA, expressing $Color_{436}$, was 65.37 % less than the DOC concentration of NHA (Table 4.6).

Table 4.6. The dissolved organic carbon concentration (DOC_{calc}) and humic acid concentration (HA_{calc}) , calculated related to the types of UV-vis parameter.

Humic acid	UV_{254}	UV_{280}	UV_{365}	$Color_{436}$	Average
	DOC_{calc}, mg L^{-1}				
Nordic	9.581	9.319	8.121	11.36	9.595
Fluka	7.329	6.718	4.124	3.932	5.526
Aldrich	7.615	7.857	3.132	5.859	6.116
Roth	7.481	7.112	3.894	3.354	5.460
All HAs	8.244	7.986	6.986	8.243	7.866
	HA_{calc}, mg L^{-1}				
Nordic	19.86	19.33	16.51	23.74	19.86
Fluka	19.14	17.64	11.25	10.78	14.70
Aldrich	21.13	21.72	10.13	16.91	17.46
Roth	13.56	12.79	6.029	4.891	9.317
All HAs	19.00	18.77	16.26	19.23	18.32

NHA concentration consisted 48 % of DOC concentration; FHA concentration consisted 38 % of DOC concentration; AHA concentration consisted 36 % of DOC concentration; RHA concentration consisted 55 % of DOC concentration for UV254 parameter. Moreover, NHA concentration consisted 48 % of DOC concentration; FHA concentration consisted 38 % of DOC concentration; AHA concentration consisted 35 %

of DOC concentration; RHA concentration consisted 68 % of DOC concentration for $Color_{436}$ parameter.

The relationship between UV-vis parameters (UV_{254}, UV_{280}, UV_{365} and $Color_{436}$) and HA concentrations for the overall humic acids and UV-vis parameter and DOC concentrations of AHA, and were examined. As explained below, the overall reported UV-vis parameter and HA/DOC was evaluated. Moreover, in additon to UV-vis parameters, another parameter (SUVA) was examined and evaluated.

4.2.15. Evaluation of the overall Reported UV-vis Parameters and HA/DOC.

UV_{254}, UV_{280}, UV_{365} indicate organic matter content whereas, $Color_{436}$ indicates color content in a humic acid sample. In addition to these UV-vis parameter, specific UV absorbance, SUVA expresses the ratio of UV-vis parameter (m^{-1}) to DOC concentration (mg L^{-1}). SUVA measure of DOC aromatic content that is calculated by measuring the DOC and the UV absorbance at 254 nm of a 0.45-μm filtered water sample (Potter and Wimsatt, 2005). It is usually expressed in units of L mg^{-1} m^{-1}. Specific UV absorbance ($SUVA_{254}$, cm^{-1} mg^{-1} L) was used to represent DOC normalized aromatic moieties (UV_{254}) whereas specific color absorbance ($SCOA_{436}$, cm^{-1} mg^{-1} L) was defined as $Color_{436}$/DOC to signify organic carbon normalized color forming moieties. $SUVA_{365}$ was also calculated in a similar fashion as the ratio of the UV_{365} absorbing species to DOC. To calculate $SUVA_{254}$, $SUVA_{280}$, $SUVA_{365}$ and $SCOA_{436}$, the data in Table 4.1 , Table 4.2, Table 4.3 and Table 4.5, respectively were used. $SUVA_{254}$ ranged from 5.15 m^{-1}L mg^{-1} to 7.7 m^{-1}L mg^{-1} ; $SUVA_{280}$ ranged from 3.15 m^{-1}L mg^{-1} to 6.65 m^{-1}L mg^{-1}; $SUVA_{365}$ ranged from 3.31 m^{-1}L mg^{-1} to 4.13 m^{-1}L mg^{-1} and $SCOA_{436}$ ranged from 0.44 m^{-1}L mg^{-1} to 2.44 m^{-1}L mg^{-1}.

The description of the spectroscopic behavior of humic substances tradionally includes:

a. The ratios of measured spectral absorbance at particular wavelenghts as indices of the slope of absorption curves;
b. The absorbance data calculated per unit of dissolved carbon as an analog of molar absorptivity (Kononova, 1966; MacCarthy and Rice, 1985; Bloom and Leenheer, 1989; Orlov, 1990; Gjessing et al., 1998).

The ultraviolet and visible regions of the electromagnetic spectrum extend from ~10 to 400 nm and from 400 to ~800 nm, respectively. The ultraviolet and visible (UV-visible) regions are generally considered together since both correspond to electronic transitions within the absorbing species (UV-visible spectra are also referred to as electronic spectra). The UV region is classified into the far UV (10-200 nm) and the near UV (200-400 nm). Oxygen absorbs strongly in the far UV, and since evacuation of the spectrometer is the simplest means of alleviating this interference the far UV region is often referred to as the vacuum ultraviolet. The UV-visible spectra of solutions generally show broad bands that are few in number. The fine structure frequently associated with vapor-phase or solid-state spectra is "lost" in solution spectra due to broadening as a result of random interactions with neighboring molecules. The absorption of UV-visible radiation can frequently be attributed to a specific segment or functional group within the molecule; such absorbing entities may contain σ, π or n electrons. Examples of common chromophores are functional groups containing unbonded electrons (e.g., carbonyl), sulfur, nitrogen, or oxygen atoms, and conjugated carbon-carbon multiple bonds (Aiken, 1985a).

The absorbance of UV light by a molecule depends on the electronic structure of the molecule. The UV spectrum, therefore, indicates the presence of specific bonding arrangements in the molecule. The functional groups containing the electrons that are promoted when a molecule absorbs light are referred to as chromophores (Christman et al., 1989; Traina et al., 1990; Novak et al., 1992; Chin et al., 1994). These chromophores are associated primarily with the humic fraction of the NOM and these chromophores, responsible for the absorbance, consist of conjugated double bonds and unbonded electrons like those associated with oxygen, sulphur, and halogen atoms (MacCarthy and Rice, 1985). In the case of absorption in the near UV (200-380 nm), conjugated systems, such as those in aromatic molecules, generally have the greatest absorptivities (Silverstein et al., 1974). UV_{254} parameter of RHA, terrestrial humic acid, was higher than the other humic acids whereas, NHA, terrestrial origin, exhibited the lowest UV_{254} parameter, at the same humic acid concentrations (Figure 4.11). As a result, RHA comprised of the highest conjugated systems among the types of humic acids at the same humic acid concentrations. RHA displayed the highest UV_{254} parameter with the highest DOC concentration among the humic acids (Figure 4.12). Although, DOC concentration of AHA, terrestrial origin, was the lowest than the other humic acids, UV_{254} parameter, corresponding to this DOC

concentration was higher than UV_{254} parameter of FHA and NHA, for the same humic acid concentration (50 mg L^{-1}). Data presented in Figure 4.12 compared UV_{254} parameter for the overall humic acids and DOC concentration. A strong correlation existed (R^2=0.936) between UV_{254} parameter and DOC data. It could be inferred that that UV_{254} parameter had a high prediction ability of DOC concentration for both terrestrial and aquatic humic acids.

It is well known that π-π* electron transition, specific for phenolic arenes, benzoic acids, aniline derivatives, polyenes, and polycyclic aromatic hydrocarbons with two or more rings, occurs between the wavelengths approximately from 270 to 280 nm. For that reason, the application of UV absorbances within 270–280 nm is more suitable for describing aromatic carbon moieties and offers also a possibility to estimate their total quantity (Peuravuori et al., 2005). UV_{280} parameter of NHA (10 mg L^{-1}), aquatic humic acid, was 29 % less than UV_{280} parameter of RHA (10 mg L^{-1}), terrestrial humic acid. UV_{280} parameter of RHA was higher than the other humic acids (Figure 4.13). As a result, RHA has remarkably high UV_{280} parameter with respect to the other samples emphasizing strong aromatic character. With the highest UV_{280} parameter, RHA existed the highest DOC concentrations among humic acids (Figure 4.14). For 50 mg L^{-1} of humic acid, UV_{280} parameter of NHA was lower than FHA, DOC concentration of FHA was higher than NHA. With the lowest UV_{280} parameter, AHA displayed the lowest DOC concentration (Figure 4.13). The plot of the correlation between UV_{280} parameter and DOC concentration was shown in Figure 4.14, which supported that UV_{280} parameter had a high prediction ability of DOC concentration (R^2 = 0.936) for both terrestrial and aquatic humic acids. Although, terrestrial acids displayed stronger aromatic character than aquatic humics did at specífic wavelength (λ=280 nm), a linear curve was obtained between UV_{280} parameter and DOC concentration.

UV_{365} parameter was found to be irrespective of the source of the samples as expressed in a decreasing order of RHA > AHA > FHA > NHA (50 mg L^{-1} of humic acid). AHA, having the lowest dissolved organic carbon concentration, possessed the higher UV_{365} parameter than FHA and NHA had. Investigated natural soil HA was characterized by elemental analysis showing a high content of oxygen and low of carbon (Slawinska et al., 2002) which indicated that it might contain more phenolic and ketonic functional groups. Consistent with literature results (Frimmel et al., 2002), 10 mg L^{-1} of

AHA, which is a terrestrial origin humic acid, illustrated more than 1.4 times more these aromatic moieties than 10 mg L^{-1} of NHA as can be seen in Figure 4.15. Similar to UV_{254} and UV_{280} with the highest UV_{365} parameter, RHA existed the highest DOC concentrations among humic acids. For 50 mg L^{-1} of humic acid, UV_{365} parameter of NHA was lower than FHA (Figure 4.15), UV_{365} parameter of FHA was higher than UV_{365} parameter of NHA (Figure 4.16) for the same DOC concentration. Above the UV_{280} parameter absorbs aromatic moieties like quinones, aromatic ketons and polyphenols (Polewski et al., 2005). RHA had the highest aromatic moieties, absorbing UV_{365} parameter among the humic acids for the same DOC concentrations. As a result, the highest UV_{365} parameter of RHA may reflect the abundance of aromatic moieties like quinones, aromatic ketons and polyphenols. Data presented in Figure 4.16 compared UV_{365} parameter for the overall humic acids and DOC concentration. A weak correlation existed (R^2=0.655) between UV_{365} parameter and DOC data. This regression coefficient indicated that UV_{365} parameter may not be useful for quantifying the DOC concentrations of different humic acid sources.

50 mg L^{-1} of RHA, which is a terrestrial origin humic acid, exhibited 0.6030 cm^{-1} of $Color_{436}$, while 50 mg L^{-1} of NHA, which is an aquatic origin humic acid, illustrated less one over third of the value of color forming moieties than RHA as can be seen in Figure 17. Moreover, 20 mg L^{-1} of AHA, terrestrial humic acid, exhibited 0.0820 cm^{-1} of $Color_{436}$. On the other hand, 20 mg L^{-1} of NHA, aquatic humic acid, exhibited less two times than the value of color forming moieties than AHA (Figure 4.18). Similar to UV_{254},UV_{280} and UV_{365} parameter with the highest $Color_{436}$ parameter, RHA existed the highest DOC concentrations among humic acids. For 50 mg L^{-1} of humic acid, $Color_{436}$ parameter of NHA was lower than FHA and AHA (Figure 4.17). For the same DOC concentration, NHA exhibited the lowest $Color_{436}$ parameter, whereas RHA displayed the highest $Color_{436}$ parameter (Figure 4.18). As mentioned above, $Color_{436}$ parameter was poorly correlated with DOC concentration (R^2 = 0.530). This poor correlation could be expected due to the different humic acid sources (aquatic and terrestrial) used in this correlation (Figure 4.18). For the same DOC concentrations, $Color_{436}$ parameter of Nordic humic acid (aquatic) was lower than $Color_{436}$ parameter of terrestrial humic acids (FHA, RHA and AHA). This regression coefficient indicated that $Color_{436}$ parameter may not be useful for quantifying the DOC concentrations of different humic acid sources.

To facilitate the UV-vis absorptivity of different humic acids, devired parameters were assessed using specified UV-vis parameters (UV_{254}, UV_{280}, UV_{365} and $Color_{436}$) normalized to the respective DOC concentrations ($m^{-1}L\ mg^{-1}$) as mentioned above. Table 4.7 exhibites $SUVA_{254}$, $SUVA_{280}$, $SUVA_{365}$ and $SCOA_{436}$ parameters. $SUVA_{254}$ is an "average" absorptivity for all the molecules that comprise the DOC in a water sample and has been used as a surrogate measurement for DOC aromaticity (Traina et al., 1990). According to the explanation that the specific UV-vis parameter can be used to describe the composition of humic material in terms of hydrophobicity and hydrohilicity, $SUVA_{254}$ >4 indicates mainly hydrophobic and have a relatively high content of complex heterogenous macromolecular organic compounds rich in aromatics, and especially aromatic moieties while a $SUVA_{254}$<4 represents a hydrophilic organic fraction (Edzwald et al., 1985) and have a relatively high content of complex heterogenous macromolecular organic compounds rich in aromatics. As shown in Table 4.7, all of these values were more than 4, thus $SUVA_{254}$ represented hydrophobic organic fraction. Depending on these results, the diversity of humic acids had high content of complex heterogenous macromolecular organic compounds rich in aromatics (Peuravuori and Pihlaja, 2006). According to Table 4.7, specific ultraviolent absorbance parameter of terrestrial humic acids was higher than aquatic humic acids. It could be inferred that the origin of humic acids could affect the results. Under the same conditions, the humic acids, dependent upon their origins, could behave different. The specific ultraviolet parameter of terrestrial humic acid was higher than the specific ultraviolet parameter of aquatic humic acid (Table 4.7). Having the higher hydrophocity of terrestrial humic acid than aquatic humic acids was not unexpected result. UV-parameter is probably mainly due to the aromatic ring structure (Bloom and Leenheer, 1989). UV-vis parameter increases with pH, aromaticity, total C-content and molecular weight (Chen et al., 1977). The strong correlation between the spesific ultraviolet parameter and aromatic carbon content of significant utility in assessing the nature or general chemical composition of dissolved organic carbon of humic acid because it provides an integrated estimate of aromatic content across functional classes (Weishaar et al., 2003). The highest specific ultraviolet parameter was 7.74 $m^{-1}L\ mg^{-1}$ (Table 4.7) of RHA (50 mg L^{-1}). $SUVA_{254}$, representing the aromaticity of dissolved organic carbon was correlated with UV_{280} parameter (Chin et al., 1994; Traina et al., 1990). The regression coefficient was found to be as R^2=0.920. Consistent with the literature results (Weishaar et al., 2003), the efficiency of $SUVA_{254}$ used as an indicator of

aromaticity for aquatic organic matter, was found to be enough. Considering the data reported by Uyguner and Bekbölet 2005c, $SUVA_{280}$ parameter was the highest for FHA, terrestrial humic acid, whereas was the lowest for NHA, aquatic humic acid (Table 4.7). Considering the data reported by Uyguner and Bekbölet 2005c, $SUVA_{365}$ parameter was the highest for RHA, terrestrial humic acid, whereas this parameter was the lowest for NHA, aquatic humic acid (Table 4.7). The specific color parameter ($SCOA_{436}$, m^{-1} L mg^{-1}) was defined as $Color_{436}$/DOC to signify organic carbon normalized color forming moieties (Uyguner and Bekbölet, 2005a).

Table 4.7. The list of HA concentration and Source, and Specific absorbance ratios of humic substances.

HA Source	HA Concentration mg L^{-1}	$SUVA_{254}$ $m^{-1}L\ mg^{-1}$	$SUVA_{280}$ $m^{-1}L\ mg^{-1}$	$SUVA_{365}$ $m^{-1}L\ mg^{-1}$	$SCOA_{436}$ $m^{-1}L\ mg^{-1}$
RHA, T	2.5	5.15	3.15	2.55	1.88
RHA, T	5	5.77	4.94	3.12	1.79
RHA, T	10	5.59	4.80	3.00	1.75
AHA,T	10	7.20	5.89	3.47	1.22
FHA,T	10	6.87	5.93	2.57	1.26
NHA, A	10	5.12	4.19	1.50	0.58
RHA, T	20	5.77	4.94	3.12	1.79
AHA,T	20	6.69	5.49	4.25	1.18
FHA,T	20	6.69	5.82	2.70	1.36
NHA, A	20	4.87	3.98	1.33	0.44
RHA, T	30	7.25	6.44	3.92	2.27
AHA,T	30	6.42	4.97	3.33	1.29
FHA,T	30	6.93	6.01	2.75	1.36
NHA, A	30	5.62	4.59	1.57	0.52
RHA, T	40	7.29	6.12	3.84	2.24
AHA,T	40	6.19	4.44	3.19	1.67
FHA,T	40	6.71	5.81	2.68	1.33
NHA, A	40	5.34	4.62	1.31	0.43
RHA, T	50	7.74	6.65	4.15	2.44
AHA,T	50	6.48	5.05	3.60	2.21
FHA,T	50	6.37	5.50	2.54	1.25
NHA, A	50	5.34	4.36	1.48	0.50

T signifies terrestrial, A signifies aquatic sources.

Considering the data reported by Uyguner and Bekbölet (2005b), $SCOA_{436}$ parameter was the highest for RHA, terrestrial humic acid, whereas this parameter was the lowest for NHA, aquatic humic acid (Table 4.7).

Similar with fulvic acids (Gan et al., 2007), although the structure, configuration, functional moieties, molar mass, and intra and inter-molecular interactions may have been significantly different, the overall optical behavior of humic acids from different sources was similar.

4.3. Oxidative Treatment of Humic Acids by Photocatalysis

In this section, Nordic humic acid and Aldrich humic acid were treated by photocatalytic oxidation using TiO_2 Degussa as the photocatalysis in the presence of light irradiation. The degradation data were followed by UV-vis parameter as UV_{254}, UV_{280}, UV_{365} and $Color_{436}$. In addition to the UV-vis parameter, the alterations in DOC concentrations were examined (Ilgun, 2010). By using Equations, obtained from the correlation graphs in section 4.1 and 4.2, DOC concentrations were calculated for Nordic humic acid.

Humic acids (HAs) are macromolecular yellow-to-black colored natural organic matter derived from the degradation of plant, algal, and microbial material (Stevenson, 1994). Although their formation mechanism and chemical structures are not well understood, they are known to be high in carbon content (50–60%) of both aliphatic and aromatic character and rich in oxygen-containing functionalities such as carboxyl, phenolic, alcoholic, and quinoid groups. HAs account for a significant fraction of natural organic carbons in surface waters and soils and play many important roles as a photosensitizer in aquatic photochemical processes, a complexing agent for heavy metal ions, and an organic coating material on mineral surfaces that affects the mobility and bioavailability of aquatic contaminants. Recently, photocatalytic oxidation using TiO_2 is gaining wide attentions as an advanced water treatment technology (Hoffman et al., 1995; Bekbolet and Ozkosemen, 1996).

During the photocatalytic treatment, the decrease in UV_{254} parameter of humic acid suggested that the hyroxyl radical attack proceeded mainly on the aromatic moieties of the molecules. The formation of new species exhibiting a significant absorption at 254 nm during oxidative degradation (Uyguner and Bekbolet, 2005c). The decrease in UV_{280}, UV_{365} parameter, represents the removal of total aromaticity, while $Color_{436}$ parameter is used to measure color removal of humic substances during the photocatalytic treatment.

4.3.1. Photocatalytic Treatment of NHA

NHA was prepared in 10, 20, 30 and 50 mg L^{-1} concentration and it was subjected to photocatalyic degradation in the presence of 0.25 mg mL^{-1} TiO_2. The degradation results were reported by Ilgun, 2010. UV–vis parameters and DOC concentrations of treated humic acid as a function of irradiation time during the oxidation process were presented in Table 4.8. While 63 % of UV_{254} and UV_{280} removed in 15 minutes of irradiation, 95 % removal attained after 60 minutes for 10 mg L^{-1} humic acid. Similar to UV_{254} and UV_{280} parameter UV_{365} alterations demostrated declining pattern with 65 % and 92 % of UV_{365} reduction after 15 minutes and 60 minutes, respectively for 10 mg L^{-1} of NHA (Table 4.8). $Color_{436}$ was removed by 62 % in 15 minutes of irradiation, whereas 90 % removal was obtained at the end of 60 minutes of irradiation time for 10 mg L^{-1} of humic acid concentration. UV_{254} parameter was degraded by 43 % in 15 minutes of irradiation, whereas 75% removal achieved after 60 minutes for 20 mg L^{-1} of humic acid. Similar to UV_{254} parameter, UV_{280} changes demostrated declining pattern with 45 % and 77 % of UV_{280} reduction after 15 minutes and 60 minutes, respectively. While 60 % of $Color_{436}$ removed in 15 minutes of irradiation, 98 % removal obtained at the end of 60 minutes for 20 mg L^{-1} of NHA. While 32 % of UV_{254} removed in 15 minutes of irradiation, 48 % removal attained after 60 minutes for 30 mg L^{-1} of NHA. Similar to UV_{254} parameter, 32 % of UV_{280} parameter removed in 15 minutes of irradiation, whereas 50% removal achieved after 60 minutes for 30 mg L^{-1} of NHA. On the other hand considering selected UV-visible parameters while 35 % of UV_{365} and $Color_{436}$ removal was recorded at the end of short period experiments 15 minutes, 58 % of UV_{365} and 61 % of $Color_{436}$ elimination achieved by 60 minutes of irradiation with 30 mg L^{-1} of humic acid. Moreover, 60 minutes of photocatalytic oxidation caused 42 % of DOC removal for 30 mg L^{-1} of NHA. 16 % of UV_{254} parameter degraded in 15 minutes of irradiation, whereas 26 % removal achieved after 60 minutes for 50 mg L^{-1} of NHA. Similar to UV_{254} parameter, UV_{280} alterations demostrated declining pattern with 16 % and 28 % UV_{280} reduction after 15 minutes and 60 minutes, respectively. On the other hand considering selected UV-visible parameter while 20 % of UV_{365} and 21 % of $Color_{436}$ removal was recorded at the end of short period experiments 15 minutes, 36% of UV_{365} and 41% of $Color_{436}$ eliminations achieved by 60 minutes of irradiation with 50 mg L^{-1} of NHA. Moreover, 60 minutes of photocatalytic oxidation caused 41 % of DOC removal from 50 mg L^{-1} of NHA concentration.

Table 4.8. The removal of UV-vis parameter and DOC concentration depending on the irradiation time after the photocatalytic treatment of Nordic humic acid (10-50 mg L^{-1}) (Ilgun, 2010).

10 mg L^{-1}	UV-vis parameters (cm^{-1}) and DOC (mg L^{-1})				
Irr. Time, min	UV_{254}	UV_{280}	UV_{365}	$Color_{436}$	DOC
0	0.1377	0.1143	0.0402	0.0168	5.530
15	0.1027	0.0834	0.0283	0.0118	5.010
30	0.0957	0.0361	0.0106	0.0051	3.250
45	0.0305	0.0239	0.0069	0.0039	2.590
60	0.0134	0.0105	0.0046	0.0032	2.030
RAW	0.2792	0.2285	0.0820	0.0317	5.500
20 mg L^{-1}	UV-vis parameters (cm^{-1}) and DOC (mg L^{-1})				
Irr. Time, min	UV_{254}	UV_{280}	UV_{365}	$Color_{436}$	DOC
0	0.2543	0.2106	0.0675	0.0213	5.542
15	0.2632	0.2100	0.0620	0.0167	6.709
30	0.2233	0.1747	0.0467	0.0106	6.218
45	0.1678	0.1269	0.0294	0.0049	5.295
60	0.1170	0.0864	0.0139	0.0010	4.744
RAW	0.4690	0.3834	0.1285	0.0420	9.635
30 mg L^{-1}	UV-vis parameters (cm^{-1}) and DOC (mg L^{-1})				
Irr. Time, min	UV_{254}	UV_{280}	UV_{365}	$Color_{436}$	DOC
0	0.5035	0.4160	0.1376	0.0468	13.91
15	0.5070	0.4154	0.1340	0.0451	13.74
30	0.4658	0.3766	0.1178	0.0390	12.52
45	0.4422	0.3579	0.1086	0.0345	12.13
60	0.3831	0.3049	0.0878	0.0268	10.41
RAW	0.7436	0.6071	0.2071	0.0694	18.00
50 mg L^{-1}	UV-vis parameters (cm^{-1}) and DOC (mg L^{-1})				
Irr. Time, min	UV_{254}	UV_{280}	UV_{365}	$Color_{436}$	DOC
0	1.0565	0.8674	0.2902	0.0961	19.63
15	1.0298	0.8377	0.2724	0.0899	19.29
30	0.9861	0.7968	0.2528	0.0815	18.25
45	0.9248	0.7431	0.2280	0.0712	16.90
60	0.9039	0.7238	0.2165	0.0675	15.96
RAW	1.2294	1.0041	0.3398	0.1137	26.98

The concentration of natural organic matter is very important for the degradation rate during the photocatalytic treatment. The degradation rate of organic substances usually display saturation behavior. At low concentrations, photogenerated electron-hole pairs

reaction with organic compounds dominate the process, and, therefore, the degradation rate increases linearly with concentration. However, at high concentrations, the generation and migration of photogenerated electron-hole pairs will become the governing step, and the degradation rate increases slowly (Carp et al., 2004). 10 mg L^{-1} of humic acid exhibited 63 % DOC removal, whereas 50 mg L^{-1} of humic acid exhibited 41 % DOC removal. Consistent with the literature (Carp et al., 2004), 10 mg L^{-1} of humic acid exhibited 95 % UV_{254} removal, whereas 50 mg L^{-1} of NHA exhibited 26% UV_{254} removal in 60 minutes.

According to the data given in Table 4.8, DOC concentration of NHA (DOC_{calc}) was calculated by using Equation (Equation 4.2, Equation 4.4, Equation 4.6 and Equation 4.8) obtained by the correlation between UV-vis parameters (UV_{254}, UV_{280}, UV_{365} and $Color_{436}$) and DOC concentrations of nonoxidized NHA. DOC_{calc} was represented depending on irradiation time for 10, 20, 30 and 50 mg L^{-1} of NHA in Table 4.9. According to the irradiation time (0, 15, 30, 45 and 60 minutes), DOC_{calc} was presented as a function of the removed UV_{254} parameter (Table 4.8) during the photocatalytic treatment for all concentrations (10, 20, 30, and 50 mg L^{-1}), and also DOC_{calc} was presented as a function of the removed UV_{280} parameter, UV_{365} parameter , $Color_{436}$ parameter (Table 4.8) during the photocatalytic treatment for all concentrations (10, 20, 30, and 50 mg L^{-1}).

DOC_{calc} exhibited in range of 5.568 mg L^{-1} to 0.736 mg L^{-1}, in range of 9.017 mg L^{-1} to 2.619 mg L^{-1}, in range of 14.01 mg L^{-1} to 7.456 mg L^{-1}, and in range of 22.84 mg L^{-1} to 16.92 mg L^{-1} as a function of the removed UV_{254} parameter during the photocatalytic treatment for 10 mg L^{-1}, 20 mg L^{-1}, 30 mg L^{-1} and 50 mg L^{-1}. DOC_{calc}, as a function of the removed UV_{280} parameter during the photocatalytic treatment, exhibited 84 %, 71 %, 47 % and 27 % removal, for 10 mg L^{-1}, 20 mg L^{-1}, 30 mg L^{-1} and 50 mg L^{-1}. DOC_{calc}, as a function of the removed UV_{365} parameter during the photocatalytic treatment, exhibited 92 %, 87 %, 57 % and 36 % removal, for 10 mg L^{-1}, 20 mg L^{-1}, 30 mg L^{-1} and 50 mg L^{-1} . DOC_{calc}, as a function of the removed $Color_{436}$ parameter during the photocatalytic treatment, exhibited 94 %, 100 %, 63 % and 41 % removal, for 10 mg L^{-1}, 20 mg L^{-1}, 30 mg L^{-1} and 50 mg L^{-1}.

Table 4.9. The dissolved organic carbon concentration, calculated as a function of UV_{254}, UV_{280}, UV_{365} and $Color_{436}$ parameters of NHA by using Equation 4.2, 4.4, 4.6 and 4.8, respectively, after the photocatalytic treatment (NHA, 10-50 mg L^{-1}).

10 mg L^{-1}	UV_{254}	UV_{280}	UV_{365}	$Color_{436}$
Irr. Time, min	DOC_{calc}, mg L^{-1}			
0	2.996	3.160	2.956	3.273
15	2.360	2.494	2.134	2.215
30	2.232	1.474	0.912	0.797
45	1.047	1.211	0.656	0.543
60	0.736	0.922	0.497	0.395
RAW	5.568	5.622	5.842	6.427
20 mg L^{-1}	UV_{254}	UV_{280}	UV_{365}	$Color_{436}$
Irr. Time, min	DOC_{calc}, mg L^{-1}			
0	5.115	5.236	4.841	4.225
15	5.277	5.223	4.461	3.251
30	4.552	4.462	3.404	1.960
45	3.543	3.432	2.210	0.753
60	2.619	2.559	1.139	0.000
RAW	9.017	8.961	9.053	8.606
30 mg L^{-1}	UV_{254}	UV_{280}	UV_{365}	$Color_{436}$
Irr. Time, min	DOC_{calc}, mg L^{-1}			
0	9.645	9.664	9.681	9.622
15	9.708	9.651	9.433	9.262
30	8.959	8.815	8.314	7.971
45	8.530	8.412	7.679	7.019
60	7.456	7.269	6.242	5.389
RAW	14.01	13.78	14.48	14.41
50 mg L^{-1}	UV_{254}	UV_{280}	UV_{365}	$Color_{436}$
Irr Time, min	DOC_{calc}, mg L^{-1}			
0	19.70	19.40	20.22	20.06
15	19.21	18.76	18.99	18.74
30	18.42	17.87	17.64	16.97
45	17.30	16.72	15.92	14.79
60	16.92	16.30	15.13	14.00
RAW	22.84	22.34	23.64	23.78

As mentioned above, DOC_{calc} (Table 4.9), calculated by using Equation 4.2 as a function of UV_{254} parameter, including non-oxidative data prior to photocatalytic treatment and oxidative data after each irradiation time of photocatalytic treatment was presented in Figure 4.22. The photocatalytic treatment was applied for 60 minutes. '0' irradiation time

represents initial DOC_{calc} concentration in Table 4.9. '0.1' presentation was chosen to signify t=0 condition. DOC_{calc}, dependent on the initial concentration of NHA, increased as expected at time'0'.

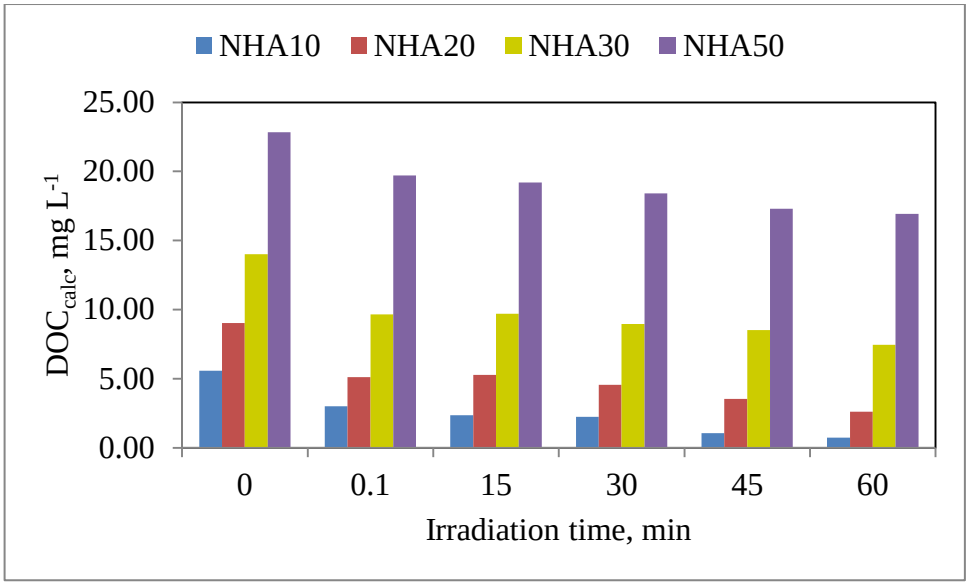

Figure 4.22. DOC_{calc} concentration, obtained by using Equation 4.2 for UV_{254} parameter, as a function of irradiation time for NHA.

At t=0.1, adsorption effect was examined in DOC_{calc}, dependent on the initial concentration of NHA with irrespective to time. At the end of adsorption period, 46 %, 43 %, 31 % and 14 % removal exhibited decreasing trend for 10, 20, 30 and 50 mg L^{-1} of NHA, respectively. Dependent upon irradiation time of 15 minutes, DOC_{calc} values displayed a consistent decreasing trend with respect to time. Moreover, the irradiation time of 30 minutes, 58 %, 41 %, 31 % and 16 % removal exhibited decreasing trend in DOCcalc, depending on the initial concentration of NHA of 10 mg L^{-1}, 20 mg L^{-1}, 30 mg L^{-1} and 50 mg L^{-1}, respectively. After the irradiation time of 60 minutes, 87 %, 71 %, 47 % and 26 % removal displayed decreasing trend in DOC_{calc}, dependent on the initial concentration of NHA.

DOC_{calc} (Table 4.9), calculated by using Equation 8 as a function of $Color_{436}$ parameter, including non-oxidative data prior to photocatalytic treatment and oxidative

data for each irradiation time of photocatalytic treatment for 10, 20, 30 and 50 mg L^{-1} of NHA was presented in Figure 4.23.

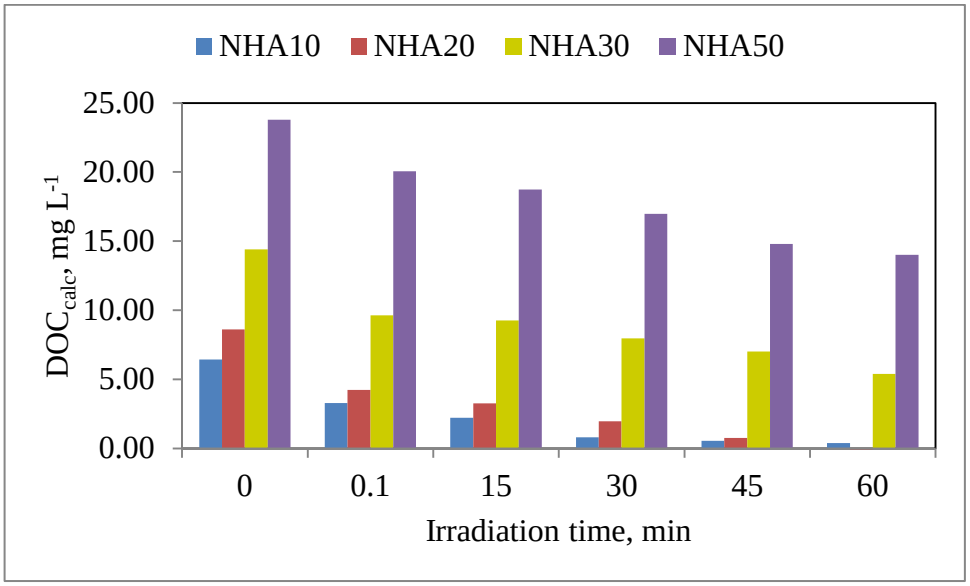

Figure 4.23. DOC_{calc} concentration, obtained by using Equation 8 for $Color_{436}$ parameter, as a function of irradiation time for NHA.

At 't=0', adsorption effect on DOC_{calc}, dependent upon the initial concentration of NHA, was determined. At the end of adsorption period, 49 %, 51 %, 33 % and 16 % removal displayed decreasing trend in DOC_{calc} for 10 mg L^{-1}, 20 mg L^{-1}, 30 mg L^{-1} and 50 mg L^{-1} of NHA, respectively. Moreover, after the irradiation time of 30 minutes, 88 %, 77 %, 45 % and 29 % removal, exhibited decreasing trend in DOC_{calc}, dependent upon the initial concentration of 10, 20, 30 and 50 mg L^{-1} NHA, respectively. After the irradiation time of 60 minutes, 94 %, 94 %, 63 % and 41 % removal displayed decreasing trend in DOC_{calc}, depending on the initial concentration of NHA.

According to the data given in Table 4.8, DOC concentration of NHA (DOC_{calc}) was calculated by using Equation (Equation 4.43, Equation 4.45, Equation 4.47 and Equation 4.49) obtained by the correlation between UV-vis parameters (UV_{254}, UV_{280}, UV_{365} and $Color_{436}$) and DOC concentrations of non-oxidized NHA. DOC_{calc} was represented depending on irradiation time for 10, 20, 30 and 50 mg L^{-1} of NHA in Table 4.10.

Table 4.10. The dissolved organic carbon concentration, calculated as a function of UV_{254}, UV_{280}, UV_{365} and $Color_{436}$ parameters of NHA by using Equation 4.43, 4.45, 4.47 and 4.49, respectively, after the photocatalytic treatment (NHA, 10-50 mg L^{-1}).

10 mg L^{-1}	UV_{254}	UV_{280}	UV_{365}	$Color_{436}$
Irr. Time, min	DOC_{calc}, mg L^{-1}			
0	3.150	3.395	5.324	7.014
15	2.658	2.899	5.060	6.853
30	2.560	2.139	4.667	6.638
45	1.643	1.943	4.584	6.599
60	1.403	1.727	4.533	6.577
RAW	5.140	5.230	6.253	7.493
20 mg L^{-1}	UV_{254}	UV_{280}	UV_{365}	$Color_{436}$
Irr. Time, min	DOC_{calc}, mg L^{-1}			
0	4.790	4.943	5.931	7.159
15	4.915	4.933	5.809	7.011
30	4.354	4.366	5.469	6.815
45	3.574	3.598	5.084	6.632
60	2.859	2.947	4.740	6.506
RAW	7.808	7.719	7.286	7.825
30 mg L^{-1}	UV_{254}	UV_{280}	UV_{365}	$Color_{436}$
Irr .Time, min	DOC_{calc}, mg L^{-1}			
0	8.293	8.243	7.489	7.979
15	8.342	8.233	7.409	7.924
30	7.763	7.610	7.049	7.728
45	7.431	7.309	6.844	7.584
60	6.600	6.458	6.382	7.336
RAW	11.67	11.31	9.033	8.706
50 mg L^{-1}	UV_{254}	UV_{280}	UV_{365}	$Color_{436}$
Irr Time, min	DOC_{calc}, mg L^{-1}			
0	16.07	15.50	10.88	9.565
15	15.69	15.02	10.48	9.365
30	15.08	14.36	10.05	9.095
45	14.22	13.50	9.497	8.764
60	13.92	13.19	9.242	8.645
RAW	18.50	17.69	11.98	10.13

According to the irradiation time (0, 15, 30, 45 and 60 minutes), DOC_{calc} was presented as a function of the removed UV_{254} parameter (Table 4.8) during the photocatalytic treatment for all concentrations (10, 20, 30, and 50 mg L^{-1}), and also DOC_{calc} was presented as a function of the removed UV_{280} parameter, UV_{365} parameter , $Color_{436}$ parameter (Table 4.8) during the photocatalytic treatment for all concentrations (10, 20, 30, and 50 mg L^{-1}). DOC_{calc} exhibited, in range of 5.140 mg L^{-1} to 1.403 mg L^{-1}, in

range of 7.808 mg L^{-1} to 2.859 mg L^{-1}, in range of 11.67 mg L^{-1} to 6.600 mg L^{-1}, and in range of 18.50 mg L^{-1} to 13.92 mg L^{-1} as a function of the removed UV_{254} parameter during the photocatalytic treatment for 10 mg L^{-1}, 20 mg L^{-1}, 30 mg L^{-1} and 50 mg L^{-1}. DOC_{calc}, as a function of the removed UV_{280} parameter during the photocatalytic treatment, exhibited 67 %, 62 %, 43 % and 25 % removal, for 10 mg L^{-1}, 20 mg L^{-1}, 30 mg L^{-1} and 50 mg L^{-1}. DOC_{calc}, as a function of the removed UV_{365} parameter during the photocatalytic treatment, exhibited 28 %, 35 %, 29 % and 23 % removal, for 10 mg L^{-1}, 20 mg L^{-1}, 30 mg L^{-1} and 50 mg L^{-1} . DOC_{calc}, as a function of the removed $Color_{436}$ parameter during the photocatalytic treatment, exhibited 12 %, 17 %, 16 % and 15 % removal, for 10 mg L^{-1}, 20 mg L^{-1}, 30 mg L^{-1} and 50 mg L^{-1} after the irradiation time of 60 minutes.

DOC_{calc} (Table 4.10), obtained by using Equation 4.43, as a function of UV_{254} parameter, including non-oxidative data prior to photocatalytic treatment and oxidative data after irradiation time of photocatalytic treatment for 10, 20, 30, and 50 mg L^{-1} of NHA, respectively was presented in Figure 4.24. At the end of adsorption period of NHA, 39% , 37 %, 29 % and 13% removal exhibited decrease in DOC_{calc}, dependent on the initial concentration of NHA with respect to time ‘0’.

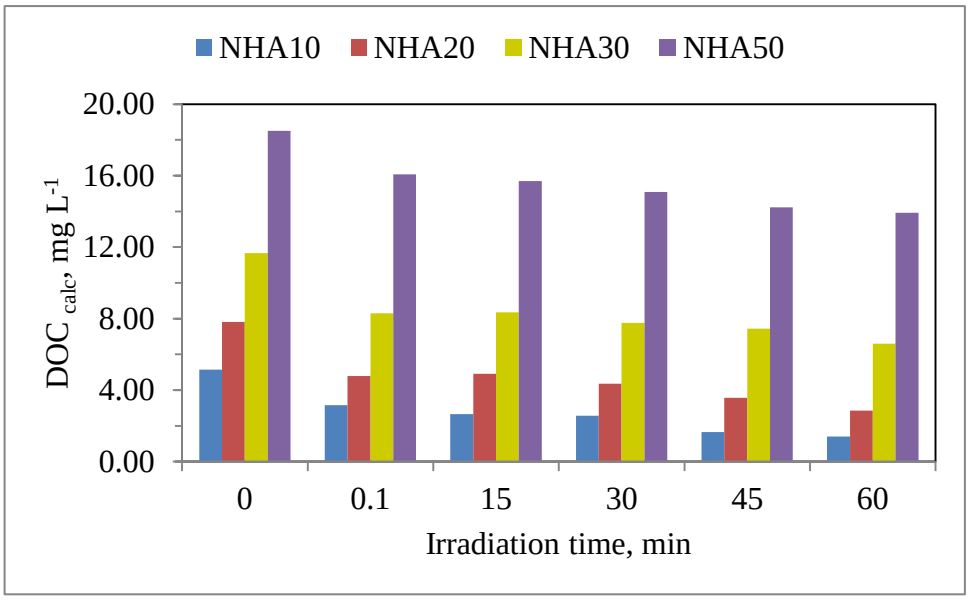

Figure 4.24. DOC_{calc} concentration, obtained by using Equation 4.43 for UV_{254} parameter, as a function of irradiation time for NHA.

Dependent upon irradiation time of 15 minutes, DOC_{calc} values displayed consistent decreasing trend for each Nordic humic acid concentrations. After the irradiation time of 30 minutes, 50 %, 44 %, 33 % and 18 % removal exhibited decreasing trend in DOC_{calc}, dependent on the initial concentration of NHA for 10 mg L^{-1}, 20 mg L^{-1}, 30 mg L^{-1} and 50 mg L^{-1} of Nordic humic acid, respectively. After the irradiation time of 60 minutes, 73%, 63 %, 43% and 25% removal displayed decreasing trend in DOC_{calc}, depending on the initial concentration of NHA of 10 mg L^{-1}, 20 mg L^{-1}, 30 mg L^{-1} and 50 mg L^{-1}, respectively for UV_{254} parameter.

DOC_{calc} (Table 4.10), attained by using Equation 4.49, as a function of $Color_{436}$ parameter, including nonoxidative data prior to photocatalytic treatment and oxidative data after irradiation time of photocatalytic treatment for the initial concentration of NHA, was presented in Figure 4.25. At the end of adsorption period of NHA, 6 %, 9 %, 8 % and 6 % removal displayed decrease in DOC_{calc}, depending on the initial concentration of NHA with respect to time '0' (Figure 4.25). Dependent upon irradiation time of 15 minutes, DOC_{calc} values displayed consistent decreasing trend for each Nordic humic acid concentrations. After the irradiation time of 30 minutes, 11 %, 13 %, 11 % and 10 % removal exhibited decreasing trend in DOC_{calc}, dependent on the initial concentration of NHA for 10 mg L^{-1}, 20 mg L^{-1}, 30 mg L^{-1} and 50 mg L^{-1}, respectively. After the irradiation time of 60 minutes, 12 %, 17 %, 16 % and 15 % removal displayed decreasing trend in DOC_{calc}, depending on the initial concentration of NHA of 10 mg L^{-1}, 20 mg L^{-1}, 30 mg L^{-1} and 50 mg L^{-1}, respectively for $Color_{436}$ parameter.

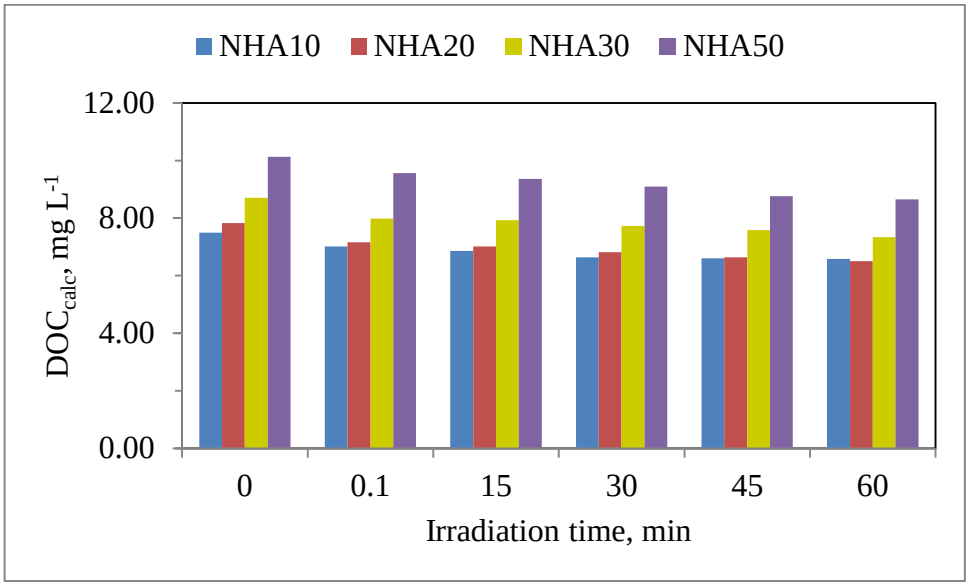

Figure 4.25. DOC_{calc} concentration, obtained by using Equation 4.49 for $Color_{436}$ parameter, as a function of irradiation time for NHA.

As mentioned before, Equation 4.2 (UV_{254}), Equation 4.4 (UV_{280}), Equation 4.6 (UV_{365}) and Equation 4.8 ($Color_{436}$) were attained by the correlation curve between UV-vis parameters and DOC concentrations of NHA. Equation 4.43 (UV_{254}), Equation 4.45 (UV_{280}), Equation 4.47 (UV_{365}) and Equation 4.49 ($Color_{436}$) were achieved by the correlation curve between UV-vis parameters and DOC concentrations of NHA, AHA, FHA and RHA. The removal rate of DOC_{calc} results (Table 4.9) were compared with DOC_{obs} degradation rate (Table 4.8).

The removal of DOC_{calc}, according to Equation 4.43 (Table 4.10) exhibited 77 % removal of DOC_{calc}, depending on Equation 4.2 (Table 4.9) for UV_{254} parameter of 10 mg L^{-1} NHA. The highest difference between Equation 4.2, obtained from the correlation of NHA and Equation 4.43, attained from the correlation of the overall humic acids, was observed for $Color_{436}$ parameter of 10 mg L^{-1} NHA. The degradation of DOC_{calc} calculated depending on Equation 4.49 (Table 4.10) displayed 15 % removal of DOC_{calc}, according to Equation 4.8 (Table 4.9) for $Color_{436}$ parameter of 10 mg L^{-1} NHA. The removal of DOC_{calc} (20 mg L^{-1} humic acid), depending on Equation 4.43 (Table 4.10) exhibited 77 % removal of DOC_{calc}, according to Equation 4.2 (Table 4.9) for UV_{254} parameter. Moreover, the removal of DOC_{calc} (20 mg L^{-1} NHA), according to Equation 4.49 (Table 4.10),

displayed 15 % of DOC degradation calculated, depending on Equation 4.8 (Table 4.9) for $Color_{436}$ parameter. The removal of DOC_{calc} (30 mg L^{-1}), according to Equation 4.43 and Equation 4.47 (Table 4.10), displayed 77 % and 32 % of the degraded DOC_{calc}, depending on Equation 4.2 and Equation 4.6 (Table 4.9) for UV_{254} parameter and UV_{365} parameter, respectively. The degradation of DOC (50 mg L^{-1} NHA), depending on Equation 4.43, Equation 4.45, Equation 4.47 and Equation 4.49 (Table 4.10), exhibited 77 %, 74 %, 32 % and 15 % removal of DOC_{calc}, depending on Equation 4.2, Equation 4.4, Equation 4.6 and Equation 4.8 (Table 4.9) for UV_{254}, UV_{280}, UV_{365} and $Color_{436}$ parameter, respectively.

The removal of DOC concentrations of NHA were correlated with the removal of UV-vis parameters (UV_{254}, UV_{280}, UV_{365} and $Color_{436}$). As mentioned above, the degradation of humic acid was completed in 60 minutes. At the end of each irradiation period (15, 30, 45 and 60 minutes), reported above, DOC and UV-vis parameter results (Table 4.8) were used in graphs below for 10, 20, 30 and 50 mg L^{-1} of NHA.

4.3.1.1. The Relationship between UV-vis Parameters and DOC Concentration, Including Non-oxidative Data before the Photocatalytic Treatment and Oxidative Data after each Irradiation Period of Photocatalytic Treatment for NHA. 10, 20, 30 and 50 mg L^{-1} of NHA were treated by the photocatalytic treatment. The treatment was applied for 60 minutes. As mentioned above, the removal of UV_{254} parameter, UV_{280} parameter, UV_{365} parameter and $Color_{436}$ parameter and the removal of DOC concentration in 60 minutes (Table 4.8) were explained. For the irradiation time of 60 minutes, the degraded rate of DOC concentration, and UV-vis parameters (UV_{254}, UV_{280}, UV_{365} and $Color_{436}$) resulted in the different values. The removal concentrations of 10, 20, 30 and 50 mg L^{-1} NHA were correlated with the removal of UV-vis parameters (UV_{254}, UV_{280}, UV_{365} and $Color_{436}$). DOC_{obs}, obtained after 15 minutes period of photocatalytic treatment, and UV-vis parameter corresponding to theses DOC_{obs} were used in graphs. In addition to the photo-oxidation data, the initial values and the values, representing at t=0, were used in graphs. As mentioned above, the types of UV-vis parameters indicated the different removal rate for each irradiation period. For example, 10 mg L^{-1} of NHA exhibited 63 % DOC removal, 95 % UV_{254} and UV_{280} removal, 94 % UV_{365} and 90 % $Color_{436}$ removal after the irradiation time of 15 minutes. Moreover, with increasing initial humic acid concentration, the removal rate changed. As the concentration of humic acid increased, the removal rate of UV-vis parameters and

DOC concentrations decreased. To examine these removals, the correlation graphs, the relationship between the removal of UV-vis parameters (UV_{254}, UV_{280}, UV_{365} and $Color_{436}$) and DOC concentrations with different initial humic acid concentrations (10, 20, 30 and 50 mg L^{-1}), were drawn (Figure 4.26).

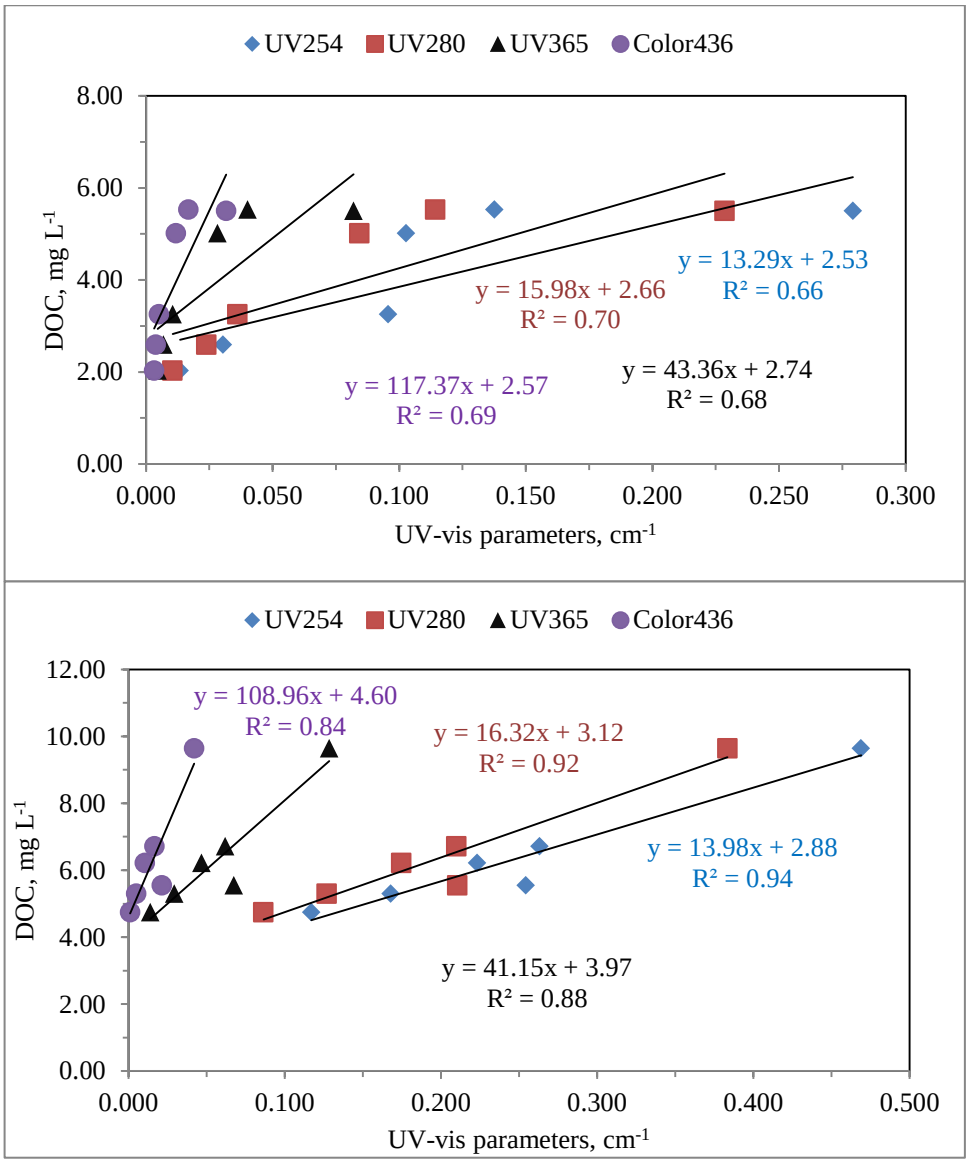

Figure 4.26. The correlation between UV-vis parameters (UV_{254}, UV_{280}, UV_{365} and $Color_{436}$) and DOC concentration , including oxidative data for each irradiation period of the photocatalytic treatment and non-oxidative data before the photocatalytic treatment (10 and 20 mg L^{-1} of NHA).

According to the data given in Table 4.8, the remained DOC concentration of NHA (10, 20, 30 and 50 mg L^{-1}) after each irradiation time (15, 30, 45 and 60 minutes) of the photocatalytic treatment and DOC concentration in adsorption period, were correlated with UV-vis parameters (UV_{254}, UV_{280}, UV_{365} and $Color_{436}$) (Figure 4.26). Figure 4.26 represented the correlation between UV-vis parameters (UV_{254}, UV_{280}, UV_{365} and $Color_{436}$) and DOC concentrations, including the non-oxidative data before the photocatalytic treatment and the oxidative data for each irradiation period of the photocatalytic treatment (10 and 20 mg L^{-1} of NHA). The correlation between UV-vis parameters and DOC concentration (10 mg L^{-1} of NHA) exhibited low regression coefficient (UV_{254}, R^2=0.66; UV_{280}, R^2=0.70; UV_{365}, R^2=0.68; $Color_{436}$, R^2=0.69). The correlation between UV-vis parameters and DOC concentration (20 mg L^{-1} of NHA) exhibited high regression coefficient (UV_{254}, R^2=0.94; UV_{280}, R^2=0.92; UV_{365}, R^2=0.88; $Color_{436}$, R^2=0.84).

Figure 4.27 represented the correlation between UV-vis parameters (UV_{254}, UV_{280}, UV_{365} and $Color_{436}$) and DOC concentrations, including the non-oxidative data before the photocatalytic treatment and the oxidative data for each irradiation period of the photocatalytic treatment (30 and 50 mg L^{-1} of NHA). The correlation between UV-vis parameters and DOC concentration (30 mg L^{-1} of NHA) displayed high regression coefficient (UV_{254}, R^2=0.98; UV_{280}, R^2=1.00; UV_{365}, R^2=1.00; $Color_{436}$, R^2=1.00). The correlation between UV-vis parameters and DOC concentration (50 mg L^{-1} of NHA) displayed high regression coefficient (UV_{254}, R^2=0.97; UV_{280}, R^2=0.96; UV_{365}, R^2=0.91; $Color_{436}$, R^2=0.89).

More specifically, Equations, obtained the correlation between UV-vis parameters (UV_{254}, UV_{280}, UV_{365} and $Color_{436}$) and DOC concentrations under the photocatalytic tratment (Figure 4.26 and Figure 4.27) were listed in Table 4.11. Equation 4.54, Equation 4.55, Equation 4.56 and Equation 4.57 were presented the correlation between DOC concentration, including the adsorption period and the irradiation period (15, 30, 45 and 60 minutes), and UV-vis parameters for 10 mg L^{-1} of NHA. Equation 4.58, Equation 4.59, Equation 4.60 and Equation 4.61 obtained from the correlation between DOC concentration, including the adsorption period and the irradiation period (15, 30, 45 and 60 minutes), and UV_{254}, UV_{280}, UV_{365} and $Color_{436}$ parameter, respectively for 20 mg L^{-1} of NHA.

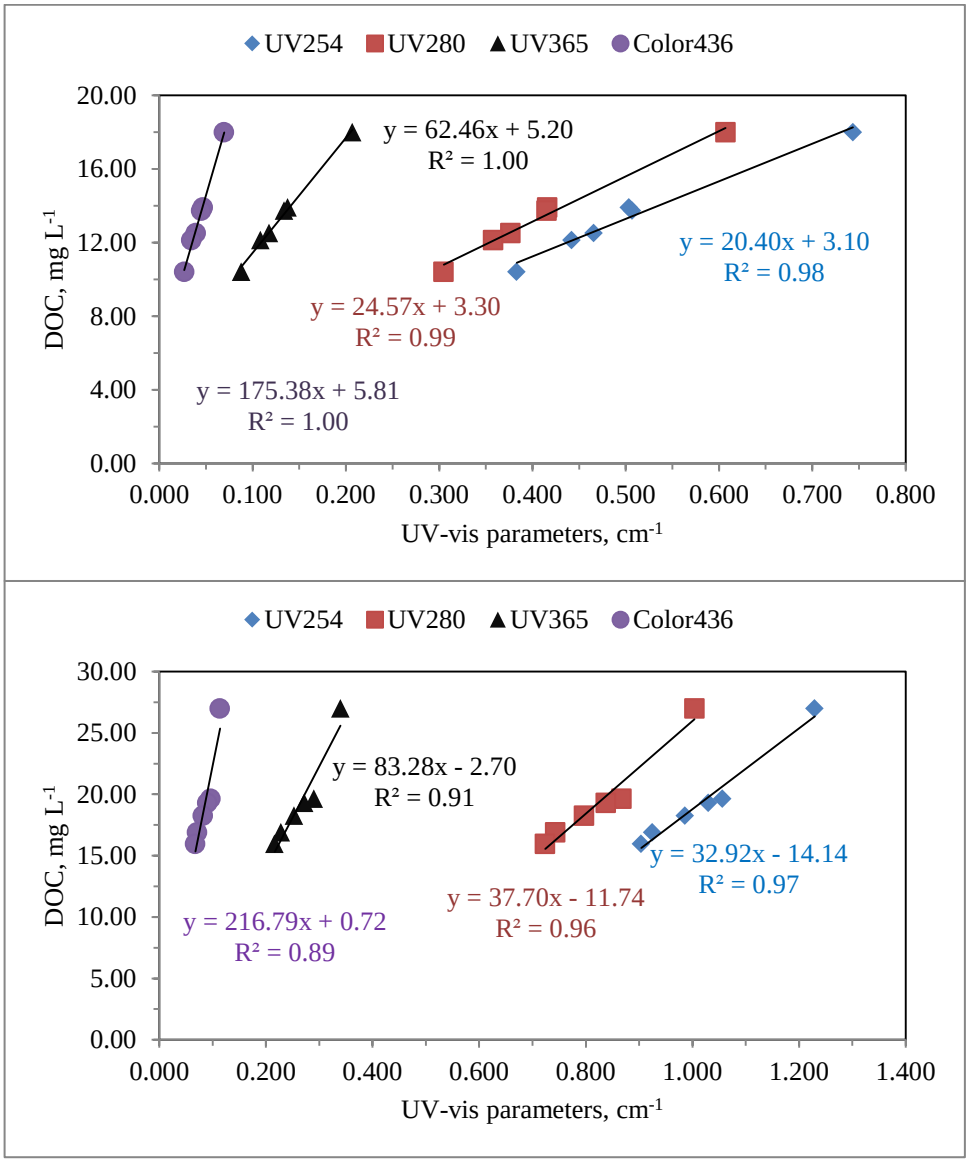

Figure 4.27. The correlation between UV-vis parameters (UV_{254}, UV_{280}, UV_{365} and $Color_{436}$) and DOC concentration, including oxidative data during the photocatalytic treatment and nonoxidative data before the photocatalytic treatment (30 and 50 mg L^{-1} of NHA).

Equation 4.62, Equation 4.63, Equation 4.64 and Equation 4.65 was obtained from the correlation between DOC concentration, including the adsorption period and the irradiation period (15, 30, 45 and 60 minutes), and UV_{254}, UV_{280}, UV_{365} and $Color_{436}$ parameter, respectively for 30 mg L^{-1} of NHA.

Table 4.11. The correlation equation, obtained from the correlation between UV-vis parameters and DOC concentration, including nonoxidative data before the photocatalytic treatment and oxidative data during the photocatalytic treatment, for NHA, and the regression coefficients of these correlation equations.

Equation No	Correlation Equation	R^2
Humic acid concentration: 10 mg L^{-1}		
4.54	DOC (mg L^{-1}) = 13.29*UV_{254} (cm^{-1}) + 2.53	0.664
4.55	DOC (mg L^{-1}) = 15.95*UV_{280} (cm^{-1}) + 2.67	0.699
4.56	DOC (mg L^{-1}) = 43.37*UV_{365} (cm^{-1}) + 2.74	0.680
4.57	DOC (mg L^{-1}) = 117.37*$Color_{436}$ (cm^{-1}) + 2.57	0.688
Humic acid concentration: 20 mg L^{-1}		
4.58	DOC (mg L^{-1}) = 13.98*UV_{254} (cm^{-1}) + 2.88	0.937
4.59	DOC (mg L^{-1}) = 16.32*UV_{280} (cm^{-1}) + 3.12	0.919
4.60	DOC (mg L^{-1}) = 41.15*UV_{365} (cm^{-1}) + 3.97	0.883
4.61	DOC (mg L^{-1}) = 108.96*$Color_{436}$ (cm^{-1}) + 4.61	0.841
Humic acid concentration: 30 mg L^{-1}		
4.62	DOC (mg L^{-1}) = 20.40* UV_{254} (cm^{-1}) + 3.10	0.978
4.63	DOC (mg L^{-1}) = 24.57* UV_{280} (cm^{-1}) + 3.30	0.998
4.64	DOC (mg L^{-1}) = 62.46* UV_{365} (cm^{-1}) + 5.20	0.995
4.65	DOC (mg L^{-1}) = 175.38*$Color_{436}$ (cm^{-1}) + 5.81	0.996
Humic acid concentration: 50 mg L^{-1}		
4.66	DOC (mg L^{-1}) = 32.92* UV_{254} (cm^{-1}) – 14.14	0.972
4.67	DOC (mg L^{-1}) = 37.70 * UV_{280} (cm^{-1}) – 11.74	0.956
4.68	DOC (mg L^{-1}) = 83.28*UV_{365} (cm^{-1}) – 2.70	0.915
4.69	DOC (mg L^{-1}) = 216.79* $Color_{436}$ (cm^{-1}) + 0.72	0.895

Equation 4.66, Equation 4.67, Equation 4.68 and Equation 4.69 obtained from the correlation between DOC concentration, including the adsorption period and the irradiation period (15, 30, 45 and 60 minutes), and UV_{254}, UV_{280}, UV_{365} and $Color_{436}$ parameter, respectively for 50 mg L^{-1} of NHA. As mentioned above, the regression coefficient,

representing the correlation between (R^2> 0.66) DOC concentration and UV-vis parameter (UV_{254}, UV_{280}, UV_{365} and $Color_{436}$), 10 mg L^{-1} of NHA, was lower than the regression coefficients (R^2>0.84), representing the correlation between DOC concentration and UV-vis parameter (UV_{254}, UV_{280}, UV_{365} and $Color_{436}$), 20, 30 and 50 mg L^{-1} of NHA.

4.3.1.2. Comparative Evaluation of UV-vis Parameters related to Degradation Kinetics.

When humic acid is in low concentration, spectroscopic parametes exhibit independent correlation. On the other hand, humic acid in high concentration spectroscopic parameters give limited correlation. The decomposition of NHA (Nordic) with initial concentration of 50 mg L^{-1} was shown in Figure 4.32. This means for a limited time, UV-vis parameters displayed different degradation velocity. In a study, the photocatalytic degradation rate of 100 mg L^{-1} of AHA was determined by measuring UV_{254} parameter and $Color_{400}$ parameter depending on the irradiation time. $Color_{400}$ parameter of AHA degraded faster than UV_{254} parameter for the irradiation time of 60 minutes. The degradation of the AHA appeared to be complete after 50 minutes. On the other hand, the DOC had been reduced by approximately 50 % (Eggins et al., 1997). Consistent with literature (Eggins et al., 1997), $Color_{436}$ parameter exhibited faster removal than UV_{254} parameter for irradiation time of 60 minutes. On the other hand, in contrast to literature (Eggins et al., 1997; Liu et al., 2008), for a limited irradiation time, DOC degradation rate of NHA was highest than UV-vis parameters. The photocatalytic degradation of 68 mg L^{-1} of AHA in artifial seawater was applied with 2.5 mg ml^{-1} TiO_2 for the treatment. The degradation of 68 mg L^{-1} humic acid at 400 nm exhibited faster removal than the degradation of AHA at 254 nm depending on the irradiation time. Decomposition of humic acid was completed between 50 and 60 minutes at 400 nm, whereas the degradation was completed in 60 minutes at 254 nm. Consistent with literatures (Eggins et al., 1997; Al-Rasheed and Cardin, 2003a) and experiment results, humic acid in high concentration, the degradation of humic acid at 400 nm exhibited faster removal than the degradation of humic acid at 254 nm depending on the irradiation time. The photocatalytic removal of FHA, containing 10 mg L^{-1} of DOC and 0.1 mg l^{-1} of TiO_2, examined by monitoring changes in the UV_{254} parameter, dissolved organic carbon concentrations over treatment time. The UVA/TiO_2 process was found to be effective in removing more than 76 % DOC and 90 % UV_{254} parameter after irradiation time of 60 minutes (Liu et al., 2008). Consistent with the literature results, for 10 mg L^{-1} of

NHA, the photocatalytic degradation exhibited at 254 nm (95 %) exhibited faster removal than DOCconcentration (63 %) in experimental results after irradiation time of 60 minutes.

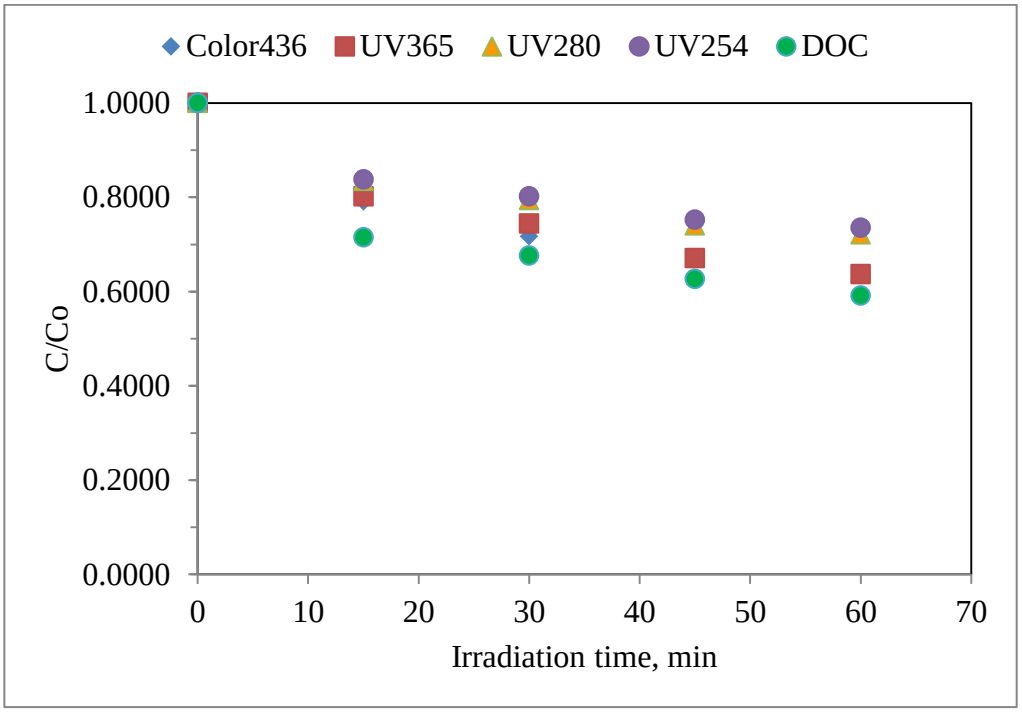

Figure 4.28. Decomposition of NHA with initial concentration 50 mg L^{-1}; TiO_2: 0.25 mg mL^{-1}; UV-vis parameters: UV_{254}, UV_{280}, UV_{365} and $Color_{436}$ and DOC concentration.

In a study, after the photocatalytic treatment of humic acids, $Color_{436}$ reductions were observed to be faster than UV_{254}, UV_{280} and UV_{365} parameter, moreover, UV_{365} reductions were faster than UV_{254} and UV_{280} parameter, which represented the carbon double bonds and aromatic structure within the humic acid molecule. Consistent with the literature (Uyguner et al., 2005b), the reduction rate showed decreasing trend as follows; $Color_{436}$ > UV_{365} > UV_{280} > UV_{254} parameter.

DOC_{obs} concentration of NHA, including oxidative data after each irradiation time of photocatalytic treatment (Table 4.8), were correlated with DOC_{calc} concentrations, that was calculated by using Equation 4.66 as a function of UV_{254} parameter, Equation 4.67 as a function of UV_{280} parameter, Equation 4.68 as a function of UV_{365} parameter and Equation 4.69 as a function of $Color_{436}$ parameter before the photocatalytic treatment and after each

irradiation time of photocatalytic treatment (Table 4.11) for 50 mg L^{-1} of NHA (Figure 4.28).

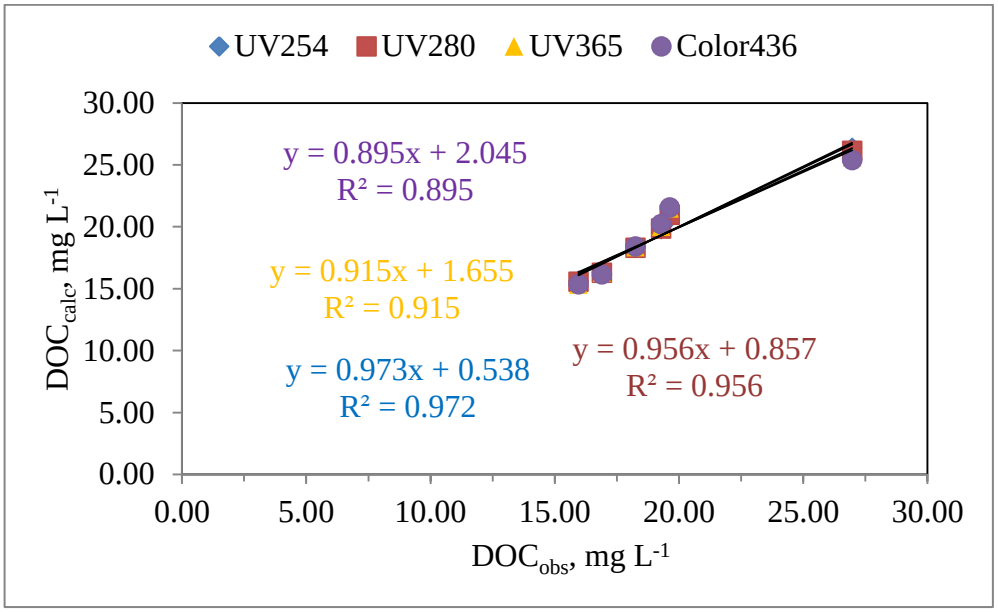

Figure 4.29. The relationship between DOC_{calc}, calculated according to Equation 4.66 for UV_{254} parameter. Equation 4.67 for UV_{280} parameter, Equation 4.68 for UV_{365} parameter and Equation 4.69 parameter for $Color_{436}$ parameter and DOC_{obs}.

Figure 4.29 illustrated the linear correlation between DOC_{obs} concentrations and DOC_{calc} concentrations. DOC equation was produced from the least-squares regression analyses (Equation 4.66, Equation 4.67, Equation 4.68 and Equation 4.69). The regression coefficient was found to be as R^2= 0.972 (UV_{254}), R^2= 0.956 (UV_{280}), R^2= 0.915 (UV_{365}) and R^2= 0.895 ($Color_{436}$). As a result, DOC_{calc}, obtained as a function UV_{254} parameter by using Equation 4.66, attained as a function of UV_{280} parameter by using Equation 4.67, obtained as a function of UV_{365} parameter by using Equation 4.68, and attained as a function of $Color_{436}$ parameter by using Equation 4.69, could predict DOC_{obs}, the data given in Table 4.8, with high regression coefficient.

4.3.1.3. The over-all Relationship between DOC and UV_{254} of NHA irrespective of Initial Humic Acid Concentration. According to Table 4.8, DOC concentrations, including the non-oxidative data before the photocatalytic treatment and the oxidative data after each

irradiation time of photocatalytic treatment, were plotted against UV_{254} parameter, corresponding to these DOC concentrations of NHA, in Figure 4.30.

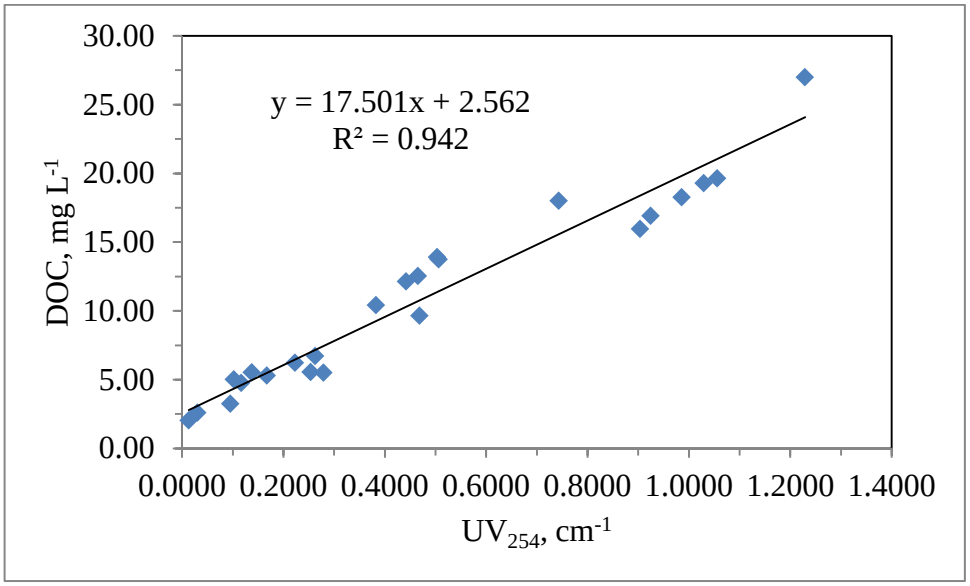

Figure 4.30. The correlation between UV_{254} parameter and DOC concentration, including oxidative data for each irradiation time during the photocatalytic treatment and nonoxidative data before the photocatalytic treatment, for 10, 20, 30 and 50 mg L^{-1} of NHA.

Figure 4.30 illustrated the linear correlation between UV_{254} parameter and DOC concentrations of NHA. Equation of the correlation between DOC concentration, including oxidative data for each irradiation time during the photocatalytic treatment and nonoxidative data before the photocatalytic treatment, for 10, 20, 30 and 50 mg L^{-1} of NHA, and UV_{254} parameter of the remaind NHA after the photocatalytic treatment and NHA concentration at adsorption period, was produced from the least-squares regression analyses (Equation 4.70). The regression coefficient was found to be as R^2= 0.942. As mentioned above, Equation 4.2 was obtained by the correlation between UV_{254} parameter and DOC concentration of non-oxidized NHA. Equation 4.70 was attained by the correlation between UV_{254} parameter and DOC concentration of NHA, including all conditions. Equation 4.43 was achieved from the graph, representing the relationship between UV_{254} parameter and DOC concentration of the nonoxidized overall humic acids (NHA, FHA, AHA and RHA). Equation 4.70a was attained by the graph, pointing out the

correlation between UV_{254} parameter results and DOC concentration results of NHA, including at t=0 and post oxidation, after the photocatalytic treatment. Equation 4.70b was achieved from the graph, representing the correlation between UV_{254} parameter and DOC concentrations, including only post oxidation data, after the photocatalytic treatment. These equations were stated below (Table 4.19). In the least square regression model, equation could give random error (Johnson and Bhattacharyya, 1996). Equation 4.2, represented the randon error as a value of 0.49, Equation 4.70 represented the randon error as a value of 2.56, Equation 70a represented the randon error as a value of 3.03, Equation 4.70b represented the randon error as a value of 3.00, and Equation 4.43 represented the randon error as a value of 1.22 (Table 4.12).

Table 4.12. The correlation equations and the regression coefficients obtained from the relationship between UV_{254} and DOC concentration of NHA, including non treatment data (Equation 4.2) and photocatalytic treatment data (Equation 4.70, 4.70a, 4.70b), and the relationship between UV_{254} and DOC concentration of the overall humic acids (NHA, FHA, AHA and RHA), including non treatment data (Equation 4.43).

Equation No	Correlation Equation	R^2
4.2	DOC (mg L^{-1}) = 18.18 * UV_{254} (cm^{-1}) + 0.49	0.995
4.70	DOC (mg L^{-1}) = 17.50 * UV_{254} (cm^{-1}) + 2.56	0.942
4.70a	DOC (mg L^{-1} = 16.14 * UV_{254} (cm^{-1}) + 3.03	0.948
4.70b	DOC (mg L^{-1}) = 16.08* UV_{254}(cm^{-1}) + 3.00	0.953
4.43	DOC (mg L^{-1}) = 14.06*UV_{254} (cm^{-1}) + 1.22	0.936

Figure 4.30 illustrated the linear correlation between UV_{254} parameter and DOC concentrations of NHA. Equation of the correlation between DOC concentration, including oxidative data for each irradiation time during the photocatalytic treatment and nonoxidative data before the photocatalytic treatment, for 10, 20, 30 and 50 mg L^{-1} of NHA, and UV_{254} parameter of the remaind NHA after the photocatalytic treatment and NHA concentration at adsorption period, was produced from the least-squares regression analyses (Equation 4.70). The regression coefficient was found to be as R^2= 0.942.

Table 4.13. DOC concentrations of NHA calculated by using Equation 4.2, Equation 4.70, Equation 4.70a, Equation 4.70 and Equation 4.43, as a function of UV_{254} parameter, including nonoxidative data before the photocatalytic treatment and oxidative data after each irradiation time period, and DOC concentration measured by TOC analyzer for 10, and 50 mg L^{-1} of NHA.

NHA: 10 mg L^{-1}	UV_{254}, cm^{-1}					
Irradiation time	0	15	30	45	60	RAW
	0.1377	0.1027	0.0957	0.0305	0.0134	0.2792
Equation	DOC, mg L^{-1}					
4.2	2.993	2.357	2.230	1.044	0.734	5.566
4.70	4.970	4.357	4.235	3.094	2.795	7.446
4.70a	5.252	4.688	4.575	3.522	3.246	7.536
4.70b	5.214	4.651	4.539	3.490	3.215	7.490
4.43	3.156	2.664	2.566	1.649	1.408	5.146
Observation	5.530	5.010	3.250	2.590	2.030	5.500
NHA: 50 mg L^{-1}	UV_{254}, cm^{-1}					
Irradiation time	0	15	30	45	60	RAW
	1.0565	1.0298	0.9861	0.9248	0.9039	1.2294
Equation	DOC, mg L^{-1}					
4.2	19.70	19.21	18.42	17.30	16.92	22.84
4.70	21.05	20.58	19.82	18.74	18.38	24.07
4.70a	20.08	19.65	18.95	17.96	17.62	22.87
4.70b	19.99	19.56	18.86	17.87	17.53	22.77
4.43	16.07	15.70	15.08	14.22	13.93	18.51
Observation	19.63	19.29	18.25	16.90	15.96	26.98

UV_{254} parameter results of 10 and 50 mg L^{-1} NHA, including before the photocatalytic treatment, at t=0 and post oxidation data (Table 4.8), were used to calculate DOC results, as shown in Table 4.13. During the adsorption period (t=0) DOC_{calc}, as a function of UV_{254} parameter by using Equation 4.2, exhibited 95 % of DOC_{calc}, depending on Equation 4.43. Moreover, DOC_{calc}, as a function of UV_{254} parameter by using Equation

4.2, exhibited 60 % of DOC_{calc}, depending on Equation 4.70 for 10 mg L^{-1} of NHA. After the irradiation time of 60 minutes, DOC_{calc}, calculated as a function of UV_{254} parameter by using Equation 4.2, exhibited 52 % of DOC_{calc}, expressed related to Equation 4.43. Moreover, DOC_{calc}, calculated as a function of UV_{254} parameter by using Equation 4.2, exhibited 26 % of DOC_{calc}, expressed related to Equation 4.70 for 10 mg L^{-1} of NHA (Table 4.13). During the adsorption period (t=0) DOC_{calc}, as a function of UV_{254} parameter by using Equation 4.43, exhibited 82 % of DOC_{calc}, dependent upon Equation 4.2. Moreover, DOC_{calc}, calculated as a function of UV_{254} parameter by using Equation 4.2, exhibited 93 % of DOC_{calc}, according to Equation 4.70 for 10 mg L^{-1} of NHA. After the irradiation time of 60 minutes, DOC_{calc}, calculated as a function of UV_{254} parameter by using Equation 4.43, exhibited 82 % of DOC_{calc}, expressed related to Equation 4.2. Moreover, DOC_{calc}, calculated as a function of UV_{254} parameter by using Equation 4.2, exhibited 92 % of DOC_{calc}, expressed related to Equation 4.70 for 50 mg L^{-1} of NHA.

Figure 4.31 showed DOC_{calc}, expressed related to Equation 4.2, Equation 4.70, 4.70a, 4.70b and Equation 4.43, and DOC_{obs}. At t=0, the adsorption effect, dependent on Equations, as mentioned above, was examined with respect to time '0'. At the adsorption period, 46 %, 33 %, 30 %, 30 % and 39 % removal exhibited decreasing trend for Equation 4.2, Equation 4.70, Equation 4.70a, Equation 4.70b and Equation 4.43, respectively. After the irradiation time of 15 minutes, 58 %, 41 %, 38 %, 38 %, 48 %, and 8.9 % removal displayed decreasing trend for Equation 4.2, Equation 4.70, Equation 4.70a, Equation 4.70b, Equation 4.43 and in the observation, respectively. After the irradiation time of 30 minutes, 60 %, 43 %, 39 %, 39 % , 50 % and 41 % removal exhibited for Equation 4.2, Equation 4.70, Equation 4.70a, Equation 4.70b, Equation 4.43 and in the observation. The conversion after 60 min, was 87 % for Equation 4.2, 62 % for Equation 4.70, 57 % for Equation 4.70a and Equation 4.70b, 73 % for Equation 4.43 and 63 % in the observation. On the other hand, after taking average of DOC_{calc}, related to Equation 4.2 and Equation 4.43, DOC average result displayed 53 % of DOC_{obs} result for 10 mg L^{-1} of NHA. When taking the average of DOC results, obtained by all equations, these DOC results exhibited 78 %, 75 % and 99 % of DOC_{obs} result just before photocatalytic treatment, at 15 minutes and at 45 minutes, respectively.

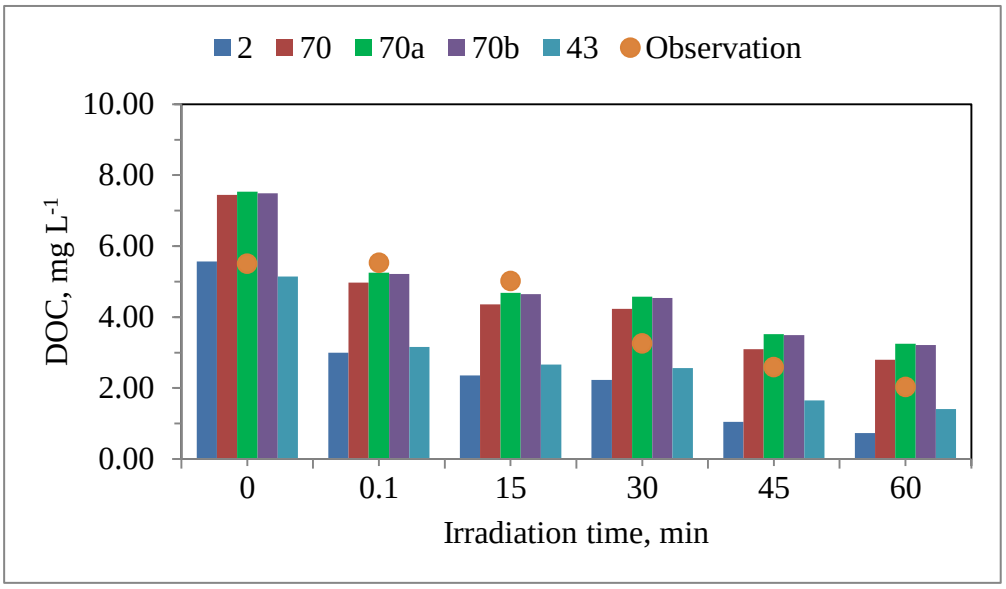

Figure 4.31. Comparison of DOC_{obs} and DOC_{calc} concentration, obtained by using Equation 4.2 (2), Equation 4.70 (70), Equation 4.70a (70a), Equation 4.70 (70b) and Equation 4.43 (43) with respect to the irradiation time as a function of UV_{254} parameter, including the non-oxidative data prior to photocatalytic treatment and the oxidative data after each irradiation period of photocatalytic treatment, for 10 mg L^{-1} of NHA.

The removal of DOC concentration, related to Equation 4.2, exhibited higher removal than DOC concentration, related to Equation 4.70, Equation 4.70a, Equation 4.70b, Equation 4.43 and the observation for 10 mg L^{-1} of NHA after 60 minutes of the photocatalytic treatment. DOC_{calc} related to Equation 4.2 and Equation 4.43, was found to be less than DOC_{obs} for 10 mg L^{-1} of NHA before the photocatalytic treatment and after each irradiation period of the photocatalytic treatment. On the other hand, DOC_{calc}, expressed related to Equation 4.70, Equation 4.70a and Equation 4.70b were found to be closed to DOC_{obs} for each irradiation time. It could be inferred that Equation 4.70a, pointing out the correlation between UV_{254} parameter results and DOC concentration results of NHA, including at t=0 and post oxidation, after the photocatalytic treatment, were found to be useful for the prediction of DOC concentration in 10 mg L^{-1} of NHA, whereas Equation 4.2, obtained from the relationship between DOC and UV_{254} parameter of nonoxidized NHA, and Equation 4.43, attained from the relationship between DOC and UV_{254} parameter of the non-oxidized overall humic acids, were not found to be useful for the prediction of DOC concentration.

Before the photocatalytic treament (t=0), when taking the average of DOC calculation results, calculated by using Equation 4.70, Equation 4.70a and Equation 4.70b, DOC average result exhibited 80 % of DOC_{obs} (Figure 4.32). 14 %, 13 %, 12 %, 13 % and 27 % removal exhibited increasing trend for Equation 4.2, Equation 4.70, Equation 4.70a and 4.70b, Equation 4.43 and in the observation, respectively.

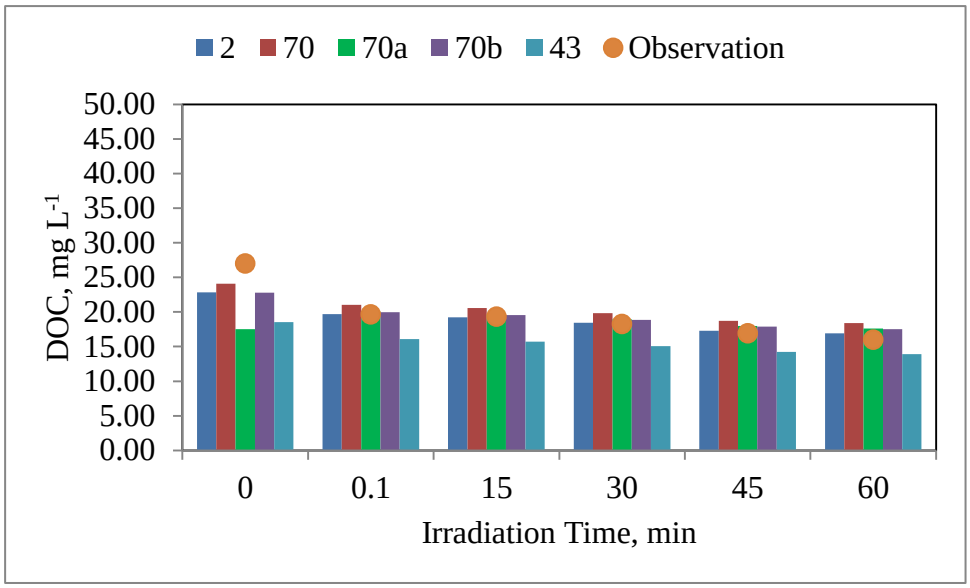

Figure 4.32. Comparison of DOC_{obs} and DOC_{calc} concentration, obtained by using Equation 4.2 (2), Equation 4.70 (70), Equation 4.70a (70a), Equation 4.70b (70b) and Equation 4.43 (43) with respect to the irradiation time as a function of UV_{254} parameter, including non-oxidative data prior to the photocatalytic treatment and oxidative data after each irradiation time of the photocatalytic treatment, for 50 mg L^{-1} of NHA.

After the irradiation time of 30 minutes, 19 %, 18 %, 17%, 17 %, 19 %, and 32 % removal displayed increasing trend for Equation 4.2, Equation 4.70, Equation 4.70a, Equation 4.70b, Equation 4.43 and in the observation, respectively. The conversion after 60 min, was 26 % for Equation 2, 24 % for Equation 4.70, 23 % for Equation 4.70b, 25 % for Equation 4.43 and 41 % in the observation. The removal of DOC_{obs} exhibited approximately two times higher removal than DOC concentration, related to Equation 4.2, Equation 4.70, Equation 4.70a, Equation 4.70b and Equation 4.43 for 50 mg L^{-1} of NHA after the irradiation time of 60 minutes. According to Figure 4.34, DOC_{calc}, calculated by using Equation 4.2, Equation 4.70, Equation 4.70a and Equation 4.70b were found to be

closed to DOC_{obs}, whereas DOC_{obs} was found to be more than DOC_{calc}, calculated by using Equation 4.43. When taking the average of DOC results, obtained by all equations, these DOC results exhibited 99 %, 98 % and 100 % of DOC_{obs} just before photocatalytic treatment, at 15 minutes and at 30 minutes, respectively. As shown in Figure 4.34, Equation 4.2, Equation 4.70, Equation 4.70 a and Equation 4.70 b were found to be useful for the prediction of DOC concentration in 50 mg L^{-1} of NHA during the photocatalytic treatment, whereas Equation 4.43, attained from the relationship between DOC result and UV_{254} parameter of the overall humic acids, were not found to be useful for the prediction of DOC result.

By using these equations (Equation 4.2, Equation 4.70, Equation 4.70a, Equation 4.70b, Equation 4.43), DOC concentration contents were calculated with given UV_{254} parameter, given in Table 4.12. By using these equations DOC_{min}, DOC_{max} and $DOC_{average}$ was calculated as a function of UV_{254}(min), UV_{254}(max) and UV_{254}(average) parameters, respectively. According to Table 4.14, the lowest UV_{254} as 0.0134 cm^{-1} (UV_{254}(min)) was obtained by the photocatalytic treatment of 10 mg L^{-1} NHA for the irradiation time of 60 minutes. On the other hand, the highest UV_{254} (UV_{254} (max)) was expressed as a value of 1.2294 cm^{-1}, representing the initial concentration of 50 mg L^{-1} of Nordic humic acid prior to the photocatalytic treatment. UV_{254}(average), expressed as a value of 0.4689 cm^{-1}, was calculated by taking the average of all of the UV_{254} parameter that were presented in Table 4.9. DOC concentrations of Nordic humic acid, related to UV_{254}(min), UV_{254}(max) and UV_{254}(average) were compared with DOC_{obs}, measured by TOC analyzer, as shown in Table 4.14. DOC_{calc}, obtained by Equation 4.70, Equation 4.70a and Equation 4.70b were closed to each other for UV_{254}(min), UV_{254}(max) and UV_{254}(average) (Table 4.14). 2.796 mg L^{-1} of DOC result, obtained by Equation 4.70, was closed to DOC_{obs}, expressed as a value of 2.030 mg L^{-1}, for UV_{254}(min). Moreover, 24.08 mg L^{-1} of DOC_{calc}, obtained by Equation 4.70, was closed to DOC_{obs}, expressed as a value of 26.98 mg L^{-1}, for UV_{254}(max). DOC_{calc}, related to Equation 4.70, displayed 86 % of DOC_{calc}, according to Equation 4.70a and Equation 4.70b for UV_{254}(min) parameter (Table 4.14). Calculated by Equation 4.70 was higher than DOC_{calc}, calculated by Equation 4.70a and Equation 4.70b for UV_{254}(average) and UV_{254}(max). Equation 4.2, exhibited 26 % of DOC, calculated according to Equation 4.70 for UV_{254}(min) parameter. Moreover, DOC_{calc} result, obtained by Equation 4.43, displayed 50 % DOC_{calc}, depending on Equation 4.70, and also exhibited

90 % more than DOC_{calc}, according to Equation 4.2 for UV_{254}(min) parameter. DOC_{calc}, obtained by using Equation 4.2, displayed 8 % of DOC_{calc}, calculated by Equation 4.70, and also exhibited 77 % of DOC_{calc}, depending on Equation 4.43 for UV_{254}(max) parameter.

Table 4.14. DOC concentrations of Nordic humic acid, related to UV_{254}(min), UV_{254}(max) and UV_{254}(average) and DOC_{obs} concentrations, measured by TOC analyzer.

Equation No	Min UV_{254}=0.0134 cm^{-1}	Max UV_{254}=1.229 cm^{-1}	Average UV_{254}=0.4689 cm^{-1}
	DOC_{calc}, mg L^{-1}		
4.2	0.7365	22.84	8.974
4.70	2.796	24.08	10.73
4.70a	3.246	22.84	10.60
4.70b	3.245	22.77	10.54
4.43	1.403	18.50	7.774
DOC_{obs}	2.030	26.98	-

DOC_{calc}, depending on Equation 4.2, displayed 84 % of DOC_{calc}, related to Equation 4.70, and also exhibited 15 % more than DOC_{calc}, related to Equation 4.43 for UV_{254} (average) parameter (Table 4.14). DOC_{calc}, related to by Equation 4.2, exhibited 23 % of DOC_{calc}, according to Equation 4.70a and Equation 4.70b for UV_{254}(min), respectively, whereas DOC_{calc}, related to Equation 4.70b, exhibited 99.6 % of DOC_{calc}, related to Equation 4.70a and Equation 2 for UV_{254}(max). DOC_{calc}, depending on Equation 43, displayed 87 %, 72 %, 73 %, and 74 % of DOC_{calc}, according to Equation 4.2, Equation 4.70, Equation 4.70a, and Equation 4.70b, respectively, for UV_{254}(average). According to the results, it was observed that the highest DOC result obtained by using Equation 4.70 whereas, the lowest DOC result was achieved by using Equation 4.2. Equation 4.70 gave the highest DOC result among the Equation 4.2 and Equation 4.43, for UV_{254}(min), UV_{254}(max) and UV_{254}(average).

DOC_{calc} results, as a function of UV_{254}(min), UV_{254}(max) and UV_{254}(average), attained by using Equation 4.2, Equation 4.43 and Equation 4.70, were compared with each other. DOC_{calc}, related to Equation 4.2 as a function of UV_{254}(max) and was 8.21 % of DOC_{calc}, as a function of UV_{254}(average). DOC, calculated by Equation 4.70 as a function of UV_{254}(min), was 12 % of DOC, calculated as a function of UV_{254}(max) and also was 26.05 % of DOC, calculated as a function of UV_{254}(average). DOC, calculated by Equation 4.43 as a function of UV_{254}(min), was 7.6 % of DOC, calculated as a function of UV_{254}(max) and also was 18 % of DOC, calculated as a function of UV_{254}(average). DOC, calculated by Equation 4.70a as a function of UV_{254}(min), was 14.21 % of DOC, calculated as a function of UV_{254}(max) and also was 30.62 % of DOC, calculated as a function of UV_{254}(average). DOC, calculated by Equation 4.70b as a function of UV_{254}(min), was 14.25 % of DOC, calculated as a function of UV_{254}(max) and also was 31 % of DOC, calculated as a function of UV_{254}(average).

DOC_{calc}, related to UV_{254}(min) and UV_{254}(max), determined by using TOC analyses (Table 4.9), were compared with DOC_{calc}, related to Equation 4.2, Equation 4.43, Equation 4.70, Equation 4.70a and Equation 4.70b .The observation and Equation results were prepared in Table 4.14. DOC_{obs}, measured by TOC analyzer, was 72 % of DOC_{calc}, related to Equation 4.70. DOC_{calc}, depending on Equation 4.43, was 69 % of DOC_{obs}, measured by TOC analyzer for UV_{254}(min). DOC_{calc}, related to Equation 4.2, was 36 % of DOC_{obs} result for UV_{254}(min). DOC_{calc}, related to Equation 4.2, was 85 % of DOC_{obs} for UV_{254}(max). DOC_{calc}, related to Equation 4.70, was 89 % of DOC_{obs} result for UV_{254}(max). DOC_{calc}, depending on Equation 4.43, was 68 % of DOC_{obs} for UV_{254}(max). Among DOC results, the highest result was observed in Equation 4.70 for UV_{254}(min), whereas the lowest result was observed in the observation result for UV_{254}(max). DOC_{obs} exhibited 62 % of DOC_{calc}, depending on Equation 4.70a and Equation 4.70b for UV_{254}(min), whereas DOC_{calc}, related to Equation 4.70b, displayed 84 % of DOC_{obs} and 99.70 % of DOC_{calc}, related to Equation 4.70a (Table 4.14).

4.3.1.4.The over-all Relationship between DOC and UV_{280} of NHA irrespective of Initial Humic Acid Concentration. According to Table 4.8, DOC concentrations, including the non-oxidative data before the photocatalytic treatment and the oxidative data after each

irradiation time of the photocatalytic treatment, were plotted against UV_{280} parameter, corresponding to the DOC concentrations of NHA, in Figure 4.33.

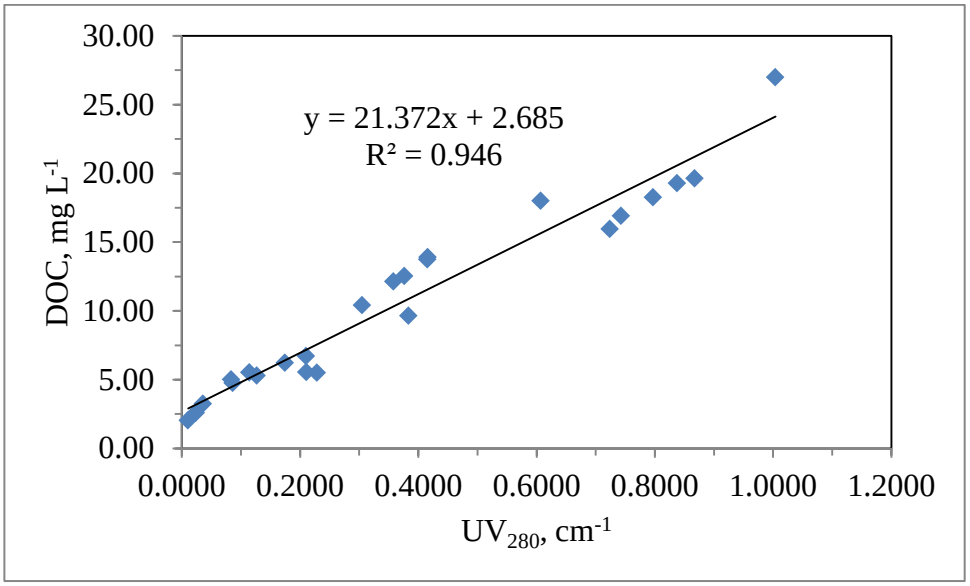

Figure 4.33. The correlation between UV_{280} parameter and DOC concentration, including oxidative data during the photocatalytic treatment and nonoxidative data before the photocatalytic treatment, for 10, 20, 30 and 50 mg L^{-1} of NHA.

Figure 4.33 illustrated the linear correlation between UV_{280} parameter and DOC concentrations of humic acid. Equation of the correlation between DOC concentration, including oxidative data for each irradiation time during the photocatalytic treatment and nonoxidative data before the photocatalytic treatment, for 10, 20, 30 and 50 mg L^{-1} of NHA, and UV_{280} parameter of the remained NHA after the photocatalytic treatment and NHA concentration at adsorption period, was produced from the least-squares regression analyses (Equation 4.71). The regression coefficient was found to be as R^2=0.946. As mentioned above, Equation 4.4 was obtained by the correlation between UV_{280} parameter and DOC concentration of the non-oxidized NHA. Equation 4.71 was attained by the correlation between UV_{280} parameter and DOC concentration of NHA including all condition data. Equation 4.45 was achieved by the relationship between UV_{280} parameter and DOC concentration of the non-oxidized overall humic acids (NHA, FHA, AHA and RHA). Equation 4.71a was attained by the graph, pointing out, the correlation between UV_{280} parameter results and DOC concentration results of NHA, including at t=0 and post

oxidation, after the photocatalytic treatment. Equation 4.71b was achieved from the graph, representing the correlation between UV_{280} parameter and DOC concentrations, including only post-oxidation data, after the photocatalytic treatment. These equations were stated below (Table 4.15). In the least square regression model, equation could exhibit random error (Johnson and Bhattacharyya, 1996). Equation 4.4, represented the randon error as a value of 0.696, Equation 4.71 represented the randon error as a value of 2.69, Equation 4.71a represented the randon error as a value of 3.15, Equation 4.70b represented the randon error as a value of 3.15, and Equation 4.45 represented the randon error as a value of 1.56 (Table 4.15).

Table 4.15. The correlation Equations and the regression coefficients obtained from the relationship between UV_{280} and DOC concentration of NHA, including the non-treatment data (Equation 4.4) and photocatalytic treatment data (Equation 4.71, 4.71a, 4.71b), and the relationship between UV_{280} and DOC concentration of the overall humic acids (NHA, FHA, AHA and RHA), including the non-treatment data (Equation 4.45).

Equation No	Correlation Equation	R^2
4.4	DOC (mg L^{-1}) = 21.56*UV_{280} (cm^{-1}) + 0.696	0.992
4.71	DOC (mg L^{-1}) = 21.37*UV_{280} (cm^{-1}) + 2.69	0.946
4.71a	DOC (mg L^{-1}) = 19.75*UV_{280} (cm^{-1}) + 3.15	0.952
4.71b	DOC (mg L^{-1}) = 19.71*UV_{280} (cm^{-1}) + 3.15	0.958
4.45	DOC (mg L^{-1}) = 16.07 *UV_{280} (cm^{-1}) + 1.56	0.939

When the Equations (Equation 4.71, Equation 4.71a, and Equation 4.71b), attained by using results after the photocatalytic treatment, were compared with each other, Equation 4.71a displayed the highest error with a value of 3.15 whereas, Equation 4.71 displayed the lowest error with a value of 2.69. On the other hand, as seen in Table 4.15, Equation 4.71, attained by DOC results and UV-vis parameter results including all conditions, Equation 4.71a, achieved by DOC results and UV-vis parameter results consisting of t=0 and post oxidation data, and Equation 4.71b, attained by DOC results and UV-vis parameter results consisting of post oxidation data exhibited very close error numbers.

UV_{280} parameter results of 10 and 50 mg L^{-1} NHA, including before the photocatalytic treatment, at t=0 and post oxidation data (Table 4.9), were used to calculate DOC results, as shown in Table 4.16. During the adsorption period (t=0) DOC_{calc}, calculated as a function of UV_{280} parameter by using Equation 4.4, exhibited 93 % of DOC_{calc}, dependent upon Equation 4.45. Moreover, DOC_{calc}, as a function of UV_{280} parameter by using Equation 4.4, exhibited 61 % of DOC_{calc}, according to Equation 4.71 for 10 mg L^{-1} of NHA.

Table 4.16. DOC concentrations of NHA calculated by using Equation 4.4, Equation 4.71, Equation 4.71a, Equation 4.71b and Equation 4.45, as a function of UV_{280} parameter and DOC concentration, measured by TOC analyzer for 10 mg L^{-1} and 50 mg L^{-1} of NHA.

NHA: 10 mg L^{-1}	UV_{280}, cm^{-1}					
Irradiation time	0	15	30	45	60	RAW
	0.1143	0.0843	0.0361	0.0239	0.0105	0.2285
Equation	DOC, mg L^{-1}					
4.4	3.160	2.514	1.474	1.211	0.922	5.622
4.71	5.133	4.491	3.461	3.201	2.914	7.573
4.71a	5.407	4.815	3.863	3.622	3.357	7.663
4.71b	5.403	4.812	3.862	3.621	3.357	7.654
4.45	3.397	2.915	2.140	1.944	1.729	5.232
Observation	5.530	5.010	3.250	2.590	2.030	5.500
NHA: 50 mg L^{-1}	UV_{280}, cm^{-1}					
Irradiation time	0	15	30	45	60	RAW
	0.8674	0.8377	0.7968	0.7431	0.7238	1.0041
Equation	DOC, mg L^{-1}					
4.4	19.40	18.76	17.88	16.72	16.30	22.34
4.71	21.23	20.59	19.72	18.57	18.16	24.15
4.71a	20.28	19.69	18.57	17.83	17.45	22.98
4.71b	20.25	19.66	18.16	17.80	17.42	22.94
4.45	15.50	15.02	14.36	13.50	13.19	17.69
Observation	19.63	19.29	18.25	16.90	15.96	26.98

After the irradiation time of 60 minutes, DOC_{calc}, as a function of UV_{280} parameter by using Equation 4.4, exhibited 53 % of DOC_{calc}, dependent upon Equation 4.45. Moreover, DOC_{calc}, as a function of UV_{280} parameter by using Equation 4.4, exhibited 32 % of DOC_{calc}, depending on Equation 4.71 for 10 mg L^{-1} of NHA (Table 4.16). During the adsorption period (t=0) DOC_{calc}, calculated as a function of UV_{280} parameter by using Equation 4.45, exhibited 80 % of DOC_{calc}, depending on Equation 4.4. Moreover, DOC_{calc}, as a function of UV_{280} parameter by using Equation 4.4, exhibited 91 % of DOC_{calc}, depending on Equation 4.71 for 50 mg L^{-1} of NHA. After the irradiation time of 60 minutes, DOC_{calc}, as a function of UV_{280} parameter by using Equation 4.45, exhibited 81 % of DOC_{calc}, calculated as a function of UV_{280} parameter by using Equation 4.4. Moreover, DOC_{calc}, as a function of UV_{280} parameter by using Equation 4.4, exhibited 90 % of DOC_{calc}, as a function of UV_{280} parameter by using Equation 4.71 for 50 mg L^{-1} of NHA.

Figure 4.34 showed DOC_{calc}, calculated by using Equation 4.4, Equation 4.71, Equation 4.71a, Equation 4.71b and Equation 4.45, and DOC_{obs}. At t=0, the adsorption effect, depending on Equations, as mentioned above, was examined with respect to time '0'. At adsorption period (t=0.1), 44 %, 32 %, 29 %, 29 % and 35 % removal exhibited decreasing trend for Equation 4.4, Equation 4.71, Equation 4.71a, Equation 4.71b and Equation 4.45, respectively. After the irradiation time of 30 minutes, 74 %, %, 54 %, 50 %, 50 % , 59 % and 41 % removal exhibited decrease for Equation 4.4, Equation 4.71, Equation 4.71a, Equation 4.71b, Equation 4.45 and in the observation. The conversion after 60 min, was 84 % for Equation 4.4, 62 % for Equation 4.71, 56 % for Equation 4.71a, and 4.71b, 67 % for Equation 4.45 and 63 % in the observation. The removal of DOC_{calc}, related to Equation 4.4, displayed higher removal than DOC_{calc}, related to Equation 4.71, Equation 4.71a, Equation 4.71b, Equation 4.45 and DOC_{obs} for 10 mg L^{-1} of NHA. DOC_{calc}, depending on Equation 4.71, Equation 4.71a, Equation 4.71b, was found to be closed to DOC_{obs}, whereas DOC_{calc}, related to Equation 4.4 and Equation 4.45, was found to be less than DOC_{obs} for 10 mg L^{-1} of NHA before the photocatalytic treatment and after the photocatalytic treatment. As seen in Figure 4.34, it could be inferred that equations were not found to be useful for the prediction of DOC concentration in NHA during the photocatalytic treatment.

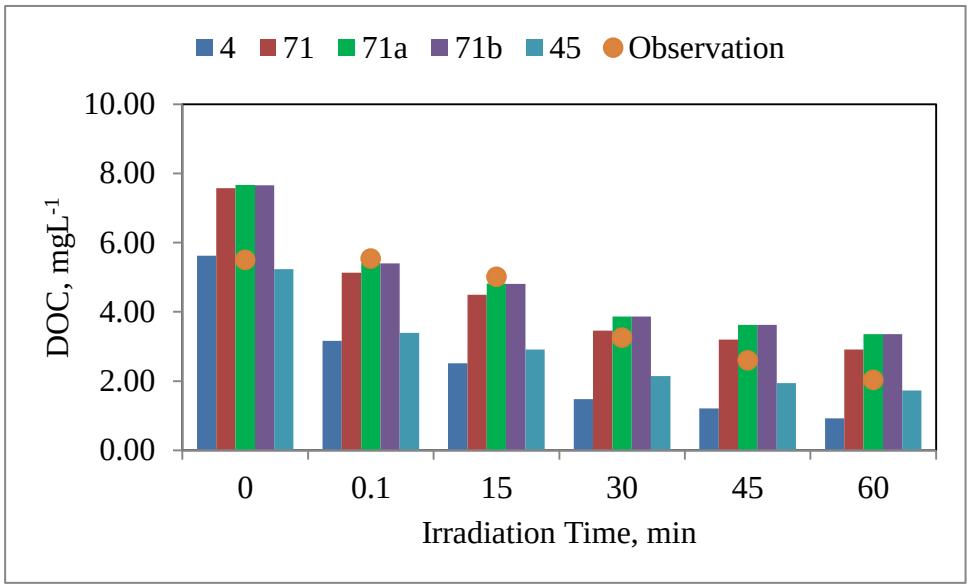

Figure 4.34. Comparison of DOC_{obs} and DOC_{calc} concentration obtained by using Equation 4.4 (4), Equation 4.71 (71), Equation 4.71a (71a), Equation 4.71b (71b), and Equation 4.45 (45) as a function of UV_{280} parameter with respect to irradiation time, including the non-oxidative data prior to the photocatalytic treatment and the oxidative data after each irradiation time of the photocatalytic treatment, for 10 mg L^{-1} of NHA.

Before the photocatalytic treatment (t=0), when taking the average of DOC_{calc}, related to Equation 4.71, Equation 4.71a and Equation 4.71b, DOC average result exhibited less DOC concentration than DOC_{obs} (Figure 4.35). At t=0, the adsorption effect, dependent on Equations, as mentioned above, was examined with respect to time '0'. At the adsoption period, 13 %, 12 %, and 27 % removal exhibited increasing trend for Equation 4.4, Equation 4.71, Equation 4.71a, Equation 4.71b, Equation 4.45, and in the observation, respectively. After the irradiation time of 15 minutes, 16 %, 15 %, 14 %, 14, 15 % and 26 % removal exhibited for Equation 4.4, Equation 4.71, Equation 4.71a, Equation 4.71b, Equation 4.45 and in the observation, respectively. The conversion after 60 min, was 27 % for Equation 4.4, 25 % for Equation 4.71, 24 % for Equation 4.71a and 4.71b, 25 % for Equation 4.45 and 41 % in the observation.

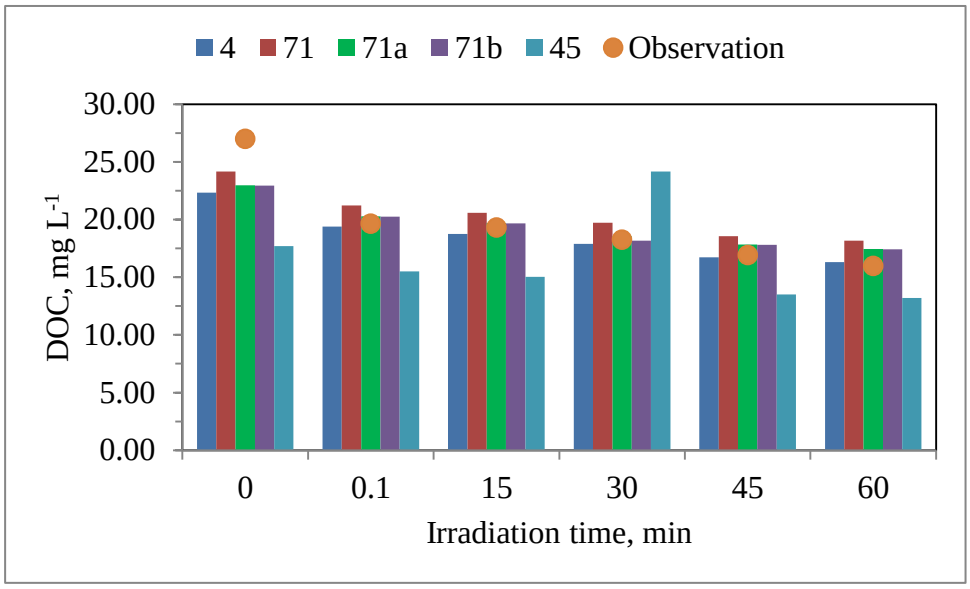

Figure 4.35. Comparison of DOC_{obs} and DOC_{calc} concentration, obtained by using Equation 4.4 (4), Equation 4.71 (71), Equation 4.71a (71a), Equation 4.71b (71b) and Equation 4.45 (45) with the irradiation time as a function of UV_{280} parameter including the non-oxidative data prior to the photocatalytic treatment and the oxidative data after each irradiation time of the photocatalytic treatment, for 50 mg L^{-1} of NHA.

The removal of DOC_{obs}, displayed higher removal than DOC_{calc} concentration, related to Equation 4.4, Equation 4.71, Equation 4.71a, Equation 4.71b and Equation 4.45 for 50 mg L^{-1} of NHA. According to Figure 4.35, DOC_{calc}, related to Equation 4.4, Equation 4.71, Equation 4.71a and Equation 4.71b were found to be closed to DOC_{obs}, whereas DOC_{obs} exhibited more DOC content than DOC_{calc}, related to Equation 4.45. As a consequence, it could be inferred that Equation 4.4, Equation 4.71, Equation 4.71a and Equation 4.71b were found to be useful for the prediction of DOC concentration for 50 mg L^{-1} of NHA during the photocatalytic treatment, whereas Equation 4.43 were not found to be useful.

According to Table 4.17, UV_{280}(min) was stated as a value of 0.0105 cm^{-1}, obtained by the photocatalytic treatment after the irradiation time of 60 minutes. UV_{280}(max) was expressed as a value of 1.0041 cm^{-1}, representing the initial concentration of 50 mg L^{-1} of NHA. UV_{280}(average), expressed as a value of 0.3766 cm^{-1}, was calculated by taking the average of UV_{280} parameter results after photocatalytic treatment. By using these equations

(Equation 4.4, Equation 4.71, Equation 4.71a, Equation 4.71b and Equation 4.45), DOC concentrations were calculated with given UV_{280} parameter (Table 4.17). DOC_{calc}, related to Equation 4.71, Equation 4.71a and Equation 4.71b were closed to each other for UV_{280}(min), UV_{280}(max) and UV_{280}(average). 2.909 mg L^{-1} of DOC_{calc}, related to Equation 4.71, was closed to DOC_{obs}, expressed as a value of 2.030 mg L^{-1}, for UV_{280}(min). Moreover, 24.14 mg L^{-1} of DOC_{calc}, related to Equation 4.70, was closed to DOC_{obs}, expressed as a value of 26.98 mg L^{-1}, for UV_{280}(max). DOC_{calc}, related to Equation 4.4, exhibited 31.70 % of DOC_{calc}, depending on Equation 4.71 as a function of UV_{280}(min) parameter. Moreover, DOC_{calc}, related to Equation 4.45 displayed 59.40 % of DOC_{calc}, related to Equation 4.71, and also exhibited 87 % more than DOC_{calc}, depending on Equation 4.4 for UV_{280}(min) parameter. DOC_{calc}, related to Equation 4.4, displayed 92 % of DOC_{calc}, related to Equation 4.71, also exhibited 26 % more than DOC_{calc}, related to Equation 4.45 for UV_{280}(max) parameter. DOC_{calc}, depending on Equation 4.45, exhibited 71 % of DOC_{calc}, related to Equation 4.71, and also exhibited 86 % of DOC_{calc}, according to Equation 4.4 for UV_{280}(average) parameter. According to the results, it was observed that the highest DOC result, obtained by using Equation 4.71, whereas the lowest DOC result was attained by using Equation 4.4. Equation 4.71 gave the highest DOC result among the Equation (Equation 4.2 and Equation 4.43) for UV_{280}(min), UV_{280}(max) and UV_{280}(average).

Table 4.17. DOC concentrations of NHA, related to UV_{280}(min), UV_{280}(max) and UV_{280}(average) and DOC_{obs}, concentrations measured by TOC analyzer.

Equation No	Min UV_{280}= 0.0105 cm^{-1}	Max UV_{280}= 1.004 cm^{-1}	Average UV_{280}= 0.3766 cm^{-1}
	DOC_{calc}, mg L^{-1}		
4.4	0.9223	22.34	8.815
4.71	2.909	24.14	10.73
4.71a	3.357	22.98	10.59
4.71b	3.357	22.94	10.57
4.45	1.728	17.69	7.610
DOC_{obs}	2.030	26.98	-

DOC_{calc}, related to Equation 4.4, displayed 92 % of DOC_{calc}, related to Equation 4.71, also exhibited 26 % more than DOC_{calc}, related to Equation 4.45 for UV_{280}(max) parameter. DOC_{calc}, depending on Equation 4.45, exhibited 71 % of DOC_{calc}, related to Equation 4.71, and also exhibited 86 % of DOC_{calc}, according to Equation 4.4 for UV_{280}(average) parameter. According to the results, it was observed that the highest DOC result, obtained by using Equation 4.71, whereas the lowest DOC result was attained by using Equation 4.4. Equation 4.71 gave the highest DOC result among the Equation (Equation 4.2 and Equation 4.43) for UV_{280}(min), UV_{280}(max) and UV_{280}(average).

DOC_{calc}, related to Equation 4.4, Equation 4.45 and Equation 4.71 as a function of UV_{280}(min), UV_{280}(max) and UV_{280}(average) were compared with each other. DOC_{calc}, related to Equation 4.4 as a function of UV_{280} average and was 39.45 % of DOC_{calc}, as a function UV_{280}(max). DOC, calculated by Equation 4.71 as a function of UV_{280}(min), was 27.11 % of DOC_{calc}, as a function of UV_{280}(average). DOC_{calc}, related to Equation 4.45 as a function of UV_{280}(min), was 9.77 % of DOC_{calc}, as a function of UV_{280}(max) and also was 22.70 % of DOC_{calc}, as a function of UV_{280}(average). DOC_{obs} results, related to UV_{280}(min) and UV_{280}(max), determined by using TOC analyses (Table 4.8), were compared with DOC_{calc}, related to Equation 4.4, Equation 4.45 and Equation 4.71 (Table 4.17). DOC_{obs}, obtained by TOC analyzer, was 70 % of DOC_{calc}, related to Equation 4.71. DOC_{calc}, related to Equation 45, was 85 % of DOC_{obs}, measured by TOC analyzer for UV_{280}(min). DOC_{obs} was 220 % of DOC_{calc}, related to Equation 4.4 for UV_{280}(min). DOC_{calc}, obtained by using Equation 4.4, was 83 % of DOC_{obs} for UV_{280}(max). DOC_{calc}, related to Equation 4.71, was 89 % of DOC_{obs} for UV_{280}(max). Among DOC results, the highest result was observed in Equation 4.71 for UV_{280}(max), while the lowest result was observed in Equation 4.4 for UV_{280}(min).

4.3.1.5. The over-all Relationship between DOC and UV_{365} of NHA irrespective of Initial Humic Acid Concentration. According to Table 4.8, DOC concentrations, including the non-oxidative data before the photocatalytic treatment and the oxidative data after each irradiation time of photocatalytic treatment, were plotted against UV_{365} parameter, corresponding to these DOC concentrations of NHA, in Figure 4.36.

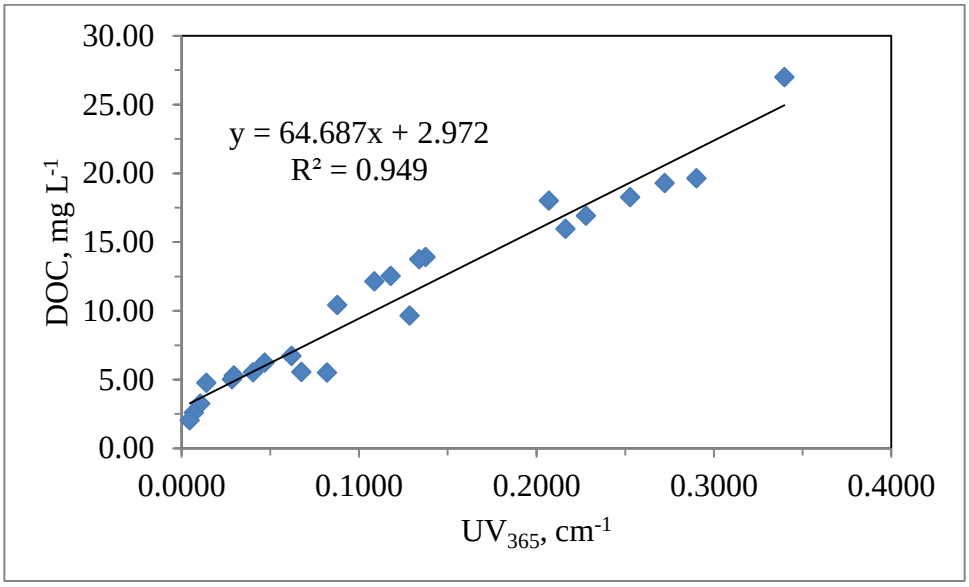

Figure 4.36. The correlation between UV_{365} parameter and DOC concentration, including the oxidative data during the photocatalytic treatment and the non-oxidative data before the photocatalytic treatment, for 10, 20, 30 and 50 mg L^{-1} of NHA.

Figure 4.36 illustrated the linear correlation between UV_{365} parameter and DOC concentrations of NHA. Equation of the correlation between DOC concentration, including oxidative data for each irradiation time during the photocatalytic treatment and nonoxidative data before the photocatalytic treatment, for 10, 20, 30 and 50 mg L^{-1} of NHA, and UV_{365} parameter of the remained NHA after the photocatalytic treatment and NHA concentration at adsorption period, was produced from the least-squares regression analyses (Equation 4.72). The regression coefficient was found to be as R^2= 0.949 (Table 4.18).

As mentioned above, Equation 4.6 was obtained by the correlation between UV_{365} parameter and DOC concentration of the non-oxidized NHA (Table 4.18). Equation 4.72 was attained by the correlation between UV_{365} parameter and DOC concentration of NHA, including all condition data. Equation 4.47 was achieved by the relationship between UV_{365} parameter and DOC concentration of the non-oxidized overall humic acids (NHA, FHA, AHA and RHA). Equation 4.72a was attained by the graph, pointing out, the correlation between UV_{365} parameter results and DOC concentration results of the non-oxidized NHA, including at t=0 and post oxidation, after the photocatalytic treatment.

Equation 4.72b was achieved from the graph, representing the correlation between UV_{365} parameter and DOC concentrations, including only post oxidation data, after the photocatalytic treatment. The equations were stated below (Table 4.18).

Table 4.18. The correlation equations and the regression coefficients obtained from the relationship between UV_{365} and DOC concentration of NHA, including non treatment data (Equation 4.6) and photocatalytic treatment data (Equation 4.72, 4.72a, 4.72b), and the relationship between UV_{365} and DOC concentration of all humic acids (NHA, FHA, AHA and RHA), including non treatment data (Equation 4.47).

Equation No	Correlation Equation	R^2
4.6	DOC (mg L^{-1}) = 69.05*UV_{365} (cm^{-1}) + 0.180	0.974
4.72	DOC (mg L^{-1}) = 64.69*UV_{365} (cm^{-1}) + 2.97	0.949
4.72a	DOC (mg L^{-1}) = 60.82*UV_{365} (cm^{-1}) + 3.43	0.951
4.72b	DOC (mg L^{-1}) = 61.64*UV_{365} (cm^{-1}) + 3.45	0.958
4.47	DOC (mg L^{-1})= 22.22*UV_{365} (cm^{-1}) + 4.43	0.655

In the least square regression model, equation could give random error (Johnson and Bhattacharyya, 1996). Equation 4.6, represented the randon error as a value of 0.180, Equation 4.72 represented the randon error as a value of 2.97, Equation 4.72a represented the randon error as a value of 3.43, Equation 4.72b represented the randon error as a value of 3.45, and Equation 4.47 represented the randon error as a value of 4.43 (Table 4.18). When the Equations (4.72, 4.72a, and 4.72b), attained by using results after the photocatalytic treatment, were compared with each other, Equation 4.72b displayed the highest error with a value of 3.45 whereas, Equation 4.72 exhibited the lowest error with a value of 2.97. On the other hand, as seen in Table 4.18, Equation 4.72, attained by DOC results and UV-vis parameter results including all conditions, Equation 4.72a, achieved by DOC results and UV-vis parameter results consisting of t=0 and post-oxidation data, and Equation 4.72b, attained by DOC results and UV-vis parameter results consisting of post-oxidation data displayed very close error numbers. Among these equations, Equation 4.47 exhibited the highest error with a value of 4.43 whereas, Equation 4.4 displayed the lowest error with a value of 0.180. As a result, Equation 4.47 obtained from the correlation

between UV_{365} parameter and DOC concentration results of the overall humic acids without treatment, exhibited more error than Equation 4.6, attained from the correlation between UV_{365} parameter and DOC concentration of non-oxidized NHA.

UV_{365} parameter results of 10 and 50 mg L^{-1} NHA, including before the photocatalytic treatment, at t=0 and post-oxidation data (Table 4.18), were used to calculate DOC results, as shown in Table 4.19. During the adsorption period (t=0) DOC_{calc}, as a function of UV_{365} parameter by using Equation 4.6, exhibited 56 % of DOC_{calc}, dependent upon Equation 4.47 (Table 4.19). DOC_{calc}, as a function of UV_{365} parameter by using Equation 4.6, exhibited 53 % of DOC_{calc}, dependent upon Equation 4.72 for 10 mg L^{-1} of NHA. After the irradiation time of 60 minutes, DOC_{calc}, as a function of UV_{365} parameter by using Equation 4.6, exhibited 11 % of DOC_{calc}, dependent upon Equation 4.47. Moreover, DOC_{calc}, as a function of UV_{365} parameter by using Equation 4.6, exhibited 15 % of DOC_{calc}, dependent upon Equation 4.72 for 10 mg L^{-1} of NHA (Table 4.19).

During the adsorption period (t=0) DOC_{calc} calculated as a function of UV_{365} parameter by using Equation 4.47, exhibited 54 % of DOC_{calc}, dependent upon Equation 4.6. Moreover, DOC_{calc}, calculated as a function of UV_{365} parameter by using Equation 4.6, exhibited 93 % of DOC_{calc}, dependent upon Equation 4.72 for 50 mg L^{-1} of NHA. After the irradiation time of 60 minutes, DOC_{calc}, calculated as a function of UV_{365} parameter by using Equation 4.47, exhibited 61 % of DOC_{calc}, according to Equation 4.6. Moreover, DOC_{calc}, calculated as a function of UV_{365} parameter by using Equation 4.6, exhibited 89 % of DOC_{calc}, according to Equation 4.72 for 50 mg L^{-1} of NHA.

Table 4.19. DOC concentrations of NHA calculated by using Equation 4.6, Equation 4.72, Equation 4.72a, Equation 4.72b and Equation 4.47, as a function of UV_{365} parameter and DOC concentration, measured by TOC analyzer for 10 mg L^{-1} and 50 mg L^{-1} of NHA.

NHA: 10 mg L^{-1}	UV_{365}, cm^{-1}					
Irradiation time	0	15	30	45	60	RAW
	0.042	0.0283	0.0106	0.0069	0.0046	0.0820
Equation	DOC, mg L^{-1}					
4.6	2.956	2.134	0.912	0.656	0.498	5.842
4.72	5.571	4.801	3.656	3.416	3.268	8.275
4.72a	5.875	5.151	4.075	3.850	3.710	8.417
4.72b	5.928	5.194	4.103	3.875	3.734	8.504
4.47	5.323	5.059	4.666	4.583	4.532	6.252
Observation	5.530	5.010	3.250	2.590	2.030	5.500
NHA: 50 mg L^{-1}	UV_{365}, cm^{-1}					
Irradiation time	0	15	30	45	60	RAW
	0.2902	0.2724	0.2528	0.2280	0.2165	0.3398
Equation	DOC, mg L^{-1}					
4.6	20.22	18.99	17.64	15.92	15.13	23.64
4.72	21.74	20.59	19.32	17.72	16.98	24.95
4.72a	5.875	5.151	4.075	3.850	3.710	8.417
4.72b	21.34	20.24	19.03	17.50	16.80	24.40
4.47	10.88	10.48	10.05	9.496	9.241	11.98
Observation	19.63	19.29	18.25	16.90	15.96	26.98

Figure 4.37 showed DOC_{calc}, calculated by using Equation 4.6, Equation 4.72, 4.72a, 4.72b and Equation 4.47, and DOC_{obs}. At t=0, the adsorption effect, dependent on Equations, as mentioned above, was examined with respect to time '0'. At the adsorption period, 49 %, 33 %, 30 %, 30 % and 15 % removal exhibited decreasing trend for Equation 4.6, Equation 4.72, Equation 4.72a, Equation 4.72b and Equation 4.47, respectively.

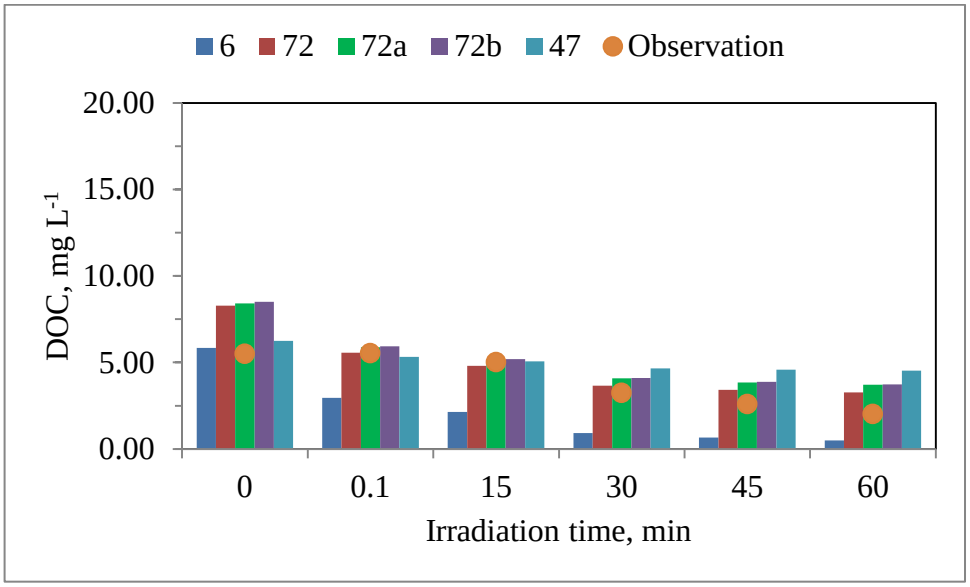

Figure 4.37. Comparison of DOC_{obs} and DOC_{calc} concentration, obtained by using Equation 4.6 (6), Equation 4.72 (72), Equation 4.72a (72a), Equation 4.72b (72b) and Equation 4.47 (47) with the irradiation time as a function of UV_{365} parameter, including the non-oxidative data prior to the photocatalytic treatment and the oxidative data after each irradiation time of the photocatalytic treatment, for 10 mg L^{-1} of NHA.

After the irradiation time of 30 minutes, 84 %, 56 %, 52 %, 52 %, 25 %, and 41 % removal displayed decreasing trend for Equation 4.6, Equation 4.72, Equation 4.72a, Equation 4.72b, Equation 4.47 and in the observation. The conversion after 60 min, was 91 % for Equation 4.6, 61 % for Equation 4.72, 56 % for Equation 4.72a and 4.72b, 28 % for Equation 4.47 and 63 % in the observation. The removal of DOC concentration, related to Equation 4.6, exhibited higher removal than DOC concentration, related to Equation 4.72, Equation 4.72a, Equation 4.72b, Equation 4.47 and the observation. DOC_{calc}, calculated by using Equation 4.72, 4.72a, 4.72b, and 4.47 was found to be closed to DOC_{obs}, whereas DOC_{calc}, calculated by using Equation 4.6, was found to be less than DOC_{obs} for 10 mg L^{-1} of NHA just before the photocatalytic treatment (during the adsorption period) and for each photocatalytic treatment period. It could be inferred these equations were not found to be useful for the prediction of DOC concentration in 10 mg L^{-1} of NHA.

Before the photocatalytic treatment (t=0), DOC_{calc}, calculated by using Equation 4.47, exhibited 44 % of DOC_{obs} (Figure 4.38). At t=0, the adsorption effect, dependent on

Equations, as mentioned above, was examined with respect to time '0'. At the adsorption period, 14 %, 13 %, 30 %, 13 % and 9.1 % removal exhibited decreasing trend for Equation 4.6, Equation 4.72, Equation 4.72a, Equation 4.72b and Equation 4.47, respectively. After the irradiation time of 30 minutes, 25 %, 23 %, 52 %, 22 % , 16 %, and 41 % removal displayed increasing trend for Equation 4.6, Equation 4.72, Equation 4.72a, Equation 4.72b, Equation 4.47 and in the observation.

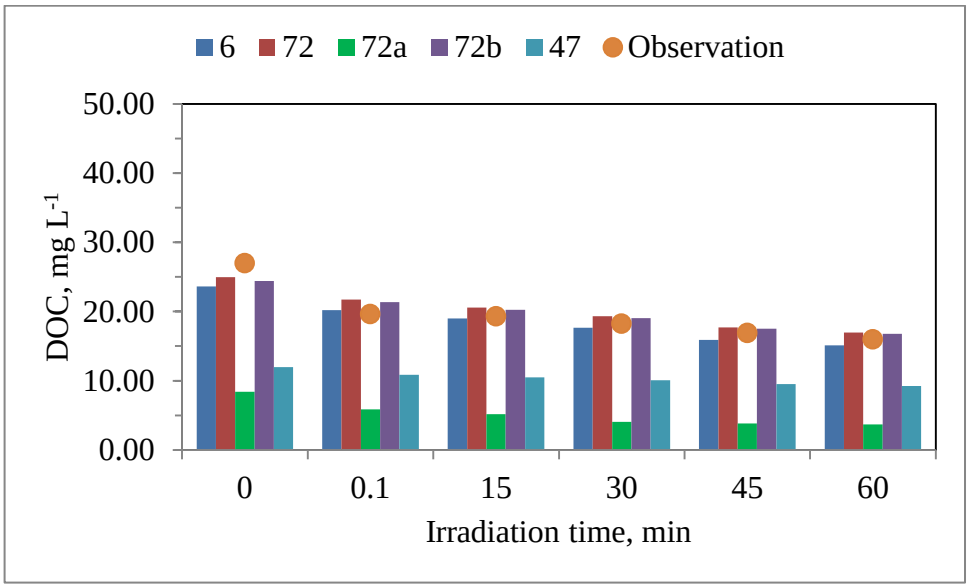

Figure 4.38. Comparison of DOC_{obs} and DOC_{calc} concentration, obtained by using Equation 4.6 (6), Equation 4.72 (72), Equation 4.72a (72a), Equation 4.72b (72b) and Equation 4.47 (47) with the irradiation time as a function of UV_{365} parameter, including oxidative data before the photocatalytic treatment and non-oxidative data after each irradiation time of the photocatalytic treatment, for 50 mg L^{-1} of NHA.

The conversion after 60 min, was 36 % for Equation 4.6, 25 % for Equation 4.72, 56 % for Equation 4.72a, 31 % for Equation 4.72b, 23 % for Equation 4.47 and 41 % in the observation. The removal of DOC_{obs}, exhibited higher removal than DOC_{calc}, related to Equation 4.6, Equation 4.72, Equation 4.72a, Equation 4.72b and Equation 4.47. According to Figure 4.38, DOC_{calc}, calculated by using Equation 4.6, Equation 4.72, Equation 4.72b were found to be closed to DOC_{obs}, whereas DOC_{obs} was found to be more than DOC_{calc}, calculated by using Equation 4.72a and Equation 4.47. As shown in Figure 4.38, Equation 4.6, Equation 4.72, Equation 4.72b were found to be useful for the

prediction of DOC concentration for 50 mg L^{-1} of NHA during the photocatalytic treatment, whereas Equation 4.47 and Equation 4.72a were not found to be useful.

According to Table 4.8, UV_{365}(min) was expressed as a value of 0.0046 cm^{-1}, obtained by the photocatalytic treatment after the irradiation time of 60 minutes. UV_{365}(max) was expressed as a value of 0.3398 cm^{-1}, representing the initial concentration of 50 mg L^{-1} of Nordic humic acid. UV_{365}(average), expressed as a value of 0.1189 cm^{-1}, was calculated by taking the average of UV_{365} parameter results after the photocatalytic treatment (Table 4.20). By using these Equations (Equation 4.6, Equation 4.72, Equation 4.72a, Equation 4.72b and Equation 4.47), DOC contents were calculated with given UV_{365} parameter (Table 4.20).

Table 4.20. DOC concentrations of NHA, related to UV_{365}(min), UV_{365}(max) and UV_{365}(average), calculated by using Equation 4.6, Equation 4.72, Equation 4.72a, Equation 4.72b and Equation 4.43, and DOC_{obs}, measured by TOC analyzer.

Equation No	Min UV_{365}=0.0046 cm^{-1}	Max UV_{365}= 0.3398 cm^{-1}	Average UV_{365}= 0.1189 cm^{-1}
	DOC_{calc}, mg L^{-1}		
4.6	0.4976	23.64	8.390
4.72	3.269	24.95	10.66
4.72a	3.710	24.10	10.66
4.72b	3.734	24.39	10.78
4.47	4.533	11.98	7.073
DOC_{obs}	2.030	26.98	-

DOC_{calc}, related to Equation 4.6, exhibited 15 % of DOC_{calc} depending on Equation 4.72 for UV_{365}(min). Moreover, DOC_{calc}, related to Equation 4.72, displayed 72 % of DOC_{calc}, depending on Equation 4.47 for UV_{365}(min) (Table 4.20). DOC_{calc}, related to Equation 4.6, displayed 95 % of DOC_{calc}, depending on Equation 4.72 for UV_{365}(max). DOC_{calc}, related to Equation 4.47, exhibited 48 % of DOC_{calc}, related to Equation 4.72 and displayed 51 % of DOC_{calc}, related to Equation 4.6 for UV_{365}(max). DOC_{calc}, related to

Equation 47, displayed 84 % of DOC_{calc}, depending on Equation 4.6 and exhibited 66 % of DOC_{calc}, related to Equation 4.72 for UV_{365}(average). According to the results, it was observed that the highest DOC result obtained by Equation 4.72 (UV_{365}(max)), whereas the lowest DOC result was achieved by Equation 4.6 (UV_{365}(min)). Equation 4.72 gave the highest DOC result among the Equation (Equation 4.2 and Equation 4.43) for UV_{365}(min), UV_{365}(max) and UV_{365}(average).

DOC results, related to UV_{365}(min), UV_{365}(max) and UV_{365}(average), calculated by using Equation 4.6, Equation 4.47 and Equation 4.72 , were compared with each other (Table 4.20). DOC_{calc}, related to Equation 4.6 as a function of UV_{365}(min), was 5.93 % of DOC_{calc}, as a function UV_{365}(average). DOC_{calc}, depending on Equation 4.72 as a function of UV_{365}(min), exhibited 31 % of DOC_{calc}, as a function of UV_{365}(average), and also displayed 13 % of DOC_{calc}, as a function of UV_{365}(max). DOC_{calc}, depending on Equation 4.47 as a function of UV_{365}(min), exhibited 64 % of DOC_{calc}, as a function of UV_{365}(average), and also displayed 38 % of DOC_{calc}, calculated as a function of UV_{365}(max). DOC_{calc}, related to Equation 4.72 as a function of UV_{365}(min), was 2.1 % of DOC_{calc}, as a function of UV_{365}(max). DOC_{calc}, depending on Equation 4.47 as a function of UV_{365}(min), was 9.77 % of DOC_{calc}, as a function of UV_{365}(max) and also was 22.70 % of DOC_{calc}, as a function of UV_{365}(average). DOC results, related to UV_{365}(min) and UV_{365}(max), determined by using TOC analyses (Table 4.8), were compared with DOC_{calc}, depending on Equation 4.6, Equation 4.47 and Equation 4.72 (Table 4.20). DOC_{obs}, exhibited 62 % of DOC_{calc}, depending on Equation 4.72. Furthermore, DOC_{obs} displayed 45 % of DOC_{calc}, related to Equation 4.47 for UV_{365}(min). DOC_{calc}, related to Equation 4.6, displayed 88 % of DOC_{obs} result for UV_{365}(max). DOC_{calc}, related to Equation 4.72, exhibited 92 % of DOC_{obs} for UV_{365}(max).

4.3.1.6. The over-all Relationship between DOC and $Color_{436}$ of NHA irrespective of Initial Humic Acid Concentration. According to Table 4.8, DOC concentrations, including the non-oxidative data before the photocatalytic treatment and the oxidative data after each irradiation time of the photocatalytic treatment, were plotted against $Color_{436}$ parameter, corresponding to these DOC concentrations of NHA, in Figure 4.39.

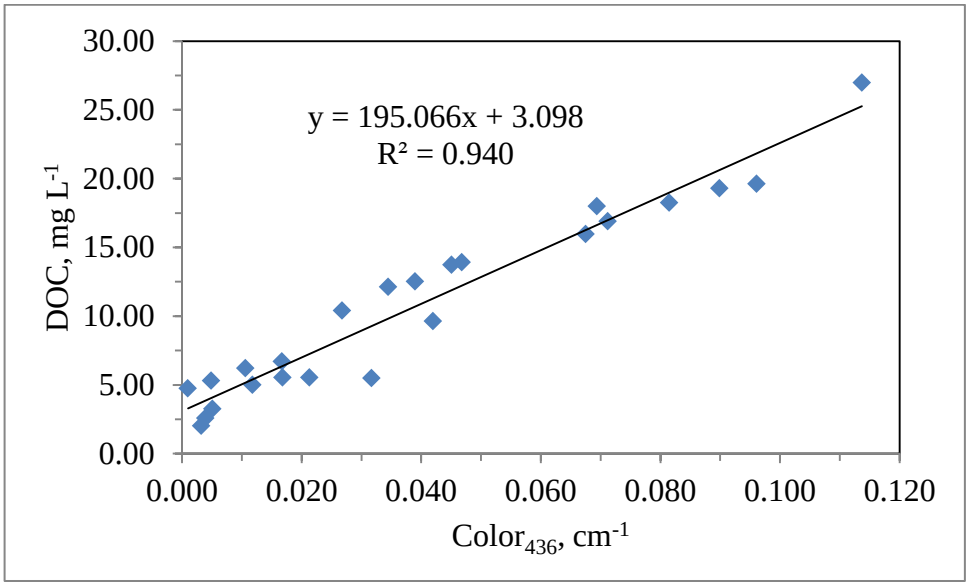

Figure 4.39. The correlation between $Color_{436}$ parameter and DOC concentration, including oxidative data during the photocatalytic treatment and nonoxidative data before the photocatalytic treatment, for 10, 20, 30 and 50 mg L^{-1} of NHA.

Figure 4.39 illustrated the linear correlation between $Color_{436}$ parameter and DOC concentrations of humic acid. Equation of the correlation between DOC concentration, including oxidative data for each irradiation time during the photocatalytic treatment and nonoxidative data before the photocatalytic treatment, for 10, 20, 30 and 50 mg L^{-1} of NHA, and $Color_{436}$ parameter of the remaind NHA after the photocatalytic treatment and NHA concentration at adsorption period, was produced from the least-squares regression analyses (Equation 4.73). The regression coefficient was found to be as R^2= 0.940. As mentioned above, Equation 4.8 was obtained by the correlation between $Color_{436}$ parameter and DOC concentration of non-oxidized NHA.

Equation 4.73 was attained by the correlation between $Color_{436}$ parameter and DOC concentration of NHA, including all condition data. Equation 4.49 was achieved by the relationship between $Color_{436}$ parameter and DOC concentration of the non-oxidized overall humic acids (NHA, FHA, AHA and RHA). Equation 4.73a was attained by the graph, pointing out, the correlation between $Color_{436}$ parameter results and DOC concentration results of NHA, including at t=0 and post oxidation, after the photocatalytic treatment. Equation 4.73b was achieved from the graph, representing the correlation

between $Color_{436}$ parameter and DOC concentrations, including only post oxidation data, after the photocatalytic treatment. These equations were stated below (Table 4.21).

Table 4.21. The correlation Equations and the regression coefficients obtained from the relationship between $Color_{436}$ and DOC concentration of NHA, including the non-treatment data (Equation 4.8) and the photocatalytic treatment data (Equation 4.73, 4.73a, 4.73b), and the relationship between $Color_{436}$ and DOC concentration of the overall humic acids (NHA, FHA, AHA and RHA), including the non-treatment data (Equation 4.49).

Equation No	Correlation Equation	R^2
4.8	DOC (mg L^{-1}) = 211.66 * $Color_{436}$ (cm^{-1}) − 0.284	0.963
4.73	DOC (mg L^{-1}) = 195.07 * $Color_{436}$ (cm^{-1}) + 3.10	0.940
4.73a	DOC (mg L^{-1}) = 185.29 * $Color_{436}$ (cm^{-1}) + 3.56	0.943
4.73b	DOC (mg L^{-1}) = 188.70 * $Color_{436}$ (cm^{-1}) + 3.64	0.949
4.49	DOC (mg L^{-1}) = 32.16* $Color_{436}$ (cm^{-1}) + 6.47	0.530

In the least square regression model, equation could give random error (Johnson and Bhattacharyya, 1996). Equation 4.8, represented the randon error as a value of - 0.284, Equation 4.73 represented the randon error as a value of 3.10, Equation 4.73a represented the randon error as a value of 3.56, Equation 4.73b represented the randon error as a value of 3.64, and Equation 4.49 represented the randon error as a value of 6.47. When the Equations (Equation 4.73, Equation 4.73a, and Equation 4.73b), attained by using results after the photocatalytic treatment, were compared with each other. Equation 4.73b gave the highest error with a value of 3.64 whereas, Equation 4.73 gave the lowest error with a value of 3.10. On the other hand, as seen in Table 4.21, Equation 4.73, attained by DOC results and UV-vis parameter results including all conditions, Equation 4.73a, achieved by DOC results and UV-vis parameter results consisting of t=0 and post-oxidation data, and Equation 4.73b, attained by DOC results and UV-vis parameter results (UV_{254}, UV_{280}, UV_{365} and $Color_{436}$) consisting of post-oxidation data gave very close error numbers. Equation 4.49 obtained from the correlation between $Color_{436}$ parameter and DOC concentration results of the overall humic acids without treatment, exhibited more error

than Equation 4.8, attained from the correlation between $Color_{436}$ parameter and DOC concentration results without treatment (Table 4.21).

$Color_{436}$ parameter results of 10 and 50 mg L^{-1} humic acid, including before the photocatalytic treatment, at t=0 and the post-oxidation data, were used to calculate DOC results, as shown in Table 4.22. During the adsorption period (t=0) DOC_{calc}, calculated as a function of $Color_{436}$ parameter by using Equation 4.8, exhibited 47 % of DOC_{calc}, according to Equation 4.49. Moreover, DOC_{calc}, calculated as a function of $Color_{436}$ parameter by using Equation 4.8, exhibited 51 % of DOC_{calc}, depending on Equation 4.73 for 10 mg L^{-1} of NHA. After the irradiation time of 60 minutes, DOC_{calc}, calculated as a function of $Color_{436}$ parameter by using Equation 4.8, exhibited 0.06 % of DOC_{calc}, according to Equation 4.49. Moreover, DOC_{calc}, calculated as a function of $Color_{436}$ parameter by using Equation 4.8, exhibited 11 % of DOC_{calc}, dependent upon Equation 4.73 for 10 mg L^{-1} of NHA.

During the adsorption period (t=0) DOC_{calc}, as a function of $Color_{436}$ parameter by using Equation 4.49, exhibited 48 % of DOC_{calc}, depending on Equation 4.8. Moreover, DOC_{calc}, as a function of $Color_{436}$ parameter by using Equation 4.8, exhibited 92 % of DOC_{calc}, depending on Equation 4.73 for 10 mg L^{-1} of NHA. After the irradiation time of 60 minutes, DOC_{calc}, as a function of $Color_{436}$ parameter by using Equation 4.49, exhibited 62 % of DOC_{calc}, depending on Equation 4.8. Moreover, DOC_{calc}, as a function of $Color_{436}$ parameter by using Equation 4.8, exhibited 86 % DOC_{calc}, depending on Equation 4.73 for 50 mg L^{-1} of NHA. At the adsorption period (t=0), 49 %, 31 %, 29 %, 29 % and 6.4 % removal exhibited decreasing trend for Equation 4.8, Equation 4.73, Equation 4.73a, Equation 4.73b and Equation 4.49, respectively. After the irradiation time of 30 minutes, 88 %, 56 %, 52 %, 52 % , 11 % and 41 % removal exhibited for Equation 4.8, Equation 4.73, Equation 4.73a, Equation 4.73b, Equation 4.49 and in the observation, respectively. The conversion after 60 min, was 94 % for Equation 4.2, 60 % for Equation 4.73, 56 % for Equation 4.73a and Equation 4.73b, 12 % for Equation 4.49 and 63 % in the observation. The removal of DOC concentration, related to Equation 4.8, displayed higher removal than DOC concentrations, related to Equation 4.73, Equation 4.73a, Equation 4.73b, Equation 4.49 and the observation.

Table 4.22. DOC concentrations of NHA calculated by using Equation 4.8, Equation 4.73, Equation 4.73a, Equation 4.73b and Equation 4.49, as a function of $Color_{436}$ parameter, including the non-oxidative data before the photocatalytic treatment and the oxidative data after each irradiation time period, and DOC concentration, corresponding to $Color_{436}$ parameter and measured by TOC analyzer for 10, 20, 30 and 50 mg L^{-1} of NHA.

NHA: 10 mg L^{-1}	$Color_{436}$, cm^{-1}					
Irradiation time	0	15	30	45	60	RAW
	0.0168	0.0118	0.0051	0.0039	0.0032	0.0317
Equation	DOC, mg L^{-1}					
4.8	3.272	2.214	0.795	0.541	0.393	6.426
4.73	6.377	5.402	4.095	3.861	3.724	9.284
4.73a	6.673	5.746	4.505	4.283	4.153	9.434
4.73b	6.810	5.867	4.602	4.376	4.244	9.622
4.49	7.010	6.850	6.634	6.595	6.573	7.490
Observation	5.530	5.010	3.250	2.590	2.030	5.500
NHA: 50 mg L^{-1}	$Color_{436}$, cm^{-1}					
Irradiation time	0	15	30	45	60	RAW
	0.0961	0.0899	0.0815	0.0712	0.0675	0.1137
Equation	DOC, mg L^{-1}					
4.8	20.06	18.74	16.97	14.79	14.00	23.78
4.73	21.85	20.64	19.00	16.99	16.27	25.28
4.73a	21.37	20.22	18.66	16.75	16.07	24.63
4.73b	21.77	20.60	19.02	17.08	16.38	25.10
4.49	9.561	9.362	9.091	8.760	8.641	10.13
Observation	19.63	19.29	18.25	16.90	15.96	26.98

Figure 4.40 showed DOC_{calc}, calculated by using Equation 4.8, Equation 4.73, Equation 4.73a, Equation 4.73b and Equation 4.49, and DOC measurement depending on the irradation time. At t=0, the adsorption effect, dependent on Equations, as mentioned above, was examined with respect to time '0'. DOC_{calc}, calculated by using Equation 4.73, Equation 4.73a, Equation 4.73b and Equation 4.49, were found to be higher than DOC_{obs}

for each irradiation period. On the other hand, DOC_{calc}, depending on Equation 4.8, obtained from the correlation between $Color_{436}$ parameter and DOC concentration of NHA, was found to be lower than DOC_{obs} just before the photocatalytic treatment, at 15 minutes, at 30 minutes, at 45 minutes and at 60 minutes. According to Figure 4.40, the Equations were not found to be useful for the prediction of DOC concentration content for 10 mg L^{-1} of NHA during the photocatalytic treatment.

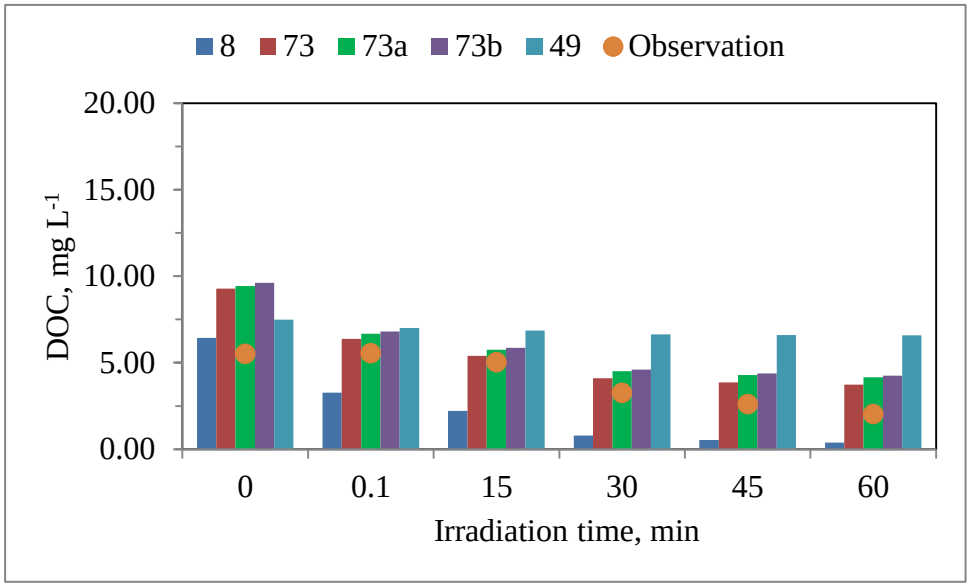

Figure 4.40. Comparison of DOC_{obs} and DOC_{calc} concentration, obtained by using Equation 4.8 (8), Equation 4.73 (73), Equation 4.73a (73a), Equation 4.73b (73b) and Equation 4.49 (49) with the irradiation time as a function of $Color_{436}$ parameter, including the non-oxidative data prior to the photocatalytic treatment and the oxidative data after each irradiation time of the photocatalytic treatment, for 10 mg L^{-1} of NHA.

Before the photocatalytic treatment, (t=0), DOC_{calc}, calculated by using Equation 49, exhibited 36 % of DOC_{obs} (Figure 4.41). At t=0, the adsorption effect, dependent on Equations, as mentioned above, was examined with respect to time '0'. At the adsorption period, 16 %, 14 %, 30 %, 30 % and 39 % removal exhibited decreasing trend for Equation 4.8, Equation 4.73, Equation 4.73a, Equation 4.73b and Equation 4.49, respectively. After the irradiation time of 30 minutes, 60 %, 43 %, 39 %, 39 % , 50 % and 41 % removal exhibited for Equation 4.8, Equation 4.73, Equation 4.73a, Equation 4.73b, Equation 4.49 and in the observation. The conversion after 60 min, was 87 % for Equation 4.2, 62 % for

Equation 4.73, 57 % for Equation 4.73a and Equation 4.73b, 73 % for Equation 4.49 and 63 % in the observation. When taking the average of DOC results, obtained by all equations, these DOC_{calc} results exhibited 96 %, 93 %, 91 %, 88 % and 89 % of DOC_{obs} just before photocatalytic treatment, at 15 minutes, at 30 minutes, at 45 minutes and at 60 minutes, respectively for 50 mg L^{-1} of NHA. Similar to 10 mg L^{-1} of NHA, the removal of DOC concentration, related to Equation 4.8, exhibited higher removal than DOC concentration related to Equation 4.73, Equation 4.73a, Equation 4.73b, Equation 4.49 and the observation for 50 mg L^{-1} of NHA. According to Figure 4.41, DOC_{calc}, calculated by using Equation 4.8, Equation 4.73, Equation 4.73a, and Equation 4.73b were found to be closed to DOC_{obs}, whereas DOC_{obs} was found to be more than DOC_{calc}, calculated by using Equation 4.49.

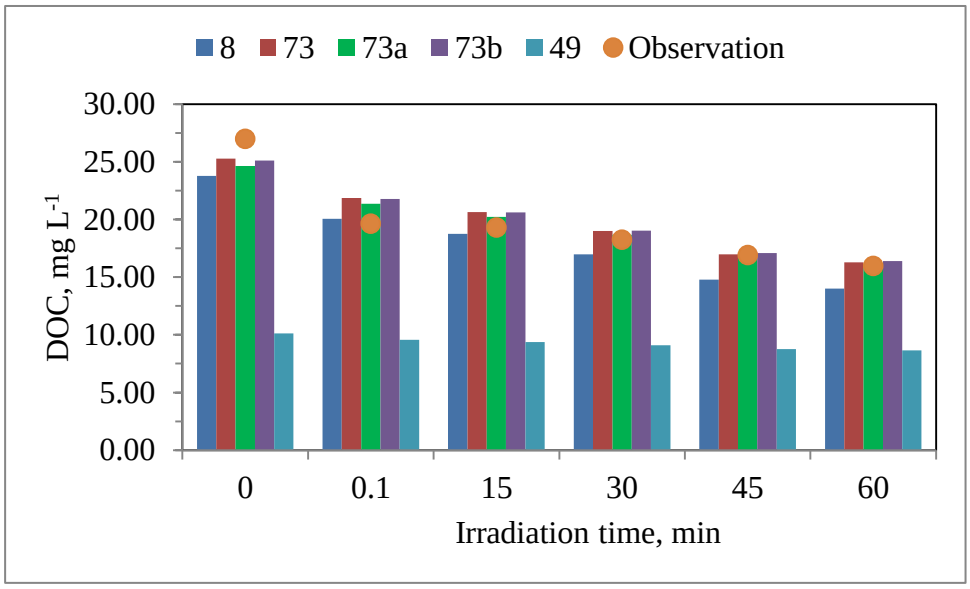

Figure 4.41. Comparison of DOC_{obs} and DOC_{calc} concentration, obtained by using Equation 4.8 (8), Equation 4.73 (73) , Equation 4.73a (73a), Equation 4.73b (73b) and Equation 4.49 (49) with the irradiation time as a function of $Color_{436}$ parameter, including the non-oxidative data prior to the photocatalytic treatment and the oxidative data after each irradiation time of the photocatalytic treatment, for 50 mg L^{-1} of NHA.

As shown in Figure 4.41, Equation 4.73, attained from the relationship between DOC result and $Color_{436}$ parameter, including all condition data and Equation 4.73a, attained from the relationship between DOC result and $Color_{436}$ parameter, consisting of t=0 and

post oxidation data, were found to be useful for the prediction of DOC concentration in 50 mg L^{-1} of NHA during the photocatalytic treatment whereas, Equation 4.49, attained from the relationship between DOC result and $Color_{436}$ parameter of the overall humic acids, were not found to be useful.

$Color_{436}$(min), $Color_{436}$(max) and $Color_{436}$(average) parameters was put in Equation 4.8, Equation 4.73 and Equation 4.49 to calculate DOC_{min}, DOC_{max} and $DOC_{average}$. According to Table 4.8, $Color_{436}$ (min) was expressed as a value of 0.0032 cm^{-1}, obtained by the photocatalytic treatment after the irradiation time of 60 minutes. $Color_{436}$(max) was expressed as a value of 0.1137 cm^{-1}, representing the initial concentration of 50 mg L^{-1} of NHA. $Color_{436}$(average), expressed as a value of 0.0379 cm^{-1}, was calculated by taking the average of $Color_{436}$ parameter results after the photocatalytic treatment. By using these equations (Equation 4.8, Equation 4.73, Equation 4.73a, Equation 4.73b, Equation 4.49), DOC concentration were calculated with given $Color_{436}$ parameter (Table 4.23).

Table 4.23. DOC concentrations of NHA, related to $Color_{436}$ (min), $Color_{436}$ (max) and $Color_{436}$ (average), calculated by using Equation 4.8, Equation 4.73, Equation 4.73a, Equation 4.73b and Equation 4.49, and DOC_{obs}, measured by TOC analyzer.

Equation No	Min $Color_{436}$=0.0032 cm^{-1}	Max $Color_{436}$= 0.1137 cm^{-1}	Average $Color_{436}$ = 0.0379 cm^{-1}
	DOC_{calc}, mg L^{-1}		
4.8	0.3933	23.78	7.865
4.73	3.722	25.28	10.61
4.73a	4.153	24.63	10.58
4.73b	4.244	25.10	10.79
4.49	6.573	10.13	7.708
DOC_{obs}	2.030	26.98	-

DOC_{calc}, related to Equation 4.8, displayed 10.5 % of DOC_{calc}, according to Equation 4.73 for $Color_{436}$ (min), and also displayed 0.06 % of DOC_{calc}, depending on Equation 4.49 for $Color_{436}$ (min). DOC_{calc}, related to Equation 4.49, exhibited 42.5 % of DOC_{calc},

according to Equation 4.73, and also displayed 40 % of DOC_{calc}, related to Equation 4.8 for $Color_{436}$ (max). DOC_{calc}, depending on Equation 4.49, displayed 73 % of DOC_{calc}, related to Equation 4.73, and also exhibited 40 % of DOC_{calc}, related to Equation 4.8 for $Color_{436}$ (average). By using Equation 4.8, DOC_{calc}, as a function of $Color_{436}$(min), exhibited 1.65 % of DOC_{calc}, as a function of $Color_{436}$(max). DOC_{obs}, related to $Color_{436}$(min) and $Color_{436}$(max), determined by using TOC analyses (Table 4.8), were compared with DOC_{calc}, related to Equation 4.8, Equation 4.49 and Equation 4.73 (Table 4.23). DOC_{calc}, related to Equation 4.73 and Equation 4.49, exhibited, respectively, 54.5 % and 30.8 % of DOC_{obs} for $Color_{436}$(max), whereas, DOC_{calc}, depending on Equation 4.8, displayed 19.3 % of DOC_{obs}, for $Color_{436}$ (min). Furthermore, the lowest DOC result was observed in Equation 4.8, while, the highest DOC was attained from the observation result (Table 4.23).

As seen below, DOC_{obs} results were correlated with DOC_{calc} results. DOC_{obs} results represented DOC values, attained at the end of each irradiation period by using TOC analyzer. DOC_{calc} of NHA pointed out DOC values, achieved by using Equations (Equation 4.2, Equation 4.4, Equation 4.6 and Equation 4.8) related to UV-vis parameters (Table 4.9). Moreover, Equations 4.43, Equation 4.45, Equation 4.47 and Equation 4.49, obtained by using the correlation between UV-vis parameters and DOC concentrations of the overall humic acids (NHA, FHA, AHA and RHA), were used for DOC calculation of NHA (Table 4.10).

4.3.1.7. The Relationship between Initial and Oxidized DOC_{obs} Concentration and DOC_{calc} Concentration of NHA depending on the Non-treatment Equations of NHA. DOC_{obs} concentration of NHA, including the non-oxidative data before the photocatalytic treatment and oxidative data after each irradiation time of the photocatalytic treatment (Table 4.8), were correlated with DOC_{calc} concentrations, that was calculated by using Equation 4.2 as a function of UV_{254} parameter, Equation 4.4 as a function of UV_{280} parameter before the photocatalytic treatment and after each irradiation time of the photocatalytic treatment (15, 30, 45 and 60 minutes) (Table 4.9) for 10, 20, 30 and 50 mg L^{-1} of NHA. DOC_{obs} was correlated with DOC_{calc} concentrations, that was calculated by using Equation 4.6. as a function of UV_{365} parameter and Equation 4.8 as a function of $Color_{436}$ parameter before the photocatalytic treatment and after each irradiation time of the

photocatalytic treatment (15, 30, 45 and 60 minutes) (Table 4.9) for 10, 20, 30 and 50 mg L^{-1} of NHA.

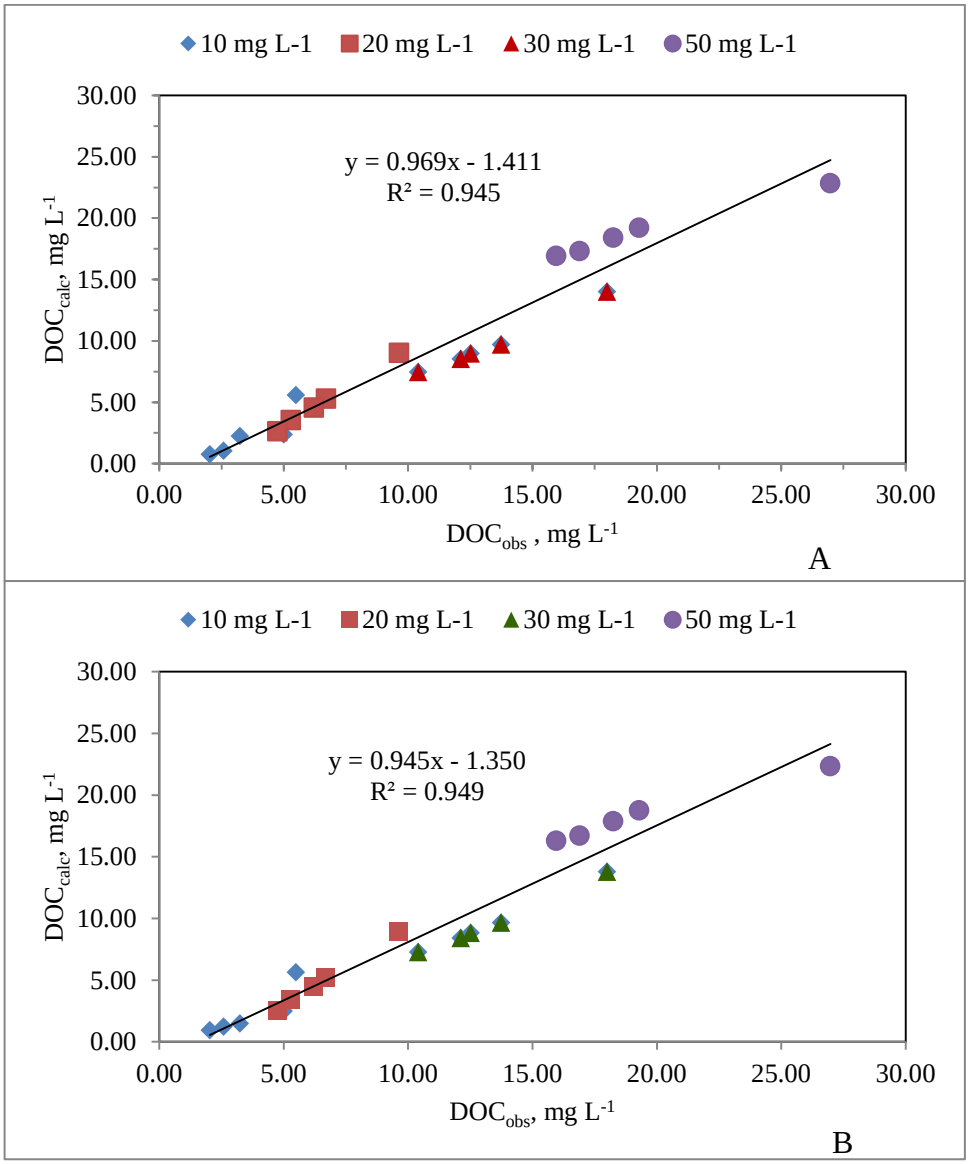

Figure 4.42. The correlation between DOC_{obs}, measured by TOC analyzer, and DOC_{calc} obtained by using Equation 4.2 as a function of UV_{254} parameter and Equation 4.4 as a function of UV_{280} parameter, including the non-oxidative data before the photocatalytic treatment and the oxidative data after each irradiation time of the photocatalytic treatment for the initial concentration of NHA. ((A) UV_{254}, (B) UV_{280}).

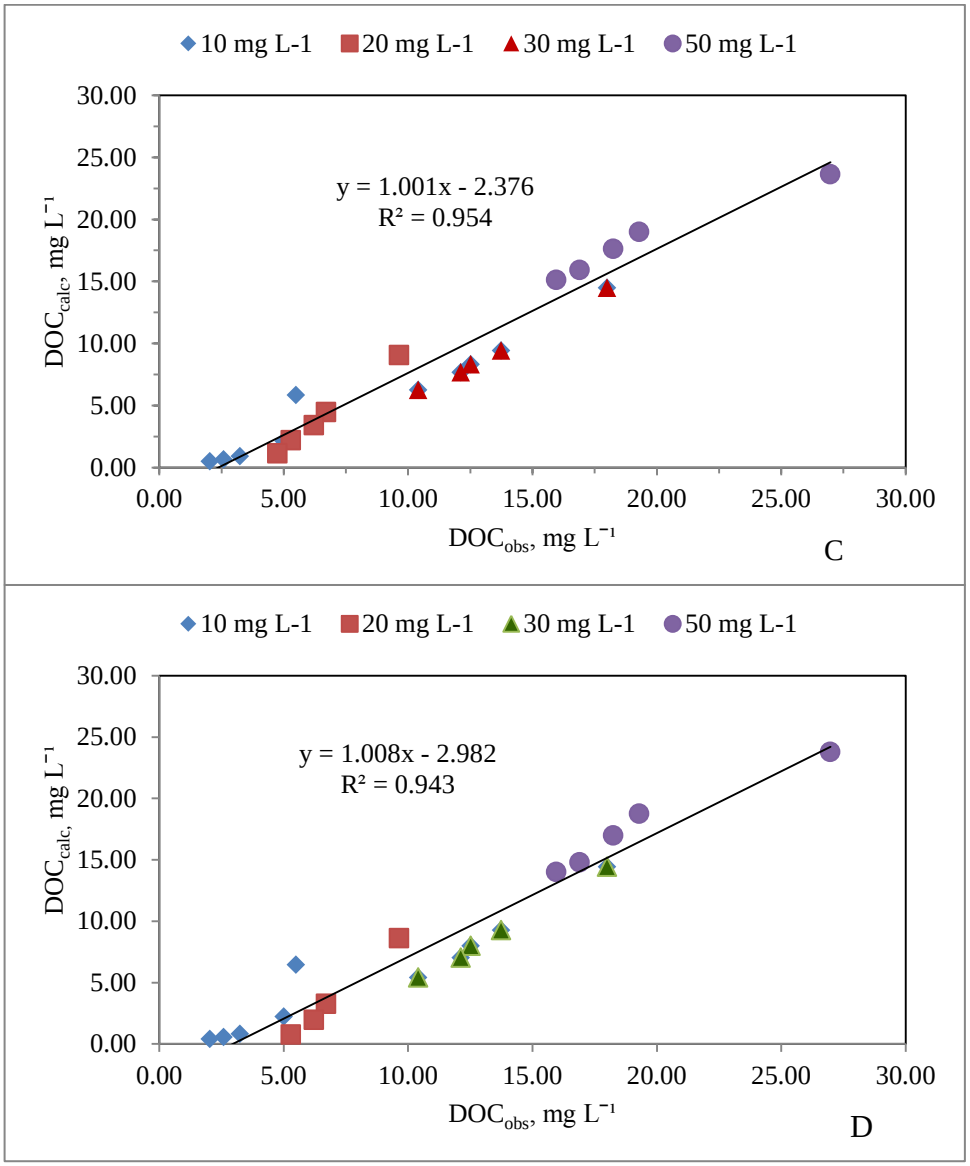

Figure 4.43. The correlation between DOC_{obs}, measured by TOC analyzer, and DOC_{calc} obtained by using Equation 4.6 as a function of UV_{365} parameter and Equation 4.8 as a function of $Color_{436}$ parameter, including the non-oxidative data before the photocatalytic treatment and the oxidative data after each irradiation period of the photocatalytic treatment for the initial concentration of NHA. ((C) UV_{365}, (D) $Color_{436}$).

As seen above, Figure 4.42 ,DOC_{obs}, obtained by using TOC analyzer, (Table 4.8) was correlated with DOC_{calc}, obtained as a function of UV_{254} and UV_{280} parameter, including the adsorption and the irradiation period (15, 30, 45 and 60 minutes) for 10, 20, 30 and 50 mg L^{-1} of NHA. The regression coefficient was found to be as R^2=0.945 for UV_{254} parameter. Moreover, the regression coefficient was found to be as R^2=0.949 for

UV_{280} parameter. DOC_{obs} could predict DOC_{calc} with high regression coefficient for both UV_{254} and UV_{280} parameter. Figure 4.43 illustrated the linear correlation between DOC_{obs} concentrations and DOC_{calc} concentrations. The Equation of DOC_{obs}, obtained by using TOC analyzer, and DOC_{calc}, as a function of UV_{365} and $Color_{436}$ parameter, was produced from the least-squares regression analyses (Equation 4.76 and Equation 4.77). The regression coefficient was found to be as R^2= 0.954 (UV_{365}; Equation 4.76) and R^2= 0.943 ($Color_{436}$; Equation 4.77).

As seen in Table 4.24, DOC_{obs} result was obtained by using TOC analyzer. Persulfate oxidation method was applied for determination of dissolved organic carbon content in Nordic humic acid. TOC analyzer detects all organic carbon content in a sample whereas, UV-vis spectroscopy detects conjugated double bonds and aromatic moieties (Her et al., 2002).

Table 4.24. The relationship between DOC_{calc}, obtained as a function of UV-vis parameters (UV_{254}, UV_{280}, UV_{365} and $Color_{436}$, including initial and oxidized data) by using Equation 4.2, Equation 4.4, Equation 4.6 and Equation 4.8 and DOC_{obs}, measured by TOC analyzer.

NHA Photocatalytic treatment			
No	UV-vis Parameter	Correlation Equation	R^2
4.74	UV_{254}	DOC_{calc} (mg L^{-1}) = 0.969*DOC_{obs} (mg L^{-1}) – 1.411	0.945
4.75	UV_{280}	DOC_{calc} (mg L^{-1}) = 0.945*DOC_{obs} (mg L^{-1}) – 1.350	0.949
4.76	UV_{365}	DOC_{calc} (mg L^{-1}) = 1.001*DOC_{obs} (mg L^{-1}) – 2.376	0.954
4.77	$Color_{436}$	DOC_{calc} (mg L^{-1}) = 1.008 *DOC_{obs} (mg L^{-1}) – 2.982	0.943

DOC_{obs} result represented the remaining dissolved organic carbon in Nordic humic acid after irradiation time. DOC_{calc} was calculated by using Equations, achieved by the correlation between untreated UV-vis parameters and DOC contents of NHA. DOC_{calc} represented results calculated by using Equation 4.2 as a function of UV_{254} parameter, Equation 4.4 as a function of UV_{280} parameter, Equation 4.6 as a function of UV_{365} parameter and Equation 4.8 as a function of $Color_{436}$ parameter, remained after the

photocatalytic treatment (Table 4.24). According to the nontreatment Equations, DOC_{calc} attained as a function of UV_{254} parameter, UV_{280} parameter, UV_{365} parameter and $Color_{436}$ parameter remaining after the irradiation time was found to be closed to DOC_{obs}, including oxidized and initial values with high regression coefficient. The remaining UV_{254} parameter and UV_{280} parameter, representing conjugated double bonds and aromatic moieties, UV_{365} parameter, representing aromatic moieties, and $Color_{436}$ parameter, representing color forming moieties, included enough carbon content depending on nontreatment equations (Equation 4.2, Equation 4.4, Equation 4.6 and Equation 4.8) that DOC_{calc} gave a good prediction of organic carbon content in NHA, observed by TOC analyzer as seen in Figure 4.43. As a result, DOC in NHA could be determined by using nontreatment Equations (Equation 4.2, Equation 4.4, Equation 4.6 and Equation 4.8) as a function of the remaning UV_{254}, UV_{280}, UV_{365} and $Color_{436}$ parameter after the irradiation time instead of using TOC analyzer.

4.3.1.8. The Relationship between Oxidized DOC_{obs} Concentration and DOC_{calc} Concentration of NHA dependent on the Non-treatment Equations of NHA. DOC_{obs} concentration of NHA, including oxidative data after each irradiation time of photocatalytic treatment (Table 4.8), were correlated with DOC_{calc} concentrations, that was calculated by using Equation 4.2 as a function of UV_{254} parameter, Equation 4.4 as a function of UV_{280} parameter, Equation 4.6 as a function of UV_{365} parameter and Equation 4.8 as a function of $Color_{436}$ parameter before the photocatalytic treatment and after each irradiation time of the photocatalytic treatment (Table 4.11) for 10, 20, 30 and 50 mg L^{-1} of NHA (Figure 4.44).

The correlation between DOC_{obs}, measured by TOC analyzer, and DOC_{calc} obtained by using Equation 4.2 as a function of UV_{254} parameter and Equation 4.4 as a function of UV_{280} parameter, including the oxidative data after each irradiation time of the photocatalytic treatment for the initial concentration of NHA was presented in Table 4.9. Moreover, the correlation between DOC_{obs}, measured by TOC analyzer, and DOC_{calc} obtained by using Equation 4.6 as a function of UV_{365} parameter and Equation 4.8 as a function of $Color_{436}$ parameter, including the oxidative data after each irradiation time of the photocatalytic treatment for the initial concentration of NHA was presented in Table 4.5. DOC_{calc}-DOC_{obs} equation was produced from the least-squares regression analyses

(Equation 4.78, Equation 4.79, Equation 4.80 and Equation 4.81). The regression coefficient was found to be as R^2= 0.953 (Equation 4.78; UV_{254} parameter), R^2= 0.958 (Equation 4.79; UV_{280} parameter), R^2= 0.958 (Equation 4.80; UV_{365} parameter) and R^2= 0.949 (Equation 4.81; $Color_{436}$ parameter).

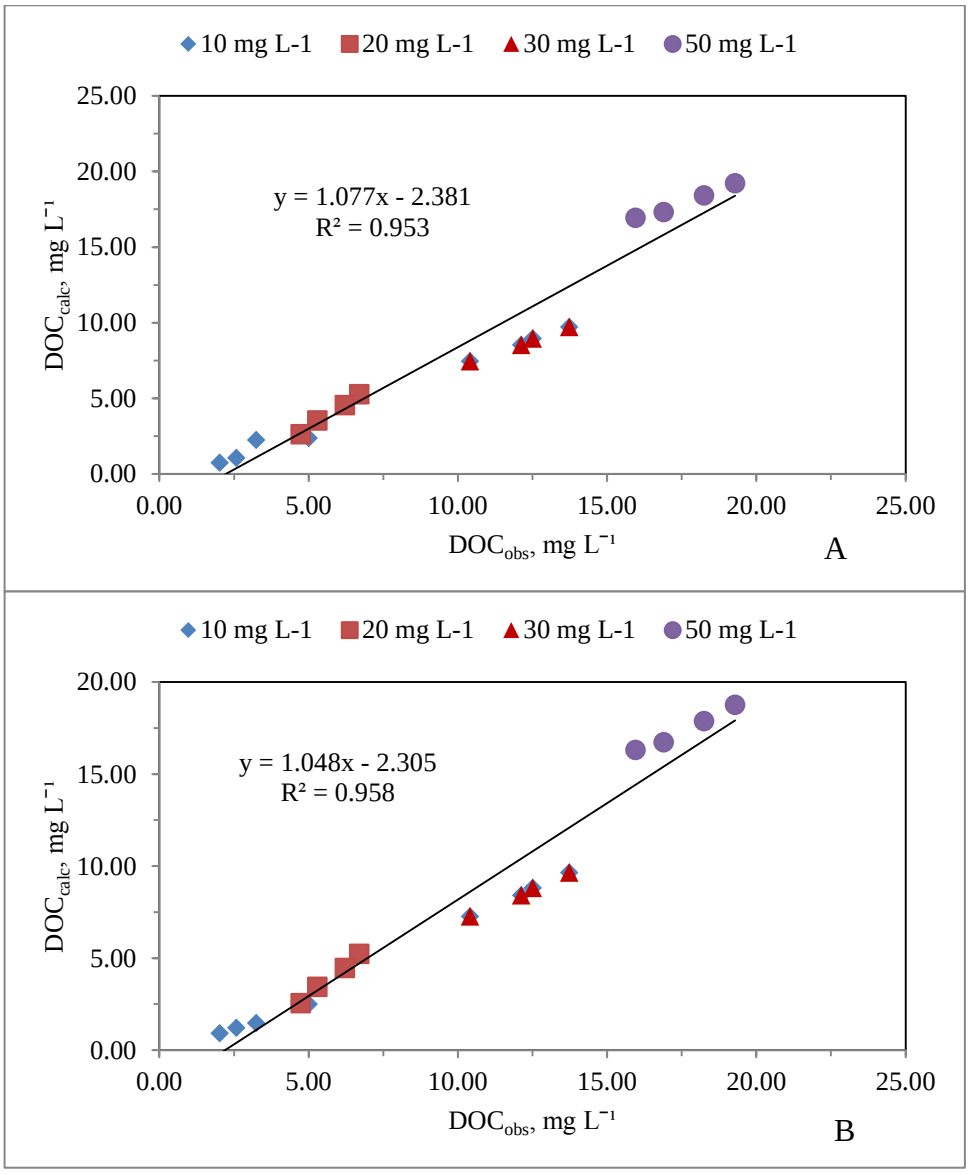

Figure 4.44. The correlation between DOC_{obs}, measured by TOC analyzer, and DOC_{calc} obtained by using Equation 4.2 as a function of UV_{254} parameter and Equation 4.4 as a function of UV_{280} parameter, including the oxidative data after each irradiation time of the photocatalytic treatment for the initial concentration of NHA.((A) UV_{254}, (B) UV_{280}).

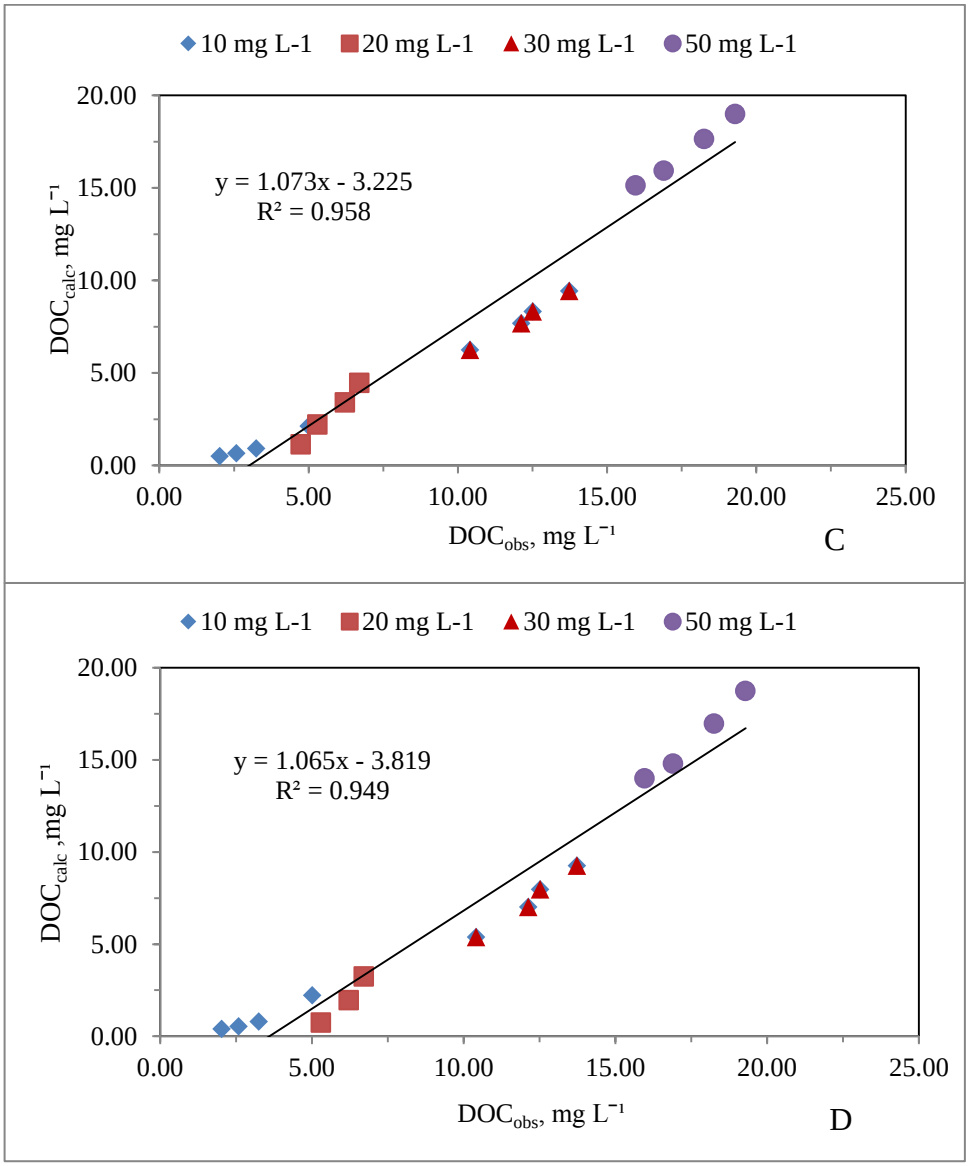

Figure 4.45. The correlation between DOC_{obs}, measured by TOC analyzer, and DOC_{cal} obtained by using Equation 4.6 as a function of UV_{365} parameter and Equation 4.8 as a function of $Color_{436}$ parameter, including the oxidative data after each irradiation time of the photocatalytic treatment for the initial concentration of NHA ((C) UV_{365}, (D) $Color_{436}$).

Similar to the correlation between DOC_{calc} and DOC_{obs}, including oxidized and initial values, the relationship between DOC_{calc} and DOC_{obs}, including oxidized values, exhibited high regression coefficient (Table 4.25). It was established correlation between DOC_{obs} and DOC_{calc} as a function of UV_{254} parameter (Equation 4.78), as a function of UV_{280} parameter (Equation 4.79), as a function of UV_{365} parameter (Equation 4.80) and as

a function of $Color_{436}$ parameter (Equation 4.81) of the remained humic acid after the photocatalytic treatment.

Table 4.25. The relationship between DOC_{calc}, obtained as a function of UV-vis parameters (UV_{254}, UV_{280}, UV_{365} and $Color_{436}$, including oxidized data) by using Equation 4.2, Equation 4.4, Equation 4.6 and Equation 4.8 and DOC_{obs}, measured by TOC analyzer.

No	UV-vis parameter	Linear Equation	R^2
4.78	UV_{254}	DOC_{calc}(mg L^{-1}) = 1.077*DOC_{obs} (mg L^{-1}) – 2.381	0.953
4.79	UV_{280}	DOC_{calc} (mg L^{-1}) = 1.048*DOC_{obs} (mg L^{-1}) – 2.305	0.958
4.80	UV_{365}	DOC_{calc} (mg L^{-1}) = 1.073*DOC_{obs} (mg L^{-1}) – 3.225	0.958
4.81	$Color_{436}$	DOC_{calc} (mg L^{-1}) = 1.065*DOC_{obs} (mg L^{-1}) – 3.819	0.949

As a result, DOC in Nordic humic acid could be determined by using nontreatment Equations (Equation 4.2, Equation 4.4, Equation 4.6 and Equation 4.8) as a function of UV_{254} parameter, UV_{280} parameter, UV_{365} parameter and $Color_{436}$ parameter of the remained humic acid after the irradiation time instead of using TOC analyzer.

4.3.1.9. The Relationship between Initial and Oxidized DOC_{obs} Concentration and DOC_{calc} Concentration of NHA depending on the Non-treatment Equation of the over-all HAs (NHA, FHA, AHA and RHA). DOC_{obs} concentration of NHA, including the non-oxidative data before the photocatalytic treatment and the oxidative data after each irradiation time of photocatalytic treatment (Table 4.8), was correlated with DOC_{calc} concentrations, calculated by using Equation 4.43 as a function of UV_{254} parameter. Moreover, DOC_{obs} concentration of NHA was correlated with DOC_{calc} concentrations, calculated by using Equation 4.45 as a function of UV_{280} parameter, Equation 4.47 as a function of UV_{365} parameter and Equation 4.49 as a function of $Color_{436}$ parameter before the photocatalytic treatment and after each irradiation time of photocatalytic treatment (Table 4.10) for 10, 20, 30 and 50 mg L^{-1} of NHA.

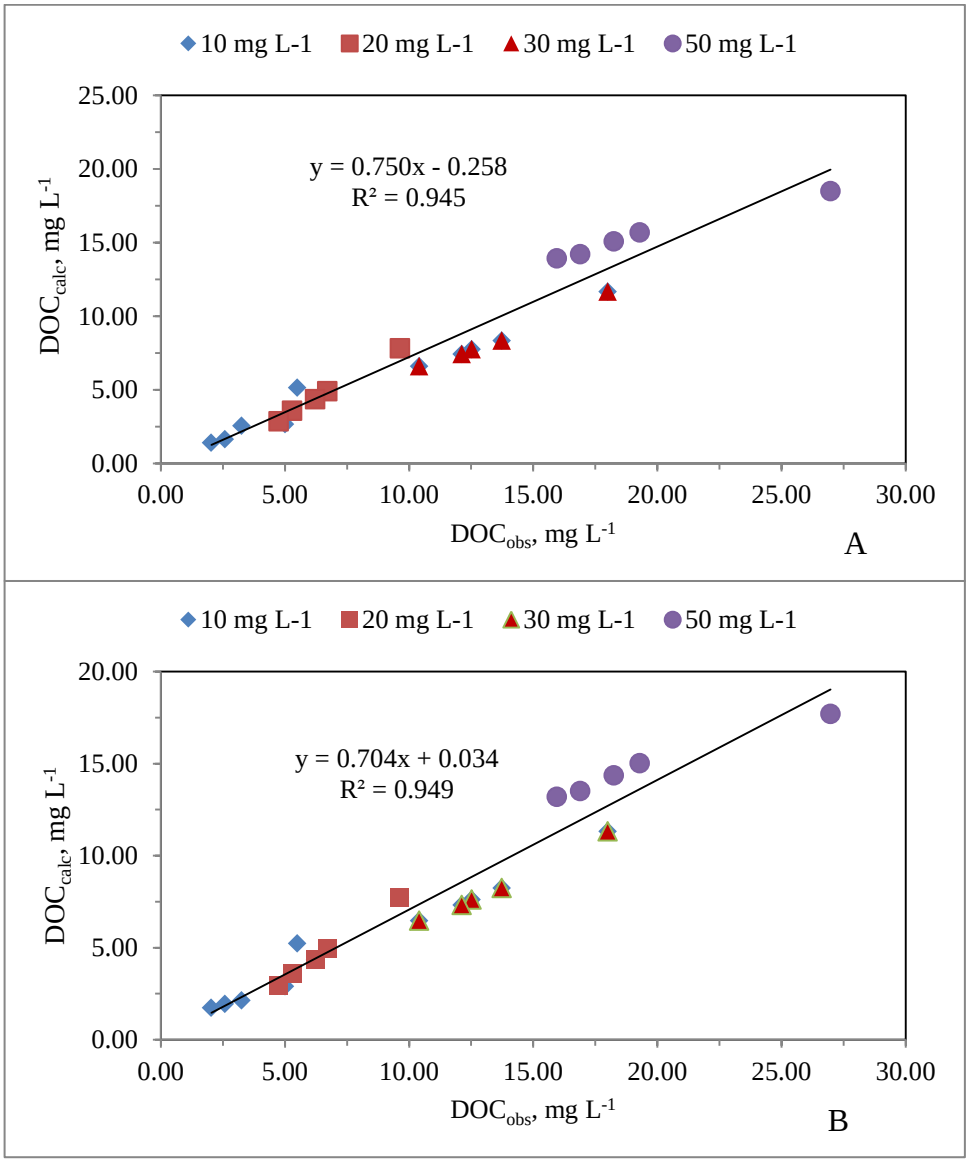

Figure 4.46. The correlation between DOC_{obs}, measured by TOC analyzer, and DOC_{calc} obtained by using Equation 4.43 as a function of UV_{254} parameter and Equation 4.45 as a function of UV_{280} parameter, including the non-oxidative data before the photocatalytic treatment and the oxidative data after each irradiation time of the photocatalytic treatment for the initial concentration of NHA. ((A)UV_{254}, (B) UV_{280}).

Figure 4.46 and 4.47 illustrated the linear correlation between DOC_{obs} concentrations and DOC_{calc} concentrations. DOC equation was produced from the least-squares regression analyses (Equation 4.82, Equation 4.83, Equation 4.84 and Equation 4.85).

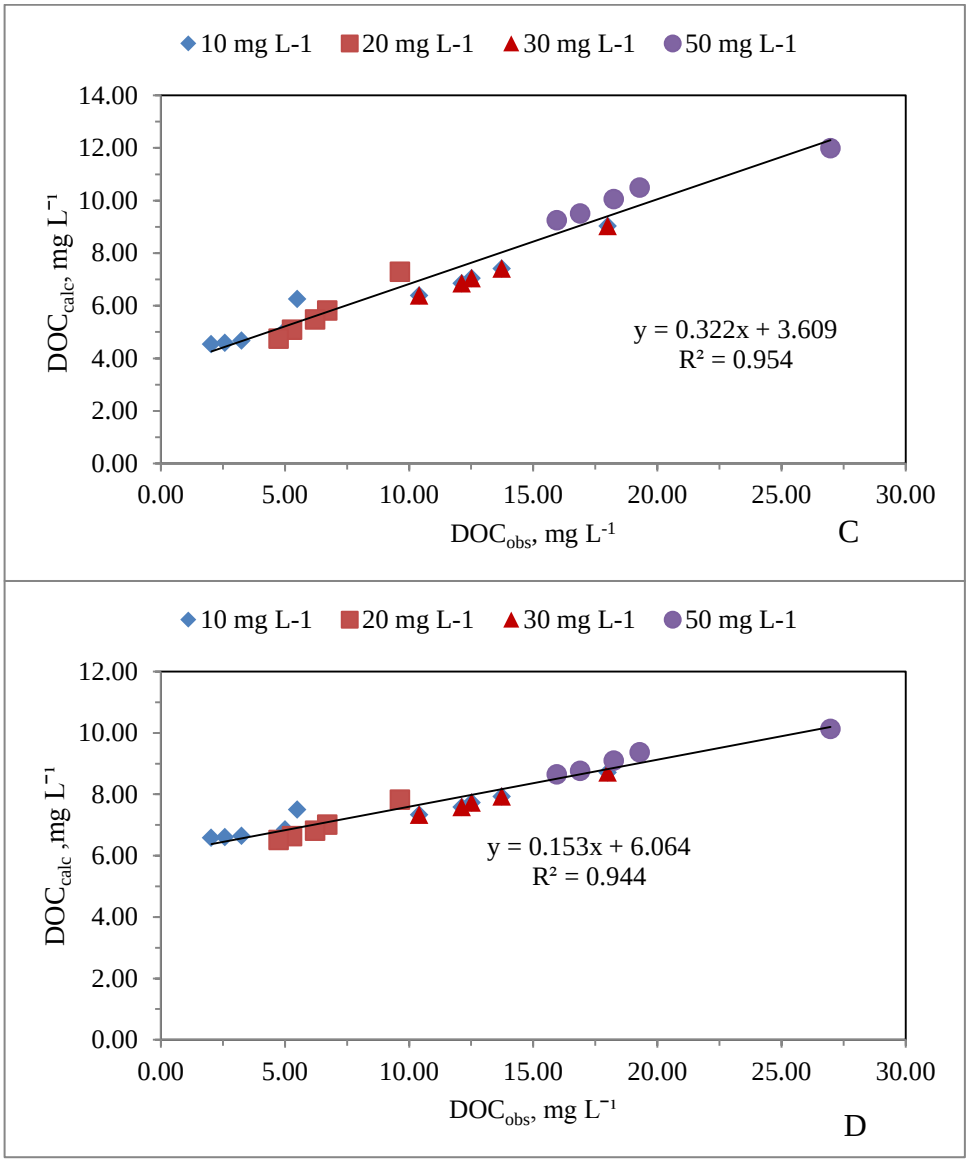

Figure 4.47. The correlation between DOC_{obs}, measured by TOC analyzer, and DOC_{calc}, obtained by using Equation 4.47 as a function of UV_{365} parameter and Equation 4.49 as a function of $Color_{436}$ parameter, including the nonoxidative data before the photocatalytic treatment and the oxidative data after each irradiation time of photocatalytic treatment for the initial concentration of NHA. ((C) UV_{365}, (D) $Color_{436}$).

DOC_{obs} result represented the remain dissolved organic carbon in NHA after irradiation time (Table 4.26). DOC_{calc} was calculated by using Equations, achieved by the correlation between nontreated UV-vis parameters (UV_{254}, UV_{280}, UV_{365} and $Color_{436}$) and DOC contents of NHA, FHA, AHA and RHA. DOC_{calc} represented results calculated by using Equation 4.43 as a function of UV_{254} parameter, Equation 4.45 as a function of

UV_{280} parameter, Equation 4.47 as a function of UV_{365} parameter and Equation 4.49 as a function of $Color_{436}$ parameter of the remained humic acid after the photocatalytic treatment.

Table 4.26. The relationship between DOC_{calc}, obtained as a function of UV-vis parameters (UV_{254}, UV_{280}, UV_{365} and $Color_{436}$, including initial and oxidized data) by using Equation 4.43, Equation 4.45, Equation 4.47 and Equation 4.49 and DOC_{obs}, measured by TOC analyzer.

No	UV-vis parmeter	Linear Equation	R^2
4.82	UV_{254}	DOC_{calc} (mg L^{-1}) = 0.750*DOC_{obs} (mg L^{-1}) – 0.258	0.945
4.83	UV_{280}	DOC_{calc}(mg L^{-1}) = 0.704*DOC_{obs} (mg L^{-1}) + 0.034	0.949
4.84	UV_{365}	DOC_{calc} (mg L^{-1}) = 0.322*DOC_{obs} (mg L^{-1}) + 3.609	0.954
4.85	$Color_{436}$	DOC_{calc} (mg L^{-1}) = 0.153*DOC_{obs}(mg L^{-1}) + 6.064	0.944

According to the nontreatment Equations (Equation 4.43, Equation 4.45, Equation 4.47 and Equation 4.49), DOC_{calc} achieved as a function of the remaining UV_{254} parameter, UV_{280} parameter, UV_{365} parameter and $Color_{436}$ parameter after the irradiation time was found to be closed to DOC_{obs} with high regression coefficient. The remaining UV_{254} parameter and UV_{280} parameter, representing conjugated double bonds and aromatic moieties, UV_{365} parameter, representing aromatic moities and $Color_{436}$ parameter, representing color forming moieties, consisting of enough carbon content according to non-treatment Equations (Equation 4.43, Equation 4.45, Equation 4.47 and Equation 4.49) that DOC_{calc} gave a good prediction of dissolved organic carbon content in NHA, observed by TOC analyzer. It could be inferred that UV_{254}, UV_{280}, UV_{365} and $Color_{436}$ parameter of the remained HA, represented enough the dissolved organic carbon that DOC_{calc}, obtained by using Equation (Equation 4.82, Equation 4.83, Equation 4.84, and Equation 4.85) could exhibit good prediction of DOC_{calc}, obtained by utilizing TOC analyzer in humic acid solution. As a result, it could be inferred that DOC content in NHA, could be determined

by calculating Equations as a function of UV-vis parameters (UV_{254}, UV_{280}, UV_{365} and $Color_{436}$) of the remained NHA after the irradiation time without applying TOC analyzer.

4.3.1.10. The Relationship between Oxidized DOC_{obs} Concentration and DOC_{calc} Concentration of NHA depending on the Non-treatment Equations of the over-all HAs (NHA, FHA, AHA and RHA). DOC_{obs} concentration of NHA, including the oxidative data after each irradiation time of photocatalytic treatment (Table 4.8), were correlated with DOC_{calc} concentrations, that was calculated by using Equation 4.43 as a function of UV_{254} parameter, Equation 4.45 as a function of UV_{280} parameter, Equation 4.47 as a function of UV_{365} parameter and Equation 4.49 as a function of $Color_{436}$ parameter before the photocatalytic treatment and after each irradiation time of the photocatalytic treatment (Table 4.10) for 10, 20,30 and 50 mg L^{-1} of NHA.

Figure 4.48 illustrated the linear correlation between DOC_{obs} concentrations and DOC_{calc} concentrations. Equation of the DOC_{obs}, obtained by using TOC analyzer (Table 4.8), and DOC_{calc}, by using Equation 4.43 as a function of UV_{254} parameter, Equation 4.45 as a function of UV_{280} parameter, before the photocatalytic treatment and after each irradiation time of the photocatalytic treatment (Table 4.10) for 10, 20,30 and 50 mg L^{-1} of NHA, was produced from the least-squares regression analyses (Equation 4.86, Equation 4.87). The regression coefficient was found to be as R^2= 0.956 (UV_{254}), R^2= 0.958 (UV_{280}). DOC_{calc} could predict DOC_{obs} with high regression coefficient for UV_{254} and UV_{280} parameter.

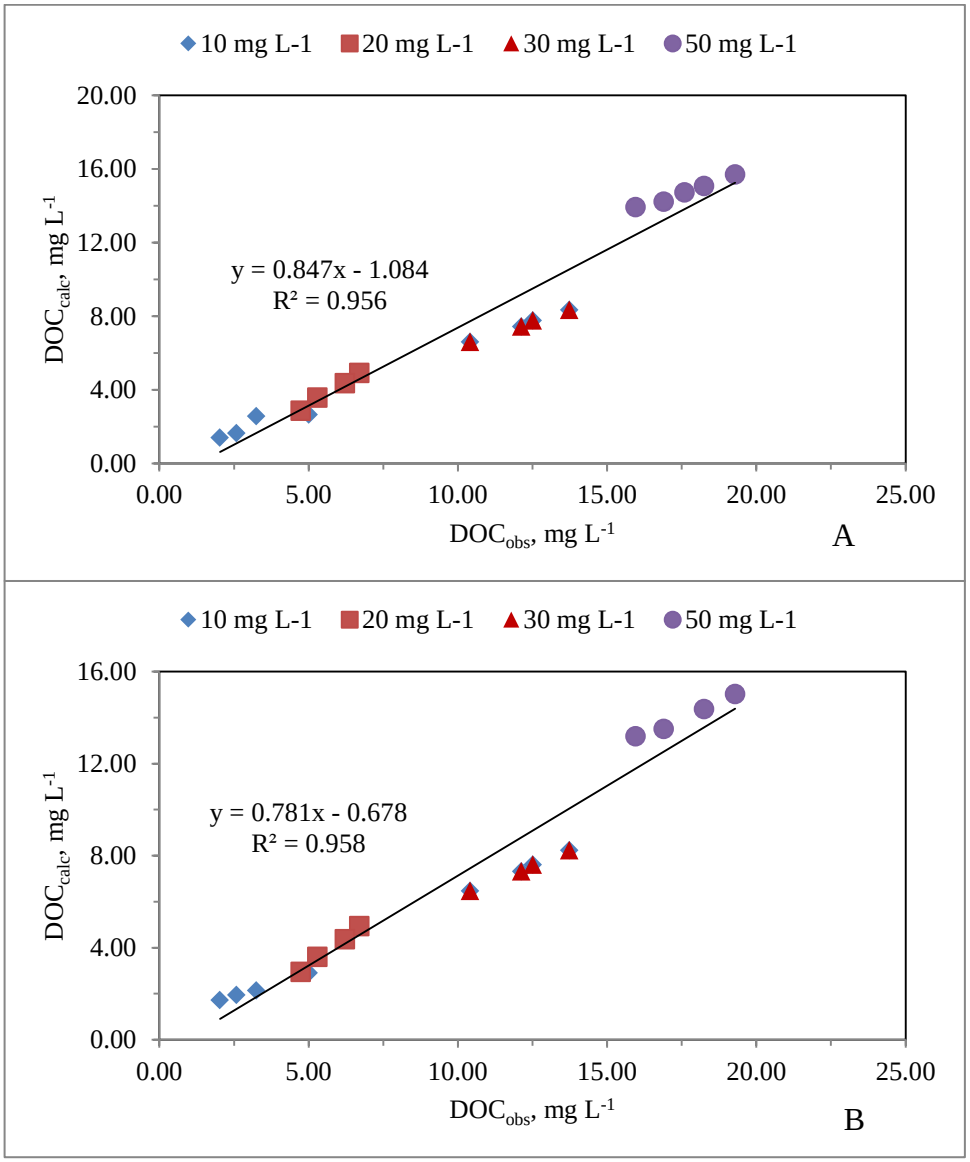

Figure 4.48. The correlation between DOC_{obs}, measured by TOC analyzer, and DOC_{calc} obtained by using Equation 4.43 as a function of UV_{254} parameter and Equation 4.45 as a function of UV_{280} parameter, including the oxidative data after each irradiation time of the photocatalytic treatment for the initial concentration of NHA. ((A)UV_{254}, (B) UV_{280}).

Figure 4.49 illustrated the linear correlation between DOC_{obs} concentrations and DOC_{calc} concentrations. DOC_{obs}, obtained by using TOC analyzer (Table 4.8), was correlated with DOC_{calc}, attained by using Equation 4.47 as a function of UV_{365} parameter, Equation 4.49 as a function of $Color_{436}$ parameter, before the photocatalytic treatment and after each irradiation time of the photocatalytic treatment (Table 4.10) for 10, 20,30 and 50

mg L^{-1} of NHA (Equation 4.86, Equation 4.87). The regression coefficient was found to be as R^2= 0.958 (UV_{365}), R^2= 0.949 ($Color_{436}$).

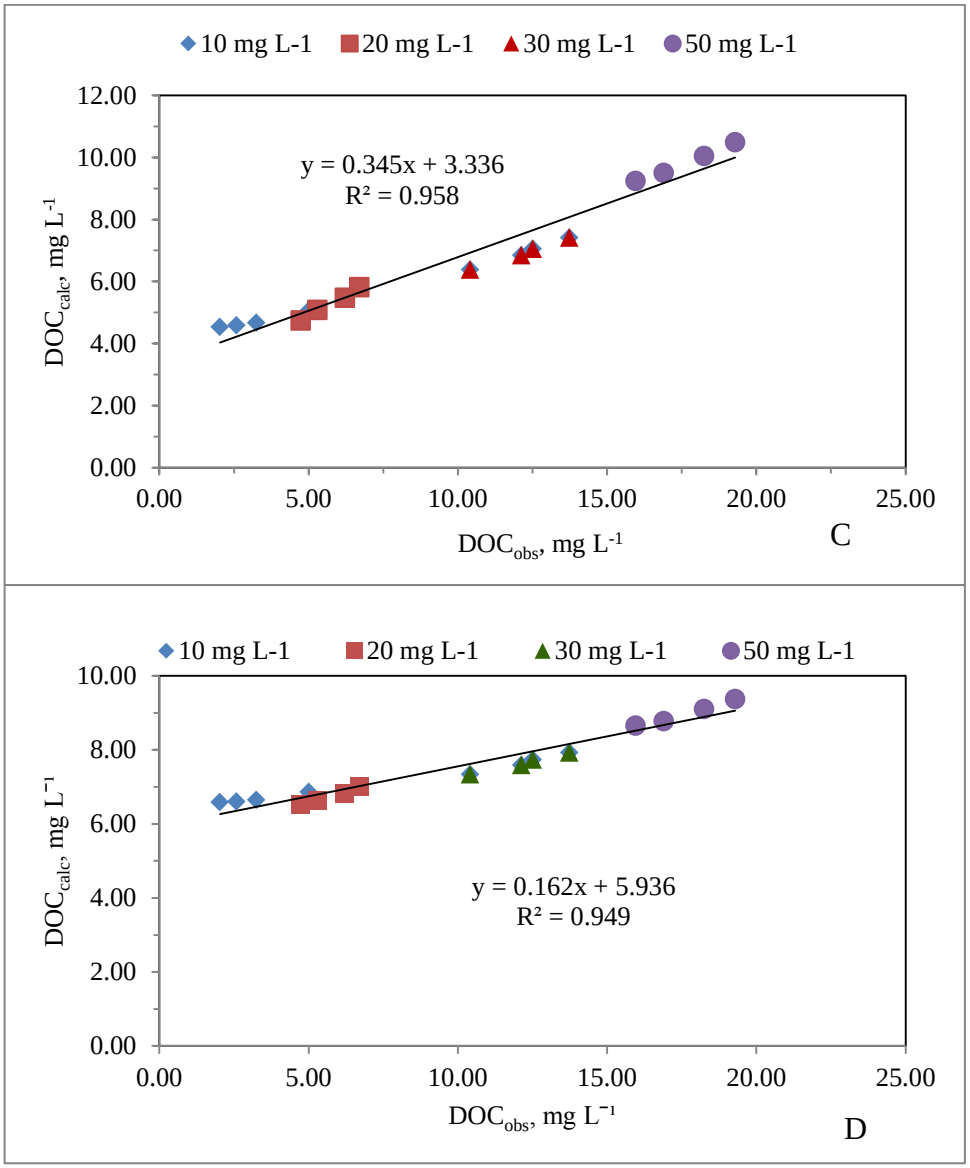

Figure 4.49. The correlation between $DOC_{obs}$and DOC_{calc} obtained by using Equation 4.47 as a function of UV_{365} parameter and Equation 4.49 as a function of $Color_{436}$ parameter, including the oxidative data after each irradiation time of the photocatalytic treatment for the initial concentration of NHA. ((C) UV_{365}, (D) $Color_{436}$).

As mentioned above, DOC_{obs} concentrations, including only oxidized values, were correlated with DOC_{calc} concentrations (Table 4.27). Similar to DOC_{calc}, consisting of

oxidized and initial values, DOC_{calc} values were found to be closed to DOC_{obs} with high regression coefficient. As a consequence, it could be inferred that DOC content in NHA, could be determined by calculating Equations (Equation 4.43, Equation 4.45, Equation 4.47 and Equation 4.49) as a function of UV_{254} parameter, UV_{280} parameter, UV_{365} parameter and $Color_{436}$ parameter of the remained NHA after the irradiation time without utilizing TOC analyzer.

Table 4.27. The relationship between DOC_{calc}, obtained as a function of UV-vis parameters (UV_{254}, UV_{280}, UV_{365} and $Color_{436}$, including oxidized data) by using Equation 4.43, Equation 4.45, Equation 4.47 and Equation 4.49 and DOC_{obs}, measured by TOC analyzer.

No	UV-vis parameter	Linear Equation	R^2
4.86	UV_{254}	DOC_{calc} (mg L^{-1}) = 0.847*DOC_{obs}(mg L^{-1}) – 1.084	0.956
4.87	UV_{280}	DOC_{calc} (mg L^{-1}) = 0.781*DOC_{obs}(mg L^{-1}) – 0.678	0.958
4.88	UV_{365}	DOC_{calc} (mg L^{-1}) = 0.345*DOC_{obs}(mg L^{-1}) + 3.336	0.958
4.89	$Color_{436}$	DOC_{calc} (mg L^{-1}) = 0.162*DOC_{obs}(mg L^{-1}) + 5.936	0949

To compare the Equations with each other, a sample was calculated by using them. Considering a humic acid sample expressing UV_{254}: 0.5000 cm^{-1}, UV_{280}: 0.4000 cm^{-1}, UV_{365}: 0.1000 cm^{-1} and $Color_{436}$: 0.0400 cm^{-1} DOC contents were calculated according to the respective equations (Equation 4.2, Equation 4.4, Equation 4.6 and Equation 4.8 for NHA (the non-treatment equations); Equation 4.43, Equation 4.45, Equation 4.47 and Equation 4.49 for the overall humic acids; Equation 4.70, Equation 4.71, Equation 4.72 and Equation 4.73 for NHA (the photocatalytic treatment equations) presented.

DOC concentration of the humic acid sample (the overall humic acids; Equation 4.43) as a function of UV_{254} parameter exhibited 86 % DOC concentration of the humic acid sample (the non-treatment Equation of NHA; Equation 4.2) as a function of UV_{254} parameter, whereas DOC concentration of humic acid sample (the non-treatment Equation of NHA; Equation 4.2) as a function of UV_{254} parameter displayed 85 % DOC concentration of humic acid sample (the photocatalytic treatment Equation of NHA;

Equation 4.70) as a function of UV_{254} parameter. DOC concentration of humic acid sample (the non-treatment Equation of the overall humic acid; Equation 4.45) as a function of UV_{280} parameter exhibited 86 % DOC concentration of humic acid sample (the non-treatment Equation of NHA; Equation 4) as a function of UV_{280} parameter, whereas DOC concentration of humic acid sample (the non-treatment Equation of NHA; Equation 4.4) displayed 83 % DOC concentration of humic acid sample (the photocatalytic treatment Equation of NHA; Equation 4.71) as a function of UV_{280} parameter.

Table 4.28. The dissolved organic carbon concentration, calculated related to the types of UV-vis parameter.

UV-vis parameter	UV_{254}, cm^{-1}	UV_{280}, cm^{-1}	UV_{365}, cm^{-1}	$Color_{436}$, cm^{-1}
	DOC (mg L^{-1})			
NHA (the photocatalytic treatment)	11.31	11.23	9.441	10.90
NHA (the non-treatment)	9.581	9.319	7.085	8.183
The overall HAs (NHA, FHA, AHA and RHA) (the non-treatment)	8.244	7.982	6.653	7.760

DOC concentration of humic acid sample (the non-treatment Equation of the overall humic acids; Equation 4.47) as a function of UV_{365} parameter displayed 94 % DOC concentration of humic acid sample (the non-treatment Equation of NHA; Equation 6) as a function of UV_{365} parameter while, DOC concentration of humic acid sample (the nontreatment Equation of NHA; Equation 4.6) exhibited 75 % DOC concentration of humic acid sample (the photocatalytic treatment Equation of NHA; Equation 4.72) as a function of UV_{365} parameter. DOC concentration of humic acid sample (the non-treatment Equation of the overall humic acid; Equation 4.49) as a function of $Color_{436}$ parameter, exhibited 95 % DOC concentration of humic acid sample (the non-treatment Equation of NHA; Equation 4.8) as a function of $Color_{436}$ parameter whereas, DOC concentration of humic acid sample (the non-treatment Equation of NHA; Equation 4.8) as a function of $Color_{436}$ parameter displayed 75 % DOC concentration of humic acid sample (the

photocatalytic treatment Equation of NHA; Equation 4.73) as a function of $Color_{436}$ parameter.

It could be inferred that DOC concentration results for the Equations, obtained from the determination without photocatalytic treatment, was lower than DOC concentration results for Equations, determined after the photocatalytic treatment, for each UV-vis parameters (UV_{254}, UV_{280}, UV_{365} and $Color_{436}$). Although, there was a decreasing trend for DOC concentration, NHA (photocatalytic treatment) > NHA (determination) > The Overall HAs (determination), DOC concentration results were closed to each other for UV-vis parameters (UV_{254}, UV_{280}, UV_{365} and $Color_{436}$) (Table 4.28).

4.3.2. Photocatalytic Treatment of AHA

AHA was prepared in 20 mg L^{-1} concentration and it was subjected to the photocatalytic degradation in the presence of 0.10, 0.25, and 1.00 mg mL^{-1} TiO_2. UV-vis parameters (UV_{254}, UV_{280}, UV_{365} and $Color_{436}$) and DOC concentrations of treated humic acid as a function of irradiation time during the oxidation process were presented (Table 4.29). UV-vis parameters (UV_{254}, UV_{280}, UV_{365} and $Color_{436}$) displayed a decreasing trend with respect to increasing wavelength (254-436 nm), for the photocatalytic degradation profiles of AHA.

While 40 % of UV_{254} removed in 10 minutes of irradiation, 70 % removal attained after 60 minutes in the presence of 0.1 mg mL^{-1} TiO_2. Similar to UV_{254}, $Color_{436}$ alterations demostrated declining pattern with 49 % and 83 % of $Color_{436}$ reduction after 10 minutes and 60 minutes of irradiation (Table 4.29). Moreover, DOC removal data were also determined to exhibit the expected declining profile with respect to UV-vis parameter. 65 % of DOC removal was obtained after 60 minutes of irradiation in the presence of 0.1 mg mL^{-1} TiO_2. On the other hand, with increasing of TiO_2 loading, the increase in removal rate of UV-vis parameter and DOC was observed. 59 % of UV_{254} removed in 10 minutes of irradiation, whereas 89 % removal attained after 60 minutes. Similar to UV_{254} parameter, UV_{280} parameter alterations demostrated declining pattern with 56 % and 91 % of UV_{280} reduction after 10 minutes and 60 minutes, in the presence of 0.25 mg mL^{-1} TiO_2. While 64 % of UV_{365} and 65 % of $Color_{436}$ removal was recorded at the end of short period experiments, 15 minutes. 95 % of UV_{365} and 96 % of $Color_{436}$ removal was attained by 60 minutes of irradiation, in the presence of 0.25 mg mL^{-1} TiO_2. 60 minutes of photocatalytic oxidation caused 83 % of DOC removal. 91 % of UV_{254} and UV_{280} removal was recorded at the end of short period experiments 10 minutes, 98 % of UV_{254} and UV_{280} elimination attained by 60 minutes of irradiation time in the presence of 1.00 mg mL^{-1} TiO_2. 60 minutes of photocatalytic oxidation caused 84 % of DOC removal from the initial AHA solutions (Table 4.29). A very important parameter influencing the performance of photocatalyst in photocatalytic oxidation is the surface morphology, namely the particle size and agglomerate size (Dinga et al., 2005).

Table 4.29. The removal of UV-vis parameters (UV_{254}, UV_{280}, UV_{365} and $Color_{436}$) and DOC depending on the irradiation time and photocatalyst loading (AHA, 20 mg L^{-1}) (İlgün, 2010).

	UV-vis parameters (cm^{-1}) and DOC (mg L^{-1})				
Photocatalyst loading: 0.10 mg mL^{-1} TiO_2					
Irr. Time, min	UV_{254}	UV_{280}	UV_{365}	$Color_{436}$	DOC
0	0.2730	0.2330	0.0950	0.0430	3.460
10	0.2650	0.2270	0.0900	0.0400	3.440
20	0.2590	0.2150	0.0840	0.0380	3.420
30	0.1920	0.1570	0.0570	0.0240	3.230
40	0.1760	0.1430	0.0490	0.0210	3.140
60	0.1320	0.1040	0.0320	0.0130	2.810
RAW	0.4420	0.3800	0.1630	0.0780	6.210
	UV-vis parameters (cm^{-1}) and DOC (mg L^{-1})				
Photocatalyst loading: 0.25 mg mL^{-1} TiO_2					
Irr. Time, min	UV_{254}	UV_{280}	UV_{365}	$Color_{436}$	DOC
0	0.2190	0.1910	0.0750	0.0330	2.743
10	0.1820	0.1670	0.0590	0.0270	2.393
20	0.1450	0.1160	0.0400	0.0160	2.117
30	0.1130	0.0920	0.0270	0.0120	2.108
40	0.0950	0.0750	0.0230	0.0080	1.494
60	0.0490	0.0350	0.0080	0.0030	1.044
RAW	0.4420	0.3800	0.1630	0.0780	6.210
	UV-vis parameters (cm^{-1}) and DOC (mg L^{-1})				
Photocatalyst loading: 1.00 mg mL^{-1} TiO_2					
Irr. Time, min	UV_{254}	UV_{280}	UV_{365}	$Color_{436}$	DOC
0	0.0500	0.0420	0.0120	0.0050	1.450
10	0.0400	0.0350	0.0090	0.0030	1.400
20	0.0370	0.0280	0.0060	0.0020	1.370
30	0.0280	0.0210	0.0030	0.0010	1.200
40	0.0140	0.0090	0.0020	0.0000	1.150
60	0.0090	0.0060	0.0010	0.0000	0.980
RAW	0.4420	0.3800	0.1630	0.0780	6.210

Numerous forms of TiO_2 have been synthesized by different methods to arrive at a photocatalyst exhibiting desirable physical properties, activity and stability for photocatalytic application (Gao and Matter, 2005). Evidently, there is a clear connection

between the surface properties, the rational development of improved synthesis routes and the possible usefulness of the material prepared in application (Diebold, 2003; Mohammadi, 2006). For instance, smaller nano-particle size is reported to give higher conversion in gaseous phase photomineralisation of organic compounds over nano-sized titanium dioxide (Maira et al., 2001). The rate of photocatalytic reaction is strongly influenced by concentration of the photocatalyst. Heterogeneous photocatalytic reactions are known to show proportional increase in photodegradation with catalyst loading (Krỳsa et al., 2004). Generally, in any given photocatalytic application, the optimum catalyst concentration must be determined, in order to avoid excess catalyst and ensure total absorption of efficient photons (Saquib and Muneer, 2003). This is because an unfavourable light scattering and reduction of light penetration into the solution is observed with excess photocatalyst loading (Chun et al., 2000). 20 mg L^{-1} of AHA was subjected to photocatalyic degradation in the presence of 0.10, 0.25 and 1.00 mg mL^{-1} TiO_2. 20 mg L^{-1} of AHA exhibited 55 % DOC removal in the presence of 0.10 mg mL^{-1} while 20 mg L^{-1} of AHA displayed 84 % DOC removal in the presence of 1.00 mg mL^{-1}. 20 mg L^{-1} of AHA exhibited 70 % UV_{254} removal in the presence of 0.10 mg mL^{-1} TiO_2, while 20 mg L^{-1} of AHA displayed 98 % UV_{254} removal in the presence of 1.00 mg mL^{-1} TiO_2.

Table 4.31 represents DOC_{calc} results, as a function of UV_{254}, UV_{280}, UV_{365} and $Color_{436}$ parameter, depending on the adsorption and the irradiation period. DOC_{calc}, obtained as a function of UV_{254} parameter (Table 4.29), exhibited 75 %, 94 % and 100 % removal after the irradiation time of 60 minutes in the presence of 0.10 mg mL^{-1} TiO_2, 0.25 mg mL^{-1} TiO_2, and 1.00 mg mL^{-1} TiO_2, respectively. DOC_{calc}, obtained as a function of UV_{280} parameter (Table 4.29), exhibited 79 %, 99 % and 100 % removal after the irradiation time of 60 minutes in the presence of 0.10 mg mL^{-1} TiO_2, 0.25 mg mL^{-1} TiO_2, and 1.00 mg mL^{-1} TiO_2, respectively. DOC_{calc}, obtained as a function of UV_{365} parameter (Table 4.29), exhibited 84 %, 100 % and 100 % removal after the irradiation time of 60 minutes in the presence of 0.10 mg mL^{-1} TiO_2, 0.25 mg mL^{-1} TiO_2, and 1.00 mg mL^{-1} TiO_2, respectively. DOC_{calc}, obtained as a function of $Color_{436}$ parameter (Table 4.29), exhibited % removal after the irradiation time of 60 minutes in the presence of 0.10 mg mL^{-1} TiO_2, 0.25 mg mL^{-1} TiO_2, and 1.00 mg mL^{-1} TiO_2, respectively. .

Table 4.30. The dissolved organic carbon concentration, calculated related to the types of UV-vis parameters by using Equation 4.20, 4.22, 4.24 and 4.26 (UV_{254}, UV_{280}, UV_{365} and $Color_{436}$) (AHA, 20 mg L^{-1}).

20 mg L^{-1}	UV_{254}	UV_{280}	UV_{365}	$Color_{436}$
Photocatalyst loading: 0.1 mg mL^{-1} TiO_2				
Irr. Time, min	DOC_{calc}, mg L^{-1}			
0	3.969	4.301	2.551	5.408
10	3.841	4.173	2.406	5.289
20	3.744	3.917	2.231	5.209
30	2.668	2.682	1.447	4.653
40	2.411	2.384	1.214	4.534
60	1.705	1.554	0.721	4.216
RAW	6.683	7.431	4.526	6.798
	UV_{254}	UV_{280}	UV_{365}	$Color_{436}$
Photocatalyst loading: 0.25 mg mL^{-1} TiO_2				
Irr. Time, min	DOC_{calc}, mg L^{-1}			
0	3.102	3.406	1.970	5.011
10	2.508	2.895	1.505	4.772
20	1.914	1.809	0.953	4.336
30	1.400	1.298	0.575	4.177
40	1.111	0.936	0.459	4.018
60	0.372	0.084	0.023	3.819
RAW	6.683	7.431	4.526	6.798
	UV_{254}	UV_{280}	UV_{365}	$Color_{436}$
Photocatalyst loading: 1.00 mg mL^{-1} TiO_2				
Irr. Time, min	DOC_{calc}, mg L^{-1}			
0	0.3880	0.2334	0.1396	3.899
10	0.2274	0.0843	0.0525	3.819
20	0.1792	0.000	0.000	3.779
30	0.0347	0.000	0.000	3.740
40	0.000	0.000	0.000	3.700
60	0.000	0.000	0.000	3.700
RAW	6.683	7.431	4.526	6.798

Moreover, UV_{280} parameter exhibited 61 %, 76 %, 83 %, and 88 % removal, in the presence of 0.25 mg mL^{-1} TiO_2 after the irradiation time of 10, 20, 30 and 40 minutes, respectively. UV_{365} parameter displayed 67 %, 79 %, 87 % and 90 % removal in the presence of 0.25 mg mL^{-1} TiO_2, after the irradiation time of 10, 20, 30 and 40 minutes, respectively.

DOC_{calc} (Table 4.30), related to Equation 4.20 as a function of UV_{254} parameter, including the non-oxidative data prior to the photocatalytic treatment and the oxidative data after each irradiation time of the photocatalytic treatment, was presented in Figure 4.50. The photocatalytic treatment was applied for 60 minutes. '0' irradiation time represents initial DOC_{calc} concentration in Table 4.30 (Figure 4.50). '0.1' presentation was selected to signify t=0 condition. DOC_{calc}, dependent on the initial concentration, increased as expected at time '0'. At=0.1, adsorption effect was examined in DOC_{calc}, dependent on the initial concentration of AHA with irrespective to time. At the end of adsorption period, 41 %, 55 % and 94 % removal displayed increasing trend in the presence of 0.10, 0.25, and 1.00 mg mL^{-1} TiO_2, respectively for 20 mg L^{-1} of AHA.

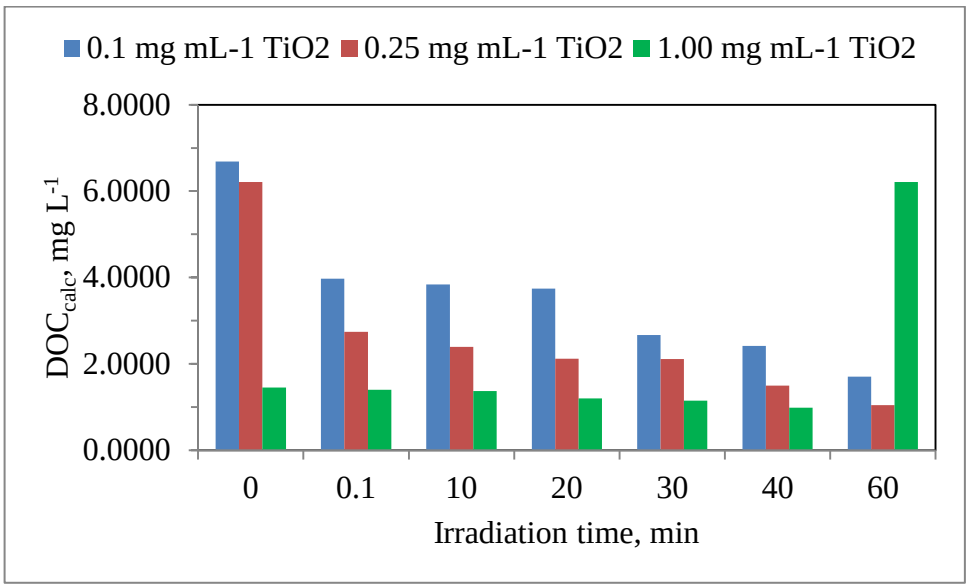

Figure 4.50. DOC_{calc} concentration, obtained by using Equation 4.20 as a function of UV_{254} parameter, according to irradiation time for AHA.

Dependent upon irradiation time of 10 minutes, DOC_{calc} values exhibited a consistent increasing trend with respect to increasing TiO_2 catalyst loading. Moreover, the irradiation time of 30 minutes, 65 %, 79 % and 97 % removal exhibited decreasing trend in DOC_{calc} in the presence of 0.10, 0.25 and 1.00 mg mL^{-1} TiO_2, respectively. After the irradiation time of 60 minutes, 74 %, 94 % and 100 % removal exhibited increasing trend in DOC_{calc} in the presence of 0.10, 0.25 and 1.00 mg mL^{-1} TiO_2, respectively.

DOC_{calc}, related to Equation 4.26 as a function of $Color_{436}$ parameter, including the non-oxidative data prior to the photocatalytic treatment and the oxidative data for each irradiation time of the photocatalytic treatment in the presence of 0.10, 0.25 and 1.00 mg mL^{-1} TiO_2, was presented in Figure 4.51. At the adsorption period (t=0.1), 22 %, 26 % and 43 % removal displayed increasing trend in DOC_{calc} in the presence of 0.10, 0.25 and 1.00 mg mL^{-1} of TiO_2, respectively. Furthermore, after the irradiation time of 30 minutes, 32 %, 36 %, and 45 % removal displayed increasing trend in DOC_{calc} dependent upon TiO_2 catalyst loading, in the presence of 0.10, 0.25 and 1.00 mg mL^{-1} TiO_2, respectively. After the irradiation time of 60 minutes, 38 %, 44 % and 46 % removal exhibited increasing trend in DOC_{calc}, depending on increasing of TiO_2 catalyst loading.

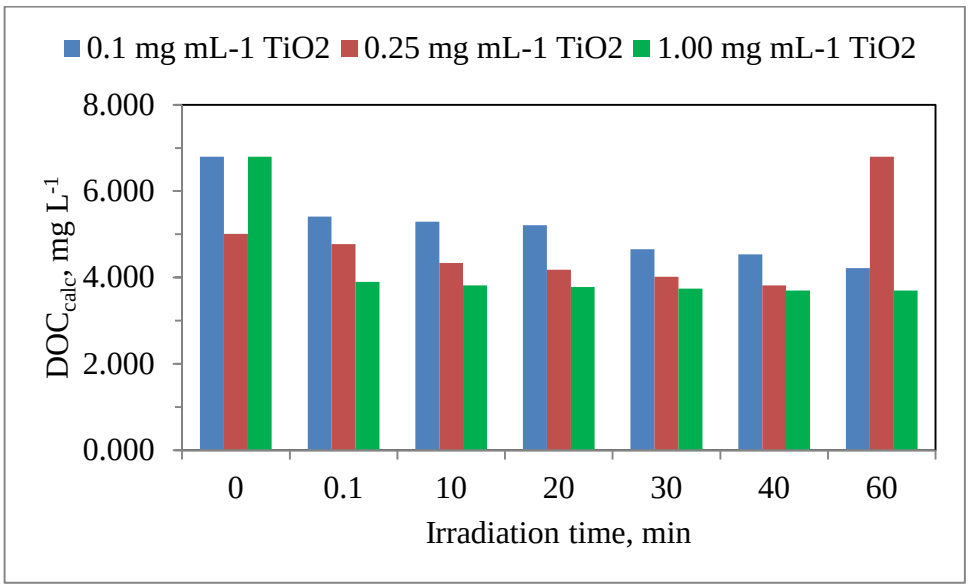

Figure 4.51. DOC_{calc} concentration, obtained by using Equation 4.26 as a function of $Color_{436}$ parameter, according to irradiation time for AHA.

Table 4.31 represents DOC_{calc} results, as a function of UV_{254}, UV_{280}, UV_{365} and $Color_{436}$ parameter, depending on the adsorption and the irradiation period. DOC_{calc}, obtained as a function of UV_{254} parameter (Table 4.29), exhibited 59 %, 74 % and 82 % removal after the irradiation time of 60 minutes in the presence of 0.10 mg mL^{-1} TiO_2, 0.25 mg mL^{-1} TiO_2, and 1.00 mg mL^{-1} TiO_2, respectively.

Table 4.31. The dissolved organic carbon concentration, calculated related to the types of UV-vis parameters by using Equation 4.43, 4.45, 4.47 and 4.49 (UV_{254}, UV_{280}, UV_{365} and $Color_{436}$) (AHA, 20 mg L^{-1}).(The Overall Humic Acids).

	UV_{254}	UV_{280}	UV_{365}	$Color_{436}$
Photocatalyst loading: 0.1 mg mL^{-1} TiO_2				
Irr. Time, min	DOC_{calc}, mg L^{-1}			
0	5.053	5.303	6.542	7.857
10	4.940	5.206	6.431	7.761
20	4.856	5.014	6.298	7.696
30	3.914	4.082	5.698	7.246
40	3.689	3.857	5.520	7.149
60	3.071	3.230	5.142	6.892
RAW	7.429	7.665	8.053	8.983
	UV_{254}	UV_{280}	UV_{365}	$Color_{436}$
Photocatalyst loading: 0.25 mg mL^{-1} TiO_2				
Irr .Time, min	DOC_{calc}, mg L^{-1}			
0	4.294	4.628	6.098	7.535
10	3.774	4.242	5.742	7.342
20	3.253	3.423	5.320	6.989
30	2.804	3.037	5.031	6.860
40	2.551	2.764	4.942	6.731
60	1.904	2.121	4.609	6.570
RAW	7.429	7.665	8.053	8.983
	UV_{254}	UV_{280}	UV_{365}	$Color_{436}$
Photocatalyst loading: 1.00 mg mL^{-1} TiO_2				
Irr. Time, min	DOC_{calc}, mg L^{-1}			
0	1.918	2.234	4.698	6.635
10	1.777	2.121	4.631	6.570
20	1.735	2.009	4.564	6.538
30	1.609	1.896	4.498	6.506
40	1.412	1.704	4.475	6.474
60	1.342	1.655	4.453	6.474
RAW	7.429	7.665	8.053	8.983

DOC_{calc}, obtained as a function of UV_{280} parameter (Table 4.29), exhibited 58 %, 72 %, and 78 % removal after the irradiation time of 60 minutes in the presence of 0.10 mg mL^{-1} TiO_2, 0.25 mg mL^{-1} TiO_2, and 1.00 mg mL^{-1} TiO_2, respectively (Table 4.31). DOC_{calc}, obtained as a function of UV_{365} parameter (Table 4.29), exhibited 36 %, 43 % and

45 % removal after the irradiation time of 60 minutes in the presence of 0.10 mg mL^{-1} TiO_2, 0.25 mg mL^{-1} TiO_2, and 1.00 mg mL^{-1} TiO_2, respectively. DOC_{calc}, obtained as a function of $Color_{436}$ parameter (Table 4.29), exhibited 23 %, 27 % and 28 % removal after the irradiation time of 60 minutes in the presence of 0.10 mg mL^{-1} TiO_2, 0.25 mg mL^{-1} TiO_2, and 1.00 mg mL^{-1} TiO_2, respectively. Moreover, UV_{280} parameter exhibited 45 %, 55 %, 60 % and 72 % removal, in the presence of 0.25 mg mL^{-1} TiO_2 after the irradiation time of 10, 20, 30, and 40 minutes, respectively. UV_{365} parameter displayed 29 %, 34 %, 38 % and 39 % and removal in the presence of 0.25 mg mL^{-1} TiO_2, after the irradiation time of 10, 20, 30 and 40 minutes, respectively.

DOC_{calc} (Table 4.31), related to Equation 4.43 as a function of UV_{254} parameter, including the non-oxidative data prior to the photocatalytic treatment and the oxidative data after irradiation time of the photocatalytic treatment in the presence of 0.10, 0.25 and 1.00 mg mL^{-1} TiO_2, was presented in Figure 4.52. At the end of adsorption period of AHA, 32 %, 42 % and 74 % removal displayed increase in DOC_{calc}, dependent on TiO_2 loading with respect to time '0'.

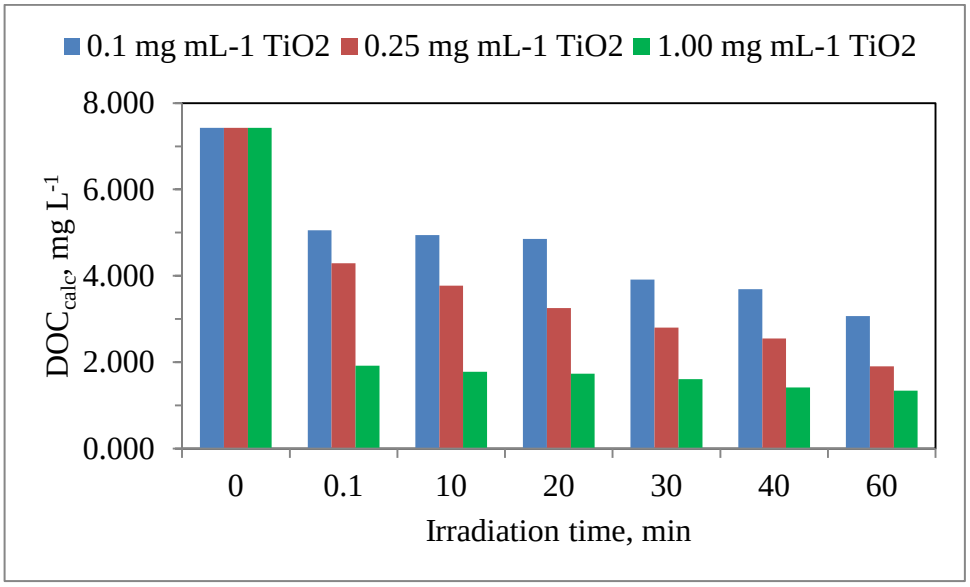

Figure 4.52. DOC_{calc} concentration, obtained by using Equation 4.43 for UV_{254} parameter, as a function of irradiation time for AHA.

Dependent upon irradiation time of 10 minutes, DOC_{calc} values exhibited consistent increasing trend with respect to increasing of TiO_2 loading. After the irradiation time of 30 minutes, 47 %, 62 % and 78 % removal displayed increasing trend in DOC_{calc}, dependent on the increase in TiO_2 loading. After the irradiation of 60 minutes, 59 %, 74 % and 84 % removal exhibited increasing trend in DOC_{calc}, in the presence 0.10, 0.25, and 1.00 mg mL^{-1} TiO_2. DOC_{calc} (Table 4.31), related to Equation 4.49 as a function of $Color_{436}$ parameter, consisting of the non-oxidative data prior to the photocatalytic treatment, and the oxidative data after the photocatalytic treatment, in the presence of 0.10, 0.25 and 1.00 mg mL^{-1} TiO_2, was presented in Figure 4.52.

At the end of adsorption period, 13 %, 16 % and 26 % removal displayed increasing trend in DOC_{calc}, dependent on the TiO_2 loading with respect to '0' (Figure 4.53). Dependent upon irradiation time of 15 minutes, DOC_{calc} values exhibited consistent increasing trend for AHA concentration. After the irradiation time of 30 minutes, 19 %, 24 % and 28 % removal exhibited increasing trend in DOC_{calc}, in the presence of 0.10, 0.25 and 1.00 mg mL^{-1} TiO_2.

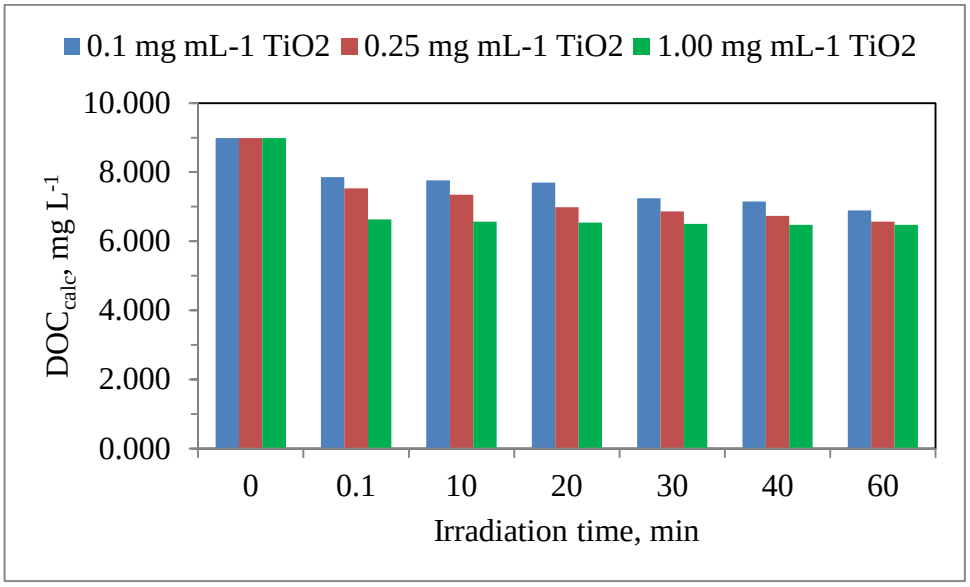

Figure 4.53. DOC_{calc}, obtained by using Equation 4.49, as a function of $Color_{436}$ parameter according to irradiation time for AHA.

As mentioned above, after the irradiation time of 60 minutes, 23 %, 27 % and 28 % removal exhibited increasing trend in DOC_{calc}, with the increase in TiO_2 loading. The removal of DOC concentrations of AHA were correlated with UV-vis parameters (UV_{254}, UV_{280}, UV_{365} and $Color_{436}$) of the remained HA after the photocatalytic treatment. As mentioned above, the degradation of humic acid was completed in 60 minutes (Figure 4.53).

At the end of each irradiation period (15, 30, 45 and 60 minutes), reported above, DOC and UV-vis parameter results (Table 4.29) were used in graphs below for 0.10, 0.25, 1.00 mg mL^{-1} TiO_2. As a result, the relationship between DOC and UV-vis parameters (UV_{254}, UV_{280}, UV_{365} and $Color_{436}$) were examined during the photocatalytic treatment.

4.3.2.1. The Relationship between UV-vis Parameters and DOC Concentration, Including the Non-oxidative Data before the Photocatalytic Treatment and the Oxidative Data after each Irradiation Period of Photocatalytic Treatment for AHA. According to Table 4.29, correlations between peak area, measured at 254, 280, 365, and 436 nm, dissolved organic carbon (DOC) content were made from a standard curve constructed by measuring the DOC of AHA solution (20 mg L^{-1}), treated by the photocatalytic treatment in the presence of 0.10, 0.25, and 1.00 mg mL^{-1} TiO_2.

Figure 4.54 represented the correlation between UV-vis parameters (UV_{254}, UV_{280}, UV_{365} and $Color_{436}$ parameter) and DOC concentration of AHA, including the oxidative data for each irradiation period of the photocatalytic treatment and the non-oxidative data before the photocatalytic treatment in the presence of 0.10 mg mL^{-1} TiO_2. The correlation Equation 4.90, Equation 4.91, Equation 4.92 and Equation 4.93 exhibited high regression coefficients for UV-vis parameters (UV_{254}, R^2= 0.875, UV_{280}, R^2= 0.866, UV_{365}, R^2= 0.860, and $Color_{436}$, R^2= 0.877)

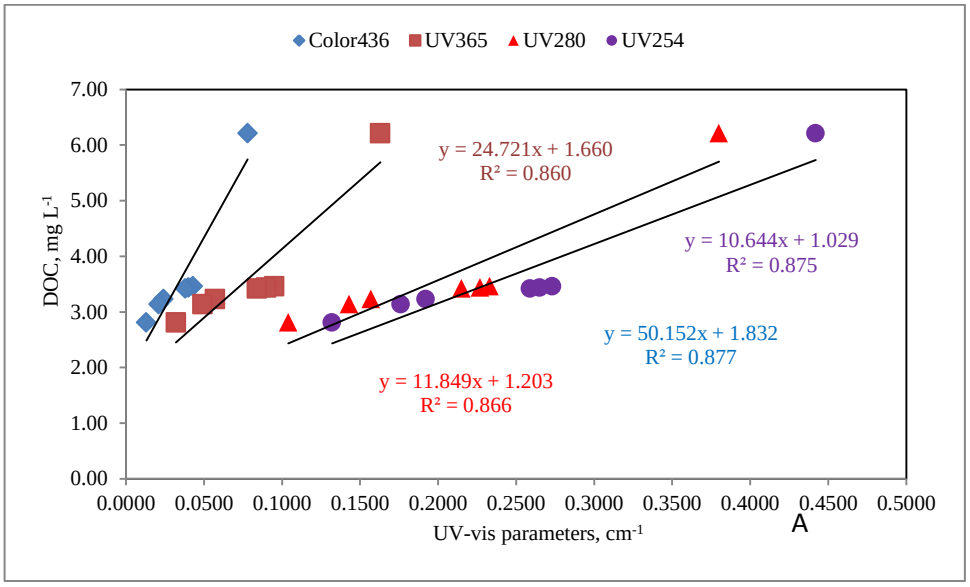

Figure 4.54. The correlation between UV-vis parameters (UV_{254}, UV_{280}, UV_{365} and $Color_{436}$) and DOC concentration , including the oxidative data for each irradiation period of the photocatalytic treatment and the non-oxidative data before the photocatalytic treatment (20 mg L^{-1} of AHA, A) TiO_2: 0.10 mg mL^{-1}).

Figure 4.55 represented the correlation between UV-vis parameters (UV_{254}, UV_{280}, UV_{365} and $Color_{436}$ parameter) and DOC concentration of AHA, including the oxidative data for each irradiation period of the photocatalytic treatment and the non-oxidative data before the photocatalytic treatment in the presence of 0.25 and 1.00 mg mL^{-1} TiO_2. The correlation Equation 4.94, Equation 4.95, Equation 4.96 and Equation 4.97 exhibited high regression coefficients for UV-vis parameters (UV_{254}, R^2=0.977, UV_{280}, R^2= 0.964, UV_{365}, R^2= 0.969, and $Color_{436}$, R^2= 0.975). The correlation Equation 4.98, Equation 4.99, Equation 4.100 and Equation 4.101 exhibited high regression coefficients for UV-vis parameters (UV_{254}, R^2= 0.999, UV_{280}, R^2= 0.999, UV_{365}, R^2= 0.999, and $Color_{436}$, R^2= 0.998).

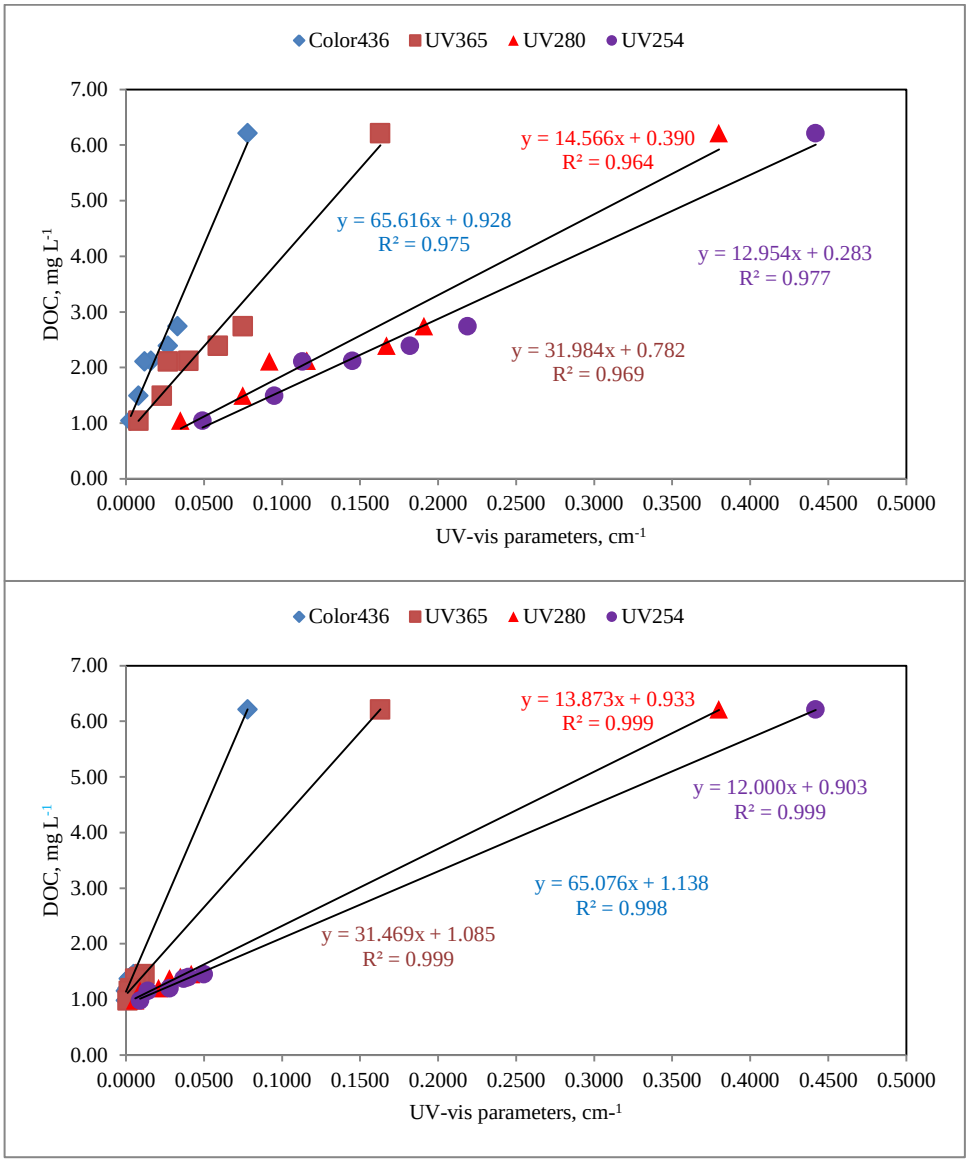

Figure 4.55. The correlation between UV-vis parameters (UV_{254}, UV_{280}, UV_{365} and $Color_{436}$) and DOC concentration , including the oxidative data for each irradiation period of the photocatalytic treatment and the non-oxidative data before the photocatalytic treatment (20 mg L^{-1} of AHA, A) TiO_2: 0.25 mg mL^{-1}, 1.00 mg mL^{-1}).

In this study, the relationship between the removal of UV_{254} parameter and DOC concentration was examined. The Equations, obtained from the correlation between the removal of DOC concentration and the removal of UV-vis parameter (UV_{254}, UV_{280}, UV_{365} and $Color_{436}$) after the photocatalytic treatment, were listed in Table 4.32.

Table 4.32. The correlation equation, obtained from the correlation between UV-vis parameters and DOC concentration, including the non-oxidative before the photocatalytic treatment and the oxidative data during the photocatalytic treatment in the presence of 0.10, 0.25, 1.00 mg mL^{-1} TiO_2, for AHA, and the regression coefficients of these correlation equations.

Equation No	Correlation Equation	R^2
Photocatalyst loading: 0.10 mg mL^{-1} TiO_2		
4.90	DOC (mg L^{-1}) = 10.64*UV_{254} (cm^{-1}) + 1.03	0.875
4.91	DOC (mg L^{-1}) = 11.85*UV_{280} (cm^{-1}) + 1.203	0.699
4.92	DOC (mg L^{-1}) = 24.72*UV_{365} (cm^{-1}) + 1.66	0.860
4.93	DOC (mg L^{-1}) = 50.15*$Color_{436}$ (cm^{-1}) + 1.83	0.877
Photocatalyst loading: 0.25 mg mL^{-1} TiO_2		
4.94	DOC (mg L^{-1}) = 12.95* UV_{254} (cm^{-1}) + 0.283	0.977
4.95	DOC (mg L^{-1}) = 14.57*UV_{280} (cm^{-1}) + 0.390	0.964
4.96	DOC (mg L^{-1}) = 31.98*UV_{365} (cm^{-1}) + 0.782	0.969
4.97	DOC (mg L^{-1}) = 65.62*$Color_{436}$ (cm^{-1}) + 0.928	0.975
Photocatalyst loading: 1.00 mg mL^{-1} TiO_2		
4.98	DOC (mg L^{-1}) = 12.00*UV_{254} (cm^{-1}) + 0.903	0.999
4.99	DOC (mg L^{-1}) = 13.87*UV_{280} (cm^{-1}) + 0.933	0.999
4.100	DOC (mg L^{-1}) = 31.47*UV_{365} (cm^{-1}) + 1.09	0.999
4.101	DOC (mg L^{-1}) = 65.08* $Color_{436}$ (cm^{-1}) + 1.14	0.998

As seen in Figure 4.54, it could be inferred that the removal of UV_{254} parameter was good indicator of the removal of DOC concentration in humic acid sample (R^2=0.875). As seen in Table 4.32, the removal of UV_{254} parameter was good indicator of the removal of DOC concentration (R^2> 0.875). In addition to UV_{254} parameter. The removal of UV_{280}, UV_{365} and $Color_{436}$ parameter were good indicator of the removal of DOC concentration(R^2>0.699, UV_{280}; R^2>0.860,UV_{365}; R^2>0.877, $Color_{436}$). The equations (Equation 4.90, Equation 4.94, Equation 4.98), obtained from the graph (Figure 4.54), were compared with each other. Equation 4.90 (0.10 mg mL^{-1} TiO_2), Equation 4.94 (0.25 mg mL^{-1} TiO_2) (Figure 4.55) and Equation 4.98 (1.00 mg m L^{-1} TiO_2) obtained from the

correlation between the removal of UV_{254} parameter, representing the removal of aromatic moieties, and the removal of DOC concentration was closed to each other in the same sample. As mentioned before, the regression coefficient of Equation 4.90, Equation 4.94 and Equation 4.98 were more than $R^2 > 0.875$.

After the photocatalytic treatment, there was enough aromatic moieties that could absorb the UV_{254} parameter and there was enough DOC concentration that could be oxidized in TOC analyzer in humic acid sample. In addition to the removal of UV_{254} parameter and DOC concentration, the removal of UV_{280}, UV_{365} and $Color_{436}$ parameter were examined in the presence of TiO_2 (Figure 4.54 and Figure 4.55). The removal of UV_{280} parameter, representing the removal of total aromaticity, was good indicator of the removal of DOC concentration ($R^2 = 0.866$), the removal of UV_{365} parameter was good indicator of the removal of DOC concentration ($R^2 = 0.860$), and the removal of $Color_{436}$ parameter, representing the removal color forming moieties, was good indicator of the removal of DOC concentration ($R^2 = 0.877$) in the presence of 0.10 mg mL^{-1} TiO_2. Similar to UV_{254} parameter, after the photocatalytic treatment, there was enough moieties that could absorb the UV_{280}, UV_{365} and $Color_{436}$ parameter and there was enough DOC concentration that could be oxidized in DOC analyzer (Equation 4.91- Equation 4.101). The regression coefficient increased with the increasing catalyst loading. According to the results, DOC_{obs}-DOC_{calc} Equation was drawn as a graph. The correlation were drawn in two different way. One way, is the correlation between DOC_{obs} and DOC_{calc} that were calculated according to the irradiation time. Another way, in addition to the irradiation time, the correlation between DOC_{obs} and DOC_{calc} that were calculated according to the initial DOC_{calc} and DOC_{obs} of AHA.

4.3.2.2. The Relationship between Initial and Oxidized DOC_{obs} Concentration and DOC_{calc} Concentration of AHA depending on the Non-treatment Equations of AHA. DOC_{obs} concentration of AHA, represented the degradation depending on the irradiation time in Table 4.29, were correlated with DOC_{calc} concentrations (Table 4.30) that was calculated by using Equation 4.20, Equation 4.22, Equation 4.24, and Equation 4.26 depending on DOC concentrations of AHA related to the irradiation time in Figure 4.56 and Figure 4.57.

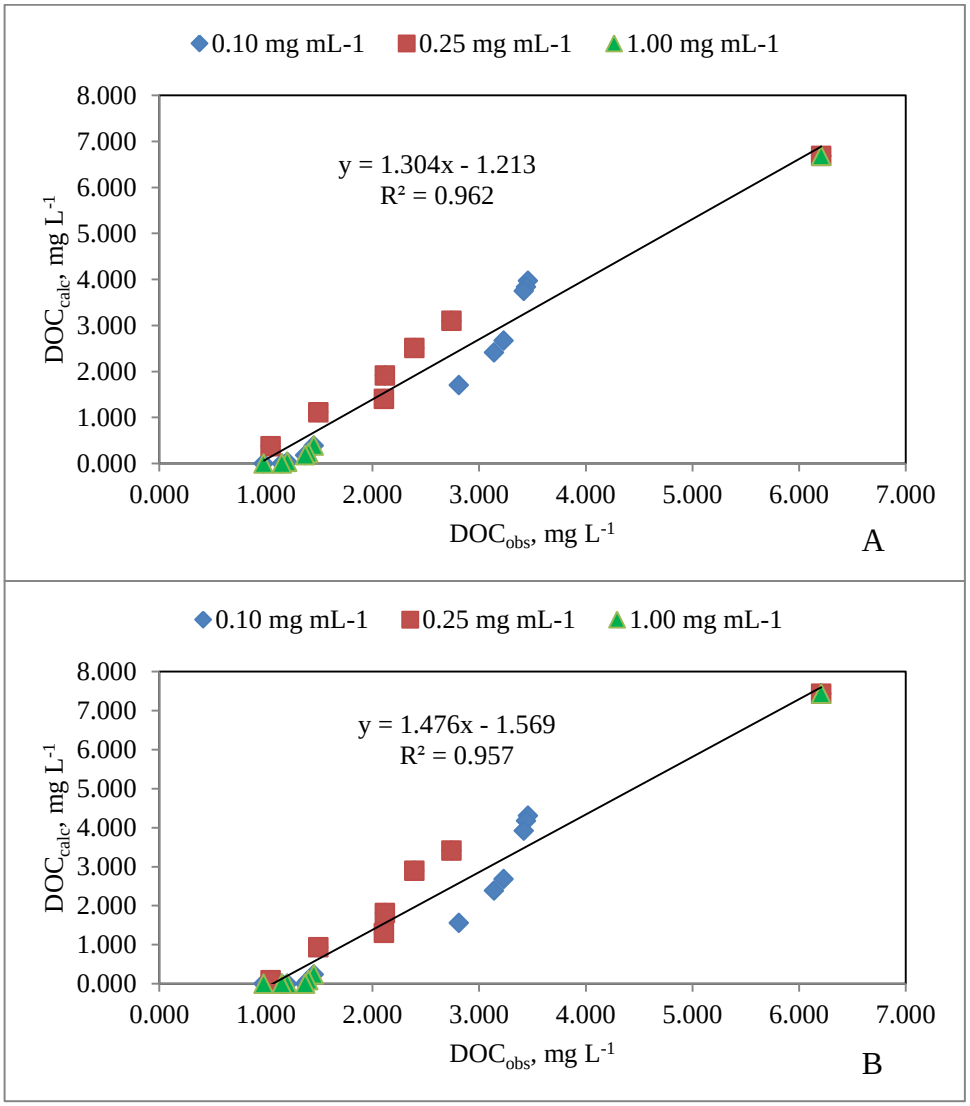

Figure 4.56. The correlation between DOC_{obs}, measured by TOC analyzer, and DOC_{calc} obtained by using Equation 4.20 as a function of UV_{254} parameter and Equation 4.22 as a function of UV_{280} parameter, including the non-oxidative data before the photocatalytic treatment and the oxidative data after each irradiation time of the photocatalytic treatment of AHA. ((A) UV_{254}, (B) UV_{280}).

The correlation between DOC_{obs}, measured by TOC analyzer, and DOC_{calc} obtained by using Equation 4.20 as a function of UV_{254} parameter and Equation 4.22 as a function of UV_{280} parameter, including the non-oxidative data before the photocatalytic treatment and the oxidative data after each irradiation time of the photocatalytic treatment of AHA was presented in Figure 4.56.

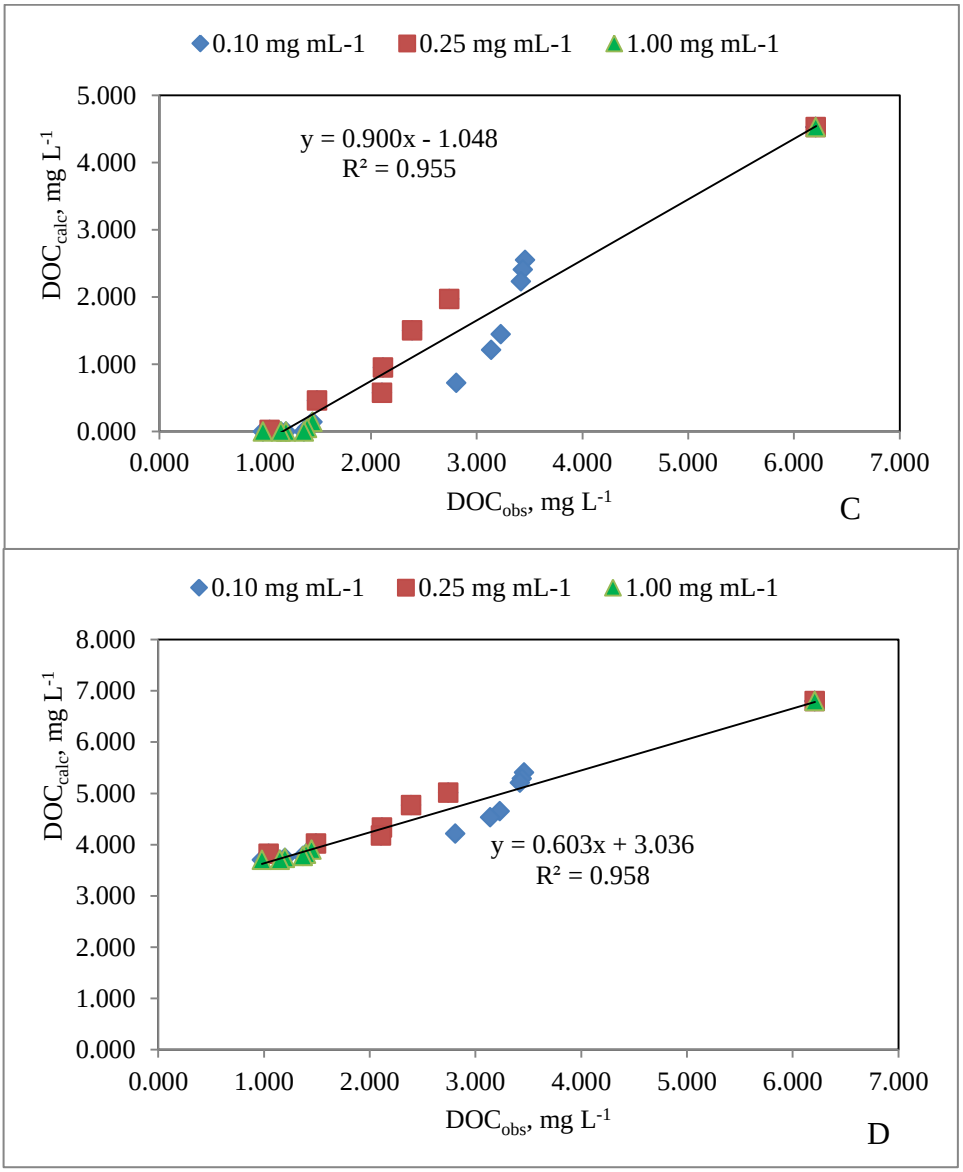

Figure 4.57. The correlation between DOC_{obs}, measured by TOC analyzer, and DOC_{calc} obtained by using Equation 4.24 as a function of UV_{365} parameter and Equation 4.26 as a function of $Color_{436}$ parameter, including the nonoxidative data before the photocatalytic treatment and the oxidative data after each irradiation period of photocatalytic treatment of AHA.((C) UV_{365}, (D) $Color_{436}$).

The correlation between DOC_{obs}, measured by TOC analyzer, and DOC_{calc} obtained by using Equation 4.24 as a function of UV_{365} parameter and Equation 4.26 as a function of $Color_{436}$ parameter, including the non-oxidative data before the photocatalytic treatment and the oxidative data after each irradiation period of photocatalytic treatment of AHA was presented in Figure 4.57. In other words, Figure 4.56 and 4.57 illustrated the linear

correlation between DOC_{obs} concentrations and DOC_{calc} concentrations. DOC_{calc}-DOC_{obs} equation was produced from the least-squares regression analyses (Equation 4.102, Equation 4.103, Equation 4.104 and Equation 4.105). The regression coefficient was found to be as R^2= 0.962 (UV_{254}), R^2= 0.957 (UV_{280}), R^2= 0.955 (UV_{365}) and R^2= 0.958 ($Color_{436}$). As seen in Figure 4.56 and 4.57, the decrease in UV_{254} parameter, UV_{280} parameter, UV_{365} parameter and $Color_{436}$ parameter were observed after the irradiation time of photocatalytic treatment.UV_{254} parameter, UV_{280} parameter and UV_{365} parameter of the remained of AHA, representing aromatic moieties, exhibited enough carbon content according to the nontreatment Equations (Equation 4.20, Equation 4.22, Equation 4.24 and Equation 4.26) that DOC_{calc} exhibited good prediction of the dissolved organic carbon content (DOC_{obs}) in AHA, measured by TOC analyzer. As a result, DOC content in AHA could be determined by using the non-treatment Equations (Equation 4.20, Equation 4.22, Equation 4.24 and Equation 4.26) as a function of UV_{254}, UV_{280}, UV_{365} and $Color_{436}$ parameter of the remained AHA after the irradiation time instead of using TOC analyzer.

Table 4.33. The relationship between DOC_{calc}, obtained as a function of UV-vis parameters (UV_{254}, UV_{280}, UV_{365} and $Color_{436}$, including initial and oxidized data) by using Equation 4.20, Equation 4.22, Equation 4.24 and Equation 4.26 and DOC_{obs}, measured by TOC analyzer.

AHA Photocatalytic treatment			
No	UV-vis parameter	Correlation Equation	R^2
4.102	UV_{254}	DOC_{calc} (mg L^{-1}) = 1.304*DOC_{obs} (mg L^{-1}) – 1.213	0.962
4.103	UV_{280}	DOC_{calc} (mg L^{-1}) = 1.476*DOC_{obs} (mg L^{-1}) – 1.569	0.957
4.104	UV_{365}	DOC_{calc} (mg L^{-1}) = 0.900*DOC_{obs} (mg L^{-1}) – 1.048	0.955
4.105	$Color_{436}$	DOC_{calc}(mg L^{-1}) = 0.603 *DOC_{obs} (mg L^{-1}) + 3.036	0.958

According to the nontreatment Equations (Equation 4.20, Equation 4.22, Equation 4.24 and Equation 4.26) DOC_{calc} obtained as a function of UV_{254} parameter, UV_{280} parameter, UV_{365} parameter and $Color_{436}$ parameter of the remained AHA, after the

irradiation time was found to be closed to DOC_{obs}, including oxidized and initial values with the high regression coefficient (Equation 4.102), (Equation 4.103), (Equation 4.104) and (Equation 4.105) (Table 4.33).

4.3.2.3. The Relationship between Oxidized DOC_{obs} Concentration and DOC_{calc} Concentration of AHA dependent on the Non-treatment Equations of AHA. DOC_{obs} concentration of AHA, representing the degradation depending on the irradiation time in Table 4.29, were correlated with DOC_{calc} concentrations that was calculated as a function of UV_{254} by using Equation 4.20. DOC_{obs} (Table 4.29) was correlated with DOC_{calc} as a function of UV_{280} parameters by using Equation 4.22, UV_{365} parameter by using Equation 4.24, and $Color_{436}$ parameter by using Equation 4.26 depending on DOC concentrations of AHA, related to the irradiation time (10, 20, 30, 40, and 60 minutes) in Table 4.31 (Figure 4.58 and 4.59).

Figure 4.58 presented the correlation between DOC_{obs}, measured by TOC analyzer, and DOC_{calc}, obtained by using Equation 4.20 as a function of UV_{254} parameter and Equation 4.22 as a function of UV_{280} parameter, including the oxidative data after each irradiation time of the photocatalytic treatment of AHA. Figure 4.59 represented the correlation between DOC_{obs}, measured by TOC analyzer, and DOC_{calc} obtained by using Equation 4.24 as a function of UV_{365} parameter and Equation 4.26 as a function of $Color_{436}$ parameter, including the oxidative data after each irradiation time of the photocatalytic treatment of AHA. Figure 4.58 and 4.59 illustrated the linear correlation between DOC_{obs} concentrations, obtained by using TOC analyzer, and DOC_{calc} concentrations, as function of UV_{254}, UV_{280}, UV_{365} and $Color_{436}$ parameter.

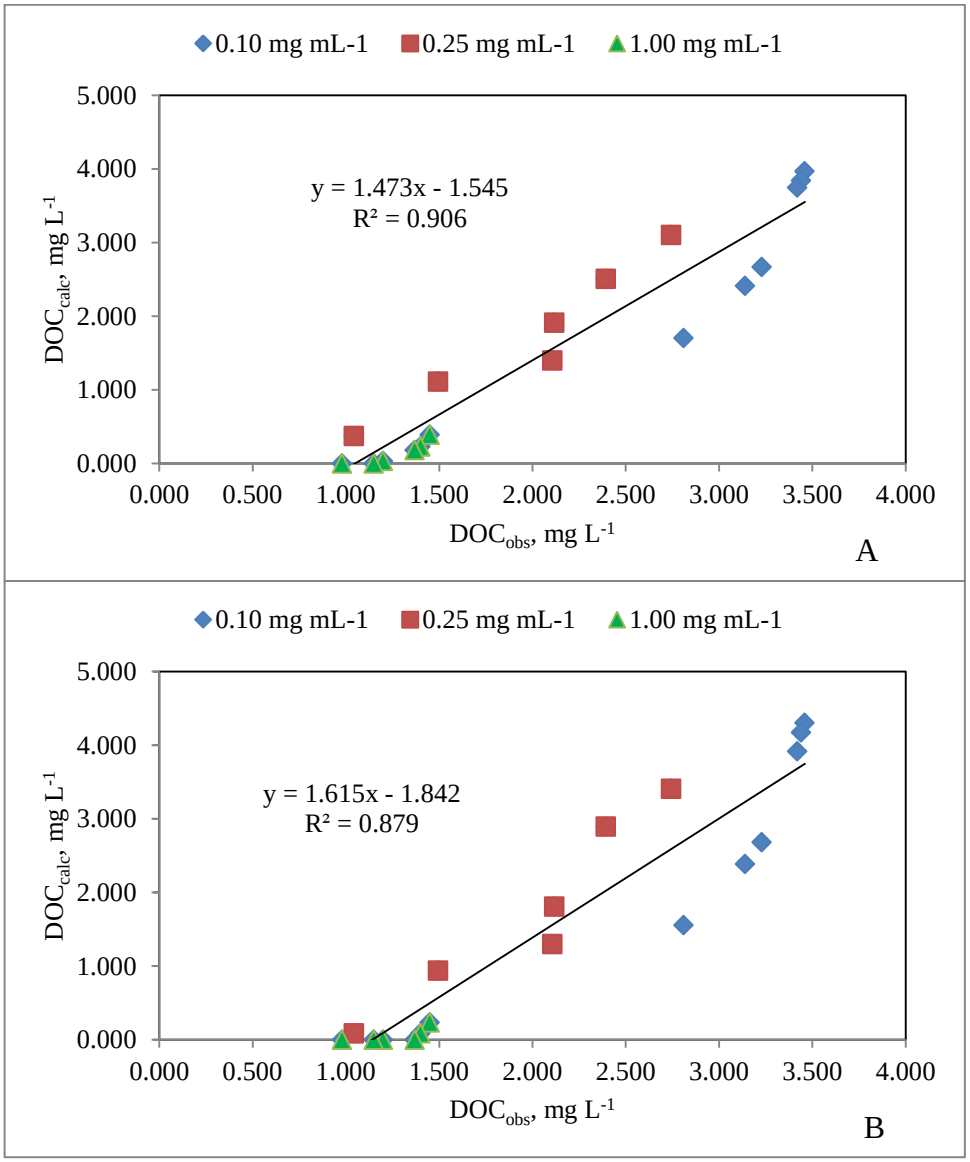

Figure 4.58. The correlation between DOC_{obs}, measured by TOC analyzer, and DOC_{calc}, obtained by using Equation 4.20 as a function of UV_{254} parameter and Equation 4.22 as a function of UV_{280} parameter, including the oxidative data after each irradiation time of the photocatalytic treatment of AHA. ((A) UV_{254}, (B) UV_{280}).

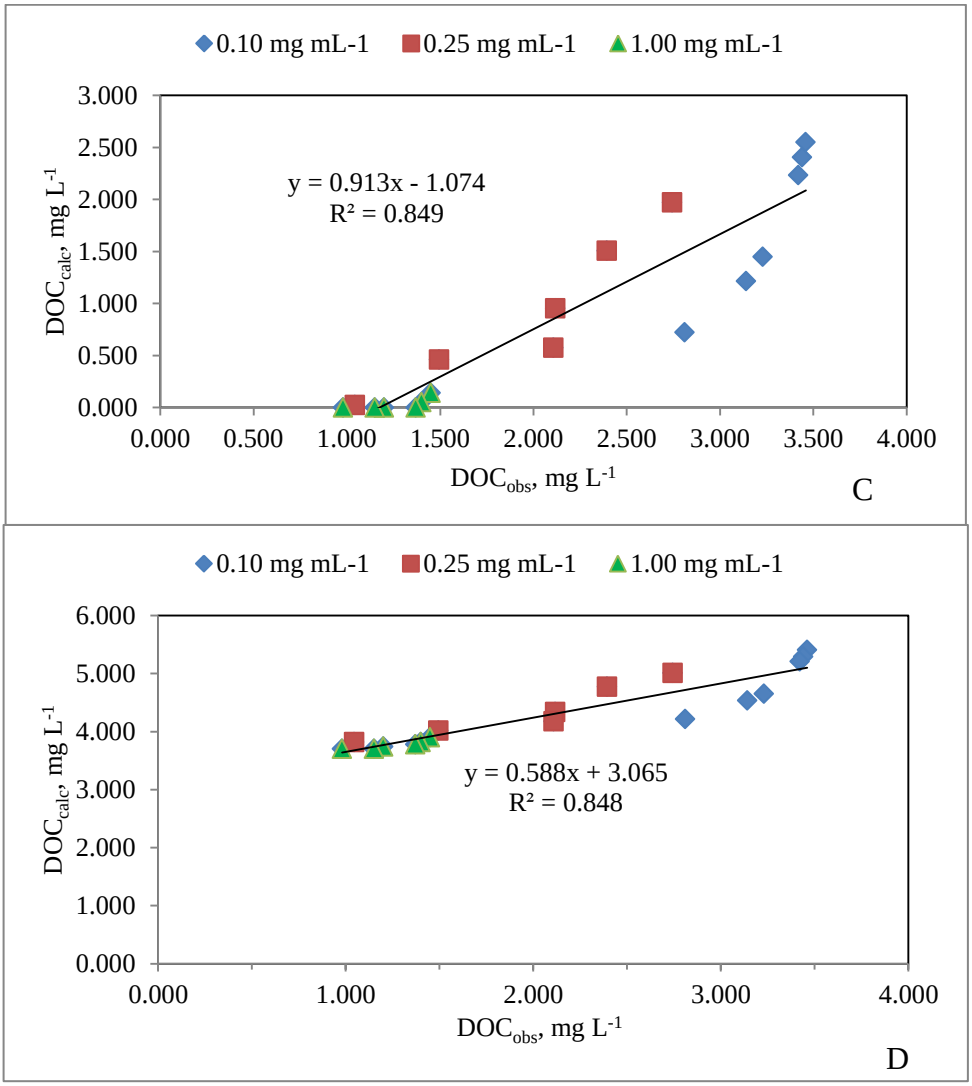

Figure 4.59. The correlation between DOC_{obs}, measured by TOC analyzer, and DOC_{calc} obtained by using Equation 4.24 as a function of UV_{365} parameter and Equation 4.26 as a function of $Color_{436}$ parameter, including the oxidative data after each irradiation time of the photocatalytic treatment of AHA. ((C)UV_{365}, (D) $Color_{436}$).

DOC_{calc}-DOC_{obs} Equation was produced from the least-squares regression analyses (Equation 4.106, Equation 4.107, Equation 4.108 and Equation 4.109). The regression coefficient was found to be as R^2= 0.906 (UV_{254}), R^2= 0.879 (UV_{280}), R^2= 0.849 (UV_{365}) and R^2= 0.848 ($Color_{436}$) (Table 4.34). The relationship between DOC_{calc}, obtained as a function of UV-vis parameters (UV_{254}, UV_{280}, UV_{365} and $Color_{436}$, including oxidized data) by using Equation 4.20, Equation 4.22, Equation 4.24 and Equation 4.26 and DOC_{obs}, measured by TOC analyzer, was presented in Table 4.34. Similar to the relationship

between DOC_{calc} and DOC_{obs}, including oxidized and initial values, the correlation between DOC_{calc} and DOC_{obs}, including oxidized values, displayed high regression coefficients.

Table 4.34. The relationship between DOC_{calc}, obtained as a function of UV-vis parameter (UV_{254}, UV_{280}, UV_{365} and $Color_{436}$, including oxidized data) by using Equation 4.20, Equation 4.22, Equation 4.24 and Equation 4.26 and DOC_{obs}, measured by TOC analyzer.

AHA Photocatalytic treatment			
No	UV-vis parameter	Correlation Equation	R^2
4.106	UV_{254}	DOC_{calc} (mg L^{-1}) = 1.473*DOC_{obs} (mg L^{-1}) – 1.545	0.906
4.107	UV_{280}	DOC_{calc} (mg L^{-1}) = 1.615*DOC_{obs} (mg L^{-1}) – 1.842	0.879
4.108	UV_{365}	DOC_{calc} (mg L^{-1}) = 0.913*DOC_{obs} (mg L^{-1}) – 1.074	0.849
4.109	$Color_{436}$	DOC_{calc} (mg L^{-1}) = 0.588*DOC_{obs} (mg L^{-1}) + 3.065	0.848

According to these results, it could be inferred that DOC content in AHA could be determined by using the nontreatment Equations (Equation 4.20, Equation 4.22, Equation 4.24 and Equation 4.26) as a function of UV_{254} parameter, UV_{280} parameter, UV_{365} parameter and $Color_{436}$ parameter of the remained AHA after the irradiation time, instead of using TOC analyzer.

4.3.2.4. The Relationship between Initial and Oxidized DOC_{obs} Concentration and DOC_{calc} Concentration of AHA depending on the Non-treatment Equation of The overall HAs (NHA, FHA, AHA and RHA). DOC_{obs} concentration of AHA, representing the degradation depending on the irradiation time in Table 4.29, were correlated with DOC_{calc} (Table 4.31) concentrations that was calculated by using Equation 4.43, Equation 4.45, Equation 4.47 and Equation 4.49 (Figure 4.60 and 4.61).

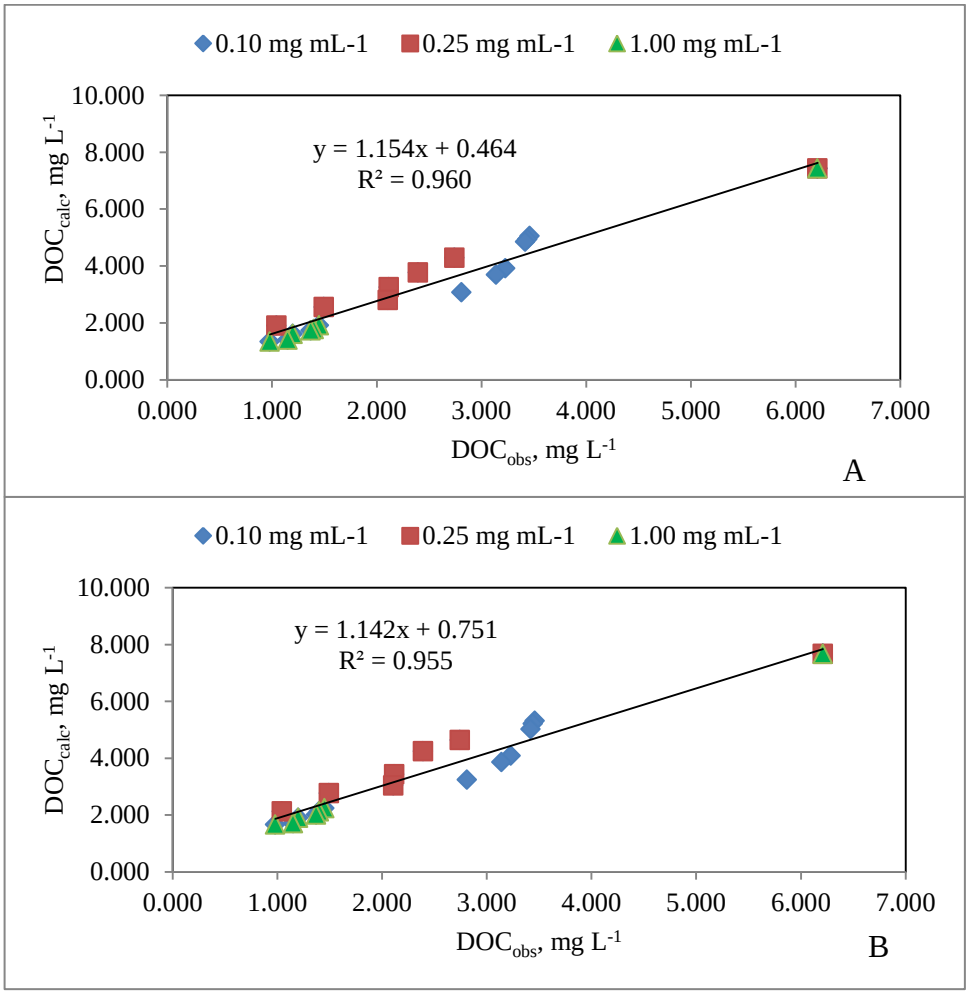

Figure 4.60. The correlation between DOC_{obs}, measured by TOC analyzer, and DOC_{calc} obtained by using Equation 4.43 as a function of UV_{254} parameter and Equation 4.45 as a function of UV_{280} parameter, including the non-oxidative data before the photocatalytic treatment and the oxidative data after each irradiation time of the photocatalytic treatment of AHA. ((A)UV_{254}, (B) UV_{280}).

Figure 4.60 illustrated the linear correlation between DOC_{obs}, measured by TOC analyzer, and DOC_{calc} obtained by using Equation 4.43 as a function of UV_{254} parameter and by using Equation 4.45 as a function of UV_{280} parameter, including the non-oxidative data before the photocatalytic treatment and the oxidative data after each irradiation time of the photocatalytic treatment of AHA. (Equation 4.110, Equation 4.111). Equations exhibited the high regression coefficient (Equation 4.110, R^2=0.960; Equation 4.111, R^2=0.955)

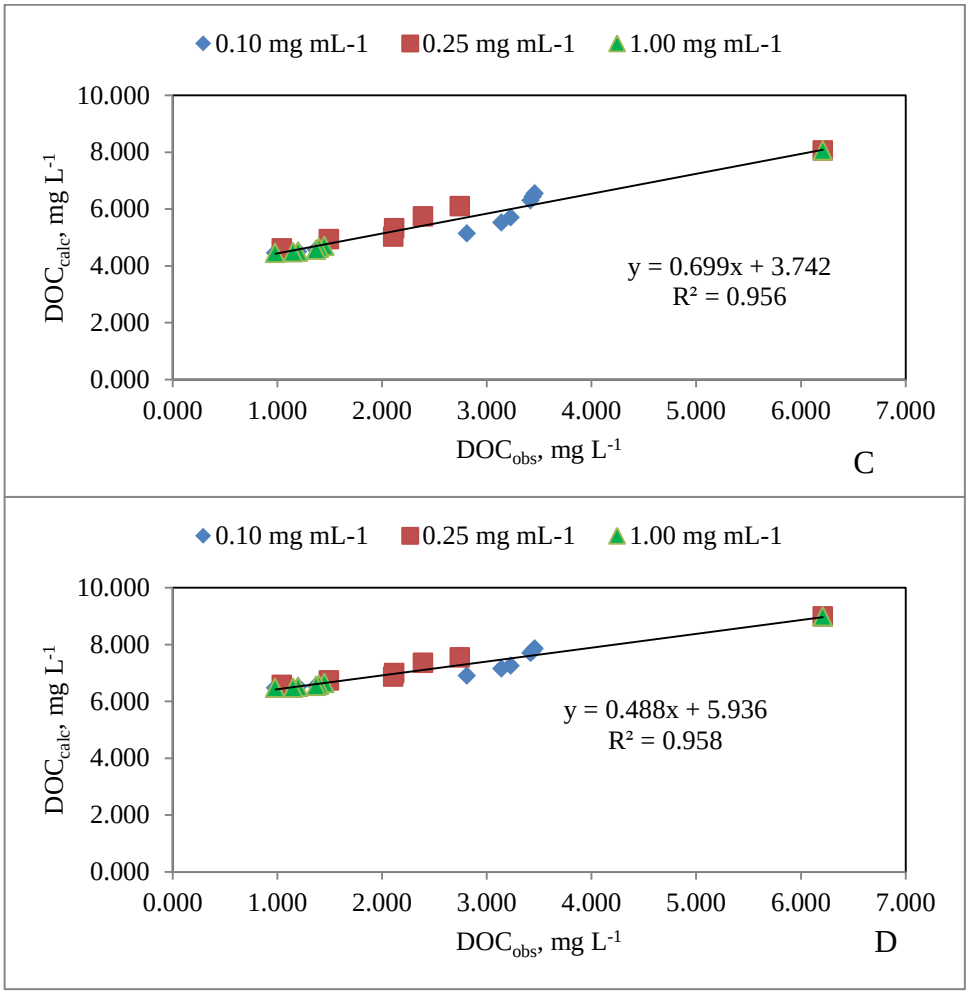

Figure 4.61. The correlation between DOC_{obs}, measured by TOC analyzer, and DOC_{calc} obtained by using Equation 4.47 as a function of UV_{365} parameter and Equation 4.49 as a function of $Color_{436}$ parameter, including the non-oxidative data before the photocatalytic treatment and the oxidative data after each irradiatio time of the photocatalytic treatment of AHA. (C) UV_{365}, (D) $Color_{436}$).

Figure 4.61 illustrated the linear correlation between DOC_{obs}, measured by TOC analyzer, and DOC_{calc}, obtained by using Equation 4.47 as a function of UV_{365} paramteter and Equation 4.49 as a function of $Color_{436}$ parameter, including the non-oxidative data before the photocatalytic treatment and the oxidative data after each irradiation time of the photocatalytic treatment of AHA. (Equation 4.112 and Equation 4.113). Equations exhibited the high regression coefficient (Equation 4.112, R^2=0.956; Equation 4.113, R^2=0.958). According to the nontreatment Equations (Equation 4.43, Equation 4.45, Equation 4.47 and Equation 4.49) DOC_{calc} obtained as a function of UV_{254} parameter,

UV_{280} parameter, UV_{365} parameter and $Color_{436}$ parameter of the remained AHA after the irradiation time was found to be closed to DOC_{obs}, including oxidized and initial values with high regression coefficient (Equation 4.110), (Equation 4.111), (Equation 4.112) and (Equation 4.113) (Table 4.35).

Table 4.35. The relationship between DOC_{calc}, obtained as a function of UV-vis parameters (UV_{254}, UV_{280}, UV_{365} and $Color_{436}$, including initial and oxidized data) by using Equation 4.43, Equation 4.45, Equation 4.47 and Equation 4.49 and DOC_{obs}, measured by TOC analyzer.

AHA Photocatalytic tretament			
No	UV-vis parameter	Correlation Equation	R^2
4.110	UV_{254}	DOC_{calc} (mg L^{-1}) = 1.154*DOC_{obs} (mg L^{-1}) + 0.464	0.960
4.111	UV_{280}	DOC_{calc} (mg L^{-1}) = 1.142*DOC_{obs} (mg L^{-1}) + 0.751	0.955
4.112	UV_{365}	DOC_{calc} (mg L^{-1}) = 0.699*DOC_{obs} (mg L^{-1}) + 3.742	0.956
4.113	$Color_{436}$	DOC_{calc} (mg L^{-1}) = 0.488*DOC_{obs} (mg L^{-1}) + 5.936	0.958

UV_{254} parameter, UV_{280} parameter and UV_{365} parameter of the remained of AHA, representing aromatic moieties, and $Color_{436}$ parameter, representing color forming moieties, including enough carbon content according to nontreatment Equations (Equation 4.43, Equation 4.45, Equation 4.47 and Equation 4.49) that DOC_{calc} exhibited a good prediction of DOC concentration content in AHA, observed by TOC analyzer. It could be inferred that DOC content in AHA could be determined by using the nontreatment Equations (Equation 4.43, Equation 4.45, Equation 4.47 and Equation 4.49) as a function of UV_{254} parameter, UV_{280} parameter, UV_{365} parameter and $Color_{436}$ parameter of the remained AHA after the irradiation time instead of using TOC analyzer.

4.3.2.5. The Relationship between Oxidized DOC_{obs} Concentration and DOC_{calc} Concentration of AHA depending on the Non-treatment Equation of the overall HAs (NHA, FHA, AHA and RHA). DOC_{obs} concentration of AHA, represented the degradation

depending on the irradiation time in Table 4.29, were correlated with DOC_{calc} concentrations (Table 4.31) that was calculated by using Equation 4.43, Equation 4.45, Equation 4.47 and Equation 4.49 (Figure 4.62 and Figure 4.63).

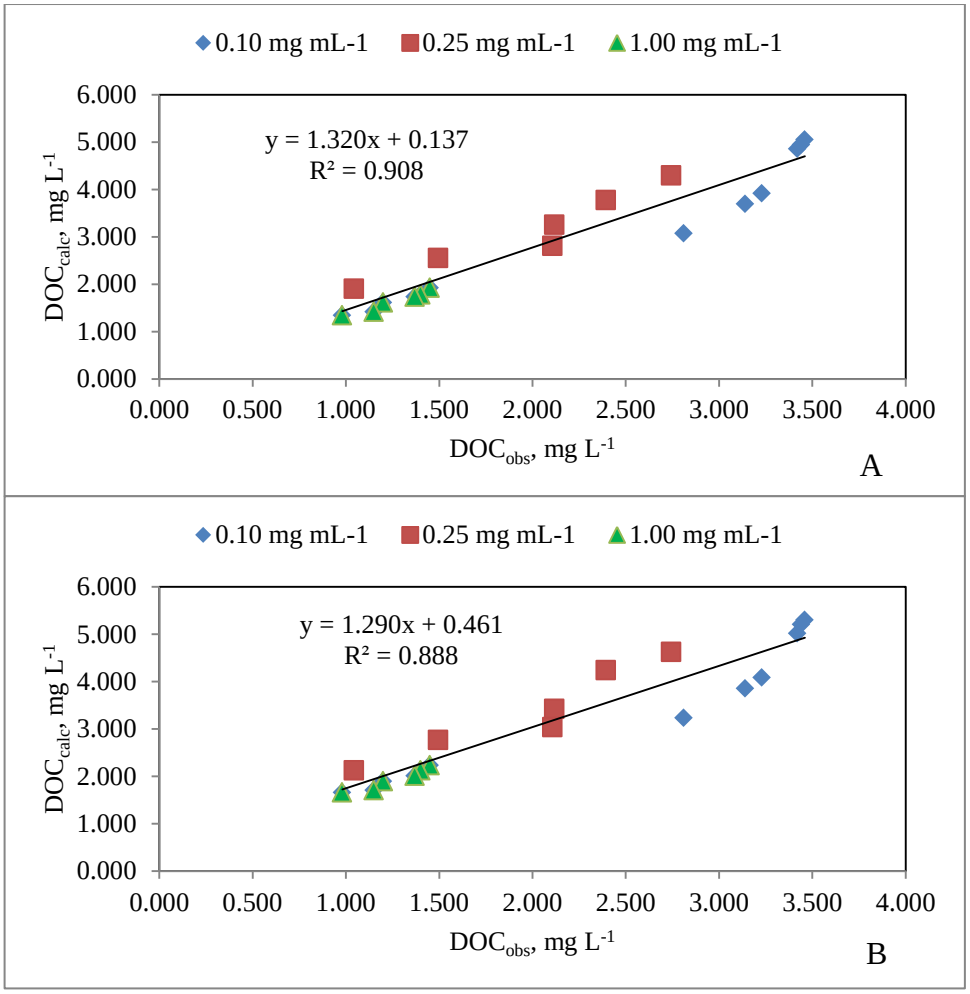

Figure 4.62. The correlation between DOC_{obs}, measured by TOC analyzer, and DOC_{calc} obtained by using Equation 4.43 as a function of UV_{254} parameter and Equation 4.45 as a function of UV_{280} parameter, including the oxidative data after each irradiation time of the photocatalytic treatment of AHA. (A)UV_{254}, (B) UV_{280}).

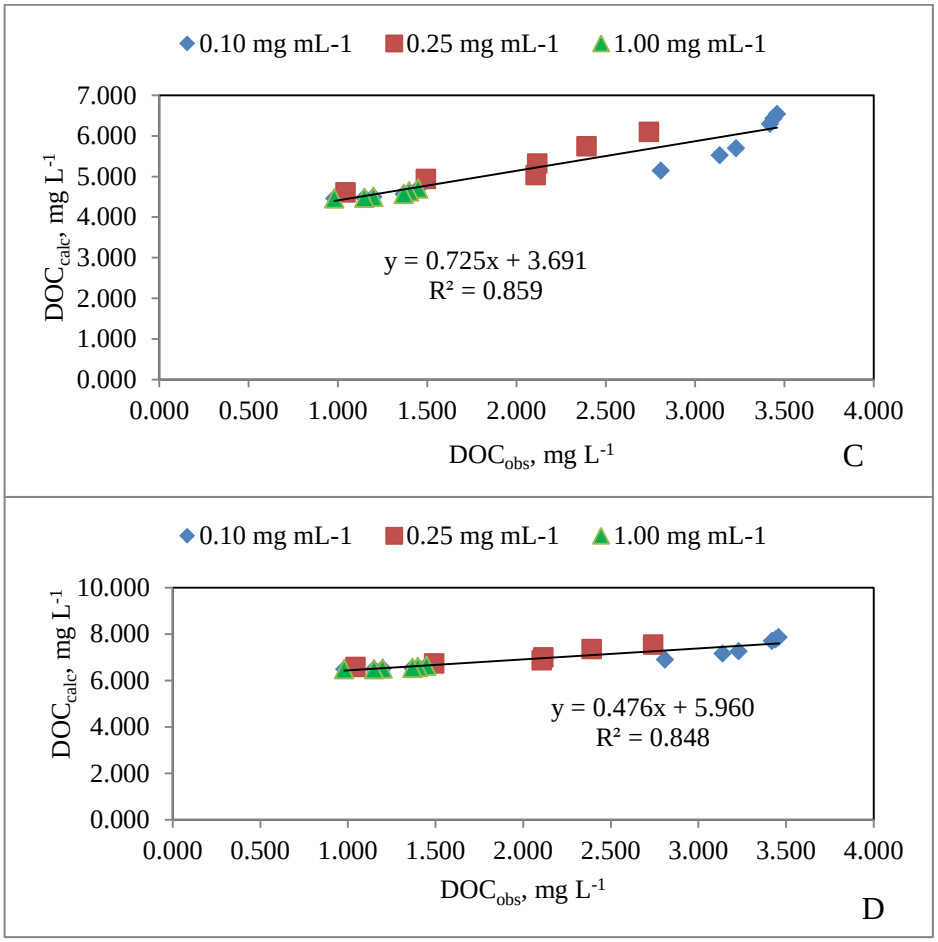

Figure 4.63. The correlation between DOC_{obs}, measured by TOC analyzer, and DOC_{calc} obtained by using Equation 4.47 as a function of UV_{365} parameter ana Equation 4.49 as a function of $Color_{436}$ parameter, including the oxidation data after each irradiation time of the photocatalytic treatment of AHA. ((C)UV_{365}, (D) $Color_{436}$).

Figure 4.62 illustrated the linear correlation between DOC_{obs}, measured by TOC analyzer, and DOC_{calc} obtained by using Equation 4.43 as a function of UV_{254} parameter and Equation 4.45 as a function of UV_{280} parameter, including the oxidative data after each irradiation time of the photocatalytic treatment of AHA. (Equation 4.114, Equation 4.115). Equations exhibited the high regression coefficient (Equation 4.114, R^2=0.908; Equation 4.115, R^2=0.888). Figure 4.63 illustrated the linear correlation between DOC_{obs}, measured by TOC analyzer, and DOC_{calc} obtained by using Equation 4.47 as a function of UV_{365} parameter and Equation 4.49 as a function of $Color_{436}$ parameter, including the oxidative data after each irradiation time of the photocatalytic treatment of AHA. (Equation 4.116,

Equation 4.117). Equations exhibited the high regression coefficient (Equation 4.116, R^2=0.859; Equation 4.117, R^2=0.848)

As mentioned above, DOC_{obs} concentrations, including only oxidized values, were correlated with DOC_{calc} concentrations (Table 4.36). Similar to DOC_{calc}, consisting of oxidized and initial values, DOC_{calc}, including only oxidized values, were found to be closed to DOC_{obs} with high regression coefficient for UV-vis parameters (UV_{254}, UV_{280}, UV_{365} and $Color_{436}$). It could be inferred that UV_{254}, UV_{280}, UV_{365} and $Color_{436}$ parameter of the remained AHA, represented enough dissolved organic carbon that DOC_{calc}, according to these Equations, can predict DOC_{calc}, obtained by utilizing TOC analyzer, in humic acid solution

Table 4.36. The relationship between DOC_{calc}, obtained as a function of UV-vis parameters (UV_{254}, UV_{280}, UV_{365} and $Color_{436}$, including oxidized data) by using Equation 4.43, Equation 4.45, Equation 4.47 and Equation 4.49 and DOC_{obs}, measured by TOC analyzer.

AHA Photocatalytic treatment			
No	UV-vis parameter	Correlation Equation	R^2
4.114	UV_{254}	DOC_{calc} (mg L^{-1}) = 1.320*DOC_{obs}(mg L^{-1}) + 0.137	0.908
4.115	UV_{280}	DOC_{calc} (mg L^{-1}) = 1.290*DOC_{obs}(mg L^{-1})+ 0.461	0.888
4.116	UV_{365}	DOC_{calc} (mg L^{-1}) = 0.725*DOC_{obs}(mg L^{-1}) + 3.691	0.859
4.117	$Color_{436}$	DOC_{calc} (mg L^{-1}) = 0.476*DOC_{obs}(mg L^{-1}) + 5.960	0.848

As a consequence, DOC content in AHA, could be determined by calculating Equations as a function of UV-vis parameters (UV_{254}, UV_{280}, UV_{365} and $Color_{436}$), remained after the irradiation time without utilizing TOC analyzer.

4.4. Critical Evaluation of The Correlations Assessed between UV-vis Parameters and Organic Carbon Contents of Humic Acids under Oxidative and Non-oxidative Conditions

Referring to the previous studies performed by Bekbolet and co-workers since 1996, the established relationships between the UV-vis parameters and DOC contents of the various humic acids under oxidative and non-oxidative conditions are evaluated.

Reference studies cover Bekbolet, 1996; Bekbolet et al., 1996; Bekbolet and Balcioglu, 1996; Bekbolet and Ozkosemen, 1996; Bekbolet et al., 1998; Bekbolet et al., 2002; Uyguner and Bekbolet, 2004; Uyguner and Bekbolet, 2005a; Uyguner and Bekbolet, 2005b; Uyguner and Bekbolet, 2005c; Uyguner and Bekbolet, 2007a; Uyguner and Bekbolet, 2007b; Uyguner and Bekbolet, 2007c; Uyguner and Bekbolet, 2009; Uyguner and Bekbolet, 2010.

The outcome of the indicated publications has been review extensively by Uyguner-Demirel and Bekbolet (Uyguner and Bekbolet, 2005; Uyguner and Bekbolet, 2006a; Uyguner and Bekbolet, 2006b; Uyguner-Demirel and Bekbolet, 2011). The significance of the indicative parameters have been revisited and the effective parameters have been compiled and presented in a table (Table 2.5. Uyguner-Demirel and Bekbolet, 2011). From clarity purposes the mentioned table is also given as Table 4.37. Aldrich humic acid (Eggins et al., 1997; Minero et al., 1999; Cho and Choi, 2002; Palmer et al., 2002; Wiszniowski et al., 2002; Wiszniowski et al., 2003; Kerc et al., 2003a; Kerc et al., 2003b; Al-Rasheed and Cardin, 2003a; Al-Rasheed and Cardin, 2003b; Wiszniowski et al., 2004; Uyguner and Bekbolet, 2005b; Portjanskaja et al., 2006; Tsarenko et al., 2006; Selcuk and Bekbolet, 2008; Syafei et al., 2008; Tsimas et al., 2009; Portjanskaja et al., 2009; Gomes et al., 2009, Zhang et al., 2009), Roth humic acid (Bekbolet, 1996; Bekbolet and Balcioglu, 1996; Bekbolet and Ozkosemen, 1996; Bekbolet et al., 1998; Bems et al., 1999; Gonenc and Bekbolet, 2001; Bekbolet et al., 2002; Uyguner and Bekbolet, 2004a; Uyguner and Bekbolet, 2007a; Uyguner and Bekbolet, 2009; Uyguner and Bekbolet, 2010) and Fluka humic acid (Tay et al., 2001; Qiao et al., 2002; Li et al., 2002; Zhang et al., 2008; Liu et al., 2008a) were used as humic sources. As mentined above, HA concentration was correlated with UV-vis parameter, and DOC concentration of various humic acid was also correlated

with UV-vis parameter during the photocatalytic treatment. TiO_2 was used as photocatalyst and TiO_2 and metal were used to degrade humic acid, effectively.

DOC concentration (Eggins et al., 1997; Palmer et al., 2002; Cho and Choi, 2002; Al-Rasheed and Cardin, 2003b; Wiszniowski et al., 2004 Doll and Frimmel, 2005; Ljubas, 2005; Murray and Parsons, 2006; Murray et al., 2007; Uyguner et al., 2007a; Rizzo et al., 2008; Syafei et al., 2008; Uyguner and Bekbolet, 2009; Liu et al., 2010) and TOC concentration (Bekbolet,1996; Bekbolet and Balcioglu, 1996; Bekbolet and Ozkosemen, 1996; Minero et al., 1999; Lee and Ohgaki,1999; Tay et al., 2001; Gonenc and Bekbolet, 2001; Molinari et al., 2002; Remoundaki et al., 2002; Li et al., 2002; Qiao et al., 2002; Wiszniowski et al., 2002; Wiszniowski et al., 2003; Selcuk et al., 2004; Uyguner and Bekbolet, 2005a; Uyguner and Bekbolet, 2005b; Bekbolet et al., 2005; Fu et al., 2006a; Fu et al., 2006b; Han et al., 2006; Le-Clech et al., 2006; Zhang et al., 2009; Gomes et al., 2009; Uyguner and Bekbolet, 2010) was determined by using TOC analyzer and UV-vis parameter (Bekbolet et al., 1996; Bekbolet, 1996; Bekbolet and Balcioglu, 1996; Bekbolet and Ozkosemen, 1996; Eggins et al., 1997; Bekbolet et al., 1998; Bems et al., 1999; Lee and Ohgaki, 1999; Tay et al., 2001; Bekbolet et al., 2002; Palmer et al., 2002; Molinari et al., 2002; Li et al., 2002; Qiao et al., 2002; Kerc et al., 2003a; Kerc et al., 2003b; Al-Rasheed and Cardin, 2003a; Al-Rasheed and Cardin, 2003b; Uyguner and Bekbolet, 2004a; Portjanskaja, 2004; Selcuk et al., 2004; Wiszniowski et al., 2004; Uyguner and Bekbolet, 2005a; Uyguner and Bekbolet, 2005b; Doll and Frimmel, 2005; Bekbolet et al., 2005; Ljubas, 2005; Portjanskaja et al., 2006; Fu et al., 2006a; Fu et al., 2006b; Han et al., 2006; Tsarenko et al., 2006; Moriguchi et al., 2006; Yang and Lee, 2006; Murray and Parsons, 2006; Murray et al., 2007; Li et al., 2007; Uyguner et al., 2007a; Rizzo et al., 2007; Huang et al., 2008; Choo et al., 2008; Selcuk and Bekbolet, 2008; Zhang et al., 2008; Huang et al., 2008; Liu et al., 2008b; Rizzo et al., 2008; Bansal et al., 2008; Syafei et al., 2008; Zhang et al., 2008; Liu et al., 2008a; Zhang et al., 2009; Tsimas et al., 2009; Portjaskaja et al., 2009; Gomes et al., 2009; Uyguner and Bekbolet, 2009; Liu et al., 2010; Uyguner and Bekbolet, 2010) was determined by using the specified spectrophotometer during the photocatalytic treatment.

The kinetic models were applied to examine the degradation of UV-vis parameter, HA concentration and DOC concentration, representing to HA. First order kinetic model

(Tay et al., 2001; Palmer et al., 2002; Kerc et al., 2003a; Kerc et al., 2003b; Al-Rasheed and Cardin, 2003b; Fu et al., 2006a; Fu et al., 2006b; Rizzo et al., 2008; Uyguner and Bekbolet, 2009; Zhang et al., 2009; Uyguner and Bekbolet, 2010) and Langmuir-Hinshelwood kinetic model (Tay et al., 2001; Al-Rasheed and Cardin, 2003a; Le-Clerch et al., 2006; Zhang et al., 2008) were used as the kinetic model. Generally, the batch reactor type (Bekbolet et al., 1996; Bekbolet, 1996; Bekbolet and Balcioglu, 1996; Bekbolet and Ozkosemen, 1996; Eggins et al., 1997; Bekbolet et al., 1998; Bems et al., 1999; Gonenc and Bekbolet, 2001; Palmer et al., 2002; Cho and Choi, 2002; Li et al., 2002; Molinori et al., 2002; Al-Rasheed and Cardin, 2003a; Al-Rasheed and Cardin, 2003b; Kerc et al., 2003a; Kerc et al., 2003b; Portjanskaja et al., 2004; Uyguner and Bekbolet, 2005a; Uyguner and Bekbolet, 2005b; Bekbolet et al., 2005; Moriguchi et al., 2006; Murray and Parsons, 2006; Uyguner et al., 2007a; Uyguner and Bekbolet, 2007a; Areenachakul et al., 2008; Rizzo et al., 2008; Bansal et al., 2008; Zhang et al; 2008; Espinoza et al., 2009; Zhang et al., 2009; Tsimas et al., 2009; Uyguner and Bekbolet, 2009; Uyguner and Bekbolet, 2010) was applied for the photocatalytic treatment and some researchers was used the membrane reactor (Qiao et al., 2002; Fu et al., 2006a; Fu et al., 2006b; Choo et al., 2008) or the fluilized photocatalysis reactor (Lee and Ohgaki, 1999) as the reactor type. Various light sources were applied for the photocatalytic treatment during the irradiation time.

UV-vis parameters were presented using different notations. Color forming moieties were presented either by as $Color_{400}$ and $Color_{436}$, $Color_{450}$, $Color_{455}$ and $Color_{465}$, aromatic moieties were presented by as UV_{250}, UV_{254} and UV_{280}, specific aromatic moieties were presented either by as UV_{300} and UV_{365}, or other specific color measurement methods such as Pt-Co, Hazen.

Aromaticity was presented using UV_{254}, A_{254} parameter, total aromaticity was presented as UV_{280}, A_{280} parameter, the specific aromatic moieties was presented as UV_{365}, A_{365} parameter, the color forming moieties was presented as using $Color_{436}$, A_{436} parameter and the specific color forming moieties was presented as using $Color_{465}$, A_{465} parameter. Organic carbon contents were determined by the gross parameters as TOC, DOC, COD and BOD_5, NPOC and DOC/TOC.

Some researchers represented the removal of HA (AHA, RHA, FHA, A sodium salt of humic acid (Acros organics) concentration as a function of UV-vis parameter during the photocatalytic treatment (Li et al., 2002; Portjanskaja et al., 2004, 2006; Tsarenko et al., 2006; Li et al., 2007; Zhang et al., 2008; Zhang et al., 2009; Portjanskaja et al., 2009; Tsimas et al., 2009). As indicated above, humic subtances represented diverse sources thereby containing a variety of different building blocks and various functional groups, leading to diversity in their structure and their behavior towards oxidation. It is widely known that the carbon contents could vary between 50 % and 60 % for humic acids (Filella et al., 2005). The part of humic acids have transformed into very refractory products in the UV-illuminated TiO_2 suspension and humic acids turn into less hydrophobic, less adsorping, and less aromatic characters, in general (Cho and Choi, 2002). These researches applied various methods to determine the HA concentration during the photocatalytic treatment.

Critical evaluation of the Table 2.5 is presented below with reference to the indicated UV-vis parameters. The whole absorbance spectrum (from 200 to 700 nm) of the reaction mixtures was recorded by using a UV-vis spectrophotometer. AHA concentration was measured monitoring the sample absorbance at three different wavelengths, namenly 254, 350 and 436 nm using respective calibration curves with respect to the concentration, these were constructed measuring the absorbance of several AHA solutions of known concentration (Tsimas et al., 2009). It was found that the discrepancy in humic acid concentration measured at these wavelengths was always less than 5 %. According to these findings, humic acid concentration was computed based on the calibration curve constructed between A_{254} and humic acid concentration.

The photocatalytic oxidation of AHA was studied at 10 mg L^{-1} and 50 mg L^{-1} initial humic acid concentrations, TiO_2 loadings in the range of 50-500 mg L^{-1} and pH=6.3. 10 mg L^{-1}, and 50 mg L^{-1} removal of humic acid concentration was presented as a function of UV_{254} parameter in the presence of 0.05 mg mL^{-1} TiO_2, 0.05 mg mL^{-1} TiO_2 and 0.10 mg mL^{-1} TiO_2, respectively. The removal of UV_{254} parameter and TOC concentration data were not presented by the researcher (Tsimas et al., 2009). The researcher reported made the calibration curve by using non-treated humic acid for the assessment of the removal of humic acid concentration. The non-treated humic acid and the treated humic acid might not

display the same compositional structure. The same amount of the treated and nontreated humic acid could exhibit the same UV-vis parameter but the structure of the nontreated humic acid may not be the same with the structure of the treated humic acid. As a result, the degraded humic acid concentration was difficult to determine by applying this method. It could be inferred that to determine the removal of humic acid concentration by applying this method could display significant error. DOC concentration can be represented as a function of UV_{254} parameter under the treatment condition, whereas humic acid concentration can not be represented as a function of UV_{254} parameter. In our study, DOC concentration, corresponding to AHA concentration, was represented as a function of UV_{254} parameter (Equation 90, 94 and 98) during the photocatalytic treatment with high regression coefficient ($R^2 > 0.875$).

A sodium salt of humic acid was obtained from a commercial source (A sodium salt of humic acid (Acros organics) and used for a static photocatalytic degradation experiment under visible-light illumination (Li et al., 2007). The photocatalytic activities of TiON/PdO nanoparticle photocatalyst were demostrated by their degradation effect on humic acid under visible-light illumination, using the TiON nanoparticle photocatalyst as a comparison basis. Photocatalytic degradation of humic acid was conducted by exposing the HA solution with various photocatalyst under visible light (> 400 nm) for varying intervals (from 2 to 10 hours). After centrifugation was performed to recover the photocatalyst, the light absorption of the clear solution was measured and the remaining percentage of HA in the solution was calculated by the ratio between the light absorptions of photocatalyst-treated and untreated HA solutions. HA was represented as a function of UV_{280} parameter during the photocatalytic treatment in the presence of TiON. The residual DOC concentration was not determined. As mentioned before, HA has complicated structure, and UV_{280} parameter, represents aromatic moieties in HA. The removal of UV_{280} parameter and the removal of TOC concentration were not determined during the photocatalytic treatment in the presence of TiON. It was difficult to examine if the evaluation of HA concentration was presented as a function of UV_{280} parameter, should be cautiously interpreted.

In another study, FHA was chosen as the model contaminant (Zhang et al., 2008). FHA solution was prepared in deionized water. The UV light source (254 nm) was

immersed into solution, 1 cm above the TiO_2 nanowire membrane. FHA concentration in solution was measured by monitoring the absorbance of 436 nm on a UV-visible spectrophotometric and the total organic matter concentration was measured on a Shimadzu TOC analyzer. $Color_{436}$ parameter was a specific parameter than UV_{254}, UV_{280} and UV_{365} parameter, and the result, obtained as a function of $Color_{436}$ parameter, exhibited lower than the result, attained as a function of UV_{254} and UV_{280} parameter, in terms of DOC, NOM, and FHA concentration. The first order kinetic model displayed decreasing trend $k_{TOC}>k_{HA}$. FHA concentration consists of DOC concentration, after the irradiation of 60 minutes, TOC exhibited more concentration HA. To present the degradation of FHA concentration as a function of $Color_{436}$ parameter, could not give the exact result. In our study, DOC concentration of AHA was correlated with $Color_{436}$ parameter in the presence of 0.10, 0.25 and 1.00 mg mL^{-1} TiO_2 with high regression coefficient ($R^2>0.877$).

Tsarenko and co-workers reported the removal of humic substances (AHA) from aqueous solutions with a photocatalyst membrane reactor (Tsarenko et al., 2006). The concentrations of humic substances (AHA) in the solution were determined by the photocolorimetry (λ=465 nm). The source of UV irradiation was a high pressure mercury lamp with an irradiance of 18.9 W m^{-2} in the 200-400 nm wavelength range. The content of humic substances in the solution as a function of $Color_{465}$ parameter was presented depending on the irradiation time in the presence of 1 mg mL^{-1} TiO_2. $Color_{465}$ parameter data were not given during the photocatalytic treatment. Moreover, similar to $Color_{436}$ parameter, $Color_{465}$ was specific parameter than UV_{254}, UV_{280}, and UV_{365} parameter. To present the degradation of AHA concentration as a function of $Color_{465}$ parameter would not represent probably the exact result expressing AHA concentration during the photocatalytic treatment.

The photocatalytic oxidation of humic substances (AHA) in aqueous solutions and natural waters with TiO_2 attached to buoyant hollow glass micro-spheres was studied (Portjanskaja et al., 2004 and 2006). A 365 nm low-pressure mercury UV lamp, 15 W UV-light source was positioned horizontally, over the reactor, providing an irradiance about 0.7 mW cm^{-2} measured at a distance corresponding to the level of the free surface of the reactor by an optical diameter. The initial solution of humic substances was filtered a 0.45

μm membrane in order to remove the indissoluble particles from the solution samples taken during the experiment to separate the catalyst before the analysis. Filtration was applied to the particles. Absorbance at 254 nm was measured by means of a spectronic Unicam spectrophotometer. The indice was correlated with the content of humic substances by calibration curve. The researcher did not mention how to measure the degraded humic subtances during the photocatalytic treatment. It was impossible to examine the relationship between humic substance and UV_{254} parameter during the photocatalytic treatment. Moreover, the performance of photocatalytic oxidation with artifial radiation sources was also characterized by the process efficiency. A few design options of attached photocatalyst reactors were tested in photocatalytic oxidation of UV/Vis-irradiated aqueous solutions containing humic acids (AHA) (Portjanskaja et al., 2009). Two 200 mL simple batch reactors with inner diameter 100 mm thermostated 19-21°C and mechanically agitated with magnetic stirrer were used in slurry, buoyant microspheres and fixed plate photocatalytic experiments. The experiments were conducted with synthetic solutions of HA purchased from AHA. The subtrates were prepared in concentrations of 10 mg L^{-1} of sodium salt of HA. The UV-absorbance of AHA sample at 254 nm was measured by Spectronic Unicam spectrophotometer, which was correlated with the content of AHA by calibration line.

The photodegradation of FHA in the presence of UV irradiation was investigated as a function of pH (Li et al., 2002). A FHA suspension was first prepared by adding the FHA chemicals into the deionized water and gently heating to temperatures up to 60°C in order to accelerate the dissolution of FHA. FHA concentration was 20 mg L^{-1} in the presence of 1 mg mL^{-1} TiO_2 loading, but different initial pH (3, 5, 7 and 9). A photoreactor consists of a cylindrial borosilicate glass reactor vessel with an effective volume of 280 mL, a cooling water jacket, and 125 W high pressure mercury lamp positioned axially at the centre of the reactor vessel as a light source to provide near UV irradiation with a light intensity of 4.38 mW cm^{-2}. The concentration of FHA (UV_{254}) was determined by a UV-vis spectrophotometer at 254 nm. Total organic carbon concentration was determined by a TOC analyzer. UV_{254} parameter is used to monitor the organic carbon in HA concentration. In this study, UV_{254} parameter was used to represent the HA concentration. It was not described clearly that UV_{254} could also express the degraded HA concentration via photocatalysis. UV_{254} parameter, calculated as a function of DOC concentration by

using Equation 98, exhibited close removal to DOC concentration of FHA, according to the irradiation time. Equation 98, obtained from the relationship between UV_{254} parameter and DOC concentration of AHA. In the presence of 1.00 mg mL^{-1} TiO_2, the pseudo kinetic order follow decreasing trend $k_{UV254}>k_{DOC}$. As a result, UV_{254} parameter could be used for the determination of FHA concentration during the photocatalytic treatment. On the other hand, there is no method to determine the removal of FHA concentration, the degraded FHA concentration, obtained by applying the researcher method, does not give the exact result. HA (Aldrich) solution of 50 mg L^{-1} was used as model pollutant for the photocatalytic treatment (Zhang et al., 2009). UV-vis absorption spectra of the solution were recorded at different time intervals to monitor the reaction and the concentration of AHA left in the aqueous system was measured by detecting the absorption at 436 nm on an UV-vis spectrophotometer. Total organic carbon content was measured using a total organic carbon analyzer. The degradation of AHA concentration was presented as a function of $Color_{436}$ parameter according to the irradiation time. According to the pseudo first kinetic model, the kinetic rate followed increasing trend $k_{HA}>k_{TOC}$. After the irradiation time of 90 minutes, the residual TOC concentration, corresponding to AHA concentration, was higher than the residual AHA concentration. Because AHA consists of TOC concentration, HA should be higher than TOC concentration. As mentioned before, Equation 93 was attained from the correlation between DOC concentration, corresponding to AHA, and $Color_{436}$ parameter during the photocatalytic treatment. $Color_{436}$ parameter, calculated by using Equation 93 as a function of DOC concentration, was found to be closed to the removal rate of DOC concentration. As a result, it could be inferred that the residue AHA concentration, was not represented as a function of $Color_{436}$ parameter during the photocatalytic treatment.

5. CONCLUSION

This study represents a significant content for the evaluation of aquatic and terrestrial origin humic acids as NHA, FHA, AHA and RHA, with respect to their UV-vis properties as representatives to natural organic matter in water supplies. Information about origin characteristics were revealed as follows: FHA, which is a terrestrial humic acid, displayed 1.2924 cm^{-1} of UV_{254}, whereas UV_{254} parameter of NHA, aquatic humic acid, exhibited 95 % UV_{254} parameter of FHA as can be seen from Table 4.1 and 4.2. Moreover, RHA, which is a terrestrial humic acid, displayed 0.6030 cm^{-1} of $Color_{436}$, whereas $Color_{436}$ parameter of NHA, aquatic humic acid, exhibited 20 % $Color_{436}$ parameter of RHA as can be seen from Table 4.1 and 4.5 for 50 mg L^{-1}. RHA and NHA concentration had similar UV_{254} and UV_{280} parameter, emphasizing strong aromatic character for 10, 20, 30, 40 and 50 mg L^{-1}. Moreover, the organic carbon content of NHA and RHA exhibited higher than the organic carbon content of FHA and AHA. Terrestrial humic acids had remarkably higher DOC content than aquatic humic acids. In our study, NHA, aquatic humic acid, displayed higher organic carbon content than FHA, and AHA, terrestrial humic acid. The order of UV_{254} and UV_{280} parameter absorbing aromatic moieties exhibited decreasing trend RHA>FHA>AHA>NHA. The order of UV_{365} parameter absorbing specific aromatic moieties displayed decreasing trend RHA>FHA>AHA>NHA. The order of $Color_{436}$ parameter, color forming moieties, exhibited decreasing trend RHA>FHA>AHA>NHA. DOC content of RHA, FHA, AHA and NHA was presented as a function of UV-vis parameter (UV_{254}, UV_{280}, UV_{365} and $Color_{436}$), respectively, under the nontreatment condition with very high regression (R^2>0.935). RHA, FHA, AHA and NHA were presented as a function of UV-vis parameter (UV_{254}, UV_{280}, UV_{365} and $Color_{436}$), respectively, under the nontreatment condition, with very high regression coefficient (R^2> 0.924). HA (NHA, FHA, AHA and RHA) were correlated with DOC concentration, corresponding to HA concentration under the non-treatment condition with very high regression coefficient (R^2>0.992). The overall HAs (NHA, FHA, AHA and RHA) were determined as a function of UV-vis parameters (UV_{254}, UV_{280}, UV_{365} and $Color_{436}$) and also DOC concentration of the overall HAs was determined as a function of UV-vis parameters (UV_{254}, UV_{280}, UV_{365} and $Color_{436}$) under the non-treatment condition.

It was examined the correlation between DOC concentration, corresponding to NHA and AHA, and UV-vis parameter under the treatment condition (the photocatalytic treatment). The photocatalytic treatment was applied as a treatment method to examine the correlation. DOC concentration of NHA was correlated with UV-vis parameter (UV_{254}, UV_{280}, UV_{365} and $Color_{436}$), for 10, 20, 30 and 50 mg L^{-1} NHA in the presence of 0.25 mg mL^{-1} TiO_2 under the treatment condition with very high regression coefficient (R^2> 0.664 for 10 mg L^{-1}; R^2> 0.841 for 20 mg L^{-1}; R^2>0.978 for 30 mg L^{-1}; R^2> 0.895 for 50 mg L^{-1}). Moreover, DOC concentration of NHA was correlated with UV-vis parameter by using all concentrations of NHA in the presence of 0.25 mg mL^{-1} TiO_2 under the treatment condition with high regression coefficient (R^2= 0.942, UV_{254}, R^2=0.946, UV_{280}, R^2= 0.949, UV_{365} and R^2=0.940, $Color_{436}$). Moreover the initial and oxidized DOC_{obs} concentration was correlated with DOC_{calc} concentration of NHA, depending on the nontreatment equations of NHA with high regression coefficient (R^2= 0.945, UV_{254}; R^2= 0.949, UV_{280}; R^2= 0.954, UV_{365} and R^2= 0.943, $Color_{436}$). The oxidized DOC_{obs} concentration was presented as a function of DOC_{calc} concentration of NHA, dependent on the nontreatment equations of NHA, with high regression coefficient (R^2= 0.953, UV_{254}; R^2= 0.958, UV_{280}; R^2= 0.958, UV_{365} and R^2= 0.949, $Color_{436}$). The initial and oxidized DOC_{obs} concentration was presented as DOC_{calc} concentration of NHA, depending on the nontreatment equation of the overall HAs, with high regression coefficient (R^2= 0.945, UV_{254}; R^2= 0.949, UV_{280}; R^2= 0.954, UV_{365} and R^2= 0.944, $Color_{436}$). The oxidized DOC_{obs} concentration was correlated with DOC_{calc} concentration of NHA, depending on the nontreatment equation of the overall HAs, with high regression coefficient (R^2= 0.956, UV_{254}; R^2= 0.958, UV_{280}; R^2= 0.958, UV_{365} and R^2= 0.949, $Color_{436}$). On the other hand, NHA concentration has a complicated structure, the determination of the removed DOC concentration , during the photocatalytic treatment, could not exhibit the exact result by using the nontreatment Equations. As a result, the removal of DOC concentration should be predicted by using TOC analyzer during the photocatalytic treatment.

DOC concentration of AHA was correlated with UV-vis parameter (UV_{254}, UV_{280}, UV_{365}, $Color_{436}$) with very high regression coefficient in the presence of 0.10 mg mL^{-1} TiO_2 (R^2>0.699), 0.25 mg mL^{-1} TiO_2 (R^2>0.969) and 1.00 mg mL^{-1} TiO_2 (R^2> 0.998) for 20 mg L^{-1} of AHA during the photocatalytic treatment. It was examined if these equations could be used to determine the removal of DOC concentration after the photocatalytic

treatment without applying TOC analyzer. According to the results, these equations did not provide exact DOC concentration result. As mentioned before, HA is a complicated chemical compound, and its behavior changes during the photocatalytic treatment, according to its origin. The DOC concentration result, obtained as a function of the correlation equation, could be different from DOC concentration result, attained by using TOC analyzer. On the other hand, the researchers represented the removal of HA concentration as a function of UV-vis parameter (UV_{254}, UV_{280}, UV_{365} and $Color_{436}$) during the photocatalytic treatment. As mentioned before, HA is a complicated organic matter, and its structure alters after the photocatalytic treatment. The methods, applied by researchers, could not display exact result of the removed HA concentration, as a function of UV-vis parameter. As a result, the removal of HA concentration could not be represented as a function of UV-vis parameter during the photocatalytic treatment. Moreover the initial and oxidized DOC_{obs} concentration was correlated with DOC_{calc} concentration of AHA, depending on the nontreatment equations of AHA with regression coefficient (R^2=0.962, UV_{254}; R^2=0.957, UV_{280}; R^2=0.955, UV_{365}; R^2=0.958, $Color_{436}$).The oxidized DOC_{obs} concentration was correlated with DOC_{calc} concentration of AHA, depending on the nontreatment equation of the overall HAs, with high regression coefficient (R^2=0.906, UV_{254}; R^2=0.879, UV_{280}; R^2=0.849, UV_{365}; R^2=0.848, $Color_{436}$).The initial and oxidized DOC_{obs} concentration was presented as DOC_{calc} concentration of AHA, depending on the nontreatment equation of the overall HAs, with high regression coefficient (R^2=0.960, UV_{254}; R^2=0.955, UV_{280}; R^2=0.956, UV_{365}; R^2=0.958, $Color_{436}$). The oxidized DOC_{obs} concentration was correlated with DOC_{calc} concentration of AHA, depending on the nontreatment equation of the overall HAs, with high regression coefficient (R^2=0.908, UV_{254}; R^2=0.888, UV_{280}; R^2=0.859, UV_{365}; R^2=0.848, $Color_{436}$). According to these high regression coeffcients, DOC_{calc} could predict DOCobs during the photocatalytic treatment. On the other hand, similar to NHA, AHA concentration has a complicated structure, the determination of the removed DOC concentration, during the photocatalytic treatment, could not exhibit the exact result by using the nontreatment Equations. As a result, the removal of DOC concentration should be predicted by using TOC analyzer during the photocatalytic treatment.

6. REFERENCES

Abbt-Braun, G., Frimmel, F.H., 2002. The Relevance of Reference Materials: Isolation and General Characterization. In: Frimmel, F. H., Abbt-Braun, G., Heumann, K. G., Hock, B., Lüdemann, H. D., Spiteller, M. (Eds), Refractory Organic substances (ROS) in the Environment, 1–38, Wiley-Verlag Chimica Helvetica Acta, Weinheim, Germany.

Abbt-Braun, G., Lankes, U., Frimmel, F.H., 2004. Structural characterization of aquatic humic substances-The need for a multiple method approach. Aquatic Sciences, 66, 2, 151–170.

Alberts, J.J., 1982. The effect of metal ions on the ultraviolet spectra of humic acid, tannic acid, and lignosulfonic acid. Water Research, 16, 7, 1273-1276.

Areerachakul, N., Vigneswaran, S., Kandasamy, J., Duangduen, C., 2008. The degradation of humic substance using continuous photocatalysis systems. Separation Science and Technology, 43, 1, 93–112.

Aiken, G.R., McKnight, D.M.,Wershaw, R.L., MacCarthy, P., 1985. Humic Substances in Soil, Sediment and Water: Geochemistry, Isolation, and Characterization. In Aiken, G.R. (Eds), John Wiley and Sons, New York, USA, 14-19.

Aiken, G.R., McKnight, D.M., Thorn, K.A., Thurman, E.M., 1992. Isolation of hydrophilic organic acids from water using non-ionic macroporous resins. Organic Geochemistry, 18, 4, 567-573.

Al-Rasheed R., Cardin D.J., 2003a. Photocatalytic degradation of humic acids in saline waters. Part 1. Artificial seawater: influence of TiO_2, temperature, pH, and air-flow. Chemosphere, 51, 9, 925-933.

Al-Rasheed R., Cardin D.J., 2003b. Photocatalytic degradation of humic acids in saline waters. Part 2. Effects of various photocatalytic materials. Applied Catalysis A: General, 246, 1, 39-48.

Amon, R.M.W., Benner, R., 1996. Bacterial utilization of different size classes of dissolved organic matter. Limnology and Oceanography, 41, 1, 41-51.

Amy, G. L, Chadik, P. A. , Chowdhury, Z., 1987. Developing models for predicting THM formation potential and kinetics. Journal American Water Works Association, 79, 7, 89-97.
Bahnemann, D., 2004. Photocatalytic water treatment: solar energy applications. Solar Energy, 77, 5, 445-459.

Bansal, A., Madhavi, S., Thatt, T., Tan, Y., Lim, T.M., 2008. Effect of silver on the photocatalytic degradation of humic acid. Catalysis Today, 131, 1-4, 250–254.

Barber, L.B., Leenheer, J.A., Noyes, T.I., Stiles, E.A., 2001. Nature and transformation of dissolved organic matter in treatment wetlands. Environmental Science and Technology, 35, 24, 4805–4816.

Barrett, S.E., Krasner, S.W., Amy, G.L., 2000. Natural organic matter and disinfection by-products: Characterization and control in drinking water. American Chemical Society, 39, 1, 226-229.

Battin, T.J., 1998. Dissolved organic matter and its optical properties in a blackwater contributary of the upper Orinoco River, Venezuela. Organic Geochemistry, 28, 9-10, 561–569.

Bekbolet, M., Balcioglu, I., 1996. Photocatalytic degradation kinetics of humic acid in aqueous TiO_2 dispersions: The influence of hydrogen peroxide and bicarbonate ion. Water Science and Technology, 34, 9, 73-80.

Bekbolet, M., 1996. Destructive removal of humic acids in aqueous media by photocatalytic oxidation with illuminated titanium dioxide. Journal of Environmental Science and health. Part A, Environmetal Science and Engineering, 31, 4, 845–858.

Bekbolet, M., Ozkosemen, G., 1996. A preliminary investigation on the photocatalytic degradation of a model humic acid. Water Science and Technology, 33, 6, 189-194.

Bekbolet, M., Uyguner, C.S., Selcuk, H., Rizzo, L., A.D. Nikolaou, A.D., Meric, S., Belgiorno, V., 2005. Application of oxidative removal of NOM to drinking water and formation of disinfection by-products. Desalination, 176, 1-3, 155-166.

Bekbolet,M., Suphandag, A. S., Uyguner, C. S., 2002. An investigation of the photocatalytic efficiencies of TiO_2 powders on the decolourisation of humic acids. Journal of Photochemistry and Photobiology A: Chemistry, 148, 1-3, 121–128.

Bekbolet, M., Boyacioglu, Z., Ozkaraova, B., 1998. The influence of solution matrix on the photocatalytic removal of color from natural waters. Water Science and Technology, 38, 6, 155-162.

Bems, B., Jentoft, F.C., Schlögl, R., 1999. Photoinduced decomposition of nitrate in drinking water in the presence of titania and humic acids. Applied Catalysis B B: Environmental, 20, 2, 155–163.

Bennett, L. E., Drikas , M., 1993. The evaluation of colour in natural waters. Water Research, 27, 7, 1209-1218.

Bhatkhande, D. S., Pangarkar V. G., Beenackers, A. A. C. M., 2002. Photocatalytic degradation for environmental applications: A Review. Journal of Chemical Technology and Biotechnology, 77, 1, 102-116.

Blake, D.M., 2001. Bibliography of work on the heterogeneous photocatalytic removal of hazardous compounds from water and air, Technical Report. National Renewable Energy Laboratory, Springfield, Colorado, USA. NREL/TP-510-31319. October.

Bloom, P.R., Leenheer, J.A., 1989. Vibrational, Electronic and High Energy Sspectroscopic Methods for Characterizing Humic Substances. In Hayes, M.H.B., MacCarthy, P., Malcolm, R.L., Swift, R.S., (Eds.), Humic Substances: II. In Search of Structure, 409-446, John Wiley and Sons, New York.

Braun, D.W, Floyd, A.J., Sainsbury, M.,1988. Organic Spectroscopy, John Wiley and Sons, New York, USA.

Brown, R.G., 1999. Emission and Flash Techniques in Environmental Photochemistry. In Boule, P., (Eds.). The Handbook of Environmental Chemistry 2, Part I, Environmental Photochemistry, 27–61, Springer-Verlag , Berlin, Germany.

Buchanan, W., Roddick, F., Porter, N., Drikas, M., 2005. Fractionation of UV and VUV pretreated natural organic matter from drinking water. Environmental Science and Technology, 39, 12, 4647–4654.

Buffle, J., Deladoey, P., Zumstein, J.,Haerdi, W., 1982. Analysis and characterization of natural organic matters in fresh waters I. Study of analytical techniques. Schweizerische Zeitschrift für Hydrologie, 44, 2, 325-362.

Buffle, J., 1988. Complexation Reactions in Aquatic Systems: An Analytical Approach Ellis Horwood, 692, Chichester, UK.

Buffle, J., 1977. Les substances humiques et leurs interactions avec les ions mineraux. In Conference Proceedings de la Commission d'Hydrologie Appliquee de I'A.G.H.T.M. L'Universite d'Orsay, 3-10.

Cabaniss, S.E., Shuman, M.S., 1988. Copper binding by dissolved organic matter: I. Suwannee river fulvic acid equilibria. Geochimica et Cosmochimica Acta, 52, 1, 185–193.

Cassano, A.E., Alfano, O.M., 2000. Reaction engineering of suspended solid heterogeneous photocatalytic reactors. Catalysis Today, 58, 2-3, 167-197.

Cassano, A.E., Martin, C.A., Brandi, R.J., Alfano, O.M., 1995. Photoreactor analysis and design: fundamentals and applications. Industrial and Engineering Chemistry Research, 34, 7, 2155-2201.

Carp, O., Huisman, G.L., Reller, 2004. Photoinduced reactivity of titanium dioxide. Progress in Solid State Chemistry, 32, 1-2, 33-177.

Collins, M.R., Amy, G.L., Steelink, C., 1986. Molecular weight distribution, carboxylic acidity, and humic substances content of aquatic organic matter: Implications for removal during water treatment. Environmental Science and Technology, 20, 10, 1028-1032.

Chen, J., Gu, B., LeBoeuf, Pan H., Dai, S., 2002. Spectroscopic characterization of the structural and functional properties of natural organic matter fractions. Chemosphere, 48, 1, 59-68.

Chen, Y., Senesi, N., Schnitzer, M., 1976. Information provided on humic substances by E_4/E_6 ratios. Soil Science Society American Journal, 41, 2, 352-358.

Cho, Y., Choi, W., 2002. Visible light-induced reactions of humic acids on TiO_2. Journal of Photochemistry and Photobiology A: Chemistry, 148, 1-3, 129-135.

Choo, K.H., Tao, R., Kim, M.J., 2008. Use of a photocatalytic membrane reactor for the removal of natural organic matter in water: Effect of photoinduced desorption and ferrihydrite adsorption. Journal of Membrane Science, 322, 2, 368–374.

Choudhry, G.G., 1984. Humic Substances: Structural, Photophysical, Photochemical and Free Radical Aspects and Interactions with Environmental Chemicals, Gordon and Breach Publishers, 7, 185, New York, USA.

Choudhry, G.G., 1981. Humic substances: Photophysical, photochemical and free radical characteristics. Environmental Chemistry, 4, 261-295.

Chow, C.W.K., Fabris, R., Drikas, M., 2004. A rapid fractionation technique to characterise natural organic matter for the optimisation of water treatment processes. The International Water Association, 53, 85–92.

Chin Y.-P., Aiken, G., O'Loughlin, E., 1994. Molecular weight, polydispersity, and spectroscopic properties of aquatic humic substances. Environmental Science and Technology, 28, 11, 1853-1858.

Christman R. F., Norwood D. L., Seo Y., Frimmel F.H., 1989. Oxidative Degradation of Humic Substances from Freshwater Environments. In Humic Substances II ,Hayes M. H. B., MacCarthy P., Malcolm R. L., Swift R. S., (Eds), John Wiley and Sons, New York. USA, 34-67.

Chun, H., Yizhong, W., Hongxio, T., 2000. Destruction of phenol aqueous solution by photocatalysis or direct photolysis. Chemosphere, 41, 6, 1205-1209.

Croue, J.P., Korshin, G.V., Benjamin, M. (Eds.), 2000. Characterization of natural organic matter in drinking water, American Water Works Association, U.S.A.

Davies, G., Ghabbour, E.A., Khairy, K.A.,1998. Humic Substances: Structures, Properties and Uses. In Davies, G. and Ghabbour, E.A. (Eds), Royal Society of Chemistry, Great Britian.

De Haan, H., De Boer, T., Kramer, H.A., Voerman, J., 1982. Applicability of light absorbance as a measure of organic carbon in humic lake water. Water Research, 16, 6, 1047-1050.

De Lourdes Pacheco, M., Havel, J., 2002. Capillary zone electrophoresis of humic acids from the American continent. Electrophoresis, 23, 2, 268-277.

Del Vecchio, R ., Blough, N.V., 2004. On the origin of the optical properties of humic substances. Environmental Science and Technology, 38, 3885-3891.

Diallo, M. S., Faulon, J.L., Goddard III, W. A., Johnson, Jr, J. H., 2001. Binding of Hydrophobic Organic Compounds to Dissolved Humic Substances: A Predictive Approach Based on Computer Assisted Structure Eludication, Atomistic Simulations and Flory-huggings Solution Theory. In Ghabbour, E.A., Davies, G. (Eds). Humic Substances: Structures, Models and Functions, 221, The Royal Society of Chemistry, Boston, Massachusetts.

Diebold, U., 2003. The surface science of titanium dioxide. Surface Science Reports, 48, 5-8, 53-229.

Dobbs, R.A., Wise, R.H., Dean, R.B., 1972. The use of ultraviolet absorbance for monitoring the total organic carbon content of water and wastewater. Water Research, 6, 10, 1173-1180.

Doll, T.E., Frimmel, F.H., 2005. Photocatalytic degradation of carbamazepine, clofibric acid and iomeprol with P25 and Hombikat UV100 in the presence of natural organic matter (NOM) and other organic water constituents. Water Research, 39, 2-3, 403–411.

Dorfman, L.M., Adams, G.E., 1973. Reactivity of the Hydroxyl Radical, National Bureau of Standards, 46, 1-56.

Duan, J., Gregory, J., 2003. Coagulation by hydrolysing metal salts. Advances in Colloid and Interface Science, 100–102, 475-502.

Dubach, P., Mehta, N. C., 1963. The chemistry of soil humic substances. Soils and Fertilizers, 26, 293-300.

Eaton, A., 1995. Measuring UV-absorbing organics: a standard method. Journal of American Water Works Association, 87, 2, 86-90.

Edzwald , J. K., Becker, W. C.,Wattier, K. L., 1985. Surrogate parameters for monitoring organic matter and THM precursorsors. Journal of American Water Works Association. 77, 4, 122-132.

Edzwald, J.K.,Van Benschoten, J., 1990. Aluminum Coagulation of Natural Organic Matter. In Hahn, H.H., and Klute, R. (Eds), Chemical Water and Wastewater Treatment, Springer-Verlag, Berlin, Germany.

Edzwald, J.K., 1993. Coagulation in drinking water treatment: particles, organics and coagulants.Water Science and Technology, 27, 11, 21– 35.

Edzwald, J.K., Tobiason, J.E., 1999. Enhanced coagulation: Us requirements and a broader view. Water Science and Technology, 40, 9, 63-70.

Eggins, B.R., Palmer F.L., Byrne, J.A., 1997. Photocatalytic treatment of humic substances in drinking water. Water Research, 31, 5, 1223-1226.

Emeline, A.V., Ryabchuk, V.K., Serpone, N., 2005. Dogmas and Misconceptions in Herogeneous Photocatalysis: Some Enlighted Reflections. The Journal of Physical Chemistry B., 109, 39, 18515-18521.

Espinoza, T.L.A., Frimmel, F.H., 2009. A simple simulation of the degradation of natural organic matter in homogeneous and heterogeneous advanced oxidation processes. Water Research, 43, 16, 3902–3909.

Etelka, T., 1999. Colloidal properties of humic acids and spontaneous changes of their colloidal state under variable solution conditions. Soil Science, 164, 11, 814-824.

Fan, L., Harris, J.L., Roddick, F. A., Booker, N., 2001. Influence of the characterictics of natural organic matter on the fouling of microfiltration membranes. Water Resources, 35, 18, 4455–4463.

Faust, B.C., 1999. Aquatic Photochemical Reactions in Atmospheric, Surface, and Marine Waters-Influences on Oxidant Formation and Pollutant Degradation. In Boule, P., (Eds.), Environmental Photochemistry, 2, Part I, 101-122, Springer-Verlag, Berlin, Germany.

Filella, M., Buffle, J., Parthasaratly, N., 2005. Humic and Fulvic Compounds. In Worsfold, P.J., Townshend, A., Pool, C.F. (Eds.), Encyclopedia of Analytical Science, 4, Second Ed., 288–298, ,Oxford, Great Britian.

Flaig, W., Beutelspacher, H., Rietz, E., 1975. Chemical Composition and Physical Properties of Humic substances. In Gieseking, J.E., (Eds), In Soil Components: 1. Organic Components, 1-211, Soil Components, New York, USA.

Fox, M.A., Dulay, M.T., 1993. Heterogeneous photocatalysis. Chemical Reviews, 93, 1, 341-357.

Frimmel, H.F., 1998. Characterization of natural organic matter as major constituents in aquatic systems. Journal of Contaminant Hydrology, 35, 1-3, 201-216.

Frimmel, H.F., 2000. Development in aquatic humic chemistry. Agronomie, 20, 5, 451-463.

Frimmel, H.F., 2001. Aquatic Humic Substances. In Hofrichter M, Steinbüchel, A. (Eds.), Lignin, Humic Substances and Coal, Wiley-VCH, 301-324.

Frimmel, F.H., Abbt-Braun, G., 2009. Dissolved Organic Matter (DOM) in Natura Environments. In: Senesi, N., Xing, B., Huang, P.M. (Eds.), Biophysico-Chemical Processes Involving Natural Nonliving Organic Matter in Environmental Systems, John Wiley and Sons, Hoboken, New Jersey.

Frimmel, H.F., Abbt-Braun, G., Heumann, K.G., Hock, B., Lüdemann, H.D. , Spiteller, M. (Eds.), 2002. Refractory Organic Substances in the Environment, Wiley-VCH, Weinheim, Germany.

Fu, J., Ji, M., Wang, Z., Jin, L., An, D., 2006a. A new submerged membrane photocatalysis reactor (SMPR) for fulvic acid removal using a nano-structured photocatalyst. Journal of Hazardous Materials, 131, 1-3, 238–242.

Fu, J., Ji, M., Zhao, Y., Wang, L., 2006b. Kinetics of aqueous photocatalytic oxidation of fulvic acids in a photocatalysis–ultrafiltration reactor (PUR). Separation and purification technology, 50, 1, 107–113.

Gaffney, J.S., Marley, N.A., Clark, S.B. (Eds.), 1996. Humic and Fulvic Acids: Isolation, Structure, and Environmental Role. ACS Symposium Series, USA.

Gao, Y., Liu, H., 2005. Preparation and catalytic property study of a novel kind of suspended photocatalyst of TiO_2-activated carbon immobilized on silicone rubber film. Materials Chemistry and Physics, 92, 2-3, 604-608.

Ghabbour, E.A., Davies, G., (Eds.), 2001. Humic Substances Structures, Models and Functions, The Royal Society of Chemistry,USA.

Ghosh, K., Schnitzer, M., 1980. Macromolecular structures of humic substance. Soil Science, 129, 5, 266–276.

Gjessing, E.T., 1976. Physical and Chemical Characteristics of Aquatic Humus. Journal Environmental Quality, 5, 4, 494-494.

Gjessing, E. T., Egeberg, P.K., Ratnaweera, H. (Eds), 1999a. Typing of natural organic matter in water. Special Issue of Environmental International, 25, 2/3.

Gjessing, E.T., Alberts, J.J., Bruchet, A., Egeberg, P.K., Lydersen, E., Mcgown, L.B., Mobed, J.J., Munster, U., Pempkowiak, J., Perdue, M., Ratnawerra, H., Rybacki, D., Takacs, M., Abbt-Braun, G., 1998. Multi-method Characterization of Natural Organic Matter Isolated from Water: Characterization of Reverse Osmosis-isolates from Water of Two Semi-Identical Dystrophic Lakes Basins in Norway. Water Resource, 2, 10, 3108–3124.

Goldstone, J.V., Pullin, M.J., Bertilsson, S., Voelker, B.M., 2002. Reactions of hydroxyl radical with humic substances: Bleaching, mineralization, and production of bioavailable carbon substrates. Environmental Science and Technology, 36, 3, 364–372.

Gomes, I., Santos, J.C., Vilar, V.J.P., Boaventura, R.A.R., 2009. Inactivation of bacteria E. coli and photodegradation of humic acids using natural sunlight. Applied Catalysis. B-Environmental,. 88, 3-4, 283–291.

Gonenc, D., Bekbolet, M., 2001. Interactions of hypochlorite ion and humic acid: photolytic and photocatalytic pathways. Water Science and Technology, 44, 5, 205-210.

Han, I., Shin, J.W., Kim, H.C., 2006. Photocatalytic oxidation of aquatic humic substances using TiO_2/UV in a rotating photoreactor. Water Science and Technology, 6, 2, 93–99.

Hatcher, P. G., Breger, I. A., Maciel, G. E., Szeverenyi, N. M., 1985. Geochemistry of Humin. In Aiken, G.R., MacCarthy, P., Malcolm, R.L., Swift, R.S. (Eds.), Humic Substances in Soil, Sediment, and Water: Geochemistry, Isolation, and Characterization, 275-302, John Wiley and Sons, NewYork.

Hayes, M.H.B., MacCarthy, P., Malcolm, R.L., Swift, R.S., 1989. The Search for the Structure: Setting the Scene. Humic substances II. In search of structure. Chichester: John Wiley and Sons, 4–30.

Hayes, M. H. B., P. MacCarthy, R. L. Malcolm, R. S. Swift (Eds.),1989. Humic Substances II: In search of structure. Part II: Spectroscopic Studies of the Structures of Humic Substances. Wiley-Interscience, 257-446, New York.

Hayes, M. H. B., Swift, R. S.,1978. The Chemistry of Soil Organic Colloids. In The Chemistry of Soil Constituents. D. J. Greenland and M. H. B. Hayes, editions. Wiley-Interscience, New York, 179-230.

Hautala, K., Peuravuori, J., Pihlaja, K., 2000. Measurement of aquatic humus content by spectroscopic analyses. Water Research, 34, 1, 246-258.

Herrmann, J.M., 1999. Heterogeneous photocatalysis: fundamentals and applications to the removal of various types of aqueous pollutants. Catalysis Today, 53, 1, 115-129.

Hernes, P. J., Benner, R. J., 2003. Photochemical and microbial degradation of dissolved lignin phenols: Implications for the fate of terrigenous dissolved organic matter in marine environments. Journal of geophysical research. Biogeosciences, 108,C9, 3291-3299.

Hoffmann, M.R., Martin, S.T., Choi, W., Bahnemann, D.W., 1995. Environmental applications of semiconductor photocatalysis. Chemical Reviews, 95, 1, 69-96.

Hofrichter, M. and Steinbüchel, A. (Eds.), 2001. Biopolymers. Lignin, Humic substances and Coal, 1, Wiley-VCH, Weinheim, Germany.

Hongve, D., Akesson G., 1996. Spectrophotometric determination of water colour in Hazen units. Water Research, 30, 11, 2771-2775.

Huang, X., Leal, M., Li, Q., 2008. Degradation of natural organic matter by TiO_2 photocatalytic oxidation and its effect on fouling of low-pressure membranes.Water Resource, 42, 4-5, 1142–1150.

Hur, J., Schlautman, M.A., 2004. Effects of pH and phosphate on the adsorptive fractionation of purified Aldrich humic acid on kaolinite and hematite. Journal of Colloid and Interface Science, 277, 2, 264-270.

Ilgun, S.A., 2010. Characterization and Reactivity of Natural Organic Matter In Drinking Water Sources, M.S.Thesis, Bogazici University.

Jaffrezic-Renault, N., Pichat, P., Foissy, A., Mercier, R., 1986. Effect of deposited Pt particles on the surface charge of TiO_2 aqueous suspensions by potentiometry, electrophoresis, and labeled ion adsorption. Journal of Physical Chemistry, 90, 2733-2738.

Janos, P., 2003. Separation methods in the chemistry of humic substances. Journal of Chromatography A, 983, 1-2, 1-18.

Johnson, R.A., Bhattocharyya, G.K., 1996. Statistics Principles of Methods, Third Edition, John Wiley and Sons, Inc., U.S.A.

Jones, M.N., Bryan, N.D., 1998. Colloidal properties of humic substances. Advances in Colloid and Interface Science , 78, 1, 1-48.

Kalbitz, K., Geyer, S., Geyer, W., 2000. A comparative characterization of dissolved organic matter by means of original aqueous samples and isolated humic substances. Chemosphere, 40,12, 1305-1312.

Kerc, A., Bekbolet, M., Saatci, A.M., 2003a. Sequential oxidation of humic acids by ozonation and photocatalysis. Ozone Science and Engineering, 25, 6, 497–504.

Kerc, A., Bekbolet, M., Saatci, A.M., 2003b. Effect of partial oxidation by ozonation on the photocatalytic degradation of humic acids. International Journal of Photoenergy, 5, 75–80.

Korshin, G.V., Li, C.W., Benjamin, M.M., 1997. Monitoring the properties of natural organic matter through UV spectroscopy: A consistent theory. Water Research, 31, 7, 1787-1795.

Kördel, W., Dassenakis, M., Lintelmann, J., Padberg, S., 1997. The importance of naturalorganic material for environmental processes in waters and soils. Pure and Applied Chemistry, 69, 7, 1571-1600.

Knabner, I.K., 2000. Analytical approaches for characterizing soil organic matter. Organic Geochemistry, 31, 7, 609-625.

Kononova, M.M., 1966. Soil Organic Matter. Pergamon, New York, USA.

Kronberg, L., 1999. Content of Humic Substances in Freshwater. In Keskitalo, J. and Eloranta (Eds.), Limnology of Humic Waters. P. Backhuys Publishers, Leiden, The Netherlands.

Krysa, J., Keppert, M., Jirkovsky, J., Stengl, V., S.J., 2004. The effect of thermal treatment treatment on the proporties of TiO_2 photocatalyst. Materials Chemistry and Physics, 86, 2-3, 333-339.

Kim, H.C., Yu, M.J, 2005. Characterization of natural organic matter in conventional water treatment processes for selection of treatment processes focused on DBPs control. Water Research, 39, 19, 4779–4789.

Kumke, M.U., Specht, C.H., Brinkmann, T., Frimmel, F.H., 2001. Alkaline hydrolysis of humic substances-spectroscopic and chromatographic investigations. Chemosphere, 45, 6-7, 1023-1031.

Langhals, H., Abbt-Braun, G., Frimmel, F. M., 2000. Association of humic substances: verification of Lambert-Beer's law. Acta Hydrochimica et Hydrobiologica, 28, 6, 329–332.

Larson, R.A. and Marley, K.A.,1999. Singlet Oxygen in the Environment In Boule, P. (Eds), Environmental Photochemistry, 2, Part I, Springer-Verlag, 123-137, Berlin.

Lawrence, J.,1980. Semi-quantitative determination of fulvic acid, tannin and lignin in natural waters. Water Research,14, 4, 373-377.

Le-Clech, P., Lee, E.K., Chen, V., 2006. Hybrid photocatalysis/membrane treatment for surface waters containing low concentrations of natural organic matters. Water Research, 40, 2, 323–330.

Lee, S., Ohgaki, S., 1999. Oxidative degradation of TOC and THMFP by fluidized bed photocatalysis reactor. Journal of Environmental Science and Health A, 34, 10, 1933–1944.

Leenheer, J.A., Croué, J.P., 2003. Aquatic organic matter. Environmental Science and Technology, 19A-26A.

Leenher, J.A., 2004. Comprehensive assessment of precursors, diagenesis, and reactivity to water treatment of dissolved and colloidal organic matter. Water Science and Technology. Water Supply, 4, 4, 1–9.

Leenheer, J.A., 1981. Comprehensive approach to preparative isolation and fractionation of dissolved organic carbon from natural waters and wastewaters. Environmental Science and Technology, 15, 5, 578–587.

Legrini, O., Oliveros E. , Braun A.M., 1993. Photochemical processes for water treatment. Chemical Reviews, 93, 2, 671-698.

Li, C.W., Korshin, G.V., Benjamin, M.M.,1998. Monitoring DBP formation with differential UV spectroscopy. Journal of American Water Works Association, 90, 8, 88-100.

Li, X.Z., Fan, C.M. , Sun, Y.T., 2002. Enhancement of photocatalytic oxidation of humic acid in TiO_2 suspensions by increasing cation strength. Chemosphere, 48, 4, 453-460.

Li, Q., Xie, R., Mintz, E.A., Shang, J.K., 2007. Enhanced visible-light photocatalytic degradation of humic acid by palladium-modified nitrogen-doped titanium oxide. Journal of American Ceramics. Society, 90, 12, 3863–3868.

Liu, S., Lim, M., Fabris, R., Chow, C., Chiang, K., Drikas, M., Amal, R., 2008a. Removal of humic acid using TiO_2 photocatalytic process- Fractionation and molecular weight characterization studies. Chemosphere, 72, 2, 263-271.

Liu, S., Lim, M., Fabris, R., Chow, C.W.K., Drikas, M., Korshin, G., Amal, R., 2010. Multi-wavelength spectroscopic and chromatographic study on the photocatalytic oxidation of natural organic matter. Water Research, 44, 8, 2525-2532.

Ljubas, D., 2005. Solar photocatalysis-a possible step in drinking water treatment. Energy, 30, 10, 1699-1710.

Ma, H., Kim, S.D., Cha, D.K., Allen, H.E., 1999. Effect of kinetics of complexation by humic acid on toxicity of copper to *Ceriodaphnia dubia*. Environmental Toxicology Chemistry, 18, 5, 828–837.

MacCarthy, P., Rice, J., 1985. Spectroscopic Methods (other than NMR) for Determining Functionality in Humic Substances. In Humic Substances in Soil, Sediment and Water, Geochemistry, Isolation and Characterization. In Aiken G. R., McKnight D. M., Wershaw R. L. and MacCarthy P. (Eds.), 527-559, John Wiley, New York, USA.

MacCarthy, P., 2001a. The Principles Of Humic Substances: An Introduction To The First Principle. Proceedings of the fifth Humic Substances Seminar, Northeastern University, Boston, Massachusetts, 221.

MacCarthy, P., 2001b. The principles of humic substances. Soil Science, 166, 11, 738-751.
MacCarthy, P., Malcolm, R.L., Clapp, C.E., Bloom, P.R., 1990. Humic Substances in Soil and Crop Sciences: Selected Readings. American Society of Agronomy and Soil Science Society of America.

Maira, A.J., Yeung, K.L., Soria, J., Coronado, J.M., Belver, C., Lee, C.Y., Augugliaro, 2001. Gas-phase photo-oxidation of toluene nanometer-size TiO_2 catalysts. Applied Catalyst B: Environmental, 29, 4, 327-336.

Malcolm, R.L., 1990. The uniqueness of humic substances in each of soil, stream and marine environments. Analytica Chimica Acta, 232, 19-30.

Marhaba, T.F., Van, D., Lippincott, R.L., 2000. Changes in NOM fractions through treatment: A comparison of ozonation and chlorination. Ozone Science and Engineering, 22, 3, 249-266.

Matilainen, A., Lindqvist, N., Korhonen, S., Tuhkanen, T., 2002. Removal of NOM in the different stages of the water treatment process. Environment International, 28 , 6, 457–465.

Matilainen, A., Sillanpää, M., 2010a. Removal of natural organic matter from drinking water by advanced oxidation processes. Chemosphere, 80, 4, 351–365.

Matilainen, A., Vepsäläinen, M., Sillanpää, M., 2010b. Natural organic matter removal by coagulation during drinking water treatment: A review. Advanced in Colloid and Interface Science, 159, 2, 189-197.

Manahan, S.E., 1991. Environmental Chemistry. Lewis Publisher, Michigan, USA.

McDonald, S., Bishop, A. G., Prenzler, P. D., Robards, K., 2004. Analytical chemistry of freshwater humic substances. Analytica Chimica Acta, 527, 2, 105–124.

Meng, Y.B., Hunag, X., Wu, Y. Wang, X., Qian, Y., 2002. Kinetic study and modeling on photocatalytic degradation of para-chlorobenzoate at different light intensities. Environmental Pollution, 117, 2, 307-313.

Mohammadi, M.R., Cordeno-Cabrera, M.C., Fray, D.J., Ghorbani, M., 2006. Preparation of high surface area titania (TiO_2) films and powders using particulate sol-gel route aided by polymeric fugitive agents. Sensors and Actuators B: Chemical, 120, 1, 86-95.

Moore, T.R., 1985. The spectroscopic determination of dissolved organic carbon in peat waters. Soil Science Society of America Journal, 49, 6, 1590-1592.

Moriguchi, T., Tahara, M., Yaguchi, K., 2006. Adsorbability and photocatalytic degradability of humic substances in water on Ti-modified silica. Journal of Colloid and Interface Science, 297, 2, 678–686.

Morrow, C. M., Minear, R. A., 1987. Use of regression models to link raw water characteristics to THM concentrations in drinking water. Water Research, 21, 1, 41-48.

Michaelis, L. and Granick, S., 1944. Molecular compounds of the quinhydrone type in solution. Journal of American Chemical Society, 66, 6, 1023-1030.

Mrkva, M., 1969. Investigation of organic pollution of surface waters by ultraviolet spectrophotometry. Journal of Water Pollution Control Federation, 41, 11, 1923-1931.

Mrkva, M., 1983. Evaluation of regressions between absorbance at 254 nm and COD of river waters. Water Research, 17, 2, 231-235.

Mills, L.H., 1997. An overview of semiconductor photocatalysis. Journal of Photochemistry and Photobiology A: Chemistry, 108, 1, 1-35.

Mills, A., Morris S., 1993. Photomineralization of 4-chlorophenol sensitized by titanium dioxide- A study of the initial kinetics of carbon dioxide photogeneration. Journal of Photochemistry and Photobiology A: Chemistry, 71, 1, 75-83.

Minero, C., 1999. Kinetic analysis of photoinduced reactions at the water semiconductor interface. Catalysis Today, 54, 2-3, 205–216.

Molinari, R., Borgese, M., Drioli, E., Palmisano, L., Schiavello, M., 2002. Hybrid processes coupling photocatalysis and membranes for degradation of organic pollutants in water. Catalysis Today, 75, 1-4, 77–85.

Murray, C.A., Parsons S.A., 2004. Comparison of AOPs for the removal of natural organic matter: Performance and economic assessment. Water Science and Technology, 49, 4, 267-272.

Murray, C.A., Parsons, S.A., 2006. Preliminary laboratory investigation of disinfection by-product precursor removal using an advanced oxidation process. Water and Environment Journal, 20, 3, 123–129.

Murray, C.A., Goslan, E.H., Parsons, S., 2007. TiO_2/UV: A single stage drinking water treatment for the removal of NOM. Journal of Environmental Engineering and Science, 6, 3, 311–317.

Najm, I.N., Patania, N.L., Jacangelo, J.G., Krasner, S.W., 1994. Evaluating surrogates for disinfection by-products. Journal of the American Water Works Association, 86, 6, 98-106.

Nikolaou, A.D., Lekkas, T.D., 2001. The role of natural organic matter during formation of chlorination by-products: A review. Acta Hydrochimica et Hydrobiologica, 29, 2-3, 63-77.

Novak, J. M., Mills, G. L., Bertsch P. M., 1992. Estimating the percent aromatic carbon in soil and aquatic humic substances using ultraviolet absorbance spectroscopy. Journal of Environmental Quality, 21, 144-147.

Ogura, N., Hanya, T.,1966. Nature of ultraviolet absorbance in seawater. Nature, 212, 758.
Ollis, D.F., 1985. Contaminant degradation in water. Environmental Science and Technology, 19, 6, 480-484.

Ollis, D.F., Pelizzetti, E., Serpone, N., 1991. Destruction of water contaminants. Environmental Science and Technology, 25, 9, 1523-1529.

Orlov, D.S., 1990. Humic Acids of Soils and General Theory of Humification, Moskova State University, Moscow, Russia.

Packham, R. F.,1964. Studies of Organic Colour in Natural Water; proceedings. Proceedings of the Society for Water Treatment and Examination, 13, 62, 316-334.

Palmer, F.L., Eggins, B.R., Coleman H.M., 2002. The effect of operational parameters on the photocatalytic degradation of humic substances. Journal of Photochemistry and Photobiology A: Chemistry, 148, 1-3, 137-143.

Peuravuori, J., Pihlaja, K., Valimaki, N., 1997a. Isolation and characterization of natural organic matter from lake water: two different adsorption chromatographic methods. Environment International, 23, 4, 453–464.

Peuravuori, J., Pihlaja, K., 1997b. Molecular size distribution and spectroscopic properties of aquatic humic substances. Analytica Chimica Acta, 337, 2, 133-149.

Peuravuori, J., Pihlaja, K., 1999. Characterization of Aquatic Humic Substances . In: Keskitalo, J., Eloranta, P. (Eds.), Limnology of Humic Waters, Backhuys, Leiden, The Netherlands.

Piccolo, A., 2001. The supramolecular structure of humic substances. Soil Science,166, 11, 810-832.

Piccolo, A., 1996. Humic Substances in Terrestrial Ecosystems. Piccolo, A. (Eds). Elsevier Science, Amsterdam, The Netherlands.

Polewski, K., Syawin´ska, D., Syawin´ski, J., Pawlak, A., 2005. The effect of UV and visible light radiation on natural humic acid EPR spectral and kinetic studies. Geoderma, 126 , 3-4, 291–299.

Portjanskaja E., Krichevskaya, M., Preis, S., Kallas, J., 2004. Photocatalytic oxidation of humic substances with TiO_2-coated glass micro spheres. Environmental Chemical Letters, 2, 3, 123-127.

Portjanskaja, E., Preis, S., Kallas, J., 2006. Aqueous photocatalytic oxidation of lignin and humic acids with supported TiO_2. International Journal of Photoenergy, 2006, 1–7.

Portjanskaja, E., Stepanova, K., Klauson, D., Preis, S., 2009. The influence of titanium dioxide modifications on photocatalytic oxidation of lignin and humic acids. Catalysis Today, 144, 1-2, 26–30.

Potter, B.B., Wimsatt, J.C., 2005. Determination of Total Organic Carbon and Specific UV Absorbance at 254 nm In Source Water and Drinking Water. Cincinatti, Ohio, EPA/600/R-05/055.

Qiao, S., Sun, D.D., Tay, J.H., Easton C., 2002. Photocatalytic oxidation technology for humic acid removal using a nano-structured TiO_2/Fe_2O_3 catalyst. Water Science and Technology, 47, 1, 211-217.

Rajeshwar, K., 1995. Photoelectrochemistry and the Environment. Journal of Applied Electrochemistry, 25, 12, 1067-1082.

Remoundaki, E., Vidali, R., Kousi, P., Hatzikioseyian, A., Tsezos, M., 2009. Photocatalytic and photocatalytic alterations of humic substances in UV (254 nm) and solar cocentric parabolic concentrator (CPC) reactors. Desalination, 248, 1-3, 843–851.

Reynolds, D.M.,Ahmad, S.R., 1997. Rapid and direct determination of wastewater BOD values using a fluorescence technique. Water Research, 31, 8, 2012-2018.

Ritchie, J.D., Perdue, E.M., 2003. Proton binding study of standard and reference fulvic acids, humic acids, and natural organic matter. Geochimica et Cosmochimica Acta, 67, 1, 85-96.

Rizzo, L., Uyguner, C.S., Selcuk, H., Bekbolet, M., Anderson, M., 2007. Activation of solgel titanium nanofilm by UV illumination for NOM removal. Water Science and Technology, 55, 12, 113–118.

Rizzo, L., Della Rocca, C., Belgiorno, V., Bekbolet, M., 2008. Application of photocatalysis as a post treatment method of a heterotrophic–autotrophic denitrification reactor effluent. Chemosphere, 72, 11, 1706–1711.

Salinaro, A., Emeline, A.V., Zhao, J., Hidaka, H., Ryabchuk, V.K. and Serpone, N.,1999. Terminology, Relative photonic efficiencies and quantum yields in heterogeneous photocatalysis. Part II: Experimental determination of quantum yields. Pure and Applied Chemistry, 71, 2, 321-335.

Saquid, M., Muneer, M., 2003. TiO_2-mediated photocatalytic degradation of a triphenylmethane dye (gentian violet), in aqueous suspensions. Dyes and Pigments, 56, 1, 37-49.

Scheuch, L.,E., Edzwald, J.,K., 1981. Removing color and chloroform precursors from low turbidity waters by direct filtration. American Water Works Association, 73, 2, 497-502.

Schnitzer, M., Khan, S.U., 1972. Humic Substances in the Environment. Marcel Dekker, New York, USA.

Schnitzer, M., 1978. Humic substances: chemistry and reactions. In: Schnitzer, M., Khan, S.U. (Eds.), Soil organic matter, 1–64, Elsevier, Amsterdam.

Schnitzer , M., 1982. Quo vadis organic matter research. Transition 12th International Congress Soil Science, New Delhi, 4, 67-78.

Schubert, W. L., 1965. Lignin Biochemistry, Academic Press, NewYork, USA.

Schlautman, M.A., Morgan, J.J., 1994. Adsorption of aquatic humic substances on colloidal-size aluminum oxide particles: influence of solution chemistry. Geochimica et Cosmochimica Acta, 58, 20, 4293– 303.

Selcuk, H., Sene, S.S., Sarikaya, H.Z., Bekbolet, M., Anderson, M., 2004. An innovative technology in the treatment of river water containing humic substances. Water Science and Technology, 49, 4, 153–158.

Selcuk, H., Bekbolet, M., 2008. Photocatalytic and photoelectrocatalytic humic acid removal and selectivity of TiO_2 coated photoanode. Chemosphere, 73, 5, 854–858.
Serpone, N. and Pelizzetti, E. (Eds), 1989. Photocatalysis, fundamentals and applications. Wiley Interscience, New York, USA.

Senesi, N., Loffredo, E., 2001. Soil Humic Substances, In Hofrichter M. and Steinbüchel A. (Eds.) Biopolymers: Lignin, Humic Substances and Coal, Wiley-VCH, 247-301.

Senesi, N., Miano, T.M., Provenzano, M.R., Brunetti G., 1991. Characterization, differentiation, and classification of humic substances by fluorescence spectroscopy. Soil Science, 152, 4, 259-271.

Serpone , N. and Pelizzetti E. (Eds.), 1989. Photocatalysis, Fundamentals and Applications. Wiley-Interscience, New York, USA.

Serpone, N., Pelizzetti E., Hidaka, H., 1992. Heterogenenous photocatalysis, issues, questions, some answers, and some success. Proceeding of 9th International Conference on Solar Energy, IPS-9, Tian Z.W., Cao, Y. (Eds.), International Academic Publishers, Beijing, China, 33-73.

Sharp, E.L., Jarvis, P., Parsons, S.A., Jefferson, B., 2006a. Impact of fractional character on the coagulation of NOM. Colloids Surfaces A: Physicochemical and Engineering Aspects, 286, 1-3, 104–111.

Sharp, E.L., Parsons, S.A., Jefferson, B., 2006b. Seasonal variations in natural organic matter and its impact on coagulation in water treatment. Science of the Total Environment, 363, 1-3, 183–194.

Shaw, D.J., 1966. Introduction to Colloid and Surface Chemistry. Butterworth, London, England.

Shirshova, L.T., Ghabbour, E.A., Davies, G., 2005. Spectroscopic characterization of humic acid fractions isolated from soil using different extraction procedures. Geoderma, 133, 3-4, 204–216.

Skoog, D.A., Leary, J.J., 1992. Principles of Instrumental Analysis, 4th Edition, Saunders College Publishing, U.S.A.

Slifkin, M. A., 1971. Charge-transfer interaction of biomolecules. Academic Press, London, Great Britain.

Smart, P.I., 1976. The relation of flourescence to dissolved organic carbon in surface waters. Water Research, 10, 9, 805-.811.

Snoeyink, V.L., Summers, R.S., 1999. Adsorption of Organic Compounds, in R.D. Letterman (Eds) Water Quality and Treatment: A Handbook of Community Water Supplies, 5th ed., American Water Works Association, McGraw-Hill, NewYork, USA.

Sontheimer, H.S., 1978. The Mülheim Process. Journal American Water Works Association, 70,7, 393.

Sontheimer, H., Crittenden, Summers, R.S., 1988. Activated Carbon for Water Treatment, 2nd ed., in English, DVGW- Forschungstelle, Engler-Bunte-Institut, Unversität Karlsruhe, Germany.

Steelink, C., 1985. In Humic Substances in Soil, Sediment and Water. Aiken, G.R., MacCarthy, P., Malcolm, R.L., Swift, R.S. (Eds), Wiley, NewYork, 460.

Stevenson, F.J., 1985. In Humic Substances in Soil, Sediment and Water. Aiken, G.R., MacCarthy, P., Malcolm, R.L., Swift, R.S. (Eds), Wiley, NewYork, 21-24.

Stevenson, F.J., 1982. Humus Chemistry, Genesis, Composition, Reactions. Wiley-International Science, New York, USA.

Stevenson, F.J., 1994. Humus Chemistry: Genesis, Composition, Reactions. John Wiley and Sons, New York, USA.

Stone, A.T. and Morgan, J.J., 1984. Reduction and dissolution of manganese (III) and manganese (IV) oxides by organics: 2. Survey of the reactivity of Organics. Environmental Science and Technology, 18, 8, 617-624.

Struyk, Z., Sposito G., 2001. Redox properties of standard humic acids. Geoderma, 102, 3-4, 329-346.

Suffet, I.H., MacCarthy, P. (Eds), 1989. Aquatic Humic Substances, Influence of Fate and Treatment of Pollutants, Advances in Chemistry Series, American Chemical Society, Washington DC, USA.

Syafei, A.D., Lin, C.-F., Wu, C.H., 2008. Removal of natural organic matter by ultrafiltration with TiO_2-coated membrane under UV-irradiation. Journal of Colloid Interface and Science, 323, 1, 112–119.

Świetlik, J., Dabrowska, A., Raczyk-Stanislawiak, U., Nawrocki, J., 2004. Reactivity of natural organic matter fractions with chlorine dioxide and ozone. Water Research, 38, 3, 547–558.

Tay, J.H., Chen D., Sun D.D., 2001. Removal of color substances using photocatalytic oxidation for membrane filtration processes. Water Science and Technology, 43, 10, 319-325.

Tchobanoglous, G., Burton, F.L., Stensel, H.D., 2003. Wastewater engineering: treatment and reuse, Fourth Ed., Metcalf and Eddy - McGraw-Hill, U.S.A., 1196.

Thurman, E.M., 1985. Organic Geochemistry of Natural Waters. Martinus Niijhoff/Dr. W. Junk Publishers, Dordrecht., 90, 304-312.

Thurman, E.M., Malcolm R.L., 1981. Preparative isolation of aquatic humic substances. Environmental Science and Technology, 15, 4, 463–466.

Tipping, E., (Eds), 2002. Cation Binding by Humic Substances, Cambridge University Press, Cambridge, UK.

Traina, S.J., Novak, J., Smeck, N.E.,1990. An ultraviolet absorbance method of estimating the percent aromatic carbon content of humic acids. Journal of Environmental Quality, 19, 1, 151-153.

Tsarenko, S.A., Kochkodan, V.M., Samsoni-Todorov, A.O., Goncharuk, V.V., 2006. Removal of humic substances from aqueous solutions with a photocatalytic membrane reactor. Colloid journal of the Russian Academy of Sciences, 68, 3, 341–344.

Tsimas, E.S., Tyrovola, K., Xekoukoulotakis, N.P., Nikolaidis, N.P., Diamadopoulos, E., Mantzavinos, D., 2009. Simultaneous photocatalytic oxidation of As(III) and humic acid in aqueous TiO_2 suspensions. Journal of hazardous materials, 169, 1-3, 376–385.

Tulonen, T., 2004. Role of allochthonous and autochthonous dissolved organic matter (DOM) as a carbon source for bacterioplankton in boreal humic lakes.Faculty of Biosciences Department of Biological and Environmental Sciences Aquatic Sciences/Hydrobiology, University of Helsinki, Academic Dissertation in Hydrobiology, PhD Thesis.

Turchi, C.S., Ollis, D.F., 1989. Mixed reactant photocatalysis: Intermediates and mutual rate inhibition. Journal of Catalysis, 119, 2, 483-496.

Turchi, C.S., Ollis, D.F., 1990. Photocatalytic degradation of organic contaminants: mechanisms involving hydroxyl attack. Journal of Catalysis, 122, 1, 178-192.

Thurman, E.M., (Eds), 1985. Organic Geochemistry of Natural Waters. Kluwer Academic Publishers Group, Dordrecht, The. Netherlands.

Thurman, E.M., Malcolm, R.L., 1981. Preparative isolation of aquatic humic substances. Environmental Science and Technology, 15, 4, 463-466.

Uyguner, C.S., Bekbolet, M., 2004a. Photocatalytic degradation of natural organic matter: Kinetic considerations and light intensity dependence. International Journal of Photoenergy, 6, 2, 73-80.

Uyguner, C.S., Bekbolet, M., 2004b. Evaluation of humic acid, chromium (VI) and TiO_2 ternary system in relation to adsorptive interactions. Applied Catalysis B: Environmental, 49, 4, 267-275.

Uyguner, C.S., Bekbolet, M., 2005a. A comparative study on the photocatalytic degradation of humic substances of various origins. Desalination, 176, 1-3, 167-176.

Uyguner C.S., Bekbolet, M., 2005b. Evaluation of humic acid photocatalytic degradation by UV-vis and fluorescence spectroscopy. Catalysis Today, 101, 3-4, 267-274.

Uyguner, C. S., Bekbolet, M., 2005c. Implementation of spectroscopic parameters for practical monitoring of natural organic matter. Desalination, 176, 1-3, 47-55.

Uyguner, C. S., Bekbolet, M., Swiétlik, J., 2006. Natural Organic Matter: Definitions and Characterization. Nova Science Publishers. Chapter 5.1.

Uyguner, C.S., Bekbolet, M., 2007. Contribution of metal species to the heterogeneous photocatalytic degradation of natural organic matter. International Journal of Photoenergy, 1, 1–8.

Uyguner, C.S., Bekbolet, M., 2009. Application of photocatalysis for the removal of natural organic matter in simulated surface and ground waters. Journal of advanced oxidation technologies, 12, 1, 87–92.

Uyguner- Demirel, Bekbolet, 2011. Significance of analytical parameters for the understanding of natural organic matter in relation to photocatalytic oxidation. Chemosphore, 84, 8, 1009-1031.

Visser, S. A., 1982. Acid functional group content of aquatic humic matter: Its dependence upon origin, molecular weight and degree of humification of the material. Journal of Environmental Science Health, 17, 6, 767-788.

Vuorio, E., Vahala, R., Rintala, J., Laukkanen, R., 1998. The evaluation of drinking water treatment performed with HPSEC. Environment International, 24, 5–6, 617– 623.

Wang, G.S., Hsieh, S., 2001. Monitoring Natural Organic Matter in Water with Scanning Spectrophotometer. Environment International, 26, 4, 205-212.

Wang, Z.D., Pant, B.C., Langford, C.H., 1990. Spectroscopic and structural characterization of a Laurentian fulvic acid: notes on the origin of the color. Analytica Chimica Acta, 232, 1, 43-49.

Wong, H., Mok, K.M., Fan, X.J., 2007. Natural organic matter and formation of trihalomethanes in two water treatment processes. Desalination, 210, 1-3, 44–51.

Wiszniowski J., Robert D., Surmacz-Gorska, J., Miksch K., Weber J.V., 2002. Photocatalytic decomposition of humic acids on TiO_2 Part I: Discussion of adsorption and mechanism . Journal of Photochemistry and Photobiology A: Chemistry, 152, 1-3, 267-273.

Wiszniowski J., Robert D., Surmacz-Gorska, J., Miksch, K., Weber, J.V., 2003. Photocatalytic mineralization of humic acids with TiO_2: Effect of pH, sulfate and chloride anions. International Journal of Photoenergy, 5, 2, 69-74.

Wiszniowski, J., Robert, D., Surmacz-Gorska, J., Miksch, K., Malato, S., Weber, J.V., 2004. Solar photocatalytic degradation of humic acids as a model of organic compounds of landfill leachate in pilot-plant. Applied Catalysis. B: Environmental, 53, 2, 127-137.

Wonnacott, T.H., Wonnacott, R.J., 1990. Introductory Statictis, Fifth Edition, John Wiley and Sons, U.S.A.

Yang, J.K., Lee, S.M., 2006. Removal of Cr(VI) and humic acid by using TiO_2 photocatalysis. Chemosphere, 63, 10, 1677–1684.

Zafiriou, O.C., Joussot-Dubien, J., Zepp, R.G., Zika, R.G., 1984. Photochemistry of natural waters. Environmental Science and Technology, 18, 12, 358A–371A.

Zavarzina, A.G., Demin, V.V., Nifanteva, T.I., Shkinev, V.M., Danilova, T.V., Spivakov,B., 2002. Extraction of humic acids and their fractions in poly (ethylene glycol)-based aqueous biphasic systems. Analytica Chimica Acta, 452, 1, 95-103.

Zhang, X., Du, A.J., Lee, P., Sun, D.D., Leckie, J.O., 2008. TiO_2 nanowire membrane for concurrent filtration and photocatalytic oxidation of humic acid in water. Journal Membrane Science, 313, 1-2, 44–51.

Zhang, X., Pan, J.H., Du, A.J., Fu, W., Sun, D.D., Leckie, J.O., 2009. Combination of one dimensional TiO_2 nanowire photocatalytic oxidation with microfiltration for water treatment. Water Research, 43, 5, 1179–1186.

Zsolnay, A., 2003. Dissolved organic matter: Artefacts, definitions, and functions. Geoderma, 113, 3-4, 187-209.